Identification and Validation of a Common Molecular Signature of Progressive Fibrosis in Human Livers

by

Mu Hao Hsu

A thesis submitted in partial fulfillment of the
requirements for the degree of

Doctor of Philosophy

in

Molecular Pathology

Department of Laboratory Medicine and Pathology

University of Alberta

Abstract

Over 25% of the world population suffer from chronic liver disease. Most common causes are long-term viral infections, alcohol abuse, and non-alcoholic fatty liver disease (NAFLD) associated with obesity, diabetes or hyperlipidemia. Chronic liver disease due to any cause is characterized by repetitive or long-lasting liver injury which may result in liver fibrosis. Regardless of underlying etiology, advanced liver fibrosis is the final common pathway that eventually leads to poor clinical outcomes. Histopathology assessment of liver biopsy plays a central role in evaluating liver fibrosis, but it is subjective, suffers from suboptimal reproducibility, and, more importantly, cannot predict fibrosis progression. The natural history of fibrosis progression varies, with a high degree of heterogeneity among patients. The factors that drive this diversity are unknown. In addition, it is unclear if there is a common molecular signature for progressive fibrosis independent of its etiology. This thesis aims to identify a common molecular signature associated with advanced fibrosis that is shared by different liver diseases in humans, and to translate this knowledge to develop a surrogate biomarker test for clinical use.

To identify a common molecular signature of advanced fibrosis, I analyzed 304 Affymetrix genome-wide microarrays of fresh livers from 312 patients with various chronic liver diseases (NAFLD, alcoholic liver disease, viral hepatitis B or C) available in open access databases. Using a discovery set (n=70), I defined a 48-gene signature with the highest discriminate ability for advanced fibrosis using multiple machine learning class prediction algorithms and class comparison methods. The 48-gene signature was validated in three independent validation sets (n=70, 91, and 73) with over 0.96 area under the receiver operating characteristic curve and over 93% accuracy for histologically-proven advanced fibrosis.

As a clinical translational approach, the 48-gene signature was then analyzed in 348 formalin-fixed paraffin-embedded (FFPE) clinical liver biopsies and 15 paired fresh and FFPE explant livers by a digital direct nucleic acid profiling method (NanoString assay) to understand if multiplex gene expression quantification in clinical liver biopsies is a feasible and reliable approach. NanoString gene expression levels were strongly correlated between paired fresh and FFPE livers ($r=0.944$, $p<0.001$). NanoString gene expression measurements were highly reproducible in repeat runs with different RNA input quantities ($r=0.946$-0.995, $p<0.001$), different operators ($r=0.949$-0.992, $p<0.001$), and different lots of reagents ($r=0.998$-0.999, $p<0.001$).

To see if gene signatures in liver biopsies can predict fibrosis progression, the 48-gene signature in FFPE clinical liver biopsies was analyzed in 299 patients with different liver diseases (122 patients with recurrent viral hepatitis C, 76 with autoimmune hepatitis, and 101 with NAFLD). Patients with a high 48-gene signature had a significantly higher probability of fibrosis progression compared to patients with a low 48-gene signature in all three liver diseases, but the probability of fibrosis progression was similar across different histological fibrosis stages. The results supported that the 48-gene signature can predict progressive fibrosis earlier than histology in different liver diseases.

For protein level validation, two of the genes in the 48-gene signature were analyzed by immunohistochemistry in 94 patients with available liver tissue after NanoString assay. The increase in mRNA expression of the two genes led to an increased expression of the corresponding protein. Patients with a high protein expression of the two genes had significantly higher probability of fibrosis progression compared to patients with a low protein expression.

The research presented in this thesis is the first comprehensive collection of a gene expression signature that drives advanced liver fibrosis in humans in the context of various

common causes of chronic liver disease. The 48-gene signature may serve as a prognostic biomarker for fibrosis progression in patients with different chronic liver diseases. This biomarker test can be easily implemented as a clinical assay.

Preface

This thesis is an original work by Mu Hao Hsu. The research project, of which this thesis is a part, received research ethics approval from the University of Alberta Research Ethics Board, Project Name "Molecular Assessment of Native and Transplant Livers", No. Pro00034669. For the liver samples from Toronto, pathological and clinical data were collected in compliance with local ethical and consent guidelines under approval by their institution and provided only deidentified clinical and pathological data and liver biopsy paraffin sections for this collaboration (CAPCR ID: 15-9479).

The experimental design referred in Chapters 2, 3, 4, 5, 6, and 7 were designed by me and my supervisor Dr. Banu Sis. The experiments in Chapters 2, 3, 4, 5, 6, and 7 were performed by me, unless otherwise stated. The immunohistochemistry experiments referred in Chapter 7 were performed by lab technicians at Alberta Health Services, Edmonton zone, immunohistochemistry lab. All data analyses in this thesis are my original work. Some of the research conducted for this thesis forms part of a research collaboration, led by Dr. Banu Sis at the University of Alberta. Clinical data of patients from Alberta referred in Chapters 3, 4, 5, 6, and 7 were collected by Dr. Aldo J. Montano-Loza and Dr. Ellina Lytvyak. Histopathological data of Alberta patients as well as their archived clinical liver biopsy paraffin blocks referred in Chapters 3, 4, 5, 6, and 7 were retrieved by Dr. Banu Sis and Dr. Jeffery Tompkins and staff of Anatomical Pathology Laboratory at the University of Alberta Hospital (Operational Approval #34817). The liver explants referred in Chapter 3 were collected by Dr. Andrew Mason's research laboratory at the University of Alberta. Clinical and histological data of patients from Toronto as well as the clinical liver biopsy paraffin

sections referred in Chapter 4 were retrieved by Dr. Oyedele Adeyi. No part of this thesis has been previously published.

Acknowledgements

The completion of this project would not have been possible without the support of a great number of people. I would like to thank first and foremost, my supervisor, Dr. Banu Sis, for her guidance and support throughout my Ph.D. studies. Her experience, knowledge, and brilliant approach to problem solving was greatly appreciated.

I am also extremely grateful to Dr. Sambasivarao Damaraju for guidance as a joint supervisor. Dr. Damaraju has taught me to think critically and pushed me to challenge myself.

Thank you to the members of my Supervisory Committee, Dr. Aldo J. Montano-Loza and Dr. Consolato Sergi for their input and the many relevant and exceptional suggestions and comments throughout this project.

I would also like to thank Reeda Gill and Kim Formenti. Thank you for teaching me all the bench works during my first year in the lab.

Last but not least, I would like to thank my wife Lifei Gu for her continued and unrelenting support. I would also like to thank my parents, Kuan-Tsung Hsu and Shun-Fen Chang, for their endless love, encouragement and support of my educational pursuits. Thank you all for being there for me, even during some of the more stressful times!

Table of Contents

List of Tables

List of Figures

List of Abbreviations

AIH: autoimmune hepatitis

ALD: alcoholic liver disease

ALT: alanine transaminase

ANA: anti-nuclear antibodies

ARFI: acoustic radiation force impulse imaging

ASK1: apoptosis signal-regulating kinase 1

AST: aspartate aminotransferase

AUROC: area under the receiver operator characteristic curve

BMI: body mass index

CI: confidence interval

CTGF: connective tissue growth factor

DAB: Diaminobenzidine

DCDC2: doublecortin domain containing 2

ECM: extracellular matrix

EPCAM: Epithelial cell adhesion molecule

EMT: epithelial-to-mesenchymal transition

EHF: ETS homologous factor

FDA: Food and Drug Administration

FFPE: formalin-fixed paraffin-embedded

FXR: Farnesoid X receptor

GGT: gamma-glutamyl transferase

HA: hyaluronic acid

HABP2: hyaluronan binding protein 2

HBV: viral hepatitis B

HCC: Hepatocellular carcinoma

HCV: viral hepatitis C

HIV: human immunodeficiency virus

HOMA-IR: homeostasis model assessment of insulin resistance

HPC: hepatic progenitor cell

HR: hazards ratio

HSC: hepatic stellate cell

HSP47: heat shock protein 47

IgG: immunoglobulin G

IHC: immunohistochemistry

INR: international normalized ratio

IQR: interquartile range

ITGBL1: integrin subunit β like 1

KRT7: keratin 7

LN: lobular necrosis

LOX: lysyl oxidase

LTBP2: latent transforming growth factor beta binding protein 2

MELD: model of end-stage liver disease

MMP: matrix metalloproteinase

MRE: magnetic resonance electrography

NAFL: non-alcoholic fatty liver

NAFLD: non-alcoholic fatty liver disease

NASH: non-alcoholic steatohepatitis

NPV: negative predictive value

OR: odds ratio

OSM: oncostatin M

PDGF: platelet-derived growth factor

PIIINP: type III procollagen

PMN: piecemeal necrosis

PNPLA3: patatin-like phospholipase domain containing 3

PPV: positive predictive value

PSC: primary sclerosing cholangitis

PLT: platelet

Ref: reference

RIN: RNA integrity number

ROC: receiver operator characteristic

SAA1: serum amyloid A1

SD: standard deviation

SERPINE2: serpin family E member 2

SMA: smooth muscle actin

SNP: single nucleotide polymorphism

SVR: sustained virological response

TGFβ: transforming growth factor-β

TIMP: tissue inhibitor of metalloproteinases

TM6SF2: the transmembrane 6 superfamily 2

TNF: tumor necrosis factor

ULN: upper limit of normal

Chapter 1: Literature Review

1.1 – The liver

1.1.1 – Gross anatomy and blood supply

The liver is the largest visceral organ that weighs about 1500 g (up to 2.5% of the total body weight in an average human adult) (1). It is located within the upper right quadrant of the abdominal cavity beneath the right hemidiaphragm. Anatomically, the liver is divided into two large lobes – the right and the left – and two smaller lobes, the quadrate and caudate (2). Functionally, the liver can be divided into eight segments based on Couinaud segmental classification (Figure 1.1) (3). Each liver segment has its own vascular inflow, outflow, and biliary drainage.

The liver is a very vascular organ that receives a dual blood supply by two main blood vessels in each segment: the hepatic artery and the portal vein, receiving approximately 25% and 75% from the total blood supply, respectively (4). The hepatic artery carries oxygenated blood that supplies the liver cells for aerobic respiration and the portal vein carries partially oxygenated blood and nutrients drained from the gastrointestinal tract and spleen (4). The hepatic artery and portal vein coalesce at the edge of the portal triad before draining into the hepatic sinusoids, which are low pressure vascular channels running between rows of hepatocytes, carrying blood from the terminal branches of the hepatic artery and portal vein to the terminal hepatic vein (central vein) (Figure 1.2). The central veins coalesce into hepatic veins that accumulate the blood leaving the liver and bring it to the heart.

1.1.2 – Histology

Microscopically, the liver is composed with tens of thousands of repeating functional

units that are uniformly distributed around the portal triads and central vein (Figure 1.2). The two most widely accepted functional unit structures are the hepatic lobule and hepatic acinus proposed by Kiernan and Rappaport, respectively (Figure 1.3) (5, 6).

The hepatic lobule is hexagonal that consist of hepatocytes and sinusoids radiating out in branches (Figure 1.2) (1). The central vein is found at the center of the lobule and the portal triads (contain portal venule, portal arteriole, and bile duct) are found at each corner of the hexagon. Compared with the hepatic lobule, hepatic acinus is more difficult to visualize. The hepatic acinus is a diamond shaped structure with the portal triads and central veins are at the periphery of the diamond (Figure 1.3) (6). The acinus can be subdivided into zones 1 (periportal), 2 (mediolobular), and 3 (centrilobular) with decreasing oxygenation and increasing susceptibility to ischemia and toxic injury.

1.1.3 – Metabolic functions

The liver is a metabolically active organ contributing to the following major functions (7):

- **Carbohydrate metabolism:** Carbohydrates are stored as glycogen in the liver that can be broken down into glucose and drained into the bloodstream to maintain normal glucose levels.
- **Bile production:** Bile is made by the liver that can be released to the small intestine to help break down and absorb cholesterol, fats, proteins, and fat-soluble vitamins (A, D, E, K).
- **Blood protein synthesis:** The liver is responsible for synthesizing coagulation factors, fibrinogen factors, albumin, complement proteins, and protease inhibitors.

- **Ammonia metabolism and urea synthesis:** A byproduct of amino acid catabolism is ammonia, which is toxic. The liver can convert ammonia into a less toxic substance called urea which is released into the bloodstream, and makes its way to the kidney and to be excreted as a component of urine.
- **Filters the blood (detoxification):** The liver is the organ for phase I (cytochrome p-450 mediated oxido-reduction reactions) and phase II enzyme mediated conjugation reactions; together, these cascade of reactions break down toxic substances such as alcohol, chemicals, heavy metals, and other drugs.
- **Storage:** The liver stores several substances that include iron, vitamins A, D, B9, and B12.

1.1.4 – Cells

The liver mass is composed of approximately 80% parenchymal cells and 20% non-parenchymal cells (8). Parenchymal cells are composed of hepatocytes and non-parenchymal cells are composed of hepatic stellate cells (HSCs), Kupffer cells (hepatic macrophages), sinusoidal endothelial cells, hepatic progenitor cells (HPCs), bile duct epithelial cells, and other rare cell types (e.g. pit cells) (8).

Hepatocytes

Hepatocytes are organized into sponge-like plates that separate sinusoidal blood from the bile duct (Figure 1.4) (1). They normally express keratin 9 and 18 and play pivotal function roles in metabolism, protein synthesis, and detoxification of substances absorbed into the blood aforementioned in section 1.1.3 (9). In the event of liver injury, hepatocytes are capable of natural regeneration. The regeneration is observed predominantly in the

periportal hepatocytes in mild injury and throughout the parenchyma in severe injury (10).

Hepatic stellate cells

HSCs, previously called lipocytes, perisinusoidal cells, or Ito cells, are located between the sinusoidal endothelial cells and hepatocytes (space of Disse) (Figure 1.4) (11). They represent about 10% of all resident liver cells (12). Under physiological conditions, HSCs maintain a quiescent phenotype and storage retinoids in lipid droplets (11). HSCs participate in angiogenesis, metabolism, and immune regulation. They are best known as a major source of liver fibrosis. The roles of HSCs in liver fibrosis are introduced in Chapter 1.4.1.

Kupffer cells

Kupffer cells are specialized macrophages in the liver that reside within the lumen of the liver sinusoids (Figure 1.4). The major function of Kupffer cells is to remove or phagocytose protein complexes, bacteria, senescent red blood cells, small particles, and cell debris from portal blood flow (13). Following liver infection or injury, Kupffer cells are activated and release an array of inflammatory mediators (e.g. interleukin-6, tumor necrosis factor alpha ([TNFα]) and reactive oxygen species (e.g. nitric oxide, superoxide) (14). These inflammatory mediators can stimulate activation of HSCs and promote liver fibrosis (15).

Sinusoidal endothelial cells

Sinusoidal endothelial cells represent the interface that separate blood cells on the one side and hepatocytes and HSCs on the other side (Figure 1.4). They represent the most abundant non-parenchymal cell population and play a role in filtration and endocytosis in the sinusoids (16).

- **Filtration:** Liver sinusoidal endothelial cells are comprised of pores, called fenestrations, which allow the transfer of macromolecules, lipoprotein, and water between the blood and the space of Disse, where they are taken up by the hepatocytes (17).
- **Endocytosis:** Liver sinusoidal endothelial cells have one of the highest endocytic capacity in the human body mediating clearance of soluble waste macromolecules and colloid materials (18).

Hepatic progenitor cells

HPCs are located in the periportal regions of the liver that show dual characteristics of both hepatocytes and bile duct epithelial cells (10). In severely injured livers where the proliferative capacity of hepatocytes is compromised, progenitor cells will be activated and repopulate the hepatocytes and bile duct epithelial cells (19).

Bile duct epithelial cells

Bile duct epithelial cells contribute to bile secretion via the net release of bicarbonate and water. Compared to hepatocytes, bile duct epithelial cells express keratin 7 and 19 in addition to keratin 8 and 18 (9). Following liver injury, bile duct epithelial cells proliferate and release fibrosis mediators including TNFα, transforming growth factor-β (TGFβ), platelet-derived growth factor (PDGF), connective tissue growth factor (CTGF), and interleukin-6 (20).

1.2 – Cirrhosis

Cirrhosis is a late stage of scarring (fibrosis) of the liver caused by many diseases and

conditions (21). It is the end-stage pathological phenotype of almost all chronic liver diseases, such as alcoholic liver disease (ALD), non-alcoholic fatty liver disease (NAFLD), viral hepatitis B (HBV), viral hepatitis C (HCV) infections, and autoimmune liver disease (22). Cirrhosis is a life-threatening condition that causes 1.03 million deaths per year worldwide (23). It is the number one cause of hepatocellular carcinoma (HCC) (24). Early diagnosis of advanced fibrosis/cirrhosis is difficult as most chronic liver diseases are asymptomatic until cirrhosis with clinical decompensation (ascites, variceal hemorrhage, hepatic encephalopathy, hepatorenal syndrome) occurs.

1.2.1 – Pathology of cirrhosis

Macroscopically, the surface of a cirrhotic liver is irregular with a firm consistency and multiple yellowish nodules on the external surface. Depending on the size of nodules, a cirrhotic liver can be classified into three macroscopic subtypes: micronodular (nodules <3mm), macronodular (nodules ≥3mm), and mixed patterns (contains both micro- and macro-nodules) (25). Common causes of micronodular cirrhosis include ALD and NAFLD, whereas macronodular cirrhosis is usually seen in chronic HBV and HCV (26).

Histologically, cirrhosis is characterized by regenerative nodules surrounded by fibrotic septa that bridge from portal to central (Figure 1.5) (27). These septa are not only simple areas of fibrosis but also contain also altered hepatic vascular architecture. When cirrhosis develops, a considerable portion of the blood bypasses hepatocytes and flow directly to the hepatic veins via the fibrovascular septa (28). As a result, xenobiotics are not completely removed from the circulation to the hepatocytes and vice-versa, blood protein, such as coagulation factors and albumin produced by the hepatocytes, do not enter the

circulation. This hepatic fibrovascular septa causes increased hepatic resistance and therefore results in portal hypertension and hepatic synthetic dysfunction.

1.2.2 – Regression of cirrhosis

Cirrhosis was considered as a terminal disease state that leads to death unless liver transplantation is done. However, several studies revealed histological evidence for regression of advanced liver fibrosis or even early cirrhosis after curing the underlying liver disease (29, 30). Therefore, if advanced liver fibrosis is predicted early and the cause is treated, early fibrosis can be reversed, and further damage can be limited. This means prevention of end-stage liver disease, HCC, and liver-related mortality. Currently, there is an unmet clinical need for early prediction of advanced liver fibrosis.

1.3 – Chronic liver disease

The burden of liver disease is rising in Canada and worldwide. Currently, there are more than two billion patients worldwide who suffer from chronic liver diseases, including over 8 million Canadians (every 1 in 4) (31-33). Chronic liver disease is a persistent, long-lasting condition that can be caused by different etiologies and involve a process of progressive damage and regeneration of the liver parenchyma (34). Most common causes worldwide are NAFLD, HBV, ALD, and HCV, with prevalence rates of 25.24%, 3.61%, 2.05% and 1.00%, respectively (31, 35-37). Other relatively rare causes include autoimmune hepatitis (AIH), primary biliary cholangitis, primary sclerosing cholangitis (PSC), drug-induced liver disease, and liver disease caused by ductal plate malformations (e.g. congenital hepatic fibrosis and Caroli disease). Despite different causes, advanced liver fibrosis is the

common final pathway, which eventually leads to cirrhosis and poor clinical outcomes (liver decompensation, HCC, need for liver transplantation, or liver-related death) (38).

1.3.1 – Non-alcoholic fatty liver disease

NAFLD is characterized by evidence of hepatic steatosis without secondary causes of hepatic fat accumulation (39). It is currently the most common chronic liver disease that affect over 25% of the population worldwide (31). Risk factors for advanced liver disease include obesity, type 2 diabetes, hyperlipidemia, hypertriglyceridemia, and hypertension (31). NAFLD is a spectrum of liver damage, ranging from simple fat accumulation (simple steatosis) to inflammation with or without fibrosis to cirrhosis (40). About 20-30% of patients with simple steatosis develop non-alcoholic steatohepatitis (NASH) and approximately 20% of patients with NASH progress to cirrhosis (41). Simple steatosis is defined as presence of ≥5% of hepatic steatosis with no or mild nonspecific inflammation (39). NASH is a progressive form of simple steatosis that is defined as presence of ≥5% of hepatitis steatosis, inflammation, and hepatocellular injury with varying degrees of fibrosis (39). Recent studies identified that among all histological features, fibrosis is the only and strongest predictor for poor clinical outcomes in patients with NAFLD (42, 43). Therefore, predicting advanced fibrosis at early disease stage is critical to prevent poor clinical outcomes.

1.3.2 – Chronic viral hepatitis B

Chronic HBV is a viral infection that attacks the liver. It is the second common chronic liver disease, affecting about 248 millions of individuals worldwide with a large regional variation (36). The Africa region and West Pacific region have the highest

prevalence of chronic HBV (range 5-9% of adults) and most were infected during infancy or at a young age (36). Countries in North America (Canada, USA, Mexico) have mostly low endemicity levels (0.2%-0.8%) (36). Risk factors for advanced liver disease include older age, male gender, alcohol consumption, elevated alanine aminotransferase (ALT) levels, high HBV DNA levels, and co-infection with HCV or human immunodeficiency virus (44). Approximately up to 40% of patients will progress to cirrhosis if untreated (45, 46). Chronic HBV infection can be divided into four phases: immunotolerance, HBeAg-positive immunoactive disease, HBeAg-negative inactive disease, and HBeAg-negative immunoactive disease (47). Patients in the immunotolerance and HBeAg-negative inactive phases are usually asymptomatic, whereas patients in the HBeAg-positive immunoactive and HBeAg-negative immunoactive phase can range from asymptomatic to cirrhosis with liver failure (47). Thus, several biomarkers are used in the clinic to determine the disease phase. These biomarkers include detecting the presence or absence of HBeAg and anti-HBe, HBV DNA level, and ALT level. However, none of these biomarkers are accurate to predict who is at high risk of progression to advanced fibrosis or poor clinical outcomes (48).

1.3.3 – Alcoholic liver disease

ALD results from excessive and long-term alcohol use and is characterized by the resulting spectrum of liver injuries ranging from simple steatosis to steatohepatitis with or without fibrosis to cirrhosis (49). It is the third common chronic liver disease that affect about 2% of the population worldwide (35). Risk factors for ALD include the amount of alcohol intake, gender (women are with a greater risk), obesity, and smoking (50). ALD can be categorized into three histological stages: (1) simple steatosis; (2) alcoholic hepatitis (steatohepatitis) with or without fibrosis; and (3) alcoholic hepatitis with advancedfibrosis

or cirrhosis (51). Up to 50% of patients who are diagnosed with alcoholic hepatitis will progress to cirrhosis if continue to drink alcohol (52, 53). However, abstinence from alcohol does not guarantee the stop of fibrosis progression. About 18% of patients with alcoholic hepatitis will still progress to cirrhosis after abstinence from alcohol (54). Therefore, there is a need to early predict patients early in the disease trajectory who are at high-risk of progression to advanced fibrosis/cirrhosis to prevent poor clinical outcomes.

1.3.4 – Chronic viral hepatitis C

Chronic hepatitis C is known as long-term infection with the hepatitis C virus. It is the fourth common chronic liver disease that affect about 252 thousand Canadians and over 70 million people worldwide (37, 55, 56). Risk factors for advanced liver disease include the duration of infection, age at infection, co-infection with hepatitis B or human immunodeficiency virus, alcohol consumption, and obesity (57). It was estimated about 20% of chronic HCV patients will develop liver cirrhosis and 5% will develop HCC within 20-30 years (58). Early diagnosis and antiviral treatment can prevent development of liver cirrhosis and liver-related complications. With the new direct-acting antiviral treatment, the rate of achieving sustained virological response (SVR) (virological cure) have tremendously increased from 50% to over 95% across all HCV genotypes with reduced side effects when compared to previously used interferon-based regimens (59). Most patients show reversal of liver fibrosis after SVR; however, a portion of patients (1%-14%) still progress to advanced fibrosis and cirrhosis despite achieving SVR (59). Predicting progressive fibrosis after SVR is still an unmet clinical need.

1.3.5 – Autoimmune hepatitis

AIH is an immune-mediated inflammatory liver disease characterized by hypergammaglobulinemia, presence of circulating autoantibodies, interface hepatitis on liver histology, and response to immunosuppression treatment (60). It is a rare chronic liver disease, with prevalence ranging from 15 to 25 cases per 100,000 people with large variance across different ethnicities (61). Patients are usually subscribed of immunosuppressive treatment to prevent progression of liver disease and the dosage of treatment should be adapted to the activity of the disease (61). A previous study reported fibrosis score decreased by 53% of treated AIH patients during a mean of 57 months of follow-up (62). However, another study reported cirrhosis develops in up to 40% in 10 years of follow-up despite of immunosuppressive treatment (63). Previous research had identified several common risk factors of fibrosis progression in AIH, including the presence of human leukocyte antigen DR3 and higher histology activity index (64). However, no single clinical variable is accurate to predict who is at high-risk for fibrosis progression at disease onset. Identifying high-risk patients can help guide clinical management to prevent fibrosis progression.

1.4 – Pathogenesis of liver fibrosis

Liver fibrosis is characterized by excessive accumulation of extracellular matrix (ECM), such as collagens, laminins, and elastins (65). Excessive deposition of ECM in the liver forms fibrotic scars. In a healthy liver, scar tissue removal (fibrolysis) and scar tissue deposition (fibrogenesis) are in balance. However, during chronic liver injury, the equilibrium between deposition and dissolution of scar tissues is disrupted, which leads to accumulation of scar tissue in the liver. The distribution of scar tissues in the liver differs in

different diseases. In chronic viral hepatitis and cholestatic disorders, the scar tissues are initially located around the portal tracts. In ALD and NAFLD, fibrosis is initially located in pericentral and perisinusoidal areas (66). As liver disease progresses and more scar tissues deposit in the liver, cirrhosis develops and eventually affect liver function. At this stage, the liver contains about 6 times more ECM proteins than a normal liver (38). These ECM proteins are composed of fibrillar collagens, elastins, fibronectins, undulins, hyaluronan, and proteoglycans (38). Cirrhosis is well-known as the final common pathway of chronic liver diseases. Moreover, the structural components of ECM, growth factors, chemokines, and cytokines, as well as central signaling cascades in fibrogenesis, are similar across other organs, such as lungs, hearts, and kidneys (67, 68). In the liver, it is yet unknown if there is a common molecular signature of progressive liver fibrosis that is shared by a variety of chronic liver diseases in humans.

1.4.1 – Cellular pathways of liver fibrogenesis

Multiple cells of the liver contribute to the deposition of ECM. The major matrix-producing cells in the liver are activated myofibroblasts, which are characterized by cells that express α-smooth muscle actin (SMA) (69). Activated HSCs are the major source of activated myofibroblasts (70). Other sources of myofibroblasts include portal fibroblasts, hepatocytes and bile duct epithelial cells undergoing epithelial-to-mesenchymal transition (EMT), and fibrocytes (70). Non-myofibroblastic fibrosis contributors include HPCs, sinusoidal endothelial cells, and macrophages.

Hepatic stellate cells

HSCs are non-proliferative and quiescent in a normal liver. Following liver injury,

increased hepatic levels of profibrogenic cytokines and chemokines such as TGFβ1 stimulate HSCs activation and cause quiescent HSCs transdifferentiate into myofibroblasts, which synthesize and deposit increasing amounts of ECM (65, 71). The major profibrogenic cytokines and chemokines that stimulate HSCs activation are reviewed in Chapter 1.4.2.

Portal fibroblasts

Portal fibroblast refers to any fibroblast in the portal region (72). In the normal liver, portal fibroblasts surround the portal vein to maintain the integrity of the portal tract (73). In response to chronic injury (mostly in biliary diseases), portal fibroblasts proliferate and differentiate into portal myofibroblasts, which is defined as any myofibroblast in the portal area that is not derived from HSCs and synthesize ECM (72, 73).

Epithelial-to-mesenchymal transition

Epithelial-to-mesenchymal transition (EMT) is a biological process in which adherent epithelial cells undergo multiple biochemical changes and convert to a mesenchymal cell phenotype (74). The mesenchymal cell phenotype is characterized by increased cell motility, invasiveness, and production of ECM components (74). Mesenchymal cells participate in tissue repair and pathological processes, which include tissue fibrosis, tumor invasiveness, and metastasis (75). Therefore, EMT occurs when tissues are being built or remodeled. It can be categorized into three different subtypes based on the biological context: embryogenesis and organ development (type 1); chronic fibrogenic disorders (type 2), and carcinogenesis (type 3) (76). During liver injury, liver epithelial cells undergo type 2 EMT and acquire myofibroblastic features that generate fibrosis (75). In the meantime, some epithelial-derived mesenchymal cells undergo mesenchymal-to-epithelial transition, which revert mesenchymal cells to normal hepatocytes or cholangiocytes and

result in fibrosis regression (75). EMT was proposed as one of the important mechanisms of fibrogenesis. However, the importance of EMT in liver fibrosis has been actively debated (75, 77, 78).

Fibrocytes

Fibocytes are circulating bone marrow-derived, spindle-like shape cells that have co-expression of progenitor and hematopoietic cell markers (79, 80). Following liver injury, fibrocytes downregulate the expression of hematopoietic markers and differentiate into α-SMA-expressing myofibroblasts that produce ECM proteins (79). Fibrocytes are involved not only in liver fibrosis but also in skin, lung, and kidney fibrosis (81).

Hepatic progenitor cells

HPCs, located within the canals of Hering, are bipotential adult stem-like cells that can differentiate to hepatocytes and cholangiocytes during liver injury (82). In a normal liver, HPCs are non-proliferative and quiescent. During liver injury, quiescent HPCs become activated and stimulate increased numbers of ductules (ductular reaction), which represent a regenerative response of the liver and these proliferating ductules express keratin 7 (83). Ductular reaction produces also profibrogenic factors, such as TGFβ, that exacerbate ECM deposition (84). Ductular reactions was found to be correlated with the severity of fibrosis in different chronic liver diseases, including chronic HCV (85), ALD (86), and NASH (83).

Sinusoidal endothelial cells

In response to liver injury, sinusoidal endothelial cells undergo morphological changes with significantly increased production of basement membrane proteins including type IV collagen, perlecan, entactin, and laminin (16). These proteins play an important role

in the capillarization of the sinusoids during liver injury (87). Capillarization is a process characterized by progressive loss of fenestrae and transformation to a vascular phenotype (87). This is an early event during liver injury that precedes activation of HSCs and macrophages and therefore suggesting it could be a preliminary step of fibrogenesis (88).

Macrophages

Macrophages are the largest non-parenchymal cell population in the liver. It is composed of Kupffer cells and circulating monocytes. These cells are involved in the pathogenesis of liver inflammation and fibrosis (89). During liver injury, macrophages become activated and phagocyte necrotic liver cells, which causes secretion of proinflammatory cytokines and chemokines such as TNF, TGFβ1, and PDGF (90). These cytokines and chemokines can stimulate HSCs transdifferentiate into activated myofibroblasts, which cause fibrosis deposition (91).

1.4.2 – Molecular pathways of liver fibrogenesis

The molecular processes driving liver fibrosis are wide-ranging and complex. Of all the molecular pathways that contribute to liver fibrosis, TGFβ is one of the major contributor (68). Other important molecular pathways that contribute to liver fibrosis include integrins, PDGF, CTGF, and vasoactive peptides such as angiotensin II and endothelin-1 (68).

TGFβ

TGFβ signaling is present in all phases of liver injury, from inflammation and fibrosis, to cirrhosis and cancer (92). It is secreted by inflammatory and fibrogenic effector cells, which include fibroblasts, fibrocytes, and myofibroblasts (93). TGFβ signaling shows its effects on fibrogenic effector cells by binding to TGFβ receptors on the cell surface and

the signal is transmitted through the membrane to activate SMAD transcription factors (68). Activated SMAD proteins induce transcription of profibrotic molecules (collagens, fibronectin, and α-SMA) and causes myofibroblast activation (92). Activation of myofibroblasts stimulate synthesis of ECM proteins and result in fibrosis progression (94).

Integrins

Integrins are a large family of cell surface receptors that mediate interactions between cells and ECM (95). These receptors can relay information from cell interior to ECM (inside-out signaling) and from ECM to cell interior (outside-in signaling) (96). Integrins consist of non-covalently linked α- and β-subunits that can form over 24 different combinations of subtypes (97). These different subtypes of integrins are differentially expressed by various liver cell types and some can contribute to liver fibrosis (97). For example, αvβ6 and αvβ8 integrins can activate TGFβ1, which is a strong regulator of ECM by HSCs, and cause enhanced matrix deposition (98). On the other hand, αvβ3 and αvβ5 integrins can upregulate ECM-degrading proteases matrix metalloproteinase (MMP) -2, -3, and -9 and result in enhanced matrix degradation. Clinical studies found abnormal expression of integrins in patients with different chronic liver diseases. In patients with HCV, the expression of α1, α5, α6, β1 integrins were significantly upregulated in histologically-proven advanced fibrosis when compared to no or mild fibrosis (99). The expression of β6 integrin was found to be significantly increased in patients with HBV, HCV, and ALD (100). These results showed integrins are involved in liver fibrosis regardless of the underlying etiology.

Platelet-derived growth factor

PDGF signaling plays an important role in activated HSCs and portal fibroblast proliferation (101). When the liver is injured, fibrotic mediators such as TGFβ and TNFα are

released and stimulate activation of PDGF and its receptor (102). The PDGF family is composed of four different polypeptide chains encoded by four different genes (PDGF-A, PDGF-B, PDGF-C, and PDGF-D) (103). These polypeptide chains can be assembled into five different disulphide-linked dimers (PDGF-AA, PDGF-AB, PDGF-BB, PDGF-CC, and PDGF-DD) (103). Of these isoforms, PDGF-BB is the major stimulus for HSCs and portal fibroblast proliferation, and the corresponding PDGFβ receptor is primarily involved in this cellular effect of PDGF (101).

Connective tissue growth factor

CTGF is a central mediator of tissue remodeling and fibrosis. It induces formation of myofibroblasts through transdifferentiation of stellate cells (104), portal fibroblast (105), and fibrocytes (106). CTGF also participates in myofibroblast activation and stimulate deposition of ECM proteins that leads to tissue remodeling and fibrosis (107). If the tissue remodeling happens in the blood vessels, it can create local portal hypertension and induce increased CTGF expression, which leads to more tissue remodeling (108). CTGF also induces increased expression of a variety of cytokines involved in liver fibrosis (109). These multiple positive feedback loops demonstrated CTGF is one of the central mediators of liver fibrogenesis.

Angiotensin II

Angiotensin II, a vasoconstrictor peptide, is the main effector of the renin-angiotensin system. The renin-angiotensin system regulates key steps in tissue remodeling through angiotensin type 1 receptors (110). During liver injury, the components of the renin-angiotensin system are expressed in myofibroblasts and generate angiotensin II (111). Angiotensin II can induce an array of fibrogenic actions in activated HSCs, including

myofibroblast proliferation, secretes fibrogenesis cytokines such as TGFβ1, and promotes collagen synthesis (112, 113).

Endothelin-1

Endothelin-1 is a vasoconstrictor peptide, which is produced by sinusoidal endothelial cells, with a potent effect on endothelin receptors. Endothelin receptors are present mostly in HSCs, but also in hepatocytes, sinusoidal endothelial cells, and Kupffer cells (114, 115). Endothelin-1 can induce activation of myofibroblasts from HSCs, portal fibroblasts, epithelial cells, and fibrocytes (116). A study revealed patients with cirrhosis have three times higher plasma endothelin-1 concentrations compared to patients without a liver disease (117). Cirrhotic patients have enhanced expression of endothelin receptors on HSCs and the expression is correlated to the degree of portal hypertension (118, 119). The enhanced concentration of endothelin-1 acts on endothelin-1 receptors on the HSCs and induces increased fibrosis deposition and intrahepatic sinusoidal resistance, which results in portal hypertension (120).

1.5 – Assessment of liver fibrosis

Current available methods for assessing liver fibrosis can be subcategorized into two main categories: (1) invasive technique (histopathological assessment of liver biopsy) and (2) non-invasive techniques (imaging tools and serological biomarkers).

1.5.1 – Histopathological assessment of liver biopsy

Histopathological assessment of liver biopsy has three major roles in clinical management: (1) for diagnosis, (2) for assessment of prognosis, and (3) to assist clinicians

in making therapeutic/clinical management decisions (121). This is currently the gold standard method to assess liver fibrosis (122). Biopsy samples are routinely scored by a pathologist using activity grading and fibrosis staging systems. There are several different proposed scoring systems for chronic liver diseases. The Metavir and Ishak systems are most commonly used for grading and staging viral hepatitis and autoimmune hepatitis (123, 124). The Metavir grade represents the degree of inflammation, which is evaluated by the combination of the degree of piecemeal necrosis (aka interface hepatitis) (scale 0-3) and lobular necrosis (scale 0-2) (Table 1.1). The Metavir stage represents the degree of fibrosis, which is scaled from 0 to 4. The Ishak system is a more complex system that grade the degree of inflammation scaled from 0 to 18 and fibrosis staging scaled from 0 to 6 (Table 1.2). NAFLD is usually scored by the NAFLD activity score and staging system (125). NAFLD activity score is the sum of the separate scores for steatosis (0-3), lobular inflammation (0-3) and hepatocellular ballooning (0-2). NASH is usually defined as patients having a NAFLD activity score of ≥5 (Table 1.3). NAFLD fibrosis stage scores fibrosis at a scale from 0 to 4 (Table 1.3).

Despite histological assessment of liver needle biopsy is the gold standard for assessing liver fibrosis, liver biopsy is an invasive procedure and has several limitations (126-128). It only represents 1/50,000 of the liver (129) and suffers from sampling variability and both inter- and intra-observer variability. According to previous studies, over 33% of biopsy samples from patients with HCV or NAFLD have discordance in fibrosis staging between different pathologists (130, 131). Even very large needle biopsy samples (>2.5cm) could not exceed 75% accuracy in assessing fibrosis in patients with HCV (127). More importantly, histology cannot accurately predict the risk of a patient for fibrosis progression

(132). The invasive nature and limitations of liver biopsy led to the development of non-invasive methods to assess liver fibrosis.

1.5.2 – Imaging methods

The most promising imaging methods for assessing liver fibrosis non-invasively are transient electrography (Fibroscan), acoustic radiation force impulse (ARFI) imaging and magnetic resonance electrography (MRE).

Fibroscan

Fibroscan was the first introduced ultrasound-based technique to measure liver stiffness in 2003 (133). It measures the velocity of a low-frequency (50Hz) elastic shear wave propagating through the liver and the velocity is directly related to liver stiffness. The results range from 2.5 to 75 kilopascals, with a normal value around 4-6 kilopascals and presence of advanced fibrosis or cirrhosis (Metavir fibrosis stage 3 or 4) >10-14 kilopascals (134, 135). A valid, accurate result is based on the median value of at least 10 validated measurements, with at least 60% of success rate (the ratio of valid measurements to the total number of measurement) and interquartile range (IQR) less than 30% of the median value (136). Fibroscan is currently the most widely used and best-validated technique for noninvasive assessment of liver fibrosis. However, liver stiffness measurement confounds with several factors such as obesity, inflammation, cholestasis, and congestion (137). Other important limitations of Fibroscan include it cannot discriminate intermediate stages of fibrosis and predict fibrosis progression (138). Although Fibroscan cannot reliably predict fibrosis progression, it is widely used to diagnose advanced fibrosis or cirrhosis in clinic.

Acoustic radiation force impulse imaging

ARFI assesses liver stiffness by evaluating the wave propagation speed through a region of interest in the liver using a ultrasound scanner with a conventional probe without external compression (139). The results are usually reported in meters per second, with advanced fibrosis >2.2 meters/second (135). ARFI has a significantly lower failure rate than Fibroscan (2.9% vs. 6.4%, $p<0.001$) and both have similar performance for advanced fibrosis and cirrhosis (138, 140). However, ARFI also cannot discriminate intermediate stages of fibrosis nor can predict fibrosis progression (138).

Magnetic resonance electrography

MRE assesses the whole liver stiffness by evaluating propagating mechanical shear waves using a conventional magnetic resonance system with added hardware to generate mechanical waves (141). The results are usually reported in kilopascals, with a normal value less than 3 kilopascals and presence of advanced fibrosis or cirrhosis > 5 kilopascals (135, 142). MRE has higher applicability for patients with ascites or obesity and has better performance to discriminate intermediate stages of fibrosis compared to Fibroscan (138). However, MRE is too costly and time consuming to be used in routine practice (138). It also cannot reliably predict fibrosis progression.

1.5.3 – Serum biomarkers

Current serum biomarkers algorithms adopted into the clinical setting for assessment of liver fibrosis usually include a combination of direct markers, which measure proteins related to scar tissue components (138), and indirect markers, which are simple biochemical tests that reflect disease severity and liver function (143). Many scores or algorithms have been proposed in different chronic liver diseases for staging liver fibrosis and they are

summarized in Table 1.4. Five are protected by patents and commercially available: the Enhanced liver fibrosis score, the Fibrometer, the Fibrotest, the FibroSpectII, and the Hepascore (Table 1.4). The advantages of serum biomarkers include high applicability, good inter-laboratory reproducibility, and potential widespread availability (non-patented) (144, 145). However, serum biomarkers cannot reliably predict fibrosis progression and have limitations such as not being liver-specific, inability to differentiate intermediate fibrosis stages, and confounder effect of liver inflammation and steatosis (146).

1.6 – Treatments of liver fibrosis

Despite many encouraging findings of effective antifibrotic drugs in preclinical models, currently, none were successfully translated and applied in clinic. The antifibrotic therapeutic approaches can be classified into four main categories: (1) control the underlying liver disease; (2) inhibit activation of fibrosis promoter cells; (3) inhibition of profibrogenic pathways; and (4) promote resolution of fibrosis (147). A list of antifibrotic clinical trials in liver fibrosis searched on ClinicalTrials.gov are summarized in Table 1.5. These clinical trials are most relevant to NAFLD, as this disease affects over 25% of the population worldwide and the role of underlying metabolic risk factors such as diabetes or hyperlipidemia are recognized but several yet undefined etiological factors contribute to the disease and hence a targeted therapy remain elusive.

1.6.1 – Control the underlying liver disease

Removing the cause of liver injury is the most effective way to prevent fibrosis progression. Previous published data have established that clearance of HCV, suppression of

HBV, alcohol abstinence in ALD, and reduced lipid synthesis, cholesterol, and triglycerides in NASH can prevent fibrosis progression and possibly lead to fibrosis regression (148, 149). This strategy can reverse fibrosis at all stages. However, not all patients cured from the underlying liver disease demonstrate fibrosis regression, especially patients with NAFLD due to metabolic diseases (i.e., diabetes) or cirrhosis. Reversal of cirrhosis depends on the duration the patient has cirrhotic liver, the cellularity of the scar, the degree of vascular remodeling, and the degree of collagen cross-linking (150). Therefore, drugs with direct therapeutic targets of liver fibrosis have been developed and several are currently being evaluated in clinical trials (Table 1.5).

1.6.2 – Inhibit activation of fibrosis promoter cells

During liver injury, multiple cells of the liver contribute to activation of myofibroblasts that stimulate fibrosis deposition. Activated HSCs are the primary source of liver myofibroblasts and therefore inhibit activation of HSCs is a key aspect to prevent fibrosis progression (65). Several antifibrotic drugs were developed to inhibit activation of HSCs such as Elafibranor, Pamrevlumab, and GR-MD-02 (Table 1.5) (107, 151, 152). These drugs can inhibit activation of HSCs and have other biological effects to reduce fibrosis. Elafibranor is a peroxisome proliferator-activated receptor-alpha and -delta agonist that has hepatoprotective effects by regulation of metabolic homeostasis, inflammation, and cell differentiation. This drug is currently in a phase III clinical trial for NASH (153). Pamrevlumab is a CTGF agonist that can reduce activation of HSCs and ECM deposition (107). GR-MD-02 is a Galectin-3 agonist that reduce inflammation, fibrosis and the number of galectin-3-positive macrophages (151).

1.6.3 – Inhibition of profibrogenic pathways

The major molecular pathways involved in fibrogenesis were discussed in Chapter 1.4.2. Drugs in this category include Selonsertib, Oltipraz, and BMS-986263 (Table 1.5). Selonsertib is an inhibitor of apoptosis signal-regulating kinase 1 (ASK1) that is currently in a phase III clinical trial for NASH. Activation of ASK1 mediates phosphorylation of c-Jun N-terminal kinase and p38 mitogen-activated kinase, which leads to hepatocyte apoptosis, hepatic inflammation, and myofibroblast activation (154). Oltipraz is a nuclear factor (erythroid-derived 2)-like 2 activator that inhibits TGFβ1 in activated HSCs (155). In a phase II clinical trial with HBV and HCV patients, Oltipraz decreases plasma TGFβ1, but no significant histological improvement in fibrosis (156). BMS-986263 is a vitamin A-coupled lipid nanoparticle containing a small interfering ribonucleic acid that inhibits the production of heat shock protein 47 (HSP47) in HSCs (157). Inhibition of HSP47 was discovered to inhibit collagen deposition and collagen fibril formation in preclinical models (158). This drug is currently in a phase II clinical trial recruiting patients that are cured of HCV with advanced liver fibrosis.

1.6.4 – Promote resolution of fibrosis

Promote resolution of fibrosis could be achieved by preventing collagen cross-linking. Cross-linking of collagen is largely mediated by lysyl oxidase-like molecule 2 (LOXL2) (159). Simtuzumab, a humanized monoclonal antibody targeting LOXL2, can promote the degradation of fibrosis in different preclinical models by preventing collagen cross-linking (160). This drug was further tested in advanced fibrosis patients with different chronic liver diseases (NASH, HCV, PSC) (Table 1.5). Despite the encouraging results in

the preclinical models, Simtuzumab was ineffective to reduce fibrosis in NASH, HCV, and PSC (161-163). This reflects inhibiting LOXL2 may be insufficient to reduce fibrosis as there are other LOX isoforms that may also mediate collagen cross-linkage (164).

1.7 – Molecular studies of liver fibrosis in humans

The understanding of molecular mechanisms underlying liver fibrosis has greatly advanced in the recent 20 years. These understandings led to the development of biomarkers to assess liver fibrosis and discovery of new antifibrotic drug targets. However, very limited findings in preclinical models were successfully translated and applied to the clinic. This is because there is lack of single, highly relevant animal model of human liver fibrosis (165). Commonly used rodent models such as CCL_4, common bile duct ligation, and methionine-choline-deficient diet are effective in establishing advanced fibrosis, but they do not faithfully represent key elements of fibrosis progression in humans. These models usually result in cirrhosis in a few weeks, whereas it takes years to decades for a patient with chronic liver disease to progress to cirrhosis, and the animal models do not simulate the comorbidities experienced by humans (166). Therefore, there is a need to understand if the molecular findings of liver fibrosis through access to highly annotated liver biopsy specimens from various stages of the disease trajectory and access to publicly available data sets help reanalyze different end points, not effectively addressed in the original study cohorts. Current methods of genome-wide transcriptomic and genome-wide association studies potentially offer a holistic approach to understand the heterogeneity and underlying biological mechanisms of liver fibrosis. Gene expression profiling and genetic association studies of sampled liver biopsies or blood samples at various stages of fibrosis may help delineate

mRNAs that are differentially expressed and reveal gene variants (single nucleotide polymorphism [SNP]). Several previous studies analyzed the global transcriptomic changes associated with fibrosis in human livers. However, most of them addressed only a single type of liver disease. Here, I will summarize the important findings of gene expression profiling and genetic variants of liver fibrosis in humans with chronic liver disease.

1.7.1 – Non-alcoholic fatty liver disease

Gene expression profiles of advanced fibrosis

The first gene expression profiling study to delineate the gene expression patterns of advanced fibrosis in NAFLD was conducted by Moylan et al. in 2014 (167). They used whole genome transcriptomics approach (Affymetrix microarrays) to characterize differentially expressed genes in liver needle biopsies between mild NAFLD (no or mild fibrosis, n=40) and severe NAFLD (advanced fibrosis, n=32). They identified a 64-gene expression signature that distinguishes NAFLD patients with advanced fibrosis from those with no or mild fibrosis, with 93% accuracy for histology-proven advanced fibrosis. This 64-gene signature was validated in a second, independent cohort (n=17), with 82.4% accuracy for histology-proven advanced fibrosis. Limitation of this study was they had a small validation set and their findings were not yet replicated by other groups, nor does these findings address other liver diseases culminating in fibrosis.

Genetic variants of advanced fibrosis

In 2008, Romeo and colleagues analyzed the association between 9229 coding SNPs and liver steatosis in 2111 adults of diverse ethnicities (168). They discovered a strong association between a common non-synonymous polymorphism (rs738409 C>G) in the

patatin-like phospholipase domain containing 3 (PNPLA3) and NAFLD. This finding was replicated by several other groups and they extended the association of this SNP to NASH, fibrosis, and cirrhosis. (169-173). This finding was one of the most robust discoveries in the field of genetic predisposition of cirrhosis in NAFLD. Later in 2014, Kozlitina et al. did an exome-wide association study and analyzed the association of 138,374 SNPs and hepatic triglyceride content in 2,736 adults of diverse ethnicities (174). They verified the sequence variant of PNPLA3 (rs738409) and discovered a new common non-synonymous polymorphism (rs58542926 c.499 C>T) in the transmembrane 6 superfamily 2 (TM6SF2) was strongly associated with hepatic triglyceride content. This discovery was replicated by Liu et al. and they found this variant was also associated with fibrosis progression in NAFLD (175).

Despite the strong and reproducible association between these two gene variants and advanced fibrosis in patients with NAFLD, whether these markers can serve as a potential predictor for advanced fibrosis in clinical practice is unknown. The strong association between gene variants and advanced fibrosis was based on an odds ratio (OR) greater than 2 per risk allele, which is a prominent magnitude for a common variant (176). However, large ORs do not necessarily assure that the variants are clinically relevant, nor a single variant associated with disease can explain the multitude of phenotypes associated with the polygenic disease (177). The premise of SNP association studies is that multiple variants, each conferring a small but finite risk with disease or phenotype may eventually help explain the heritable basis for risk but do not address the environmental factors nor the gene-environmental interactions in conferring the risk. The SNP based association studies help identify hitherto unidentified and uncharacterized genes in capturing the heritable component

of the disease. Population based SNP association studies and fine mapping of disease loci may help identify the causal gene(s) in polygenic diseases which are not amenable to linkage or pedigree-based association studies which are appropriate for monogenic diseases. Therefore, other classification parameters such as sensitivity, specificity, positive predictive value (PPV), negative predictive value (NPV), and area under the receiver operator characteristic curve (AUROC) are needed to test the predictive value of a genetic variant (177, 178). Moreover, since NAFLD as explained above is a multisystem disease, and it is unlikely that two SNPs alone can accurately predict advanced fibrosis in all patients (179). Combination of other genetic variants and environmental factors are needed to generate a good predictive model. Danford and colleagues used a combination of age, genetic variants of PNPLA3 and TM6SF2, and insulin resistance to build a model for advanced fibrosis using 177 NAFLD patients with various fibrosis stages (180). The model had an AUROC of 0.82 for advanced fibrosis.

1.7.2 – Chronic viral hepatitis B

Gene expression profiles of advanced fibrosis

Wang and colleagues conducted a gene expression profiling study to identify differentially expressed genes in HBV patients with various fibrosis stages (181). They found the expression of integrin subunit β like 1 (ITGBL1) (R^2=0.51, p<0.001), doublecortin domain containing 2 (DCDC2) (R2=0.49, p<0.001), platelet-derived growth factor D (R^2=0.48, p<0.001), and ETS homologous factor (EHF) (R^2=0.48, p<0.001) were significantly correlated with histological fibrosis stages. However, the diagnostic performance of these genes for advanced fibrosis or cirrhosis were not reported.

Genetic variants of advanced fibrosis

Despite a remarkable progress in understanding the natural history of chronic HBV, the host genetic factor(s) associated with fibrosis progression of chronic HBV are not well addressed. Eslam and colleagues conducted a large cohort of study that included 555 chronic HBV patients and they discovered SNP (rs12979860) in the intronic region of interferon-λ4 was significantly associated with progression to advanced fibrosis (182). However, the results have not yet been replicated by other groups and the predictive performance of this SNP for fibrosis progression is currently unknown.

1.7.3 – Alcoholic liver disease

Gene expression profiles of advanced fibrosis

The first gene expression profiling study to delineate gene expression patterns of advanced fibrosis in ALD was conducted by Seth et al. in 2003 (183). They used preselected genes represented on human 6K cDNA glass microarrays and not whole genome array to characterize differentially expressed genes in liver biopsies between non-diseased donor livers (n=7) and explant ALD cirrhotic livers without other liver diseases (n=7). They discovered several fibrotic associated genes (α-SMA, collagen type IV, CTGF, tissue inhibitor of metalloproteinase 2 [TIMP2]) were significantly up-regulated in cirrhotic livers. As these differentially expressed genes were generated by comparing between biopsies with very extreme phenotypes, it is unknown if these genes are applicable for advanced fibrosis in patients with ALD.

Genetic variants of advanced fibrosis

In 2009, Tian and colleagues conducted a large candidate gene study in 1221 heavy

drinkers at various stages of ALD (184). They found rs738409[G] in PNPLA3 was strongly associated with alcoholic cirrhosis. This association was further replicated in other independent cohorts of patients with ALD (185, 186). In 2015, Buch et al. conducted a genome-wide association study comparing 1426 heavy drinkers without liver injury to 712 patients with alcoholic cirrhosis (187). They confirmed PNPLA3 and identified TM6SF2 polymorphism, the same loci in NAFLD, were associated with alcoholic cirrhosis. Despite the strong and reproducible association between these two gene variants and cirrhosis in patients with ALD, whether these markers can serve as a potential predictor for advanced fibrosis or cirrhosis in clinical practice is unknown.

1.7.4 – Chronic viral hepatitis C

Gene expression profiles of advanced fibrosis

In 2003, Smith and colleagues conducted the first gene expression profiling study to identify differentially expressed genes between HCV-infected cirrhotic liver explants (n=8) and non-diseased livers (n=4) (188). In this limited sample size, they found 87 genes were significantly upregulated in cirrhosis and these genes were mostly involved in ECM remodeling, activated lymphocytes and macrophages. As the genes were generated by comparing between biopsies with extreme phenotypes, the performance of these genes for advanced fibrosis in patients with HCV is unknown.

Later in 2006, Smith and colleagues conducted another gene expression profiling study analyzing liver tissues from 13 liver transplant patients (11 infected and 2 uninfected with HCV) and identified fibrotic genes by comparing patients with and without fibrosis progression (189). They identified 21 genes were upregulated in patients who had fibrosis

progression compared to non-progressors in the first-year post-transplantation. Of the 21 genes, 15 were encoded for markers of myofibroblasts and myofibroblast cells. Their data suggest that early fibrosis progression may be associated with a reduction of quiescent HSCs and increased number of myofibroblast-like cells. Due to the small sample size and lack of independent replication of findings, the performance of these genes for fibrosis progression is unknown.

Genetic variants of advanced fibrosis

Variants in the PNPLA3 region were also analyzed in patients with HCV. A significant association of rs738409[G] with advanced fibrosis were found in several European cohorts after adjustment for other known environmental factors (190-192). Despite the strong association of PNPLA3 variant with fibrosis, the performance of this variant for advanced fibrosis in HCV is unknown.

In 2006, Huang and colleagues analyzed 24,832 putative functional SNPs in 916 patients with HCV from two centers (193). They identified a missense SNP in DEAD box polypeptide 5 gene was associated with an increased risk of advanced fibrosis in both cohorts (OR=1.8 and 2.0). Moreover, they found a carnitine palmitoyltransferase gene was associated with a decreased risk of advanced fibrosis in both centers (OR=0.3 and 0.6). However, no classification parameters were reported in this study. Later in 2007, Huang et al. identified and validated a seven-gene cirrhosis risk score (seven SNPs combined into a scoring system) is strongly associated with progression to cirrhosis in patients with HCV, with 0.75 and 0.73 of AUROC in the training cohort (n=420) and an independent validation cohort (n=154), respectively (194). The seven-gene cirrhosis risk score was further validated in 271 HCV patients with initially no or minimal to moderate fibrosis and the patients were

follow-up for at least 60 months (195). They found the mean seven-gene cirrhosis risk score was significantly higher (p=0.005) in patients with fibrosis progression compared to patients without fibrosis progression. However, this study did not report the classification performance of the seven-gene cirrhosis risk score for fibrosis progression.

1.7.5 – Autoimmune hepatitis

Several candidate genetic-association studies were performed in patients with AIH, mostly focused on predicting treatment outcomes or identifying gene variants associated with AIH (196-199). One study found a SNP in the FAS gene at position -670 was associated with cirrhosis at presentation (197). This study analyzed 149 AIH patients with 179 matched controls, patients with adenosine/adenosine or adenosine/guanine genotypes had a higher prevalence of cirrhosis at presentation than in those with the guanine/guanine genotype (29% vs 6%). However, the results have not yet been replicated.

1.8 – Thesis overview and objectives

1.8.1 – Rationale

Liver fibrosis causes significant morbidity and mortality worldwide. Liver damage due to a variety of etiologies may result in advanced fibrosis, which is the common final pathway of different chronic liver diseases. Furthermore, advanced liver fibrosis is the major prognostic factor driving poor clinical outcomes. However, the natural history of fibrosis progression varies, with a high degree of heterogeneity among patients. The factors that drive this diversity are unknown. It is also unclear if there is a common molecular signature of progressive liver fibrosis independent of its etiology. Understanding the common molecular

signature of progressive liver fibrosis can help to develop a surrogate biomarker test to accurately identify patients that are at high-risk for progressive fibrosis. This biomarker test can identify patients who may benefit from drug treatments to prevent further liver damage and poor clinical outcomes. Stratification of patients who are at high-risk for progressive liver fibrosis by incorporating molecular biomarkers may help better clinical trial designs. This thesis aims to identify a common molecular signature associated with advanced fibrosis that is shared by different chronic liver diseases in humans, and to translate this knowledge to develop a surrogate biomarker test for clinical use.

1.8.2 – Hypothesis

Biological mechanisms underlying liver fibrosis induce a common multiple gene expression signature in human livers and quantitative measurement of this multigene signature in liver biopsy tissues identifies fibrosis progression and poor clinical outcomes in patients with chronic liver disease.

1.8.3 – Objectives

To test the hypothesis, this research proposes five specific objectives:

1. To discover and validate a molecular fibrosis signature in fresh human liver tissues with a variety of chronic liver diseases by genome-wide microarrays.

   This topic is covered in **Chapter 2**, wherein I studied publicly available genome-wide Affymetrix microarrays of fresh human liver tissues with different chronic liver diseases and various fibrosis stages to discover and validate a common molecular signature for advanced liver fibrosis.

2. To translate and validate the molecular signature in formalin-fixed paraffin-embedded (FFPE) liver needle biopsies using the NanoString platform.

   This topic is covered in **Chapter 3**, wherein I analyzed the feasibility of gene expression analysis in FFPE liver needle biopsies on NanoString and compared the measured gene expression between paired fresh and FFPE biopsies.

3. To investigate if the molecular fibrosis signature can identify progressive fibrosis in patients with different chronic liver diseases.

   This topic is covered in **Chapters 4, 5, and 6**, wherein the molecular fibrosis signature was used to predict progressive fibrosis in patients with recurrent HCV, AIH, and NAFLD, respectively.

4. To investigate if the molecular fibrosis signature can predict poor clinical outcomes in patients with different chronic liver diseases.

   This topic is covered in **Chapters 4, 5, and 6**, wherein the molecular fibrosis signature was used to predict poor clinical outcomes in patients with recurrent HCV, AIH, and NAFLD, respectively.

5. To analyze if the protein expression of the molecular fibrosis signature can predict progressive fibrosis and poor clinical outcomes.

   This topic is covered in **Chapter 7**, wherein the protein expression of the molecular fibrosis signature was measured in liver biopsies with recurrent HCV, AIH, and NAFLD that were included in **Chapters 4, 5, and 6**, respectively.

Table 1.1. Metavir grading and staging system

Activity grade		Fibrosis stage	
A0	PMN=0 and LN=0	F0	No fibrosis
A1	PMN=0 and LN=1	F1	Portal fibrosis without septa
	PMN=1 and LN=0-1		
A2	PMN=0 and LN=2	F2	Portal fibrosis with rare septa
	PMN=1 and LN=2		
	PMN=2 and LN=0-1		
A3	PMN=2 and LN=2	F3	Numerous septa without cirrhosis
	PMN=3 and LN=0-2		
		F4	Cirrhosis

PMN, piecemeal necrosis: 0, none; 1, mild; 2, moderate; 3, severe; LN, lobular necrosis: 0, no or mild; 1, moderate; 2, severe; A, histological activity grade: 0, none; 1, mild; 2, moderate; 3, severe. Reference (123).

Table 1.2. Ishak grading and staging system

Activity grade	Fibrosis stage
Periportal or periseptal interface hepatitis	**Stage 0**
Absent: 0	No fibrosis
Mild (focal, few portal areas): 1	
Mild/moderate (focal, most portal areas): 2	**Stage 1**
Moderate (continuous around <50%): 3	Fibrous expansion of some portal areas,
Severe (continuous around >50%): 4	with or without short fibrous septa
Confluent necrosis	
Absent: 0	**Stage 2**
Focal: 1	Fibrous expansion of most portal areas,
Zone 3 necrosis in some areas: 2	with or without short fibrous septa
Zone 3 necrosis in most areas: 3	
Zone 3 necrosis + occasional P-C bridging: 4	**Stage 3**
Zone 3 necrosis + multiple P-C bridging: 5	Fibrous expansion of most portal areas,
Panacinar or multiacinar necrosis: 6	with occasional P-P bridging
Focal lytic necrosis, apoptosis and focal inflammation	**Stage 4**
Absent: 0	Fibrous expansion of most portal areas,
One focus or less per 10X objective: 1	with marked P-P and P-C bridging
Two to four foci per 10X objective: 2	
Five to ten foci per 10X objective: 3	**Stage 5**
More than ten foci per 10X objective: 4	Marked P-P and P-C bridging with
Portal inflammation	occasional nodules
None: 0	
Mild, some or all portal areas: 1	**Stage 6**
Moderate, some or all portal areas: 2	Cirrhosis
Moderate/marked, all portal areas: 3	
Marked, all portal areas: 4	

P-C, portal to central. P-P, portal to portal. Reference (124).

Table 1.3. NAFLD activity scoring and fibrosis staging system

Activity score	Fibrosis stage
Steatosis <5%: 0 5-33%: 1 34-66%: 2 >66%: 3	**Stage 0** No fibrosis
Lobular inflammation None: 0 <2: 1 2-4: 2 >4: 3	**Stage 1** Zone 3 perisinusoidal fibrosis • Mild: 1a • Moderate: 1b • Portal/periportal: 1c
Hepatocyte ballooning None: 0 Few ballooned cells: 1 Many ballooned cells: 2	**Stage 2** Both perisinusoidal and portal/ periportal fibrosis
NAFLD activity score (sum of steatosis, lobular inflammation, and hepatocyte ballooning) <3: not NASH ≥5: NASH	**Stage 3** Bridging fibrosis
	Stage 4 Cirrhosis

Reference (125).

Table 1.4. Serum biomarkers for assessing liver fibrosis

Name	Formula	Etiology	Ref
AST to platelet ratio	AST (ULN)/PLT (10^9/L) x100	HCV	(200)
BARD score	(BMI ≥28 = 1; AST/ALT ratio ≥0.8 = 2; diabetes = 1; score ≥2, odds ratio for advanced fibrosis = 17)	NAFLD	(201)
Enhanced liver fibrosis score	Patented formula combining age, hyaluronate, MMP3, and TIMP1	Mixed	(202)
Fibroindex	1.738-0.064 x PLT (10^9/mm^3) + 0.005 x AST (IU/L) + 0.463 x (gamma globulin [g/dl])	HCV	(203)
Fibrometer	Patented formula combining PLT, prothrombin index, AST, α-2-macroglobulin, hyaluronate, urea, and age	Mixed	(204)
Fibrosis probability index	10.929 + (1.827 x ln[AST]) + (0.081 x age) + (0.768 x past alcohol use*) + (0.385 x HOMA-IR) – (0.447 x cholesterol)	HCV	(205)
Fibrotest	Patented formula combining α-2-macroglobulin, γGT, apolipoprotein A1, haptoglobin, total bilirubin, age and gender	HCV	(206)
FibroSpectII	Patented formula combining α-2-macroglobulin, hyaluronate and TIMP-1	HCV	(207)
FIB-4	age (year) x AST (U/L)/(PLT (10^9/L) x (ALT [U/L])$^{1/2}$	HIV-HCV	(208)
Forns index	7.811 – 3.131 x ln(PLT) + 0.781 x ln(GGT) + 3.467 x ln(age) – 0.014 x (cholesterol)	HCV	(209)
Goteborg university cirrhosis index	AST x prothrombin – INR x 100/PLT	HCV	(210)
HALT-C model	-3.66 – 0.00995 x PLT (10^3/ml) + 0.008 x serum TIMP-1 + 1.42 x log(hyaluronate)	HCV	(211)
Hepascore	Patented formula combining bilirubin, GGT, hyaluronate, α-2- macroglobulin, age and gender	HCV	(212)
Hui score	3.148 + 0.167 x BMI + 0.088 x bilirubin – 0.151 x albumin – 0.019 x PLT	HBV	(213)
Lok index	-5.56 – 0.0089 x PLT (10^3/mm^3) + 1.26 x AST/ALT ratio = 5.27 x INR	HCV	(214)
NAFLD fibrosis score	-1.675 + 0.037 x age (year) + 0.094 x BMI (kg/m2) + 1.13 x IFG/diabetes (yes = 1, no = 0) + 0.99 x AST/ ALT ratio – 0.013 x PLT (x10^9/L) – 0.66 x albumin (g/dl)	NAFLD	(215)
MP3	0.5903 x log(PIIINP [ng/ml]) – 0.1749 x log(MMP-1 (ng/ml)	HCV	(216)
SHASTA index	-3.84 + 1.70 (1 if HA 41-85 ng/ml, 0 otherwise) + 3.28 (1 if HA >85 ng/ml, 0 otherwise) + 1.58 (albumin <3.5 g/dl, 0 otherwise) + 1.78 (1 if AST	HIV-HCV	(217)

	>60 IU/L, 0 otherwise)		
Zeng score	-13.995 + 3.220 log(α-2-macroglobulin) + 3.096 log(age) + 2.254 log(GGT) + 2.437 log(hyaluronate)	HBV	(218)

* Graded as 0-2.

Abbreviations: AST, aspartate aminotransferase; ALT, alanine transaminase GGT, gamma-glutamyl transferase; HA, hyaluronic acid; HIV, human immunodeficiency virus; HOMA-IR, homeostasis model assessment of insulin resistance; INR, international normalized ratio; MMP, matrix metalloproteinase; PIIINP, type III procollagen; PLT, platelet; Ref, reference; TIMP, tissue inhibitor of metalloproteinases.

Table 1.5. Selected antifibrotic trials registered at ClinicalTrials.gov

Drug (drug trial identifier)	Drug target (drug mechanism)	Type of disease (phase)	N of patients in trial	Drug trial results	Antifibrotic strategy
Candesartan (NCT00990639)	Angiotensin II receptor, type 1 (AGTR1 inhibitor)	ALD (1/2)	85	Improvement in fibrosis (219)	Inhibit activation of fibrosis promoter cells
Losartan (NCT01051219, NCT00298714)	Angiotensin II receptor, type 1 (AGTR1 inhibitor)	NASH (3)	45	Recruited insufficient patients (220)	Inhibit activation of fibrosis promoter cells
		HCV (4)	20	No change in fibrosis (221)	
Irbesartan (NCT00265642)	Angiotensin II receptor, type 1 (AGTR1 inhibitor)	HCV (3)	166	Pending	Inhibit activation of fibrosis promoter cells
Timolumab (NCT02239211)	Amine oxidase copper containing 3 (AOC3 inhibitor)	PSC (2)	41	Pending	Inhibit activation of fibrosis promoter cells
Cenicriviroc (NCT03028740)	C-C Motif chemokine receptor 2,5 (CCR2/CCR5 inhibitor)	NASH (3)	2000	Pending	Inhibit activation of fibrosis promoter cells
Pamrevlumab (NCT01217632)	Connective tissue growth factor (CTGF inhibitor)	HBV (2)	114	Pending	Inhibit activation of fibrosis promoter cells
BMS-986036 (NCT03486899, NCT03486912)	Fibroblast growth factor 21 (analogue of FGF21)	NASH (2)	160	Pending	Control the underlying liver disease
		NASH (2)	100	Pending	
Tropifexor (NCT03517540)	Farnesoid X receptor (FXR agonist)	NASH (2)	200	Pending	Control the underlying liver disease
Obeticholic acid (NCT01265498, NCT02548351)	Farnesoid X receptor (FXR agonist)	NASH (2)	283	Improvement in fibrosis (222)	Control the underlying liver disease
		NASH (3)	2370	Improvement in fibrosis (223)	
GR-MD-02 (NCT02421094, NCT02462967)	Galectin 3 (LGALS3 inhibitor)	NASH (2)	30	Pending	Inhibit activation of fibrosis promoter cells
		NASH (2)	162	Pending	
Simtuzumab (NCT01672866, NCT01672879, NCT01707472, NCT01672853)	Lysyl oxidase-like molecule 2 (LOXL2 inhibitor)	NASH (2)	222	No change in fibrosis (161)	Promote resolution of fibrosis
		NASH (2)	259	No change in fibrosis (161)	
		HCV (2)	18	No change in fibrosis (162)	
		PSC (2)	235	No change in fibrosis (163)	
Selonsertib (NCT02466516, NCT03449446, NCT03053063, NCT03053050)	Apoptosis signal-regulating kinase 1 (ASK1 inhibitor)	NASH (2)	72	Improvement in fibrosis (154)	Inhibition of profibrogenic pathway
		NASH (2)	350	Pending	
		NASH (3)	883	Pending	
		NASH (3)	808	Pending	

Oltipraz (NCT00956098)	Nuclear factor (erythroid-derived 2)-like 2 (NFE2L2 activator)	HBV and HCV (2)	81	No change in fibrosis (156)	Inhibition of profibrogenic pathway
Elafibranor (NCT02704403)	Peroxisome oroliferator activated receptor alpha and delta (PPARA and PPARD agonist)	NASH (3)	2000	Pending	Inhibit activation of fibrosis promoter cells
Farglitazar (NCT00244751)	Peroxisome proliferator activated receptor gamma (PPARG agonist)	HCV (2)	265	No change in fibrosis (224)	Inhibit activation of fibrosis promoter cells
Aramchol (NCT02279524)	Stearoyl-CoA desaturase-1 (SCD inhibitor)	NASH (2/3)	247	Pending	Control the underlying liver disease
Volixibat (NCT02787304)	Solute carrier family 10 member 2 (SLC10A2 inhibitor)	NASH (2)	197	Pending	Control the underlying liver disease
BMS-986263 (NCT03420768)	Heat shock protein 47 (HSP47 inhibitor)	HCV (2)	165	Pending	Inhibition of profibrogenic pathway
Metadoxine (NCT02541045)	5-Hydroxytryptamine receptor 2B (5-HT2B inhibitor)	NASH (3)	108	Suspended (lack of finance resources)	Control the underlying liver disease

Abbreviations: ALD, alcoholic liver disease; HBV, hepatitis B virus; HCV, hepatitis C virus; NAFLD, non-alcoholic fatty liver disease NASH, non-alcoholic steatohepatitis; PSC, primary sclerosing cholangitis.

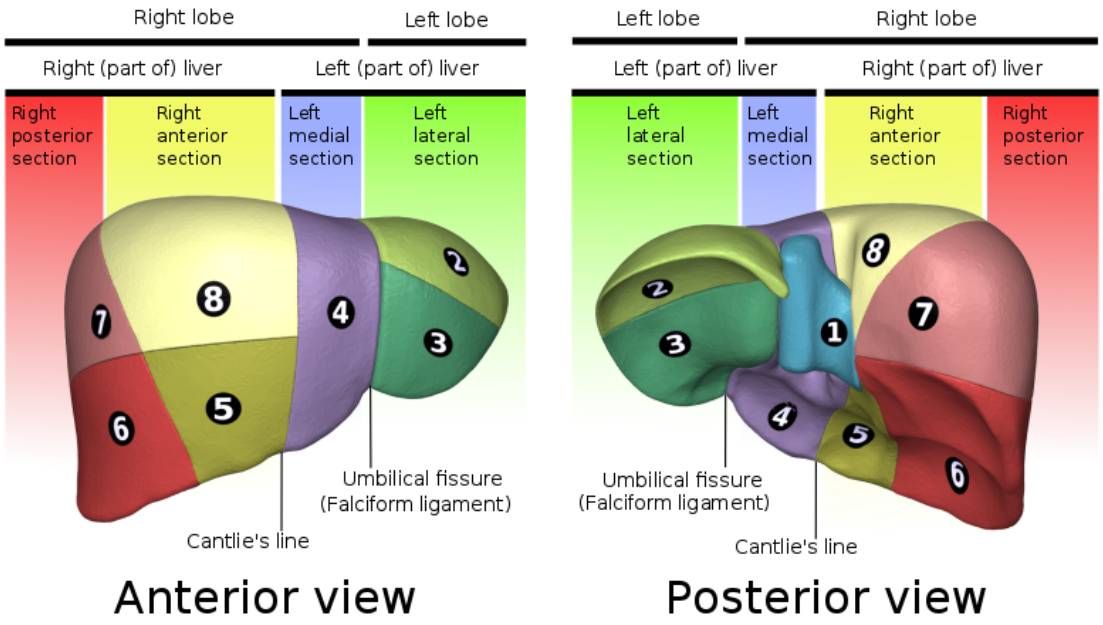

Figure 1.1. Couinaud classification of the liver.

Reprinted from BodyParts3D/Anatomography (https://lifesciencedb.jp/bp3d/) generated by Database Center for Life Science (https://dbcls.rois.ac.jp/index-en.html). This figure is licensed under Creative Commons Attribution-ShareAlike 2.1 Japan (https://creativecommons.org/licenses/by-sa/2.1/jp/deed.en).

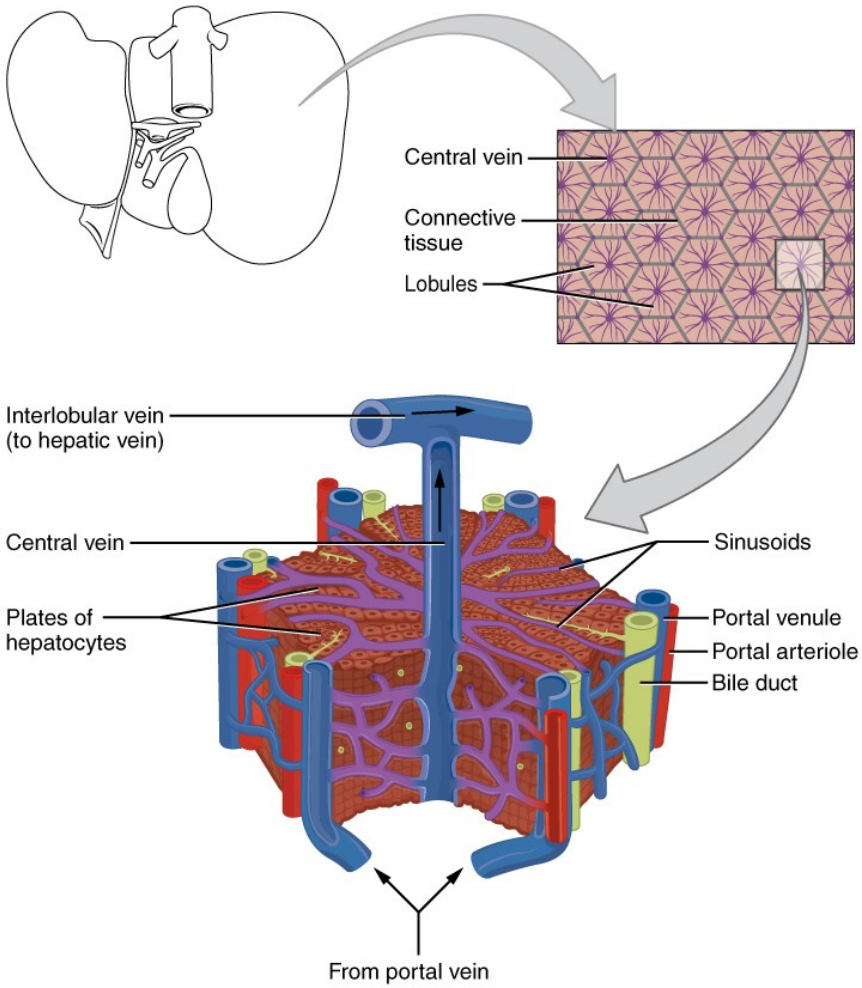

Figure 1.2. Microscopic anatomy of the liver.
Reprinted from Figure 23.25, Anatomy & Physiology, connexions web site (https://openstax.org/details/books/anatomy-and-physiology) by OpenStax College (https://cnx.org/). This image is licensed under Creative Commons Attribution v4.0 (https://creativecommons.org/licenses/by/4.0/).

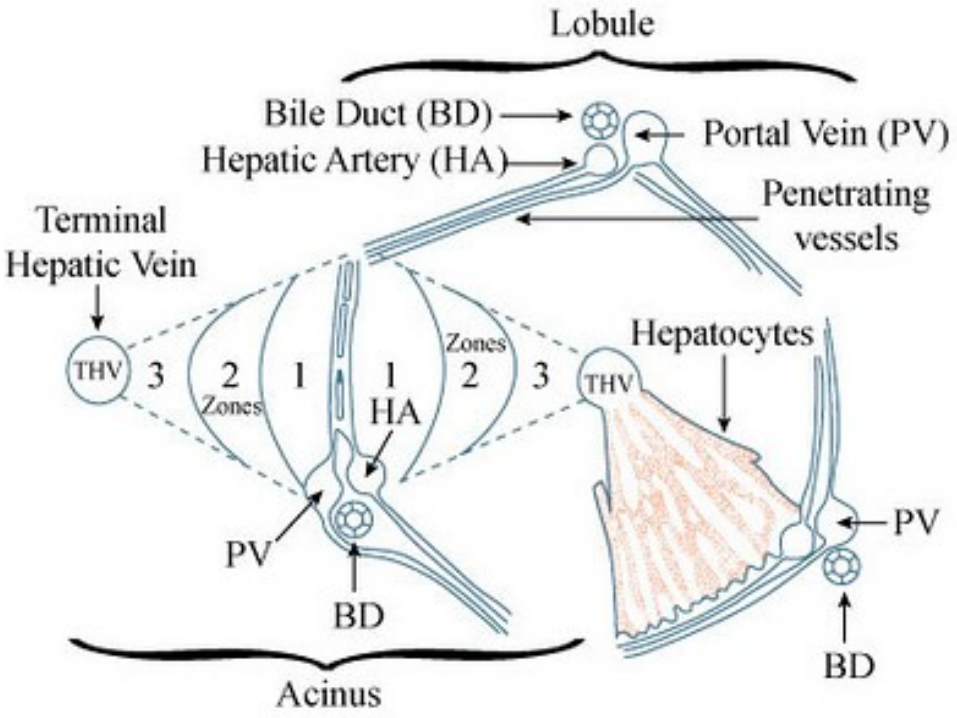

Figure 1.3. Schematic diagram of hepatic lobule and hepatic acinus.
"Schematic of liver operational units: the classic lobule and the acinus", is reprinted from 20.201 Mechanisms of Drug Actions, Fall 2005 by MIT OpenCourseWare (https://www.flickr.com/photos/mitopencourseware/3694426132). This is licensed under Creative Commons Attribution-NonCommercial-ShareAlike v4.0 (https://creativecommons.org/licenses/by-nc-sa/4.0/).

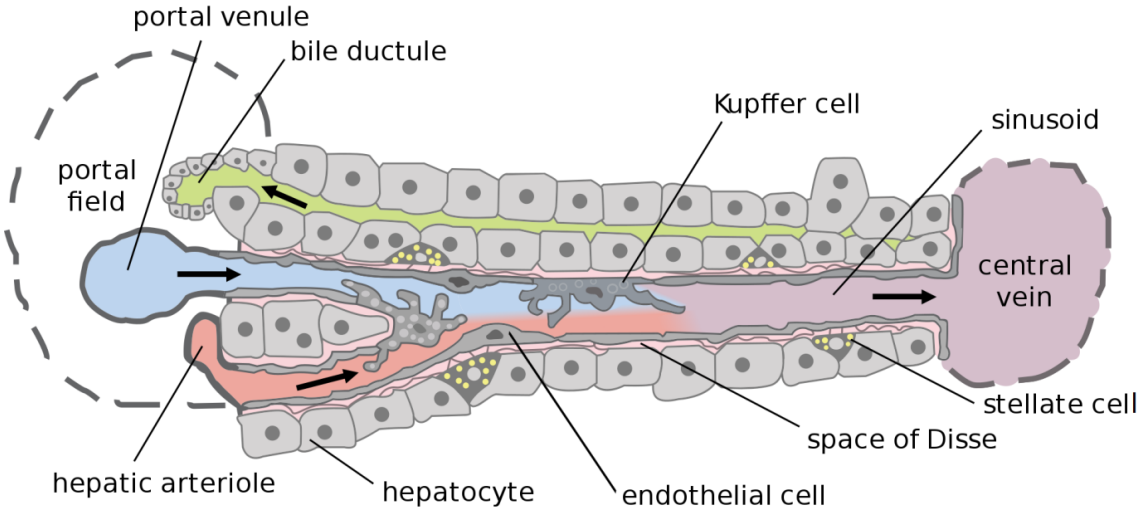

Figure 1.4. Cells in the liver.

Reprinted from reference (225). Articles and accompanying materials published by this journal (PLOS biology) are licensed under Creative Commons Attribution v4.0 (https://creativecommons.org/licenses/by/4.0/).

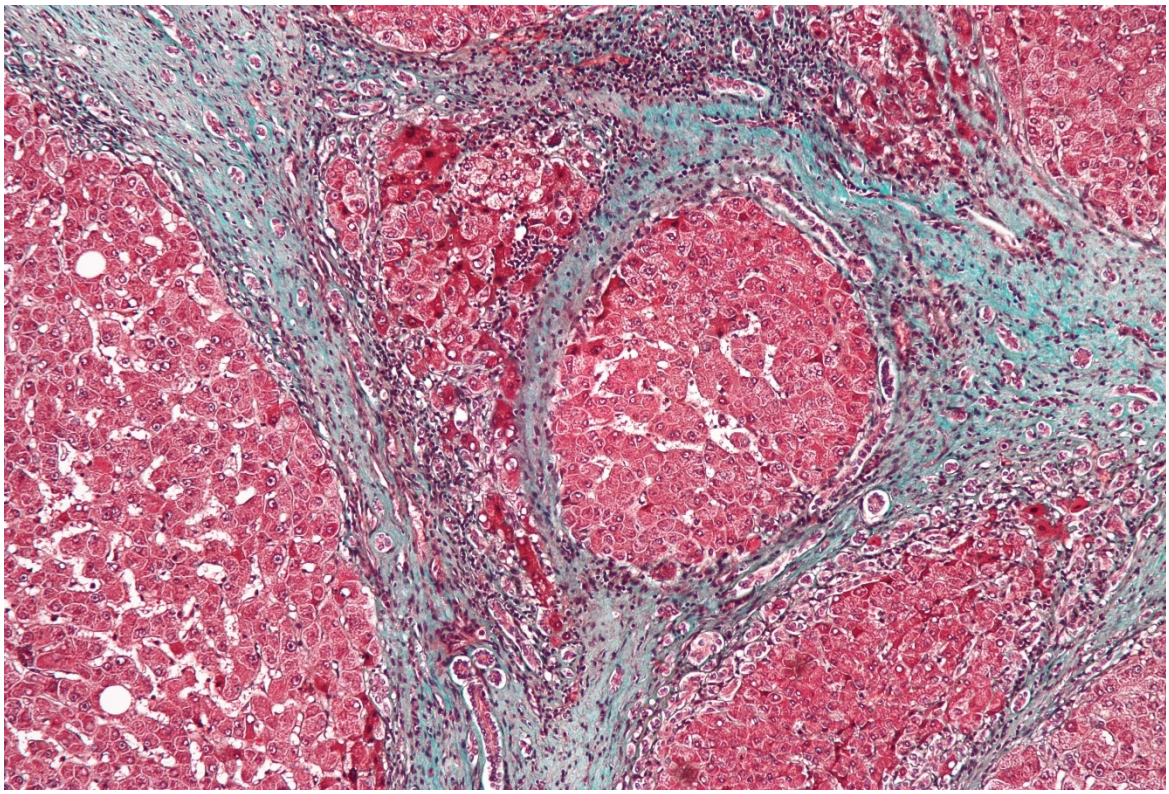

Figure 1.5. Histopathology of cirrhosis.
Reprinted from https://commons.wikimedia.org/wiki/User:Nephron/Gallery#/media/File:Cirrhosis_high_mag.jpg created by Nephron (https://commons.wikimedia.org/wiki/User:Nephron). This image is licensed under Creative Commons Attribution-Share Alike 3.0 Unported (https://creativecommons.org/licenses/by-sa/3.0/).

1.9 – References

1. Mills SE. Histology for pathologists. 4th ed. Philadelphia : Wolters Kluwer Health/Lippincott Williams & Wilkins., 2012.
2. Rutkauskas S, Gedrimas V, Pundzius J, Barauskas G, Basevicius A. Clinical and anatomical basis for the classification of the structural parts of liver. Medicina (Kaunas) 2006;42(2):98-106.
3. Couinaud C. [Dorsal sector of the liver]. Chirurgie 1998 Feb;123(1):8-15.
4. Abdel-Misih SR, Bloomston M. Liver anatomy. Surg Clin North Am 2010 Aug;90(4):643-653.
5. Kiernan F, Green J. XXIX. The anatomy and physiology of the liver. Philosophical Transactions of the Royal Society of London 1833 Jan 1.
6. Rappaort AM, BOROWY ZJ, LOUGHEED WM, LOTTO WN. Subdivision of hexagonal liver lobules into a structural and functional unit; role in hepatic physiology and pathology. Anat Rec 1954 May;119(1):11-33.
7. WAKIM KG. Physiology of the liver. Am J Med 1954 Feb;16(2):256-271.
8. Kmiec Z. Cooperation of liver cells in health and disease. Adv Anat Embryol Cell Biol 2001;161:III-151.
9. Zatloukal K, Stumptner C, Fuchsbichler A, Fickert P, Lackner C, Trauner M, et al. The keratin cytoskeleton in liver diseases. J Pathol 2004 Nov;204(4):367-376.
10. Fausto N, Campbell JS. The role of hepatocytes and oval cells in liver regeneration and repopulation. Mech Dev 2003 Jan;120(1):117-130.

11. Friedman SL. Hepatic stellate cells: protean, multifunctional, and enigmatic cells of the liver. Physiol Rev 2008 Jan;88(1):125-172.

12. Wake K. "Sternzellen" in the liver: perisinusoidal cells with special reference to storage of vitamin A. Am J Anat 1971 Dec;132(4):429-462.

13. Wardle EN. Kupffer cells and their function. Liver 1987 Apr;7(2):63-75.

14. Vrba J, Modriansky M. Oxidative burst of Kupffer cells: target for liver injury treatment. Biomed Pap Med Fac Univ Palacky Olomouc Czech Repub 2002 Dec;146(2):15-20.

15. Kolios G, Valatas V, Kouroumalis E. Role of Kupffer cells in the pathogenesis of liver disease. World J Gastroenterol 2006 Dec 14;12(46):7413-7420.

16. Poisson J, Lemoinne S, Boulanger C, Durand F, Moreau R, Valla D, et al. Liver sinusoidal endothelial cells: Physiology and role in liver diseases. J Hepatol 2017 Jan;66(1):212-227.

17. Maslak E, Gregorius A, Chlopicki S. Liver sinusoidal endothelial cells (LSECs) function and NAFLD; NO-based therapy targeted to the liver. Pharmacol Rep 2015 Aug;67(4):689-694.

18. Smedsrod B, Le CD, Ikejima K, Jaeschke H, Kawada N, Naito M, et al. Hepatic sinusoidal cells in health and disease: update from the 14th International Symposium. Liver Int 2009 Apr;29(4):490-501.

19. Itoh T. Stem/progenitor cells in liver regeneration. Hepatology 2016 Aug;64(2):663-668.

20. Kinnman N, Housset C. Peribiliary myofibroblasts in biliary type liver fibrosis. Front Biosci 2002 Feb 1;7:d496-d503.

21. Tsochatzis EA, Bosch J, Burroughs AK. Liver cirrhosis. Lancet 2014 May 17;383(9930):1749-1761.

22. Ellis EL, Mann DA. Clinical evidence for the regression of liver fibrosis. J Hepatol 2012 May;56(5):1171-1180.

23. Lozano R, Naghavi M, Foreman K, Lim S, Shibuya K, Aboyans V, et al. Global and regional mortality from 235 causes of death for 20 age groups in 1990 and 2010: a systematic analysis for the Global Burden of Disease Study 2010. Lancet 2012 Dec 15;380(9859):2095-2128.

24. EASL-EORTC clinical practice guidelines: management of hepatocellular carcinoma. J Hepatol 2012 Apr;56(4):908-943.

25. Suriawinata A, Thung S. Liver Pathology: An Atlas and Concise Guide. 2011.

26. Sharma B, John S. Hepatic Cirrhosis. StatPearls Publishing, 2019.

27. Anthony PP, Ishak KG, Nayak NC, Poulsen HE, Scheuer PJ, Sobin LH. The morphology of cirrhosis: definition, nomenclature, and classification. Bull World Health Organ 1977;55(4):521-540.

28. POPPER H, ELIAS H, PETTY DE. Vascular pattern of the cirrhotic liver. Am J Clin Pathol 1952 Aug;22(8):717-729.

29. Marcellin P, Gane E, Buti M, Afdhal N, Sievert W, Jacobson IM, et al. Regression of cirrhosis during treatment with tenofovir disoproxil fumarate for chronic hepatitis B: a 5-year open-label follow-up study. Lancet 2013 Feb 9;381(9865):468-475.

30. Morgan TR, Ghany MG, Kim HY, Snow KK, Shiffman ML, De Santo JL, et al. Outcome of sustained virological responders with histologically advanced chronic hepatitis C. Hepatology 2010 Sep;52(3):833-844.

31. Younossi ZM, Koenig AB, Abdelatif D, Fazel Y, Henry L, Wymer M. Global epidemiology of nonalcoholic fatty liver disease-Meta-analytic assessment of prevalence, incidence, and outcomes. Hepatology 2016 Jul;64(1):73-84.

32. Obesity linked to dramatic rise in liver disease: Alarming new statistics show that 1 in 4 Canadians may be affected by liver disease. 2016.

33. El-Serag HB. Epidemiology of viral hepatitis and hepatocellular carcinoma. Gastroenterology 2012 May;142(6):1264-1273.

34. Friedman SL. Liver fibrosis -- from bench to bedside. J Hepatol 2003;38 Suppl 1:S38-S53.

35. Younossi ZM, Stepanova M, Afendy M, Fang Y, Younossi Y, Mir H, et al. Changes in the prevalence of the most common causes of chronic liver diseases in the United States from 1988 to 2008. Clin Gastroenterol Hepatol 2011 Jun;9(6):524-530.

36. Schweitzer A, Horn J, Mikolajczyk RT, Krause G, Ott JJ. Estimations of worldwide prevalence of chronic hepatitis B virus infection: a systematic review of data published between 1965 and 2013. Lancet 2015 Oct 17;386(10003):1546-1555.

37. Blach S, Zeuzem S, Manns M, Altraif I, Duberg A, Mulijono D, et al. Global prevalence and genotype distribution of hepatitis C virus infection in 2015: a modelling study. Lancet Gastroenterol Hepatol 2017 Mar;2(3):161-176.

38. Bataller R, Brenner DA. Liver fibrosis. J Clin Invest 2005 Feb;115(2):209-218.

39. Chalasani N, Younossi Z, Lavine JE, Charlton M, Cusi K, Rinella M, et al. The diagnosis and management of nonalcoholic fatty liver disease: Practice guidance from the American Association for the Study of Liver Diseases. Hepatology 2018 Jan;67(1):328-357.

40. Bellentani S, Marino M. Epidemiology and natural history of non-alcoholic fatty liver disease (NAFLD). Ann Hepatol 2009;8 Suppl 1:S4-S8.

41. Rinella ME. Nonalcoholic fatty liver disease: a systematic review. JAMA 2015 Jun 9;313(22):2263-2273.

42. Ekstedt M, Hagstrom H, Nasr P, Fredrikson M, Stal P, Kechagias S, et al. Fibrosis stage is the strongest predictor for disease-specific mortality in NAFLD after up to 33 years of follow-up. Hepatology 2015 May;61(5):1547-1554.

43. Angulo P, Kleiner DE, Dam-Larsen S, Adams LA, Bjornsson ES, Charatcharoenwitthaya P, et al. Liver Fibrosis, but No Other Histologic Features, Is Associated With Long-term Outcomes of Patients With Nonalcoholic Fatty Liver Disease. Gastroenterology 2015 Aug;149(2):389-397.

44. Lai CL, Ratziu V, Yuen MF, Poynard T. Viral hepatitis B. Lancet 2003 Dec 20;362(9401):2089-2094.

45. Sarin SK, Kumar M, Lau GK, Abbas Z, Chan HL, Chen CJ, et al. Asian-Pacific clinical practice guidelines on the management of hepatitis B: a 2015 update. Hepatol Int 2016 Jan;10(1):1-98.

46. Fattovich G. Natural history and prognosis of hepatitis B. Semin Liver Dis 2003 Feb;23(1):47-58.

47. EASL 2017 Clinical Practice Guidelines on the management of hepatitis B virus infection. J Hepatol 2017 Aug;67(2):370-398.

48. Terrault NA, Lok ASF, McMahon BJ, Chang KM, Hwang JP, Jonas MM, et al. Update on prevention, diagnosis, and treatment of chronic hepatitis B: AASLD 2018 hepatitis B guidance. Hepatology 2018 Apr;67(4):1560-1599.

49. O'Shea RS, Dasarathy S, McCullough AJ. Alcoholic liver disease. Hepatology 2010 Jan;51(1):307-328.

50. Orman ES, Odena G, Bataller R. Alcoholic liver disease: pathogenesis, management, and novel targets for therapy. J Gastroenterol Hepatol 2013 Aug;28 Suppl 1:77-84.

51. MacSween RN, Burt AD. Histologic spectrum of alcoholic liver disease. Semin Liver Dis 1986 Aug;6(3):221-232.

52. Basra S, Anand BS. Definition, epidemiology and magnitude of alcoholic hepatitis. World J Hepatol 2011 May 27;3(5):108-113.

53. Alexander JF, Lischner MW, Galambos JT. Natural history of alcoholic hepatitis. II. The long-term prognosis. Am J Gastroenterol 1971 Dec;56(6):515-525.

54. Galambos JT. Natural history of alcoholic hepatitis. 3. Histological changes. Gastroenterology 1972 Dec;63(6):1026-1035.

55. Lavanchy D. The global burden of hepatitis C. Liver Int 2009 Jan;29 Suppl 1:74-81.

56. Shah H, Bilodeau M, Burak KW, Cooper C, Klein M, Ramji A, et al. The management of chronic hepatitis C: 2018 guideline update from the Canadian Association for the Study of the Liver. CMAJ 2018 Jun 4;190(22):E677-E687.

57. Benhamou Y, Bochet M, Di M, V, Charlotte F, Azria F, Coutellier A, et al. Liver fibrosis progression in human immunodeficiency virus and hepatitis C virus coinfected patients. The Multivirc Group. Hepatology 1999 Oct;30(4):1054-1058.

58. Alberti A, Chemello L, Benvegnu L. Natural history of hepatitis C. J Hepatol 1999;31 Suppl 1:17-24.

59. Lee YA, Friedman SL. Reversal, maintenance or progression: what happens to the liver after a virologic cure of hepatitis C? Antiviral Res 2014 Jul;107:23-30.

60. Krawitt EL. Autoimmune hepatitis. N Engl J Med 2006 Jan 5;354(1):54-66.

61. EASL Clinical Practice Guidelines: Autoimmune hepatitis. J Hepatol 2015 Oct;63(4):971-1004.

62. Czaja AJ, Carpenter HA. Decreased fibrosis during corticosteroid therapy of autoimmune hepatitis. J Hepatol 2004 Apr;40(4):646-652.

63. Roberts SK, Therneau TM, Czaja AJ. Prognosis of histological cirrhosis in type 1 autoimmune hepatitis. Gastroenterology 1996 Mar;110(3):848-857.

64. Czaja AJ, Carpenter HA. Progressive fibrosis during corticosteroid therapy of autoimmune hepatitis. Hepatology 2004 Jun;39(6):1631-1638.

65. Friedman SL. Mechanisms of hepatic fibrogenesis. Gastroenterology 2008 May;134(6):1655-1669.

66. Lo RC, Kim H. Histopathological evaluation of liver fibrosis and cirrhosis regression. Clin Mol Hepatol 2017 Dec;23(4):302-307.

67. Wynn TA, Ramalingam TR. Mechanisms of fibrosis: therapeutic translation for fibrotic disease. Nat Med 2012 Jul 6;18(7):1028-1040.

68. Rockey DC, Bell PD, Hill JA. Fibrosis--a common pathway to organ injury and failure. N Engl J Med 2015 Mar 19;372(12):1138-1149.

69. Gabbiani G. The myofibroblast in wound healing and fibrocontractive diseases. J Pathol 2003 Jul;200(4):500-503.

70. Xu J, Liu X, Koyama Y, Wang P, Lan T, Kim IG, et al. The types of hepatic myofibroblasts contributing to liver fibrosis of different etiologies. Front Pharmacol 2014;5:167.

71. Tsuchida T, Friedman SL. Mechanisms of hepatic stellate cell activation. Nat Rev Gastroenterol Hepatol 2017 Jul;14(7):397-411.

72. Wells RG. The portal fibroblast: not just a poor man's stellate cell. Gastroenterology 2014 Jul;147(1):41-47.

73. Dranoff JA, Wells RG. Portal fibroblasts: Underappreciated mediators of biliary fibrosis. Hepatology 2010 Apr;51(4):1438-1444.

74. Xie G, Diehl AM. Evidence for and against epithelial-to-mesenchymal transition in the liver. Am J Physiol Gastrointest Liver Physiol 2013 Dec;305(12):G881-G890.

75. Choi SS, Diehl AM. Epithelial-to-mesenchymal transitions in the liver. Hepatology 2009 Dec;50(6):2007-2013.

76. Kalluri R, Weinberg RA. The basics of epithelial-mesenchymal transition. J Clin Invest 2009 Jun;119(6):1420-1428.

77. Taura K, Miura K, Iwaisako K, Osterreicher CH, Kodama Y, Penz-Osterreicher M, et al. Hepatocytes do not undergo epithelial-mesenchymal transition in liver fibrosis in mice. Hepatology 2010 Mar;51(3):1027-1036.

78. Parola M, Pinzani M. Hepatic wound repair. Fibrogenesis Tissue Repair 2009 Sep 25;2(1):4.

79. Quan TE, Bucala R. Culture and analysis of circulating fibrocytes. Methods Mol Med 2007;135:423-434.

80. Brenner DA, Kisseleva T, Scholten D, Paik YH, Iwaisako K, Inokuchi S, et al. Origin of myofibroblasts in liver fibrosis. Fibrogenesis Tissue Repair 2012;5(Suppl 1):S17.

81. Reilkoff RA, Bucala R, Herzog EL. Fibrocytes: emerging effector cells in chronic inflammation. Nat Rev Immunol 2011 Jun;11(6):427-435.

82. Theise ND, Saxena R, Portmann BC, Thung SN, Yee H, Chiriboga L, et al. The canals of Hering and hepatic stem cells in humans. Hepatology 1999 Dec;30(6):1425-1433.

83. Richardson MM, Jonsson JR, Powell EE, Brunt EM, Neuschwander-Tetri BA, Bhathal PS, et al. Progressive fibrosis in nonalcoholic steatohepatitis: association with altered regeneration and a ductular reaction. Gastroenterology 2007 Jul;133(1):80-90.

84. Kaur S, Siddiqui H, Bhat MH. Hepatic Progenitor Cells in Action: Liver Regeneration or Fibrosis? Am J Pathol 2015 Sep;185(9):2342-2350.

85. Clouston AD, Powell EE, Walsh MJ, Richardson MM, Demetris AJ, Jonsson JR. Fibrosis correlates with a ductular reaction in hepatitis C: roles of impaired replication, progenitor cells and steatosis. Hepatology 2005 Apr;41(4):809-818.

86. Roskams T, Yang SQ, Koteish A, Durnez A, DeVos R, Huang X, et al. Oxidative stress and oval cell accumulation in mice and humans with alcoholic and nonalcoholic fatty liver disease. Am J Pathol 2003 Oct;163(4):1301-1311.

87. Xu B, Broome U, Uzunel M, Nava S, Ge X, Kumagai-Braesch M, et al. Capillarization of hepatic sinusoid by liver endothelial cell-reactive autoantibodies in patients with cirrhosis and chronic hepatitis. Am J Pathol 2003 Oct;163(4):1275-1289.

88. Marrone G, Shah VH, Gracia-Sancho J. Sinusoidal communication in liver fibrosis and regeneration. J Hepatol 2016 Sep;65(3):608-617.

89. Kazankov K, Barrera F, Moller HJ, Bibby BM, Vilstrup H, George J, et al. Soluble CD163, a macrophage activation marker, is independently associated with fibrosis in patients with chronic viral hepatitis B and C. Hepatology 2014 Aug;60(2):521-530.

90. Tacke F, Zimmermann HW. Macrophage heterogeneity in liver injury and fibrosis. J Hepatol 2014 May;60(5):1090-1096.

91. Pradere JP, Kluwe J, De MS, Jiao JJ, Gwak GY, Dapito DH, et al. Hepatic macrophages but not dendritic cells contribute to liver fibrosis by promoting the survival of activated hepatic stellate cells in mice. Hepatology 2013 Oct;58(4):1461-1473.

92. Gressner AM, Weiskirchen R, Breitkopf K, Dooley S. Roles of TGF-beta in hepatic fibrosis. Front Biosci 2002 Apr 1;7:d793-d807.

93. Dooley S, ten DP. TGF-beta in progression of liver disease. Cell Tissue Res 2012 Jan;347(1):245-256.

94. Massague J. TGFbeta in Cancer. Cell 2008 Jul 25;134(2):215-230.

95. Anderson LR, Owens TW, Naylor MJ. Structural and mechanical functions of integrins. Biophys Rev 2014 Jun;6(2):203-213.

96. Mizejewski GJ. Role of integrins in cancer: survey of expression patterns. Proc Soc Exp Biol Med 1999 Nov;222(2):124-138.

97. Luo BH, Springer TA. Integrin structures and conformational signaling. Curr Opin Cell Biol 2006 Oct;18(5):579-586.

98. Cong M, Iwaisako K, Jiang C, Kisseleva T. Cell signals influencing hepatic fibrosis. Int J Hepatol 2012;2012:158547.

99. Nejjari M, Couvelard A, Mosnier JF, Moreau A, Feldmann G, Degott C, et al. Integrin up-regulation in chronic liver disease: relationship with inflammation and fibrosis in chronic hepatitis C. J Pathol 2001 Nov;195(4):473-481.

100. Patsenker E, Stickel F. Role of integrins in fibrosing liver diseases. Am J Physiol Gastrointest Liver Physiol 2011 Sep;301(3):G425-G434.

101. Borkham-Kamphorst E, Weiskirchen R. The PDGF system and its antagonists in liver fibrosis. Cytokine Growth Factor Rev 2016 Apr;28:53-61.

102. van DF, Olinga P, Poelstra K, Beljaars L. Targeted Therapies in Liver Fibrosis: Combining the Best Parts of Platelet-Derived Growth Factor BB and Interferon Gamma. Front Med (Lausanne) 2015;2:72.

103. Fredriksson L, Li H, Eriksson U. The PDGF family: four gene products form five dimeric isoforms. Cytokine Growth Factor Rev 2004 Aug;15(4):197-204.

104. Paradis V, Dargere D, Bonvoust F, Vidaud M, Segarini P, Bedossa P. Effects and regulation of connective tissue growth factor on hepatic stellate cells. Lab Invest 2002 Jun;82(6):767-774.

105. Grotendorst GR, Rahmanie H, Duncan MR. Combinatorial signaling pathways determine fibroblast proliferation and myofibroblast differentiation. FASEB J 2004 Mar;18(3):469-479.

106. Lee CH, Shah B, Moioli EK, Mao JJ. CTGF directs fibroblast differentiation from human mesenchymal stem/stromal cells and defines connective tissue healing in a rodent injury model. J Clin Invest 2010 Sep;120(9):3340-3349.

107. Lipson KE, Wong C, Teng Y, Spong S. CTGF is a central mediator of tissue remodeling and fibrosis and its inhibition can reverse the process of fibrosis. Fibrogenesis Tissue Repair 2012;5(Suppl 1):S24.

108. Chaqour B, Goppelt-Struebe M. Mechanical regulation of the Cyr61/CCN1 and CTGF/CCN2 proteins. FEBS J 2006 Aug;273(16):3639-3649.

109. Ihn H. Pathogenesis of fibrosis: role of TGF-beta and CTGF. Curr Opin Rheumatol 2002 Nov;14(6):681-685.

110. Mezzano SA, Ruiz-Ortega M, Egido J. Angiotensin II and renal fibrosis. Hypertension 2001 Sep;38(3 Pt 2):635-638.

111. Elpek GO. Cellular and molecular mechanisms in the pathogenesis of liver fibrosis: An update. World J Gastroenterol 2014 Jun 21;20(23):7260-7276.

112. Bataller R, Schwabe RF, Choi YH, Yang L, Paik YH, Lindquist J, et al. NADPH oxidase signal transduces angiotensin II in hepatic stellate cells and is critical in hepatic fibrosis. J Clin Invest 2003 Nov;112(9):1383-1394.

113. Bataller R, Gabele E, Schoonhoven R, Morris T, Lehnert M, Yang L, et al. Prolonged infusion of angiotensin II into normal rats induces stellate cell activation and proinflammatory events in liver. Am J Physiol Gastrointest Liver Physiol 2003 Sep;285(3):G642-G651.

114. Gandhi CR, Behal RH, Harvey SA, Nouchi TA, Olson MS. Hepatic effects of endothelin. Receptor characterization and endothelin-induced signal transduction in hepatocytes. Biochem J 1992 Nov 1;287 (Pt 3):897-904.

115. Housset C, Rockey DC, Bissell DM. Endothelin receptors in rat liver: lipocytes as a contractile target for endothelin 1. Proc Natl Acad Sci U S A 1993 Oct 15;90(20):9266-9270.

116. Rodriguez-Pascual F, Busnadiego O, Gonzalez-Santamaria J. The profibrotic role of endothelin-1: is the door still open for the treatment of fibrotic diseases? Life Sci 2014 Nov 24;118(2):156-164.

117. Moore K, Wendon J, Frazer M, Karani J, Williams R, Badr K. Plasma endothelin immunoreactivity in liver disease and the hepatorenal syndrome. N Engl J Med 1992 Dec 17;327(25):1774-1778.

118. Yokomori H, Oda M, Yasogawa Y, Nishi Y, Ogi M, Takahashi M, et al. Enhanced expression of endothelin B receptor at protein and gene levels in human cirrhotic liver. Am J Pathol 2001 Oct;159(4):1353-1362.

119. Leivas A, Jimenez W, Bruix J, Boix L, Bosch J, Arroyo V, et al. Gene expression of endothelin-1 and ET(A) and ET(B) receptors in human cirrhosis: relationship with hepatic hemodynamics. J Vasc Res 1998 May;35(3):186-193.

120. Angus PW. Role of endothelin in systemic and portal resistance in cirrhosis. Gut 2006 Sep;55(9):1230-1232.

121. Rockey DC, Caldwell SH, Goodman ZD, Nelson RC, Smith AD. Liver biopsy. Hepatology 2009 Mar;49(3):1017-1044.

122. Afdhal NH, Nunes D. Evaluation of liver fibrosis: a concise review. Am J Gastroenterol 2004 Jun;99(6):1160-1174.

123. Bedossa P, Poynard T. An algorithm for the grading of activity in chronic hepatitis C. The METAVIR Cooperative Study Group. Hepatology 1996 Aug;24(2):289-293.

124. Ishak K, Baptista A, Bianchi L, Callea F, De GJ, Gudat F, et al. Histological grading and staging of chronic hepatitis. J Hepatol 1995 Jun;22(6):696-699.

125. Kleiner DE, Brunt EM, Van NM, Behling C, Contos MJ, Cummings OW, et al. Design and validation of a histological scoring system for nonalcoholic fatty liver disease. Hepatology 2005 Jun;41(6):1313-1321.

126. Bejarano PA, Koehler A, Sherman KE. Second opinion pathology in liver biopsy interpretation. Am J Gastroenterol 2001 Nov;96(11):3158-3164.

127. Bedossa P, Dargere D, Paradis V. Sampling variability of liver fibrosis in chronic hepatitis C. Hepatology 2003 Dec;38(6):1449-1457.

128. Netto GJ, Watkins DL, Williams JW, Colby TV, dePetris G, Sharkey FE, et al. Interobserver agreement in hepatitis C grading and staging and in the Banff grading schema for acute cellular rejection: the "hepatitis C 3" multi-institutional trial experience. Arch Pathol Lab Med 2006 Aug;130(8):1157-1162.

129. Friedman SL. Evolving challenges in hepatic fibrosis. Nat Rev Gastroenterol Hepatol 2010 Aug;7(8):425-436.

130. Regev A, Berho M, Jeffers LJ, Milikowski C, Molina EG, Pyrsopoulos NT, et al. Sampling error and intraobserver variation in liver biopsy in patients with chronic HCV infection. Am J Gastroenterol 2002 Oct;97(10):2614-2618.

131. Ratziu V, Charlotte F, Heurtier A, Gombert S, Giral P, Bruckert E, et al. Sampling variability of liver biopsy in nonalcoholic fatty liver disease. Gastroenterology 2005 Jun;128(7):1898-1906.

132. Berenguer J, Zamora FX, Aldamiz-Echevarria T, Von Wichmann MA, Crespo M, Lopez-Aldeguer J, et al. Comparison of the prognostic value of liver biopsy and FIB-4 index in patients coinfected with HIV and hepatitis C virus. Clin Infect Dis 2015 Mar 15;60(6):950-958.

133. Sandrin L, Fourquet B, Hasquenoph JM, Yon S, Fournier C, Mal F, et al. Transient elastography: a new noninvasive method for assessment of hepatic fibrosis. Ultrasound Med Biol 2003 Dec;29(12):1705-1713.

134. Castera L. Noninvasive methods to assess liver disease in patients with hepatitis B or C. Gastroenterology 2012 May;142(6):1293-1302.

135. Barr RG, Ferraioli G, Palmeri ML, Goodman ZD, Garcia-Tsao G, Rubin J, et al. Elastography Assessment of Liver Fibrosis: Society of Radiologists in Ultrasound Consensus Conference Statement. Radiology 2015 Sep;276(3):845-861.

136. Castera L, Forns X, Alberti A. Non-invasive evaluation of liver fibrosis using transient elastography. J Hepatol 2008 May;48(5):835-847.

137. Tapper EB, Castera L, Afdhal NH. FibroScan (vibration-controlled transient elastography): where does it stand in the United States practice. Clin Gastroenterol Hepatol 2015 Jan;13(1):27-36.

138. Patel K, Bedossa P, Castera L. Diagnosis of liver fibrosis: present and future. Semin Liver Dis 2015 May;35(2):166-183.

139. D'Onofrio M, Crosara S, De RR, Canestrini S, Demozzi E, Gallotti A, et al. Acoustic radiation force impulse of the liver. World J Gastroenterol 2013 Aug 14;19(30):4841-4849.

140. Bota S, Herkner H, Sporea I, Salzl P, Sirli R, Neghina AM, et al. Meta-analysis: ARFI elastography versus transient elastography for the evaluation of liver fibrosis. Liver Int 2013 Sep;33(8):1138-1147.

141. Talwalkar JA, Yin M, Fidler JL, Sanderson SO, Kamath PS, Ehman RL. Magnetic resonance imaging of hepatic fibrosis: emerging clinical applications. Hepatology 2008 Jan;47(1):332-342.

142. Venkatesh SK, Yin M, Ehman RL. Magnetic resonance elastography of liver: technique, analysis, and clinical applications. J Magn Reson Imaging 2013 Mar;37(3):544-555.

143. Berenguer M, Schuppan D. Progression of liver fibrosis in post-transplant hepatitis C: mechanisms, assessment and treatment. J Hepatol 2013 May;58(5):1028-1041.

144. Cales P, Veillon P, Konate A, Mathieu E, Ternisien C, Chevailler A, et al. Reproducibility of blood tests of liver fibrosis in clinical practice. Clin Biochem 2008 Jan;41(1-2):10-18.

145. Poynard T, Munteanu M, Deckmyn O, Ngo Y, Drane F, Messous D, et al. Applicability and precautions of use of liver injury biomarker FibroTest. A reappraisal at 7 years of age. BMC Gastroenterol 2011 Apr 14;11:39.

146. EASL-ALEH Clinical Practice Guidelines: Non-invasive tests for evaluation of liver disease severity and prognosis. J Hepatol 2015 Jul;63(1):237-264.

147. Yoon YJ, Friedman SL, Lee YA. Antifibrotic Therapies: Where Are We Now? Semin Liver Dis 2016 Feb;36(1):87-98.

148. Knop V, Hoppe D, Welzel T, Vermehren J, Herrmann E, Vermehren A, et al. Regression of fibrosis and portal hypertension in HCV-associated cirrhosis and sustained virologic response after interferon-free antiviral therapy. J Viral Hepat 2016 Dec;23(12):994-1002.

149. Chang TT, Liaw YF, Wu SS, Schiff E, Han KH, Lai CL, et al. Long-term entecavir therapy results in the reversal of fibrosis/cirrhosis and continued histological improvement in patients with chronic hepatitis B. Hepatology 2010 Sep;52(3):886-893.

150. Schuppan D, Kim YO. Evolving therapies for liver fibrosis. J Clin Invest 2013 May;123(5):1887-1901.

151. Henderson NC, Mackinnon AC, Farnworth SL, Poirier F, Russo FP, Iredale JP, et al. Galectin-3 regulates myofibroblast activation and hepatic fibrosis. Proc Natl Acad Sci U S A 2006 Mar 28;103(13):5060-5065.

152. Hellemans K, Michalik L, Dittie A, Knorr A, Rombouts K, De JJ, et al. Peroxisome proliferator-activated receptor-beta signaling contributes to enhanced proliferation of hepatic stellate cells. Gastroenterology 2003 Jan;124(1):184-201.

153. Staels B, Rubenstrunk A, Noel B, Rigou G, Delataille P, Millatt LJ, et al. Hepatoprotective effects of the dual peroxisome proliferator-activated receptor alpha/delta agonist, GFT505, in rodent models of nonalcoholic fatty liver disease/nonalcoholic steatohepatitis. Hepatology 2013 Dec;58(6):1941-1952.

154. Loomba R, Lawitz E, Mantry PS, Jayakumar S, Caldwell SH, Arnold H, et al. The ASK1 inhibitor selonsertib in patients with nonalcoholic steatohepatitis: A randomized, phase 2 trial. Hepatology 2017 Sep 11.

155. Kang KW, Kim YG, Cho MK, Bae SK, Kim CW, Lee MG, et al. Oltipraz regenerates cirrhotic liver through CCAAT/enhancer binding protein-mediated stellate cell inactivation. FASEB J 2002 Dec;16(14):1988-1990.

156. Kim SG, Kim YM, Choi JY, Han JY, Jang JW, Cho SH, et al. Oltipraz therapy in patients with liver fibrosis or cirrhosis: a randomized, double-blind, placebo-controlled phase II trial. J Pharm Pharmacol 2011 May;63(5):627-635.

157. Soule B, Tirucherai G, Kavita U, Kundu S, Christian R. Safety, tolerability, and pharmacokinetics of BMS-986263/ND-L02-s0201, a novel targeted lipid nanoparticle delivering HSP47 siRNA, in healthy participants: A randomised, placebo-controlled, double-blind, phase 1 study. Journal of Hepatology 2018 Apr 1;68:S112.

158. Kawasaki K, Ushioda R, Ito S, Ikeda K, Masago Y, Nagata K. Deletion of the collagen-specific molecular chaperone Hsp47 causes endoplasmic reticulum stress-mediated apoptosis of hepatic stellate cells. J Biol Chem 2015 Feb 6;290(6):3639-3646.

159. Moon HJ, Finney J, Ronnebaum T, Mure M. Human lysyl oxidase-like 2. Bioorg Chem 2014 Dec;57:231-241.

160. Barry-Hamilton V, Spangler R, Marshall D, McCauley S, Rodriguez HM, Oyasu M, et al. Allosteric inhibition of lysyl oxidase-like-2 impedes the development of a pathologic microenvironment. Nat Med 2010 Sep;16(9):1009-1017.

161. Harrison SA, Abdelmalek MF, Caldwell S, Shiffman ML, Diehl AM, Ghalib R, et al. Simtuzumab Is Ineffective for Patients With Bridging Fibrosis or Compensated Cirrhosis Caused by Nonalcoholic Steatohepatitis. Gastroenterology 2018 Oct;155(4):1140-1153.

162. Meissner EG, McLaughlin M, Matthews L, Gharib AM, Wood BJ, Levy E, et al. Simtuzumab treatment of advanced liver fibrosis in HIV and HCV-infected adults: results of a 6-month open-label safety trial. Liver Int 2016 Dec;36(12):1783-1792.

163. Muir AJ, Levy C, Janssen HLA, Montano-Loza AJ, Shiffman ML, Caldwell S, et al. Simtuzumab for Primary Sclerosing Cholangitis: Phase 2 Study Results With Insights on the Natural History of the Disease. Hepatology 2018 Aug 28.

164. Lampi MC, Reinhart-King CA. Targeting extracellular matrix stiffness to attenuate disease: From molecular mechanisms to clinical trials. Sci Transl Med 2018 Jan 3;10(422).

165. Perez TR. Is cirrhosis of the liver experimentally produced by CCl4 and adequate model of human cirrhosis? Hepatology 1983 Jan;3(1):112-120.

166. Moran CJ, Ramesh A, Brama PA, O'Byrne JM, O'Brien FJ, Levingstone TJ. The benefits and limitations of animal models for translational research in cartilage repair. J Exp Orthop 2016 Dec;3(1):1.

167. Moylan CA, Pang H, Dellinger A, Suzuki A, Garrett ME, Guy CD, et al. Hepatic gene expression profiles differentiate presymptomatic patients with mild versus severe nonalcoholic fatty liver disease. Hepatology 2014 Feb;59(2):471-482.

168. Romeo S, Kozlitina J, Xing C, Pertsemlidis A, Cox D, Pennacchio LA, et al. Genetic variation in PNPLA3 confers susceptibility to nonalcoholic fatty liver disease. Nat Genet 2008 Dec;40(12):1461-1465.

169. Speliotes EK, Butler JL, Palmer CD, Voight BF, Hirschhorn JN. PNPLA3 variants specifically confer increased risk for histologic nonalcoholic fatty liver disease but not metabolic disease. Hepatology 2010 Sep;52(3):904-912.

170. Valenti L, Al-Serri A, Daly AK, Galmozzi E, Rametta R, Dongiovanni P, et al. Homozygosity for the patatin-like phospholipase-3/adiponutrin I148M polymorphism influences liver fibrosis in patients with nonalcoholic fatty liver disease. Hepatology 2010 Apr;51(4):1209-1217.

171. Rotman Y, Koh C, Zmuda JM, Kleiner DE, Liang TJ. The association of genetic variability in patatin-like phospholipase domain-containing protein 3 (PNPLA3) with histological severity of nonalcoholic fatty liver disease. Hepatology 2010 Sep;52(3):894-903.

172. Kotronen A, Johansson LE, Johansson LM, Roos C, Westerbacka J, Hamsten A, et al. A common variant in PNPLA3, which encodes adiponutrin, is associated with liver fat content in humans. Diabetologia 2009 Jun;52(6):1056-1060.

173. Sookoian S, Castano GO, Burgueno AL, Gianotti TF, Rosselli MS, Pirola CJ. A nonsynonymous gene variant in the adiponutrin gene is associated with nonalcoholic fatty liver disease severity. J Lipid Res 2009 Oct;50(10):2111-2116.

174. Kozlitina J, Smagris E, Stender S, Nordestgaard BG, Zhou HH, Tybjaerg-Hansen A, et al. Exome-wide association study identifies a TM6SF2 variant that confers susceptibility to nonalcoholic fatty liver disease. Nat Genet 2014 Apr;46(4):352-356.

175. Liu YL, Reeves HL, Burt AD, Tiniakos D, McPherson S, Leathart JB, et al. TM6SF2 rs58542926 influences hepatic fibrosis progression in patients with non-alcoholic fatty liver disease. Nat Commun 2014 Jun 30;5:4309.

176. Welter D, MacArthur J, Morales J, Burdett T, Hall P, Junkins H, et al. The NHGRI GWAS Catalog, a curated resource of SNP-trait associations. Nucleic Acids Res 2014 Jan;42(Database issue):D1001-D1006.

177. Kraft P, Wacholder S, Cornelis MC, Hu FB, Hayes RB, Thomas G, et al. Beyond odds ratios--communicating disease risk based on genetic profiles. Nat Rev Genet 2009 Apr;10(4):264-269.

178. Parikh CR, Thiessen-Philbrook H. Key concepts and limitations of statistical methods for evaluating biomarkers of kidney disease. J Am Soc Nephrol 2014 Aug;25(8):1621-1629.

179. Trepo E, Romeo S, Zucman-Rossi J, Nahon P. PNPLA3 gene in liver diseases. J Hepatol 2016 Aug;65(2):399-412.

180. Danford CJ, Connelly MA, Shalaurova I, Kim M, Herman MA, Nasser I, et al. A Pathophysiologic Approach Combining Genetics and Insulin Resistance to Predict the Severity of Nonalcoholic Fatty Liver Disease. Hepatol Commun 2018 Dec;2(12):1467-1478.

181. Wang M, Gong Q, Zhang J, Chen L, Zhang Z, Lu L, et al. Characterization of gene expression profiles in HBV-related liver fibrosis patients and identification of ITGBL1 as a key regulator of fibrogenesis. Sci Rep 2017 Mar 6;7:43446.

182. Eslam M, Hashem AM, Leung R, Romero-Gomez M, Berg T, Dore GJ, et al. Interferon-lambda rs12979860 genotype and liver fibrosis in viral and non-viral chronic liver disease. Nat Commun 2015 Mar 5;6:6422.

183. Seth D, Leo MA, McGuinness PH, Lieber CS, Brennan Y, Williams R, et al. Gene expression profiling of alcoholic liver disease in the baboon (Papio hamadryas) and human liver. Am J Pathol 2003 Dec;163(6):2303-2317.

184. Tian C, Stokowski RP, Kershenobich D, Ballinger DG, Hinds DA. Variant in PNPLA3 is associated with alcoholic liver disease. Nat Genet 2010 Jan;42(1):21-23.

185. Stickel F, Buch S, Lau K, Meyer zu SH, Berg T, Ridinger M, et al. Genetic variation in the PNPLA3 gene is associated with alcoholic liver injury in caucasians. Hepatology 2011 Jan;53(1):86-95.

186. Trepo E, Gustot T, Degre D, Lemmers A, Verset L, Demetter P, et al. Common polymorphism in the PNPLA3/adiponutrin gene confers higher risk of cirrhosis and liver damage in alcoholic liver disease. J Hepatol 2011 Oct;55(4):906-912.

187. Buch S, Stickel F, Trepo E, Way M, Herrmann A, Nischalke HD, et al. A genome-wide association study confirms PNPLA3 and identifies TM6SF2 and MBOAT7 as risk loci for alcohol-related cirrhosis. Nat Genet 2015 Dec;47(12):1443-1448.

188. Smith MW, Yue ZN, Korth MJ, Do HA, Boix L, Fausto N, et al. Hepatitis C virus and liver disease: global transcriptional profiling and identification of potential markers. Hepatology 2003 Dec;38(6):1458-1467.

189. Smith MW, Walters KA, Korth MJ, Fitzgibbon M, Proll S, Thompson JC, et al. Gene expression patterns that correlate with hepatitis C and early progression to fibrosis in liver transplant recipients. Gastroenterology 2006 Jan;130(1):179-187.

190. Trepo E, Pradat P, Potthoff A, Momozawa Y, Quertinmont E, Gustot T, et al. Impact of patatin-like phospholipase-3 (rs738409 C>G) polymorphism on fibrosis progression and steatosis in chronic hepatitis C. Hepatology 2011 Jul;54(1):60-69.

191. Valenti L, Rumi M, Galmozzi E, Aghemo A, Del MB, De NS, et al. Patatin-like phospholipase domain-containing 3 I148M polymorphism, steatosis, and liver damage in chronic hepatitis C. Hepatology 2011 Mar;53(3):791-799.

192. Muller T, Buch S, Berg T, Hampe J, Stickel F. Distinct, alcohol-modulated effects of PNPLA3 genotype on progression of chronic hepatitis C. J Hepatol 2011 Sep;55(3):732-733.

193. Huang H, Shiffman ML, Cheung RC, Layden TJ, Friedman S, Abar OT, et al. Identification of two gene variants associated with risk of advanced fibrosis in patients with chronic hepatitis C. Gastroenterology 2006 May;130(6):1679-1687.

194. Huang H, Shiffman ML, Friedman S, Venkatesh R, Bzowej N, Abar OT, et al. A 7 gene signature identifies the risk of developing cirrhosis in patients with chronic hepatitis C. Hepatology 2007 Aug;46(2):297-306.

195. Marcolongo M, Young B, Dal PF, Fattovich G, Peraro L, Guido M, et al. A seven-gene signature (cirrhosis risk score) predicts liver fibrosis progression in patients with initially mild chronic hepatitis C. Hepatology 2009 Oct;50(4):1038-1044.

196. Agarwal K, Czaja AJ, Jones DE, Donaldson PT. Cytotoxic T lymphocyte antigen-4 (CTLA-4) gene polymorphisms and susceptibility to type 1 autoimmune hepatitis. Hepatology 2000 Jan;31(1):49-53.

197. Agarwal K, Czaja AJ, Donaldson PT. A functional Fas promoter polymorphism is associated with a severe phenotype in type 1 autoimmune hepatitis characterized by early development of cirrhosis. Tissue Antigens 2007 Mar;69(3):227-235.

198. Vogel A, Strassburg CP, Manns MP. Genetic association of vitamin D receptor polymorphisms with primary biliary cirrhosis and autoimmune hepatitis. Hepatology 2002 Jan;35(1):126-131.

199. Czaja AJ, Cookson S, Constantini PK, Clare M, Underhill JA, Donaldson PT. Cytokine polymorphisms associated with clinical features and treatment outcome in type 1 autoimmune hepatitis. Gastroenterology 1999 Sep;117(3):645-652.

200. Wai CT, Greenson JK, Fontana RJ, Kalbfleisch JD, Marrero JA, Conjeevaram HS, et al. A simple noninvasive index can predict both significant fibrosis and cirrhosis in patients with chronic hepatitis C. Hepatology 2003 Aug;38(2):518-526.

201. Harrison SA, Oliver D, Arnold HL, Gogia S, Neuschwander-Tetri BA. Development and validation of a simple NAFLD clinical scoring system for identifying patients without advanced disease. Gut 2008 Oct;57(10):1441-1447.

202. Rosenberg WM, Voelker M, Thiel R, Becka M, Burt A, Schuppan D, et al. Serum markers detect the presence of liver fibrosis: a cohort study. Gastroenterology 2004 Dec;127(6):1704-1713.

203. Koda M, Matunaga Y, Kawakami M, Kishimoto Y, Suou T, Murawaki Y. FibroIndex, a practical index for predicting significant fibrosis in patients with chronic hepatitis C. Hepatology 2007 Feb;45(2):297-306.

204. Cales P, Oberti F, Michalak S, Hubert-Fouchard I, Rousselet MC, Konate A, et al. A novel panel of blood markers to assess the degree of liver fibrosis. Hepatology 2005 Dec;42(6):1373-1381.

205. Sud A, Hui JM, Farrell GC, Bandara P, Kench JG, Fung C, et al. Improved prediction of fibrosis in chronic hepatitis C using measures of insulin resistance in a probability index. Hepatology 2004 May;39(5):1239-1247.

206. Imbert-Bismut F, Ratziu V, Pieroni L, Charlotte F, Benhamou Y, Poynard T. Biochemical markers of liver fibrosis in patients with hepatitis C virus infection: a prospective study. Lancet 2001 Apr 7;357(9262):1069-1075.

207. Patel K, Gordon SC, Jacobson I, Hezode C, Oh E, Smith KM, et al. Evaluation of a panel of non-invasive serum markers to differentiate mild from moderate-to-advanced liver fibrosis in chronic hepatitis C patients. J Hepatol 2004 Dec;41(6):935-942.

208. Sterling RK, Lissen E, Clumeck N, Sola R, Correa MC, Montaner J, et al. Development of a simple noninvasive index to predict significant fibrosis in patients with HIV/HCV coinfection. Hepatology 2006 Jun;43(6):1317-1325.

209. Forns X, Ampurdanes S, Llovet JM, Aponte J, Quinto L, Martinez-Bauer E, et al. Identification of chronic hepatitis C patients without hepatic fibrosis by a simple predictive model. Hepatology 2002 Oct;36(4 Pt 1):986-992.

210. Islam S, Antonsson L, Westin J, Lagging M. Cirrhosis in hepatitis C virus-infected patients can be excluded using an index of standard biochemical serum markers. Scand J Gastroenterol 2005 Jul;40(7):867-872.

211. Fontana RJ, Goodman ZD, Dienstag JL, Bonkovsky HL, Naishadham D, Sterling RK, et al. Relationship of serum fibrosis markers with liver fibrosis stage and collagen content in patients with advanced chronic hepatitis C. Hepatology 2008 Mar;47(3):789-798.

212. Adams LA, Bulsara M, Rossi E, DeBoer B, Speers D, George J, et al. Hepascore: an accurate validated predictor of liver fibrosis in chronic hepatitis C infection. Clin Chem 2005 Oct;51(10):1867-1873.

213. Hui AY, Chan HL, Wong VW, Liew CT, Chim AM, Chan FK, et al. Identification of chronic hepatitis B patients without significant liver fibrosis by a simple noninvasive predictive model. Am J Gastroenterol 2005 Mar;100(3):616-623.

214. Lok AS, Ghany MG, Goodman ZD, Wright EC, Everson GT, Sterling RK, et al. Predicting cirrhosis in patients with hepatitis C based on standard laboratory tests: results of the HALT-C cohort. Hepatology 2005 Aug;42(2):282-292.

215. Angulo P, Hui JM, Marchesini G, Bugianesi E, George J, Farrell GC, et al. The NAFLD fibrosis score: a noninvasive system that identifies liver fibrosis in patients with NAFLD. Hepatology 2007 Apr;45(4):846-854.

216. Leroy V, Monier F, Bottari S, Trocme C, Sturm N, Hilleret MN, et al. Circulating matrix metalloproteinases 1, 2, 9 and their inhibitors TIMP-1 and TIMP-2 as serum

markers of liver fibrosis in patients with chronic hepatitis C: comparison with PIIINP and hyaluronic acid. Am J Gastroenterol 2004 Feb;99(2):271-279.

217. Kelleher TB, Mehta SH, Bhaskar R, Sulkowski M, Astemborski J, Thomas DL, et al. Prediction of hepatic fibrosis in HIV/HCV co-infected patients using serum fibrosis markers: the SHASTA index. J Hepatol 2005 Jul;43(1):78-84.

218. Zeng MD, Lu LG, Mao YM, Qiu DK, Li JQ, Wan MB, et al. Prediction of significant fibrosis in HBeAg-positive patients with chronic hepatitis B by a noninvasive model. Hepatology 2005 Dec;42(6):1437-1445.

219. Kim MY, Cho MY, Baik SK, Jeong PH, Suk KT, Jang YO, et al. Beneficial effects of candesartan, an angiotensin-blocking agent, on compensated alcoholic liver fibrosis - a randomized open-label controlled study. Liver Int 2012 Jul;32(6):977-987.

220. McPherson S, Wilkinson N, Tiniakos D, Wilkinson J, Burt AD, McColl E, et al. A randomised controlled trial of losartan as an anti-fibrotic agent in non-alcoholic steatohepatitis. PLoS One 2017;12(4):e0175717.

221. Colmenero J, Bataller R, Sancho-Bru P, Dominguez M, Moreno M, Forns X, et al. Effects of losartan on hepatic expression of nonphagocytic NADPH oxidase and fibrogenic genes in patients with chronic hepatitis C. Am J Physiol Gastrointest Liver Physiol 2009 Oct;297(4):G726-G734.

222. Neuschwander-Tetri BA, Loomba R, Sanyal AJ, Lavine JE, Van Natta ML, Abdelmalek MF, et al. Farnesoid X nuclear receptor ligand obeticholic acid for non-

cirrhotic, non-alcoholic steatohepatitis (FLINT): a multicentre, randomised, placebo-controlled trial. Lancet 2015 Mar 14;385(9972):956-965.

223. Younossi ZM, Ratziu V, Loomba R, Rinella M, Anstee QM, Goodman Z, et al. Obeticholic acid for the treatment of non-alcoholic steatohepatitis: interim analysis from a multicentre, randomised, placebo-controlled phase 3 trial. Lancet 2019 Dec 14;394(10215):2184-2196.

224. McHutchison J, Goodman Z, Patel K, Makhlouf H, Rodriguez-Torres M, Shiffman M, et al. Farglitazar lacks antifibrotic activity in patients with chronic hepatitis C infection. Gastroenterology 2010 Apr;138(4):1365-73, 1373.

225. Frevert U, Engelmann S, Zougbede S, Stange J, Ng B, Matuschewski K, et al. Intravital observation of Plasmodium berghei sporozoite infection of the liver. PLoS Biol 2005 Jun;3(6):e192.

Chapter 2: A Common Gene Signature of Advanced Liver Fibrosis of Diverse Etiologies in Humans

2.1 – Introduction

The burden of liver disease is rising worldwide. Currently, there are more than two billion patients worldwide who suffer from chronic liver disease (1, 2). Most common causes are non-alcoholic fatty liver disease (NAFLD), viral hepatitis B, alcoholic liver disease (ALD), and viral hepatitis C (HCV) with prevalence rates of 25.24%, 3.61%, 2.05%, and 1.68% worldwide, respectively (1, 3, 4). Advanced fibrosis is the common final pathway of different chronic liver diseases, leading to cirrhosis (end-stage liver fibrosis) and poor clinical outcomes (liver decompensation, need for liver transplantation, premature death) (5). Despite being the cardinal pathology consequence of a variety of chronic liver diseases, it is unknown if there is a common molecular pathway for advanced liver fibrosis in humans.

Although several previous whole genome transcriptomic had identified hepatic gene expression profiles for advanced liver fibrosis in humans, most addressed only a single liver disease at a time, and therefore, their fibrosis gene signatures may not be applicable to other liver diseases (6-10). Of these studies, only one conducted a whole genome transcriptomics study in patients with different chronic liver diseases (55 with chronic HCV, 12 with NAFLD, and 2 with ALD) at a time (10). They identified expression of 12 fibrosis genes were significantly correlated with serum enhanced liver fibrosis score (r^2=0.39-0.50) (10). However, 80% of samples were chronic HCV and thus it is questionable if the genes they discovered can represent the common fibrosis genes in different chronic liver diseases, or only specifically to chronic HCV. There is a need for a comprehensive analysis including a larger sample size and a diverse types of chronic liver diseases to identify a common fibrosis gene signature for advanced fibrosis in humans.

There is a significant diversity in outcomes among patients with chronic liver diseases. Approximately 20-30% of patients with chronic liver disease progress to advanced fibrosis/cirrhosis, whereas others remain stable (11-13). Cirrhosis is responsible for 1.03 million deaths each year and this is why recent guidelines strongly recommended consideration of pharmacotherapy in patients with advanced fibrosis or without advanced fibrosis but at high-risk for fibrosis progression (14, 15). Although currently there is no Food and Drug Administration (FDA) approved drug for liver fibrosis, there are several liver antifibrotic drugs in phase 3 or 4 clinical trials, of which some are expected to report the initial study results around 2021 (16). These therapeutic approaches are most relevant to NAFLD, as there is no cure nor a unified approach to entirely eliminate the underlying metabolic risk factors such as diabetes or hyperlipidemia. Since there is a huge heterogeneity for disease outcomes, there is an unmet clinical need for a surrogate biomarker test to accurately identify high-risk patients who may benefit from upcoming drug treatments to prevent liver damage and adverse outcomes. Transcriptomics of sampled liver biopsies with different liver diseases at various stages of fibrosis may help delineate genes (mRNA level) that are differentially expressed and what pathways they might regulate.

This chapter aim to discover and validate a common molecular signature associated with advanced fibrosis that is shared by different liver diseases in humans using a systematic, unbiased, multi-centered, microarray based transcriptomic analysis of normal livers and livers with different chronic liver diseases.

2.2 – Materials and methods

2.2.1 – Search for microarrays of human liver tissue

I conducted a web-based search using the National Center for Biotechnology Information Gene Expression Omnibus datasets, with "liver" and "fibrosis" as keywords and identified files from Affymetrix Human Genome U133 Plus 2.0 Arrays of normal or chronic liver disease adult human liver tissues with individual-patient level of histological fibrosis staging in October 2014 (Figure 2.1). Liver tissues with hepatocellular carcinoma (HCC) or dysplastic nodules were excluded. Based on these criteria, five independent studies (GSE49541, GSE7741, GSE17548, GSE6764, GSE28619) were identified and included for a total of 140 microarrays of livers from 148 patients. These raw microarray files were downloaded from National Center for Biotechnology Information Gene Expression Omnibus datasets (6, 7, 17-19). After data preprocessing, 140 microarrays were separated equally and randomly based on disease label and fibrosis stage into a discovery set (n=70) and an independent validation set 1 (n=70) (blinded to the molecular results). A common molecular signature for advanced fibrosis was defined in the discovery set and validated in validation set 1. To analyze if the common molecular signature can be validated in different batches of microarrays from the same and different microarray platforms, two additional series of liver gene expression data set from 91 patients with viral hepatitis (GSE84044, platform: Affymetrix Human Genome U133 Plus 2.0 Array) and 73 patients with ALD (GSE103580, platform: Affymetrix Human Genome U219 Array) were included for use as an independent validation set 2 and validation set 3, respectively (9, 20).

Microarrays were characterized into two groups based on the severity of fibrosis: no

or mild fibrosis and advanced fibrosis. No or mild fibrosis was defined as histological examination without fibrosis or any degree of fibrosis without bridging fibrosis and advanced fibrosis was defined as the presence of bridging fibrosis or cirrhosis.

2.2.2 – Data preprocessing

Microarrays in the discovery set and validation set 1 were pooled in one batch and preprocessed using robust multi-array averaging method (Figure 2.2). Validation set 2 and 3 were processed independently using robust multi-array averaging method. Probe sets with less variability across the microarrays in each batch were removed using the procedure as follows (21):

Step 1. Calculate the median expression value of each probe set in each batch.

Step 2. Divide each probe set expression value by the median expression value to obtain a fold-change value.

Step 3. If less than 20% of microarrays have a >1.5 or <-1.5 fold-change value, the probe set was excluded.

Next, to select the best probe set for a gene, the maximally expressed probe set measured by average intensity in a batch was used to represent the gene.

2.2.3 – Machine learning classifiers development, cross-validation, and external validation

To avoid the idiosyncrasies of any particular machine learning method, seven different machine learning methods (Compound Covariate Predictor, Diagonal Linear Discriminant Analysis, 1-Nearest Neighbor Predictor, 3-Nearest Neighbors Predictor,

Nearest Centroid Predictor, Support Vector Machine Predictor, and Bayesian Compound Covariate Predictor) were applied to build classifiers for identifying histologically-proven advanced fibrosis using the discovery set (22). The threshold of predicted probability for a sample being assigned to a class in Bayesian Compound Covariate Predictor was 0.8 (23). Diagnostic performance of classifiers in discovery set was obtained using 10-fold cross-validation and validated in validation set 1. The 10-fold cross-validation method was used as follows:

Step 1. Microarrays in the discovery set were randomly partitioned into 10 equal-sized subsets.

Step 2. A single subset was retained as the validation data. The remaining nine subsets were used to develop classifiers and predict the retained single subset.

Step 3. Repeat step 2 ten times. Each of the 10 subsets was predicted exactly once, so that by the end of the procedure, all the microarrays in the discovery set had a single prediction result.

2.2.4 – Performance measurements of the classifiers and biomarker test for advanced fibrosis

Sensitivity, specificity, positive predictive value, negative predictive value, accuracy, and area under the receiver operating characteristic curve (AUROC) values were calculated for the classifiers and biomarker test.

2.2.5 – Pathway and functional enrichment analysis

Pathway and functional enrichment analysis were conducted using the Database for

Annotation, Visualization and Integrated Discovery (v6.7, http://david.abcc.ncifcrf.gov/) and Ingenuity Pathways Analysis (Ingenuity systems, Inc., Redwood City, CA, www.ingenuity.com).

2.2.6 – Molecular interaction analysis

ConsensusPathDB (http://cpdb.molgen.mpg.de/) was used to analyze the high confidence protein-protein interactions, gene regulatory interactions, biochemical reactions, and drug-target interactions. ConsensusPathDB combines 32 public databases for interactions and interactions curated from peer reviewed literature. Analyzed results were visualized using Cytoscape (http://www.cytoscape.org/).

2.2.7 – Cellular origin of the molecular fibrosis signature

The molecular fibrosis signature was linked to liver cell types using two human liver cell atlases via single cell RNA sequencing (24, 25). One atlas contained nine normal liver tissues (http://human-liver-cell-atlas.ie-freiburg.mpg.de/) and the other contained five normal liver tissues and five cirrhotic liver tissues (2 with NAFLD, 2 with ALD, and 1 with primary biliary cholangitis) (http://www.livercellatlas.mvm.ed.ac.uk/).

The atlas of nine normal liver tissues comprises clusters of major liver cell types including hepatocytes, EPCAM+ cells and cholangiocytes, liver sinusoidal endothelial cells, macrovascular endothelial cells, hepatic stellate cells (HSCs) and myofibroblasts, Kupffer cells, and nature killer, nature killer T, and T cells (24). A gene was labeled as up-regulated in a specific cluster of cell type if the gene expression was significantly up-regulated (Benjamini-Hochberg's corrected p-value <0.05) when compared to all other clusters of cell

types.

The atlas with normal and cirrhotic liver tissues comprises clusters of major liver cell types including B cells, cycling cells, endothelial cells, epithelial cells, innate lymphoid cells, mast cells, mesenchymal cells, mononuclear phagocytes, plasmacytoid dendritic cells, plasma cells, and T cells (25). They conducted differential gene expression analysis between single cell types from cirrhotic versus normal liver using the standard AUROC classifier to assess significance.

2.2.8 – Statistical analysis

Continuous variables were presented as mean ± standard deviation and categorical variables were presented as number and percentage. All data were compared between groups using independent t-test, Mann-Whitney U-test or Wilcoxon signed-rank test for continuous variables, where appropriate, and Fisher's exact test for categorical variables. P-values for multiple testing were corrected by Benjamini-Hochberg's method to control the false discovery rate at 5%. Correlations between variables were evaluated using Spearman's rank correlation coefficient. All tests with two-sided p-value <0.05 were considered significant. All analyses and figures were performed generated using the SPSS 25 statistical software (IBM, Armonk, NY, USA), Excel 2010 (Microsoft Corporation, Redmond, WA), BRB-ArrayTools (version 4.5.0 - stable) (http://linus.nci.nih.gov/BRB-ArrayTools.htm), or R-program (version 3.3.2; http://www.r-project.org) with the following packages: ggplot2, gplot, pROC, and corrplot.

2.3 – Results

2.3.1 – Clinical characteristics of the study population

A total of 304 microarrays of livers from 312 patients with different liver diseases were analyzed. These microarrays included 72 NAFLD, 88 ALD, 122 viral hepatitis, 5 cryptogenic hepatitis, and 17 normal livers (Figure 2.1 and 2.3, Table 2.1). Of 312 livers, 262 were obtained by needle biopsy and 50 by resection. Each microarray was hybridized with one RNA sample of a liver from a patient except for the three microarrays from center 2 (Figure 2.3). Of these three microarrays, two were hybridized with a pool of liver RNA samples from four patients and one was hybridized with a pool of liver RNA samples from three patients (6). The liver tissues that were pooled together were in the same histological fibrosis group. Of total 304 microarrays, 127 had no or mild fibrosis and 177 had advanced fibrosis (Figure 2.3).

2.3.2 – Development and validation of machine learning classifiers for identifying advanced fibrosis

Seven different classifiers were developed to identify advanced fibrosis in discovery set and then the classifiers were validated in validation set 1 (Figure 2.4). To avoid bias in gene selection, two sets of genes were used to develop classifiers: all 6,951 genes that passed data preprocessing and 1,294 differentially expressed genes between advanced and no or mild fibrosis (independent t-test, $p<0.001$) in the discovery set. In the discovery set, classifiers with 1,294 differentially expressed genes had significantly higher accuracy for histology-proven advanced fibrosis compared to classifiers with 6,951 genes (mean 83% vs.

74% accuracy, respectively, p=0.018) (Figure 2.5). In validation set 1, classifiers with 1,294 differentially expressed genes also had significantly higher accuracy for histology-proven advanced fibrosis compared to classifiers with 6,951 genes (mean 83% vs. 75% accuracy, respectively, p=0.016) (Figure 2.5). Among the seven different classifiers with 1,294 differentially expressed genes, the Support Vector Machine Predictor had the highest accuracy for histology-proven advanced fibrosis in both the discovery set (94%) and validation set 1 (94%).

2.3.3 – Use of classifiers to develop a biomarker test for advanced liver fibrosis

Despite the robust performance of machine learning classifiers, it may be difficult and costly to measure the expression of 1,294 genes in a clinical biomarker test. To shorten the gene list, I identified a top 50-gene subset of the most differentially expressed genes (top 50 genes with smallest Benjamini-Hochberg's false discovery rate corrected p-value) between advanced vs. no or mild fibrosis in the discovery set (Table 2.2). Of these 50 genes, 48 were up-regulated and two were down-regulated in advanced fibrosis. To achieve the best performance for advanced fibrosis, I analyzed three different subsets of genes: top 50 differentially expressed genes (up-regulated and down-regulated), top 48 up-regulated, differentially expressed genes, and top 51 to 100 differentially expressed genes (Figure 2.4). A molecular score was assigned for each sample by calculating geometric mean expression of the genes in each subset. The 48 up-regulated genes had the best diagnostic performance (AUROC = 0.994) for advanced fibrosis (Figure 2.6A) compared to the top 50 differentially expressed genes (AUROC = 0.993) (Figure 2.7A) and the top 51 to 100 differentially expressed genes (AUROC = 0.987) (Figure 2.8A). Unsupervised hierarchical analysis of the 48 up-regulated genes clustered patients into advanced fibrosis or no/mild fibrosis with high

accuracy (Figure 2.6A and 2.6B). A 48-gene signature score cutoff (Youden index = 6.185) for advanced fibrosis was derived by the receiver operating characteristic curve analysis in the discovery set (Figure 2.6A). This cutoff (geometric mean expression of 48 genes = 6.185) had 95% sensitivity, 97% specificity, 98% positive predictive value, 93% negative predictive value, 96% accuracy, and 0.994 AUROC (95% confidence interval 0.983-1.000) for advanced fibrosis. Based on the selected cutoff, only 3 out of 70 (4%) samples were misclassified compared to the histological label. (Figure 2.6C). The 48-gene signature had a better performance (AUROC = 0.994) for histology-proven advanced fibrosis than any 48 individual genes in the discovery set (AUROC range 0.894-0.982) (Table 2.2).

2.3.4 – External validation of the biomarker test

The molecular score cutoff of three subsets of genes derived in the discovery set were validated in validation set 1. Validated results showed the 48-gene had the best diagnostic performance (AUROC = 0.994, Figure 2.9A) for advanced fibrosis when compared to the top 50 differentially expressed genes (AUROC = 0.992, Figure 2.7B) and the top 51 to 100 differentially expressed genes (AUROC = 0.991, Figure 2.8B). Unsupervised hierarchical analysis of 48 up-regulated genes clustered patients into advanced fibrosis or no/mild fibrosis with high accuracy (Figure 2.9A and 2.9B). The 48-gene signature score cutoff (6.185) derived in the discovery set had 95% sensitivity, 97% specificity, 98% positive predictive value, 93% negative predictive value, 96% accuracy, and 0.994 AUROC (95% confidence interval 0.983-1.000) for advanced fibrosis in validation set 1 (Figure 2.9A). Based on discovery set derived cutoff, only 3 out of 70 (4%) samples were misclassified compared to the histological label (Figure 2.9C). The 48-gene signature had a better performance (AUROC = 0.994) for histology-proven advanced fibrosis than any 48 individual genes in

the validation set 1 (AUROC range 0.795-0.985) (Table 2.3).

The 48-gene signature was further validated in validation set 2 (91 patients with viral hepatitis) and validation set 3 (73 patients with ALD) and had robust performance for histology-proven advanced fibrosis in both sets (validation set 2: AUROC = 0.964, 93% accuracy, Figure 2.10A; validation set 3: AUROC = 0.993, 99% accuracy, Figure 2.10B). The robust performance of the 48-gene signature for histology-proven advanced fibrosis in all three validation sets with different chronic liver diseases supported that the 48-gene signature is a common molecular signature for advanced liver fibrosis and independent to the etiologies.

2.3.5 – Pathway and functional enrichment analysis

Gene Ontology identified the 48-gene signature was enriched in a variety of biological functions, mostly involved with extracellular matrix, such as extracellular matrix organization in the biological process category, extracellular matrix in the cellular component category, and the extracellular matrix structural constituent in the molecular function category (Table 2.4). Collagens, which play an important role in liver fibrosis, were involved in almost all biological functions. The only function without a collagen gene was calcium ion binding, which was equally important in cellular signaling cascades and may play a prominent role in fibrosis. Kyoto Encyclopedia of Genes and Genomes pathway analysis indicated that the 48-gene signature was most significantly enriched for extracellular matrix-receptor interaction (Table 2.5).

Ingenuity Pathways Analysis was used to identify the biological processes that were overrepresented in the 48-gene signature (Table 2.6). All of the 48 genes were associated

with cancer and 36 were associated with liver hyperplasia/hyperproliferation. This was reasonable because advanced liver fibrosis is known as a major risk factor for HCC and cirrhosis is characterized by regenerative liver cell nodules. Ingenuity Pathways Analysis identified that transforming growth factor-β 1 (TGFβ1), an important fibrogenic mediator, was a significant upstream regulator in the 48-gene signature ($p=1.57 \times 10^{-7}$) (Figure 2.11). All these results supported that the 48-gene signature was significantly involved in liver fibrogenesis.

2.3.6 – Protein and transcription factors interaction analysis

To investigate the mechanisms that regulate the protein functions of the 48-gene signature, the protein-protein interactions were analyzed via consensusPathDB (Figure 2.12A). Overall, the corresponding protein of the 48-gene signature interacted with proteins that were involved in liver fibrogenesis, such as hepatic stellate cells (HSCs) activation or proliferation (SAA1, HABP2, PDGFB) (26, 27), liver fibrogenesis (TGFβ1, OSM, LTBP2, SERPINE2, collagen genes) (28, 29), collagen cross-linkage (LOX) (30), and hepatocyte proliferation (hepassocin) (31). These results supported that the 48-gene signature played an important role in liver fibrogenesis at protein level.

I also analyzed gene regulatory interactions and biochemical reactions of the 48-gene signature and found microRNA 29 (has-miR-29) members reacted with several collagen genes in the 48-gene signature (Figure 2.12B). has-miR-29 members could silence the expression of collagen genes and were known to be significantly down-regulated in advanced liver fibrosis (32). This gave an insight that has-miR-29 might be a potential biomarker for advanced liver fibrosis and activating has-miR-29 may reduce liver fibrosis.

2.3.7 – Cellular origins involved in hepatic fibrosis

The proposed cellular sources of extracellular matrix accumulation during chronic liver injury are driven by a heterogeneous population of cells in the liver, majority from HSCs and hepatic progenitor cells (HPCs) (33, 34). However, most of the data were derived from rodent or in vitro experimental models, thus cellular origins of liver fibrosis in humans remains elusive. Here, I investigated the correlation between the expression of 14 HSC and 10 HPC markers (literature-selected) vs. the expression of the eight collagen genes in the 48-gene signature (Table 2.7). Two HPC markers, CD24 and KRT7, which were in the 48-gene signature, had a high correlation ($r > 0.7$) with the geometric mean expression of 8 collagen genes in all four datasets (discovery set, validation set 1, validation set 2, validation set 3). Interestingly, none of the HSC markers had high correlation ($r>0.7$) with the geometric mean expression of the collagen genes. Some well-known HSC markers (desmin, GFAP, synaptophysin) were excluded after data preprocessing and this meant the expression of these markers did not alter in different fibrosis stages (Table 2.7). Specifically, I compared the expression of each cellular origin marker gene with each collagen gene and found that CD24 and KRT7 had significant positive correlation with all eight individual collagen genes in all four datasets (Table 2.8). Correlation heatmap showed the expression of HPC markers had significantly higher correlation with the collagen genes than HSC markers in the discovery set (mean correlation 0.575 ± 0.183 vs. 0.232 ± 0.404, $p<0.001$), validation set 1 (mean correlation 0.664 ± 0.205 vs. 0.225 ± 0.393, $p<0.001$), validation set 2 (mean correlation 0.629 ± 0.141 vs. 0.369 ± 0.296, $p<0.001$), and validation set 3 (mean correlation 0.422 ± 0.213 vs. 0.193 ± 0.370, $p<0.001$) (Figure 2.13). These results suggest that HPC proliferation may play a major role in human liver fibrogenesis and HPC markers such as CD24 and KRT7

may serve as potential biomarkers for advanced fibrosis, independent of etiologies.

2.3.8 – Cellular origins of the 48-gene signature

The 48 fibrosis genes were analyzed in a human single liver cell RNA sequencing atlas derived from normal liver tissues and a HSC gene signature reported by Zhang et al. (24, 35). Of the 48 fibrosis genes, most of the genes were up-regulated in $EPCAM^+$ cells and cholangiocytes (35%), followed by HSCs and myofibroblasts (27%), macrovascular endothelial cells (21%), sinusoidal endothelial cells (13%), Kupffer cells (2%), nature killer, nature killer T, and T cells (2%), and hepatocytes (2%) (Figure 2.14, Table 2.9).

The 48 fibrosis genes were also analyzed in another human single liver cell RNA sequencing atlas constructed using five normal and five cirrhotic liver tissues (25). Of the 48 fibrosis genes, most of the genes were significantly up-regulated in epithelial cells (19%) in cirrhotic livers, followed by mesenchymal cells (vascular smooth muscle cells, HSCs, fibroblasts) (13%), and endothelial cells (10%) (Figure 2.15, Table 2.10).

These results support the correlation analyses in section 2.3.7 that single cell RNA data suggest that HPCs followed by myofibroblasts/HSC and endothelial cells are the major cellular origin of the 48-gene signature of advanced liver fibrosis.

2.3.9 – The expression of liver antifibrotic drug targets in the datasets

Currently, no animal models can faithfully represent the hepatic features of human liver disease and there is lack of molecular data of liver fibrosis in human. This explains the positive findings from an antifibrotic therapies developed in animal models, but same drugs were not effective in humans. Transcriptomic analyses in human liver tissues may overcome this gap to identify drugs that are already in trials and see if any of these drugs can be

repurposed or to offer explanation as to why certain drugs failed to prevent fibrosis in a clinical setting. Here, I selected antifibrotic drugs searched on ClinicalTrials.gov that had a primary molecular target and showed the molecular target gene expression fold-changes between advanced and no or mild fibrosis in NAFLD, viral hepatitis, and ALD samples. This was used as a representative of human hepatic fibrosis molecular data (Table 2.11). I found the expression of CCR2 and CCR5 (molecular target of Cenicriviroc, an antifibrotic drug in phase 3 trial for treating non-alcoholic steatohepatitis [NASH]) were significantly upregulated in NAFLD samples with advanced fibrosis. The fold-change for CCR2 and CCR5 was 1.33 ($p=0.002$) and 1.17 ($p=0.016$), respectively (Table 2.11). The expression of CCR2 and CCR5 were also significantly up-regulated in viral hepatitis samples with advanced fibrosis, with a fold-change of 1.16 ($p<0.001$) and 1.15 ($p<0.001$), respectively. These results supported that CCR2 and CCR5 were significantly up-regulated in advanced fibrosis and could be a driver for fibrosis progression in both NAFLD and viral hepatitis.

The expression of several antifibrotic drug targets in NASH phase 3 trials (Losartan, Obeticholic acid, Selonsertib, Elafibranor, Aramchol, Metadoxine) had no significant difference between advanced and no or mild fibrosis in the NAFLD samples (Table 2.11). I also found the expression of LOXL2, the molecular target of Simtuzumab, was not significantly upregulated in viral hepatitis samples with advanced fibrosis and this may be the reason of Simtuzumab was ineffective in decreasing liver fibrosis in a phase 2 clinical trial of patients with HCV, as the expression of LOXL2 was similar between advanced and no or mild fibrosis (36). However, LOXL2 was significantly upregulated in NAFLD samples but Simtuzumab was also ineffective in decreasing liver fibrosis in a phase 2 clinical trial (37). This could be explained as although LOXL2 was significantly up-regulated in advanced

fibrosis, inhibition of LOXL2 was insufficient to reduce liver fibrosis.

2.3.10 – Multicenter impact of the 48-gene signature

The 48-gene signature with the same liver disease and fibrosis group from different centers was assessed for multicenter impact. Only normal and viral hepatitis samples were compared because they were analyzed by the same microarray platform and had samples from multiple centers. The 48-gene signature in both normal and viral hepatitis samples were similar across different centers (Figure 2.16). This showed that the 48-gene signature was not impacted by different centers.

2.4 – Discussion

This is the first comprehensive collection of gene expression signatures that drives advanced liver fibrosis in the context of various common causes of liver disease in humans. I analyzed 304 microarrays of livers from 312 patients and identified a 48-gene signature associated with advanced liver fibrosis that is shared by different chronic liver diseases. The 48-gene signature was identified in a discovery set and validated in three independent validation sets with over 93% accuracy for advanced fibrosis. Pathway and functional enrichment analysis revealed the 48-gene signature is significantly involved in hepatic fibrosis, HSCs activation, and HCC. Molecular interaction analysis also revealed the 48-gene signature is involved in HSCs activation and HPCs proliferation. These results supported that the 48-gene signature is a common molecular signature for advanced fibrosis in different chronic liver diseases.

During the search in the National Center for Biotechnology Information Gene

Expression Omnibus, I found six other human liver studies that used different microarray platforms to analyze the relation of gene expression and different severity of fibrosis (8, 38-42). These microarrays were not included as an external validation set in this chapter due to small sample size. Three studies identified differentially expressed genes between advanced and no or mild fibrosis in patients with HCV (8, 38, 41). The fibrosis genes that they discovered had no overlap with the 48-gene signature. This might be caused by the small sample size (n=9, 18, 16 patients analyzed in reference 8, 38, and 41, respectively) with less than 10 patients in each fibrosis subgroup when identifying differentially expressed genes and resulted in limited statistical power (8, 38, 41). Two studies identified differentially expressed genes between normal and cirrhotic liver tissues (40, 42). As they compared normal vs. cirrhotic livers, I would expect collagen genes as the top differentially expressed genes in their gene list. However, no collagen genes were present in both studies. This could also be caused by small sample size (n=42, 22 patients analyzed in reference 40 and 42, respectively), which cause limited statistical power (40, 42). One study identified genes that were differentially expressed between normal and different severity of NAFLD in 63 patients (39). However, they did not have patients with advanced fibrosis (≥F3). Due to the abovementioned, these datasets were not used to validate the 48-gene signature.

Of the 48 fibrosis genes, 35 were previously associated with liver fibrosis and 13 are novel targets (Table 2.2). In our study, KRT7, CD24 and EPCAM are among top upregulated genes in advanced fibrosis and they are known to be expressed by HPCs and biliary epithelial cells. When the liver is injured, the expression of HPC markers may be increased due to ductular proliferation, as ductular reaction has been reported in some forms of chronic liver disease and is a common feature in nonbiliary type of cirrhosis. Moreover, the expression of

these three genes were significantly and highly correlated with the expression of collagen genes in all discovery and validation sets (Table 2.7). Currently, it is yet unknown if matrix deposition is beneficial for HPC-associated regenerative response or whether fibrosis is exacerbated by the HPC activation (33). The significant correlation between the expression of HPC markers and collagen genes suggests that HPC activation may cause exacerbation of fibrosis and this is a shared feature of different chronic liver diseases in humans.

In upstream analysis, TGFβ1 was a significant upstream regulator in the 48-gene signature (Figure 2.11). There are antifibrotic drug trials targeting mediators in the TGFβ1 signaling pathway to inhibit fibrogenesis in liver fibrosis (clinical trial identifier: NCT01217632) and idiopathic pulmonary fibrosis (NCT01371305, NCT03573505). Targeting mediators of TGFβ1 may be an effective antifibrotic strategy because it is an upstream regulator of many pathways involved in liver fibrogenesis.

miRNAs can regulate the expression of multiple gene transcripts. In the molecular interaction analysis, hsa-miR-29 emerges as an important regulator molecule for the 48-gene signature (Figure 2.12B). Down-regulation of hsa-miR-29 was reported to induce HSC activation and liver fibrogenesis (32). Hence, hsa-miR-29 might be a potential therapeutic target for liver fibrosis. A hsa-miR-29 mimic, MRG-201, is tested in a phase 1 clinical trial as an antifibrotic therapy for skin fibrosis (NCT02603224).

The 48-gene signature could be used to stratify patients as predictive or surrogate biomarker test in antifibrotic drug clinical trials. Individually, the 48 genes could also be explored as targets for novel therapeutics development. In phase 3 clinical trials for treating NASH, Farnesoid X receptor (FXR) and apoptosis signal-regulating kinase 1 (ASK1) were selectively targeted by Obeticholic acid and Selonsertib, respectively. I found the expression

of FXR and ASK1 had no significant difference between advanced and no or mild fibrosis samples with NAFLD (Table 2.10) in this chapter. In a NASH phase 2 trial, NASH patients with diabetes treated with Obeticholic acid had a significant fibrosis improvement (odds ratio [OR] = 4.6, 95% confidence interval [CI] 2.0-10.6, p=0.0003), but not in patients without diabetes (OR = 2.0, 95% CI 0.8-4.7, p=0.12) (43). Of the NAFLD samples in this chapter, only 37.5% (27 of 72) had diabetes (7), and this could be the reason of why FXR expression was similar between advanced and no or mild fibrosis. In a Selonsertib phase 2 trial, 43% (13 of 30) of NASH patients treated with 18 mg of Selonsertib daily had improvement in fibrosis compared to 30% (8 of 27) treated with 9 mg of Selonsertib and 20% (2 of 10) in the placebo group (44). However, the improvement was not statistically significant. Based on the expression of FXR and ASK1 in the NAFLD samples included in this chapter, these drugs may not be effective enough to yield a significant therapeutic response to reduce fibrosis. In phase 2 clinical trials, Simtuzumab, an LOXL2 inhibitor, was ineffective for patients with NASH, HCV, and primary sclerosing cholangitis (36, 37, 45). The expression of LOXL2 was similar between advanced and no or mild fibrosis in viral hepatitis samples, but significantly upregulated in NAFLD samples with advanced fibrosis. This could reflect expression levels of LOXL2 increase in NAFLD patients with advanced fibrosis but inhibiting LOXL2 was insufficient to reduce fibrosis as there are other LOX isoforms that mediate collagen cross-linkage. Moreover, fibrosis progression in NAFLD has diverse mechanisms (e.g. modulation of different metabolic pathways, different inflammatory cascades, myofibroblast activation, collagen cross-linkage) of liver injury that differ between individuals but may present with a similar histological phenotype. Therefore, single antifibrotic therapy is unlikely to be effective in all patients with NAFLD. Combining

therapies that engage different targets which were significantly upregulated in advanced fibrosis may provide a synergistic antifibrotic benefit.

The 48-gene signature has the potential to develop novel non-invasive biomarkers as surrogates for liver biopsy to assess liver fibrosis. Current serum-based approaches lack specificity, as they could detect fibrogenic activity in other organs as well. Diagnostic performance of these approaches could vary in patients with different chronic liver diseases and had only AUROC scores of ~0.8 for advanced fibrosis (46). The 48-gene signature could reflect changes of fibrogenic activity in different chronic liver diseases. The 48-gene signature had at least 0.96 AUROC for advanced fibrosis in three validation sets, which was better than any previous reported non-invasive approaches. The 48-gene signature could be further tested on specimen that can be obtained noninvasively, such as serum samples, to assess which gene is able to translate to protein and which of these proteins are detectable in blood circulation to accurately reflect liver tissue pathology.

Despite its merits, this chapter had a limitation that is important to acknowledge. The samples analyzed in this chapter had extreme histology phenotype (F0-F1 versus F3-F4) and lack of samples with intermediate level of fibrosis (F2). F2 fibrosis samples were excluded because they have mixed molecular phenotype and excluding them could increase the power to identify a more significant fibrosis gene signature. This line of reasoning also has its merits in that extremes of phenotypes are often preferred in single nucleotide polymorphism (SNP) based association studies, and gene expression-based studies are no exception. However, the concern if the 48-gene signature is also effective in fibrosis progression in chronic liver disease patients with F2 fibrosis still needs to be addressed. Therefore, I present a multicenter, longitudinal study of total 299 patients with recurrent HCV (post-transplant,

Chapter 4), autoimmune hepatitis (Chapter 5), and NAFLD (Chapter 6) with all fibrosis stages (F0 to F4) to validate the results.

In this chapter, I identified and validated a common 48-gene signature that drives advanced liver fibrosis in various chronic liver diseases. This new understanding defines a quantitative surrogate biomarker for advanced liver fibrosis. The 48-gene signature can be beneficial if incorporated into future clinical studies of the natural history of liver fibrosis and therapeutic intervention.

Table 2.1. The condition of microarrays in the discovery and validation sets

Condition	Discovery set		Validation set 1		Validation set 2		Validation set 3		Total
	No or mild fibrosis	Advanced fibrosis	No or mild fibrosis	Advanced fibrosis	No or mild fibrosis	Advanced fibrosis	No or mild fibrosis	Advanced fibrosis	
Normal, n	8	0	9	0	0	0	0	0	17
NAFLD, n	20	16	20	16	0	0	0	0	72
Alcoholic liver disease, n	0	8	0	7	0	0	6	67	88
Viral hepatitis, n	1	14	0	16	63	28	0	0	122
Cryptogenic hepatitis, n	0	3	0	2	0	0	0	0	5
Total	29	41	29	41	63	28	6	67	304

Table 2.2. The list of top 50 differentially expressed genes and fold-changes between advanced and no or mild fibrosis in the discovery set

Gene	Official gene name	Function	Fold change	Corrected p-value	AUROC	Link to fibrosis
BICC1	BicC family RNA binding protein 1	Wnt signaling	↑4.33	2.08×10^{-15}	0.982	Previously reported (7)
NALCN	Sodium leak channel, non-selective	Ion transporter	↑2.53	9.60×10^{-15}	0.976	Previously reported (7)
THBS2	Thrombospondin 2	Contribute to the structural integrity of the ECM	↑3.49	1.27×10^{-14}	0.976	Previously reported (7)
DCDC2	Doublecortin domain containing 2	Wnt signaling	↑4.73	2.63×10^{-13}	0.966	Previously reported (7)
LTBP2	Latent transforming growth factor beta binding protein 2	Contribute to the structural integrity of the ECM	↑1.79	8.47×10^{-11}	0.960	Previously reported (10)
ITGBL1	Integrin, beta-like 1	Integrin binding	↑3.18	4.92×10^{-13}	0.958	Previously reported (7)
COL4A4	Collagen, type IV, alpha 4	Contribute to the structural integrity of the ECM	↑2.41	8.74×10^{-12}	0.955	Previously reported (5)
COL1A1	Collagen, type I, alpha 1	Contribute to the structural integrity of the ECM	↑5.06	2.22×10^{-13}	0.954	Previously reported (5)
EPCAM	Epithelial cell adhesion molecule	Cell proliferation and differentiation	↑7.40	6.28×10^{-11}	0.954	Previously reported (7)
MAP1B	Microtubule-associated protein 1B	Microtubule binding	↑2.46	2.40×10^{-12}	0.954	Previously reported (7)
CD24	CD24 molecule	Cell proliferation and differentiation	↑4.37	7.66×10^{-13}	0.952	Previously reported (7)
CXCL6	Chemokine ligand 6	Inflammatory response	↑6.79	7.15×10^{-12}	0.944	Previously reported (7)
SOX9	SRY (sex determining region Y)-box 9	Cell proliferation and differentiation	↑3.37	1.10×10^{-10}	0.944	Previously reported (7)
KRT7	Keratin 7	Cell proliferation and differentiation	↑3.01	1.17×10^{-9}	0.943	Previously reported (10)
C1orf198	Chromosome 1 open reading frame 198	Unknown	↑2.12	3.68×10^{-10}	0.942	Previously reported (7)
ANTXR1	Anthrax toxin receptor 1	Interact with collagen	↑2.45	1.05×10^{-11}	0.940	Previously reported (7)
HEPH	Hephaestin	Ion transporter	↑1.88	1.44×10^{-11}	0.940	Novel
SLC38A1	Solute carrier family 38, member 1	Amino acid transporter	↑3.50	1.09×10^{-10}	0.939	Novel
COL1A2	Collagen, type I, alpha 2	Contribute to the structural integrity of the ECM	↑3.40	6.38×10^{-11}	0.937	Previously reported (7)
CACNA2D1	Calcium channel, voltage-dependent, alpha 2/delta subunit 1	Ion transporter	↑2.08	1.20×10^{-10}	0.936	Novel
COL6A3	Collagen, type VI, alpha 3	Contribute to the structural integrity of the ECM	↑2.19	1.03×10^{-10}	0.935	Previously reported (7)
TMEM200A	Transmembrane protein 200A	Unknown	↑2.24	1.86×10^{-9}	0.934	Novel
FBN1	Fibrillin 1	Contribute to the structural integrity of the ECM	↑2.33	4.06×10^{-10}	0.932	Previously reported (7)
SH3YL1	SH3 and SYLF domain containing 1	Regulation of ruffle assembly	↑2.54	3.41×10^{-9}	0.932	Novel
C7	Complement component 7	Complement activation	↑2.47	1.23×10^{-9}	0.931	Previously reported (7)
COL4A1	Collagen, type IV, alpha 1	Contribute to the structural integrity of the ECM	↑2.56	1.67×10^{-9}	0.931	Previously reported (7)
DKK3	Dickkopf WNT signaling pathway inhibitor 3	Wnt signaling	↑2.89	1.37×10^{-11}	0.929	Previously reported (7)
AQP1	Aquaporin 1	Cell proliferation and differentiation	↑4.24	1.62×10^{-10}	0.928	Previously reported (7)
EPHA3	EPH receptor A3	Inflammation	↑3.92	1.17×10^{-11}	0.925	Previously reported (7)

MAP2	Microtubule-associated protein 2	Microtubule binding	↑2.00	$3.71x10^{-10}$	0.924	Previously reported (10)
DTNA	Dystrobrevin, alpha	Dystrophin	↑2.95	$2.99x10^{-10}$	0.923	Previously reported (10)
EFEMP1	EGF containing fibulin-like extracellular matrix protein 1	Contribute to the structural integrity of the ECM	↑5.60	$7.52x10^{-12}$	0.923	Previously reported (7)
COL3A1	Collagen, type III, alpha 1	Contribute to the structural integrity of the ECM	↑2.44	$1.25x10^{-10}$	0.920	Previously reported (7)
CDH11	Cadherin 11, type 2, OB-cadherin	Contribute to the structural integrity of the ECM	↑3.53	$1.79x10^{-10}$	0.918	Novel
NAV3	Neuron navigator 3	Microtubule binding	↑1.85	$2.30x10^{-9}$	0.917	Novel
RCAN2	Regulator of calcineurin 2	Nucleic acid binding	↑2.57	$5.63x10^{-10}$	0.917	Novel
JAG1	Jagged 1	Mediation of Notch signaling	↑2.52	$4.48x10^{-9}$	0.916	Previously reported (7)
LAMB1	Laminin, beta 1	Contribute to the structural integrity of the ECM	↑2.45	$6.28x10^{-10}$	0.915	Previously reported (47)
COL14A1	Collagen, type XIV, alpha 1	Contribute to the structural integrity of the ECM	↑2.22	$2.07x10^{-9}$	0.910	Previously reported (7)
COL4A2	Collagen, type IV, alpha 2	Contribute to the structural integrity of the ECM	↑2.60	$5.37x10^{-9}$	0.909	Previously reported (5)
FAM169A	Family with sequence similarity 169, member A	Unknown	↑2.42	$1.10x10^{-9}$	0.909	Novel
FAT1	FAT atypical cadherin 1	Epithelial to mesenchymal transition	↑2.83	$4.43x10^{-10}$	0.905	Novel
EHF	Ets homologous factor	Epithelial to mesenchymal transition	↑2.69	$3.59x10^{-9}$	0.903	Previously reported (7)
LUM	Lumican	Contribute to the structural integrity of the ECM	↑2.69	$2.60x10^{-9}$	0.903	Previously reported (7)
IGFBP7	Insulin-like growth factor binding protein 7	Contribute to the structural integrity of the ECM	↑2.00	$1.70x10^{-9}$	0.902	Previously reported (7)
GPRC5B	G protein-coupled receptor, class C, group 5, member B	Signal transduction	↑2.07	$4.85x10^{-9}$	0.898	Novel
MOXD1	Monooxygenase, DBH-like 1	Ion binding	↑2.36	$7.41x10^{-10}$	0.898	Novel
GSN	Gelsolin	Regulation of apoptosis	↑2.83	$1.97x10^{-9}$	0.894	Novel
THOP1	Thimet oligopeptidase 1	Peptide degradation	↓0.51	$3.22x10^{-9}$	0.107	Novel
CYP2C19	Cytochrome P450, family 2, subfamily C, polypeptide 19	Ion binding	↓0.18	$1.90x10^{-9}$	0.101	Novel
50-gene signature			↑2.66	<0.001[1]	0.993	
48-gene signature[2]			↑2.88	<0.001[1]	0.994	

[1] Unadjusted p-value. [2] The 48 up-regulated genes in advanced fibrosis.

Abbreviations: AUROC, area under the receiver operating characteristic curve. ECM, extracellular matrix.

Table 2.3. The area under the receiver operator characteristic curve (AUROC) of the 48-gene signature for advanced fibrosis in the validation sets

Gene	Official gene name	Validation set 1 AUROC	Validation set 2 AUROC	Validation set 3 AUROC
ANTXR1	Anthrax toxin receptor 1	0.949	0.769	0.769
AQP1	Aquaporin 1	0.950	0.925	0.925
BICC1	BicC family RNA binding protein 1	0.985	0.965	0.965
C1orf198	Chromosome 1 open reading frame 198	0.936	0.918	0.918
C7	Complement component 7	0.950	0.980	0.980
CACNA2D1	Calcium channel, voltage-dependent, alpha 2/delta subunit 1	0.944	0.910	0.910
CD24	CD24 molecule	0.976	0.882	0.882
CDH11	Cadherin 11, type 2, OB-cadherin	0.968	0.781	0.781
COL14A1	Collagen, type XIV, alpha 1	0.901	0.876	0.876
COL1A1	Collagen, type I, alpha 1	0.927	0.813	0.813
COL1A2	Collagen, type I, alpha 2	0.897	0.846	0.846
COL3A1	Collagen, type III, alpha 1	0.937	0.846	0.846
COL4A1	Collagen, type IV, alpha 1	0.948	0.915	0.915
COL4A2	Collagen, type IV, alpha 2	0.897	0.970	0.970
COL4A4	Collagen, type IV, alpha 4	0.873	0.726	0.726
COL6A3	Collagen, type VI, alpha 3	0.911	0.756	0.756
CXCL6	Chemokine ligand 6	0.947	0.866	0.866
DCDC2	Doublecortin domain containing 2	0.944	0.828	0.828
DKK3	Dickkopf WNT signaling pathway inhibitor 3	0.966	0.761	0.761
DTNA	Dystrobrevin, alpha	0.899	0.928	0.928
EFEMP1	EGF containing fibulin-like extracellular matrix protein 1	0.984	0.940	0.940
EHF	Ets homologous factor	0.936	0.799	0.799
EPCAM	Epithelial cell adhesion molecule	0.958	0.908	0.908
EPHA3	EPH receptor A3	0.939	0.935	0.935
FAM169A	Family with sequence similarity 169, member A	0.839	0.734	0.734
FAT1	FAT atypical cadherin 1	0.893	0.801	0.801
FBN1	Fibrillin 1	0.927	0.887	0.887

GPRC5B	G protein-coupled receptor, class C, group 5, member B	0.944	0.861	0.861
GSN	Gelsolin	0.881	0.784	0.784
HEPH	Hephaestin	0.951	0.697	0.697
IGFBP7	Insulin-like growth factor binding protein 7	0.902	0.908	0.908
ITGBL1	Integrin, beta-like 1	0.950	0.787	0.787
JAG1	Jagged 1	0.931	0.928	0.928
KRT7	Keratin 7	0.929	0.841	0.841
LAMB1	Laminin, beta 1	0.837	0.893	0.893
LTBP2	Latent transforming growth factor beta binding protein 2	0.940	0.970	0.970
LUM	Lumican	0.976	0.960	0.960
MAP1B	Microtubule-associated protein 1B	0.958	0.915	0.915
MAP2	Microtubule-associated protein 2	0.900	0.873	0.873
MOXD1	Monooxygenase, DBH-like 1	0.947	0.886	0.886
NALCN	Sodium leak channel, non-selective	0.982	0.704	0.704
NAV3	Neuron navigator 3	0.926	0.863	0.863
RCAN2	Regulator of calcineurin 2	0.795	0.886	0.886
SH3YL1	SH3 and SYLF domain containing 1	0.897	0.749	0.749
SLC38A1	Solute carrier family 38, member 1	0.836	0.960	0.960
SOX9	SRY (sex determining region Y)-box 9	0.953	0.965	0.965
THBS2	Thrombospondin 2	0.970	0.945	0.945
TMEM200A	Transmembrane protein 200A	0.927	0.597	0.597
48-gene signature		0.994	0.964	0.993

Table 2.4. The significant biological functions associated with the 48-gene signature

Gene Ontology category	Gene Ontology description	Number of genes involved in a biological function	Genes	-log (p)[1]
Biological process	Extracellular matrix organization	12	COL4A4, COL4A2, COL14A1, COL4A1, LUM, COL3A1, COL6A3, FBN1, COL1A2, COL1A1, SOX9, LAMB1	9.10
	Collagen catabolic process	7	COL4A4, COL4A2, COL4A1, COL3A1, COL6A3, COL1A2, COL1A1	5.52
	Cell adhesion	10	FAT1, IGFBP7, COL6A3, COL1A1, CD24, LAMB1, THBS2, ITGBL1, EPHA3, CDH11	3.52
	Collagen fibril organization	5	COL14A1, LUM, COL3A1, COL1A2, COL1A1	3.48
	Skeletal system development	6	COL3A1, FBN1, COL1A2, COL1A1, SOX9, CDH11	2.63
	Cellular response to transforming growth factor beta stimulus	4	COL4A2, FBN1, COL1A1, SOX9	1.76
	Cellular response to amino acid stimulus	4	COL4A1, COL3A1, COL1A2, COL1A1	1.75
	Cellular response to retinoic acid	4	COL1A1, SOX9, AQP1, EPHA3	1.37
Cellular component	Extracellular matrix	14	COL4A2, COL4A1, LTBP2, LUM, IGFBP7, FBN1, EFEMP1, COL3A1, COL14A1, COL6A3, COL1A2, COL1A1, LAMB1, THBS2	10.46
	Extracellular region	21	COL4A4, C7, COL4A2, COL4A1, LUM, IGFBP7, COL3A1, FBN1, EFEMP1, JAG1, CXCL6, EPHA3, ITGBL1, DKK3, COL14A1, GSN, COL6A3, COL1A2, COL1A1, LAMB1, THBS2	7.47

	Endoplasmic reticulum lumen	8	COL4A4, COL4A2, COL14A1, COL4A1, COL3A1, COL6A3, COL1A2, COL1A1	4.74
	Proteinaceous extracellular matrix	8	COL4A4, COL14A1, LTBP2, LUM, COL6A3, EFEMP1, FBN1, COL1A2	4.08
	Extracellular space	15	LTBP2, LUM, IGFBP7, COL3A1, FBN1, EFEMP1, CXCL6, GPRC5B, DKK3, COL14A1, GSN, COL6A3, COL1A2, COL1A1, LAMB1	4.06
	Collagen trimer	6	COL4A4, COL14A1, COL3A1, COL6A3, COL1A2, COL1A1	4.04
	Extracellular exosome	21	C7, COL4A2, CACNA2D1, LTBP2, LUM, IGFBP7, FBN1, EFEMP1, GPRC5B, AQP1, EPCAM, COL14A1, GSN, KRT7, FAT1, COL6A3, COL1A2, ANTXR1, SLC38A1, LAMB1, CDH11	3.97
	Collagen type IV trimer	3	COL4A4, COL4A2, COL4A1	2.93
	Basement membrane	4	COL4A1, FBN1, LAMB1, THBS2	1.93
	Collagen type I trimer	2	COL1A2, COL1A1	1.32
Molecular function	Extracellular matrix structural constituent	10	COL4A4, COL4A2, COL14A1, COL4A1, LUM, COL3A1, FBN1, COL1A2, COL1A1, LAMB1	11.36
	Platelet-derived growth factor binding	4	COL4A1, COL3A1, COL1A2, COL1A1	3.97
	Calcium ion binding	8	LTBP2, GSN, FAT1, EFEMP1, FBN1, JAG1, THBS2, CDH11	1.31

[1]Fisher exact test Benjamini-Hochberg's corrected p-values are shown as –log (p).

Table 2.5. The significant pathways associated with the 48-gene signature

KEGG description	Number of genes involved in a pathway	Genes	-log (p)[1]
Extracellular matrix - receptor interaction	9	COL4A4, COL4A2, COL4A1, COL3A1, COL6A3, COL1A2, COL1A1, LAMB1, THBS2	8.30
Protein digestion and absorption	8	COL4A4, COL4A2, COL14A1, COL4A1, COL3A1, COL6A3, COL1A2, COL1A1	6.90
Focal adhesion	9	COL4A4, COL4A2, COL4A1, COL3A1, COL6A3, COL1A2, COL1A1, LAMB1, THBS2	5.79
Amoebiasis	7	COL4A4, COL4A2, COL4A1, COL3A1, COL1A2, COL1A1, LAMB1	5.16
PI3K-Akt signaling pathway	9	COL4A4, COL4A2, COL4A1, COL3A1, COL6A3, COL1A2, COL1A1, LAMB1, THBS2	4.31
Small cell lung cancer	4	COL4A4, COL4A2, COL4A1, LAMB1	1.81

[1]Fisher exact test Benjamini-Hochberg's corrected p-values are shown as –log (p).
KEGG, Kyoto Encyclopedia of Genes and Genomes.

Table 2.6. Ingenuity Pathways Analysis

Top diseases and biological functions	p-value[1]	Genes (n)
Diseases and disorders		
Cancer	$4.85 \times 10^{-11} – 5.53 \times 10^{-2}$	48
Connective tissue disorder	$4.85 \times 10^{-11} – 4.83 \times 10^{-2}$	19
Organismal injury and abnormalities	$4.85 \times 10^{-11} – 5.53 \times 10^{-2}$	48
Reproductive system disease	$4.85 \times 10^{-11} – 5.10 \times 10^{-2}$	43
Endocrine system disorder	$1.46 \times 10^{-11} – 5.21 \times 10^{-2}$	31
Molecular and cellular functions		
Cellular movement	$6.06 \times 10^{-8} – 5.21 \times 10^{-2}$	24
Cellular assembly and organization	$7.79 \times 10^{-6} – 4.83 \times 10^{-2}$	14
Cellular function and maintenance	$7.79 \times 10^{-6} – 4.83 \times 10^{-2}$	17
Cellular development	$4.22 \times 10^{-4} – 5.21 \times 10^{-2}$	16
Physiological system development and function		
Tissue development	$4.22 \times 10^{-4} – 5.21 \times 10^{-2}$	20
Embryonic development	$1.47 \times 10^{-3} – 5.21 \times 10^{-2}$	11
Hair and skin development and function	$1.47 \times 10^{-3} – 4.83 \times 10^{-2}$	7
Top toxicological functions		
Hepatotoxicity		
Liver hyperplasia/hyperproliferation	$1.93 \times 10^{-3} – 1.11 \times 10^{-1}$	36
Hepatocellular carcinoma	9.91×10^{-3}	9
Top canonical pathways		
GP6 signaling pathway	1.51×10^{-7}	8
Hepatic fibrosis / hepatic stellate cell activation	2.02×10^{-5}	7

[1]Fisher's exact test corrected by Benjamini-Hochberg's method was used to calculate a p-value to identify statistically significant over-representation of the 48-gene signature involved in a specific function or pathway.

Table 2.7. Correlation between the geometric mean expression of 8 collagen genes and cellular origin markers in the discovery and validation sets

Cellular origin	Gene symbol	Gene full name	Discovery set	Validation set 1	Validation set 2	Validation set 3	Mean correlation	Ref
Hepatic stellate cell	CYGB	Cytoglobin	0.431*	0.226	0.585*	0.100	0.336	(48)
	DES	Desmin	NA	NA	-0.158	-0.242*	-0.200	(48)
	FAP	Fibroblast Activation Protein Alpha	0.728*	0.652*	0.307*	0.670*	0.589	(48)
	GFAP	Glial Fibrillary Acidic Protein	NA	NA	NA	-0.142	-0.142	(48)
	HGF	Hepatocyte Growth Factor	0.610*	0.634*	0.707*	0.757*	0.677	(49)
	LHX2	LIM Homeobox 2	-0.236*	-0.261*	NA	-0.132	-0.210	(49)
	LRAT	Lecithin Retinol Acyltransferase	-0.504*	-0.395*	0.126	-0.374*	-0.286	(48)
	NGFR	Nerve Growth Factor Receptor	NA	NA	NA	0.463*	0.463	(48)
	NTF3	Neurotrophin 3	NA	NA	NA	-0.040	-0.040	(48)
	NTRK3	Neurotrophic Receptor Tyrosine Kinase 3	NA	NA	NA	-0.258*	-0.258	(48)
	PDGFRB	Platelet Derived Growth Factor Receptor Beta	NA	NA	0.400*	0.714*	0.557	(48)
	RBP1	Retinol Binding Protein 1	0.292*	0.178	NA	0.491*	0.320	(48)
	SYP	Synaptophysin	NA	NA	NA	-0.205	-0.205	(48)
	VIM	Vimentin	0.538*	0.666*	0.736*	0.813*	0.688	(50)
Hepatic progenitor cell	CD24	CD24 Molecule	0.843*	0.794*	0.799*	0.776*	0.803	(51)
	CD109	CD109 Molecule	0.211	0.175	0.622*	0.354*	0.341	(52)
	EPCAM	Epithelial Cell Adhesion Molecule	0.756*	0.791*	0.761*	0.586*	0.724	(53)
	KIT	KIT Proto-Oncogene Receptor Tyrosine Kinase	NA	NA	NA	0.072	0.072	(52)
	KRT7	Keratin 7	0.814*	0.886*	0.728*	0.712*	0.785	(54)
	KRT19	Keratin 19	0.616*	0.806*	0.576*	0.366*	0.591	(54)
	NCAM1	Neural Cell Adhesion Molecule 1	0.565*	0.644*	0.345*	0.206	0.440	(48)
	PROM1	Prominin 1	0.697*	0.804*	0.702*	0.525*	0.682	(55)
	PTPRC	Protein Tyrosine Phosphatase, Receptor Type C	NA	NA	0.747*	0.428*	0.588	(52)
	THY1	Thy-1 Cell Surface Antigen	0.636*	0.784*	0.707*	0.759*	0.722	(52)

High positive correlation (>0.7) was shaded grey. * Significant correlation ($p<0.05$).
NA, not applicable. The gene was excluded after data preprocessing.
Ref, reference.

Table 2.8. Correlation between the expression of 8 collagen genes in the 48-gene signature and cellular origin markers in the discovery and validation sets

Dataset	Cellular origin	Gene symbol	COL1A1	COL1A2	COL3A1	COL4A1	COL4A2	COL4A4	COL6A3	COL14A1
Discovery set	Hepatic stellate cell	CYGB	0.517*	0.446*	0.367*	0.254*	0.339*	0.374*	0.444*	0.380*
		DES	NA	NA	NA	NA	NA	NA	NA	NA
		FAP	0.626*	0.721*	0.685*	0.761*	0.701*	0.473*	0.680*	0.532*
		GFAP	NA	NA	NA	NA	NA	NA	NA	NA
		HGF	0.465*	0.521*	0.598*	0.590*	0.448*	0.656*	0.593*	0.560*
		LHX2	-0.144	-0.380*	-0.133	-0.421*	-0.429*	-0.094	-0.204	0.011
		LRAT	-0.506*	-0.561*	-0.382*	-0.524*	-0.587*	-0.343*	-0.520*	-0.237*
		NGFR	NA	NA	NA	NA	NA	NA	NA	NA
		NTF3	NA	NA	NA	NA	NA	NA	NA	NA
		NTRK3	NA	NA	NA	NA	NA	NA	NA	NA
		PDGFRB	NA	NA	NA	NA	NA	NA	NA	NA
		RBP1	0.102	0.196	0.310*	0.288*	0.194	0.337*	0.210	0.244*
		SYP	NA	NA	NA	NA	NA	NA	NA	NA
		VIM	0.345*	0.653*	0.467*	0.585*	0.644*	0.328*	0.444*	0.358*
	Hepatic progenitor cell	CD24	0.751*	0.747*	0.791*	0.856*	0.772*	0.708*	0.760*	0.664*
		CD109	0.254*	0.049	0.432*	0.243*	-0.007	0.205	0.172	0.366*
		EPCAM	0.606*	0.735*	0.615*	0.714*	0.699*	0.659*	0.714*	0.591*
		KIT	NA	NA	NA	NA	NA	NA	NA	NA
		KRT7	0.697*	0.811*	0.678*	0.793*	0.841*	0.631*	0.746*	0.606*
		KRT19	0.458*	0.685*	0.456*	0.691*	0.726*	0.418*	0.557*	0.371*
		NCAM1	0.473*	0.510*	0.527*	0.501*	0.509*	0.472*	0.591*	0.430*
		PROM1	0.549*	0.664*	0.537*	0.643*	0.694*	0.519*	0.685*	0.600*
		PTPRC	NA	NA	NA	NA	NA	NA	NA	NA
		THY1	0.579*	0.691*	0.539*	0.649*	0.677*	0.401*	0.581*	0.515*
Validation set 1	Hepatic stellate cell	CYGB	0.246*	0.065	0.234	0.174	0.129	0.334*	0.233	0.236*
		DES	NA	NA	NA	NA	NA	NA	NA	NA
		FAP	0.617*	0.669*	0.647*	0.652*	0.669*	0.473*	0.664*	0.508*
		GFAP	NA	NA	NA	NA	NA	NA	NA	NA
		HGF	0.574*	0.585*	0.637*	0.649*	0.553*	0.546*	0.585*	0.593*
		LHX2	-0.214	-0.396*	-0.252*	-0.315*	-0.323*	-0.092	-0.241*	-0.139
		LRAT	-0.453*	-0.440*	-0.329*	-0.438*	-0.441*	-0.156	-0.380*	-0.308*
		NGFR	NA	NA	NA	NA	NA	NA	NA	NA
		NTF3	NA	NA	NA	NA	NA	NA	NA	NA
		NTRK3	NA	NA	NA	NA	NA	NA	NA	NA
		PDGFRB	NA	NA	NA	NA	NA	NA	NA	NA
		RBP1	0.079	0.173	0.231	0.243*	0.244*	0.194	0.130	0.064
		SYP	NA	NA	NA	NA	NA	NA	NA	NA

		VIM	0.575*	0.801*	0.576*	0.673*	0.805*	0.428*	0.603*	0.430*
	Hepatic progenitor cell	CD24	0.790*	0.707*	0.847*	0.831*	0.705*	0.631*	0.764*	0.703
		CD109	0.195	-0.019	0.349*	0.263*	-0.006	0.186	0.196	0.236*
		EPCAM	0.740*	0.730*	0.790*	0.776*	0.700*	0.691*	0.749*	0.721*
		KIT	NA	NA	NA	NA	NA	NA	NA	NA
		KRT7	0.836*	0.829*	0.871*	0.848*	0.789*	0.759*	0.865*	0.765*
		KRT19	0.740*	0.811*	0.781*	0.820*	0.786*	0.674*	0.805*	0.606*
		NCAM1	0.603*	0.599*	0.604*	0.543*	0.572*	0.621*	0.655*	0.639*
		PROM1	0.761*	0.746*	0.742*	0.711*	0.702*	0.735*	0.820*	0.794*
		PTPRC	NA	NA	NA	NA	NA	NA	NA	NA
		THY1	0.714*	0.754*	0.760*	0.804*	0.776*	0.643*	0.717*	0.655*
Validation set 2	Hepatic stellate cell	CYGB	0.645*	0.535*	0.498*	0.525*	0.481*	0.628*	0.548*	0.546*
		DES	-0.215*	-0.016	-0.103	-0.156	-0.010	-0.261*	-0.137	-0.193
		FAP	0.433*	0.263*	0.270*	0.366*	0.248*	0.334*	0.233*	0.368*
		GFAP	NA	NA	NA	NA	NA	NA	NA	NA
		HGF	0.749*	0.606*	0.617*	0.650*	0.604*	0.731*	0.658*	0.683*
		LHX2	NA	NA	NA	NA	NA	NA	NA	NA
		LRAT	-0.010	0.166	0.159	0.063	0.172	0.052	0.163	0.080
		NGFR	NA	NA	NA	NA	NA	NA	NA	NA
		NTF3	NA	NA	NA	NA	NA	NA	NA	NA
		NTRK3	NA	NA	NA	NA	NA	NA	NA	NA
		PDGFRB	0.229*	0.482*	0.412*	0.370*	0.539*	0.254*	0.394*	0.375*
		RBP1	NA	NA	NA	NA	NA	NA	NA	NA
		SYP	NA	NA	NA	NA	NA	NA	NA	NA
		VIM	0.631*	0.862*	0.821*	0.703*	0.781*	0.503*	0.608*	0.715*
	Hepatic progenitor cell	CD24	0.855*	0.778*	0.766*	0.785*	0.762*	0.671*	0.676*	0.710*
		CD109	0.611*	0.533*	0.565*	0.616*	0.525*	0.565*	0.650*	0.636*
		EPCAM	0.843*	0.702*	0.692*	0.732*	0.672*	0.707*	0.667*	0.708*
		KRT7	0.674*	0.793*	0.742*	0.708*	0.795*	0.555*	0.619*	0.632*
		KRT19	0.539*	0.696*	0.632*	0.579*	0.680*	0.401*	0.458*	0.542*
		KIT	NA	NA	NA	NA	NA	NA	NA	NA
		NCAM1	0.377*	0.201	0.276*	0.351*	0.246*	0.388*	0.347*	0.359*
		PROM1	0.645*	0.645*	0.680*	0.678*	0.677*	0.595*	0.754*	0.661*
		PTPRC	0.788*	0.711*	0.740*	0.692*	0.638*	0.640*	0.663*	0.772*
		THY1	0.767*	0.706*	0.712*	0.696*	0.619*	0.605*	0.581*	0.649*
Validation set 3	Hepatic stellate cell	CYGB	0.080	0.150	0.085	-0.006	0.054	0.051	0.432*	0.379*
		DES	-0.197	-0.126	-0.264*	-0.290*	-0.176	-0.252*	0.098	0.146
		FAP	0.597*	0.600*	0.616*	0.664*	0.724*	0.390*	0.614*	0.578*
		GFAP	-0.167	-0.052	-0.145	-0.228	-0.198	-0.138	0.228	0.184
		HGF	0.710*	0.750*	0.684*	0.686*	0.744*	0.420*	0.646*	0.649*
		LHX2	-0.069	-0.071	-0.015	-0.191	-0.173	-0.027	-0.073	0.028
		LRAT	-0.197	-0.230	-0.150	-0.388*	-0.439*	-0.315*	-0.295*	-0.132

	NGFR	0.420*	0.431*	0.491*	0.383*	0.366*	0.287*	0.405*	0.414*
	NTF3	-0.072	-0.012	-0.009	-0.159	-0.094	-0.021	0.043	0.203
	NTRK3	-0.275*	-0.289*	-0.251*	-0.201	-0.058	-0.200	-0.119	-0.167
	PDGFRB	0.609*	0.694*	0.627*	0.604*	0.686*	0.454*	0.731*	0.709*
	RBP1	0.504*	0.517*	0.544*	0.496*	0.431*	0.227	0.518*	0.449*
	SYP	-0.290*	-0.217	-0.321*	-0.301*	-0.190	-0.037	0.109	-0.015
	VIM	0.734*	0.782*	0.700*	0.740*	0.803*	0.494*	0.674*	0.656*
Hepatic progenitor cell	CD24	0.720*	0.703*	0.737*	0.813*	0.867*	0.412*	0.461*	0.481*
	CD109	0.234*	0.302*	0.189	0.337*	0.401*	0.334*	0.296*	0.271*
	EPCAM	0.475*	0.524*	0.502*	0.549*	0.630*	0.394*	0.413*	0.480*
	KIT	0.091	0.113	0.108	0.115	0.082	-0.046	0.250*	0.263*
	KRT7	0.614*	0.684*	0.602*	0.673*	0.762*	0.418*	0.615*	0.615*
	KRT19	0.319*	0.391*	0.281*	0.348*	0.465*	0.146	0.556*	0.421*
	NCAM1	0.045	0.158	0.048	0.088	0.141	0.276*	0.336*	0.222
	PROM1	0.412*	0.476*	0.447*	0.459*	0.581*	0.335*	0.555*	0.559*
	PTPRC	0.454*	0.428*	0.483*	0.409*	0.387*	0.173	0.181	0.292*
	THY1	0.651*	0.741*	0.701*	0.679*	0.708*	0.472*	0.716*	0.737*

High positive correlation (>0.7) was shaded grey.
NA, not applicable. The gene was excluded after data preprocessing.

Table 2.9. Genes in the 48-gene signature that were up-regulated in a specific cell type when compared to other cell types in normal livers

Cluster of cell type	N out of 48 genes in a cluster (%)	Genes
EPCAM+ cells and cholangiocytes	17/48 (35%)	AQP1, BICC1, C1orf198, CD24, CXCL6, DCDC2, DTNA, EHF, EPCAM, FAT1, GPRC5B, JAG1, KRT7, LAMB1, MAP2, SH3YL1, SOX9
HSCs and myofibroblasts	13/48 (27%)	ANTXR1, COL14A1, COL1A1, COL1A2, COL3A1, COL4A1, COL4A2, COL6A3, GSN, LAMB1, MAP1B, RCAN2, THBS2
Macrovascular endothelial cells	10/48 (21%)	AQP1, COL3A1, COL4A1, COL4A2, DKK3, GSN, IGFBP7, JAG1, LAMB1, MAP1B
Sinusoidal endothelial cells	6/48 (13%)	C7, COL4A1, COL4A2, IGFBP7, LAMB1, MAP1B
Kupffer cells	1/48 (2%)	GSN
Hepatocytes	1/48 (2%)	GSN
NK, NKT, and T cells	1/48 (2%)	SLC38A1
Unknown cell type	15/48 (31%)	CACNA2D1, CDH11, COL4A4, EFEMP1, EPHA3, FAM169A, FBN1, HEPH, ITGBL1, LTBP2, LUM, MOXD1, NALCN, NAV3, TMEM200A

HSC, hepatic stellate cell; NK, nature killer; NKT, nature killer T.

Table 2.10. Genes in the 48-gene signature that were up-regulated in a specific cell type in cirrhotic livers when compared to normal livers

Cluster of cell type	N out of 48 genes in a cluster (%)	Genes
Epithelial cells	9/48 (19%)	BICC1, CD24, CXCL6, DCDC2, EHF, EPCAM, KRT7, SH3YL1, SOX9
Mesenchymal cells	6/48 (13%)	COL1A2, COL3A1, GSN, LUM, MAP1B, RCAN2
Endothelial cells	5/48 (10%)	AQP1, COL4A1, COL4A2, GSN, IGFBP7
B cells	0/48 (0%)	
Cycling cells	0/48 (0%)	
Innate lymphoid cells	0/48 (0%)	
Mast cells	0/48 (0%)	
Mononuclear phagocytes	0/48 (0%)	
Plasmacytoid dendritic cells	0/48 (0%)	
Plasma cells	0/48 (0%)	
T cells	0/48 (0%)	

Table 2.11. Fold-change of gene expression of antifibrotic drug target between advanced fibrosis and no or mild fibrosis in the NAFLD, viral hepatitis, and ALD samples

Drug (drug trial identifier)	Drug target (drug mechanism)	Type of disease	N of patients in trial	Drug trial results	Fold change of gene expression (advanced fibrosis/no or mild fibrosis)		
					NAFLD	Viral hepatitis	ALD[1]
Candesartan (NCT00990639)	Angiotensin II receptor, type 1 (AGTR1 inhibitor)	ALD	85	Improvement in fibrosis (56)	0.91	1.23[2]	1.21
Losartan (NCT01051219, NCT00298714)	Angiotensin II receptor, type 1 (AGTR1 inhibitor)	NASH	45	Recruited insufficient patients (57)	0.91	1.23[2]	1.21
		HCV	20	No change in fibrosis (58)			
Irbesartan (NCT00265642)	Angiotensin II receptor, type 1 (AGTR1 inhibitor)	HCV	166	Pending	0.91	1.23[2]	1.21
Timolumab (NCT02239211)	Amine oxidase copper containing 3 (AOC3 inhibitor)	PSC	41	Pending	NA	NA	NA
Cenicriviroc (NCT03028740)	C-C Motif chemokine receptor 2,5 (CCR2/CCR5 inhibitor)	NASH	2000	Pending	CCR2: 1.33** CCR5: 1.17*	CCR2: 1.16*** CCR5: 1.15***	CCR2: 1.72*** CCR5: 1.09
Pamrevlumab (NCT01217632)	Connective tissue growth factor (CTGF inhibitor)	HBV	114	Pending	1.73***	1.44***	2.43***
BMS-986036 (NCT03486899, NCT03486912)	Fibroblast growth factor 21 (analogue of FGF21)	NASH	160	Pending	1.04	1.03	0.81
		NASH	100	Pending			
Tropifexor (NCT03517540)	Farnesoid X receptor (FXR agonist)	NASH	200	Pending	0.9	1.33[2]*	NA
Obeticholic acid (NCT01265498, NCT02548351)	Farnesoid X receptor (FXR agonist)	NASH	283	Improvement in fibrosis (43)	0.9	1.33[2]*	NA
		NASH	2370	Pending			
GR-MD-02 (NCT02421094, NCT02462967)	Galectin 3 (LGALS3 inhibitor)	NASH	30	Pending	1.48**	1.21***	1.92*
		NASH	162	Pending			
Simtuzumab (NCT01672866, NCT01672879, NCT01707472, NCT01672853)	Lysyl oxidase-like molecule 2 (LOXL2 inhibitor)	NASH	222	No change in fibrosis (37)	1.34***	1.14[2]	1.97**
		NASH	259	No change in fibrosis (37)			
		HCV	18	No change in fibrosis (36)			
		PSC	235	No change in fibrosis (45)			
	Apoptosis signal-regulating kinase 1 (ASK1 inhibitor)	NASH	72	Improvement in fibrosis (44)	0.98	0.95[2]	0.77
		NASH	350	Pending			

Selonsertib (NCT02466516, NCT03449446, NCT03053063, NCT03053050)		NASH	883	Pending			
		NASH	808	Pending			
Oltipraz (NCT00956098)	Nuclear factor (erythroid-derived 2)-like 2 (NFE2L2 activator)	HBV HCV	81	No change in fibrosis (59)	0.95	1.68***	0.87
Elafibranor (NCT02704403)	Peroxisome oroliferator activated receptor alpha and delta (PPARA and PPARD agonist)	NASH	2000	Pending	PPARA: 1.00 PPARD: 1.05	PPARA: 0.99 PPARD: 1.18[2]	PPARA: 0.69* PPARD: 1.47**
Farglitazar (NCT00244751)	Peroxisome proliferator activated receptor gamma (PPARG agonist)	HCV	265	No change in fibrosis (60)	0.93	1.09[2]	NA
Aramchol (NCT02279524)	Stearoyl-CoA desaturase-1 (SCD inhibitor)	NASH	247	Pending	1.01	1.02*	0.75
Volixibat (NCT02787304)	Solute carrier family 10 member 2 (SLC10A2 inhibitor)	NASH	197	Pending	NA	NA	NA
BMS-986263 (NCT03420768)	Serpin family H member 1 (SERPINH1 inhibitor)	HCV	165	Pending	1.22***	1.28[2]*	1.24
Metadoxine (NCT02541045)	5-Hydroxytryptamine receptor 2B (5-HT2B inhibitor)	NASH	108	Suspended (lack of finance resources)	1.26	1.08**	1.01

Genes that are significantly ($p<0.05$) upregulated in advanced fibrosis are highlighted in grey.

[1] Included only ALD samples in validation set 3.

[2] The gene did not pass data preprocessing in validation set 2.

*$p<0.05$, **$p<0.01$, ***$p<0.001$

Abbreviations: ALD, alcoholic liver disease; HBV, hepatitis B virus; HCV, hepatitis C virus; NAFLD, non-alcoholic fatty liver disease NASH, non-alcoholic steatohepatitis; PSC, primary sclerosing cholangitis. NA, not applicable, target gene did not pass data preprocessing.

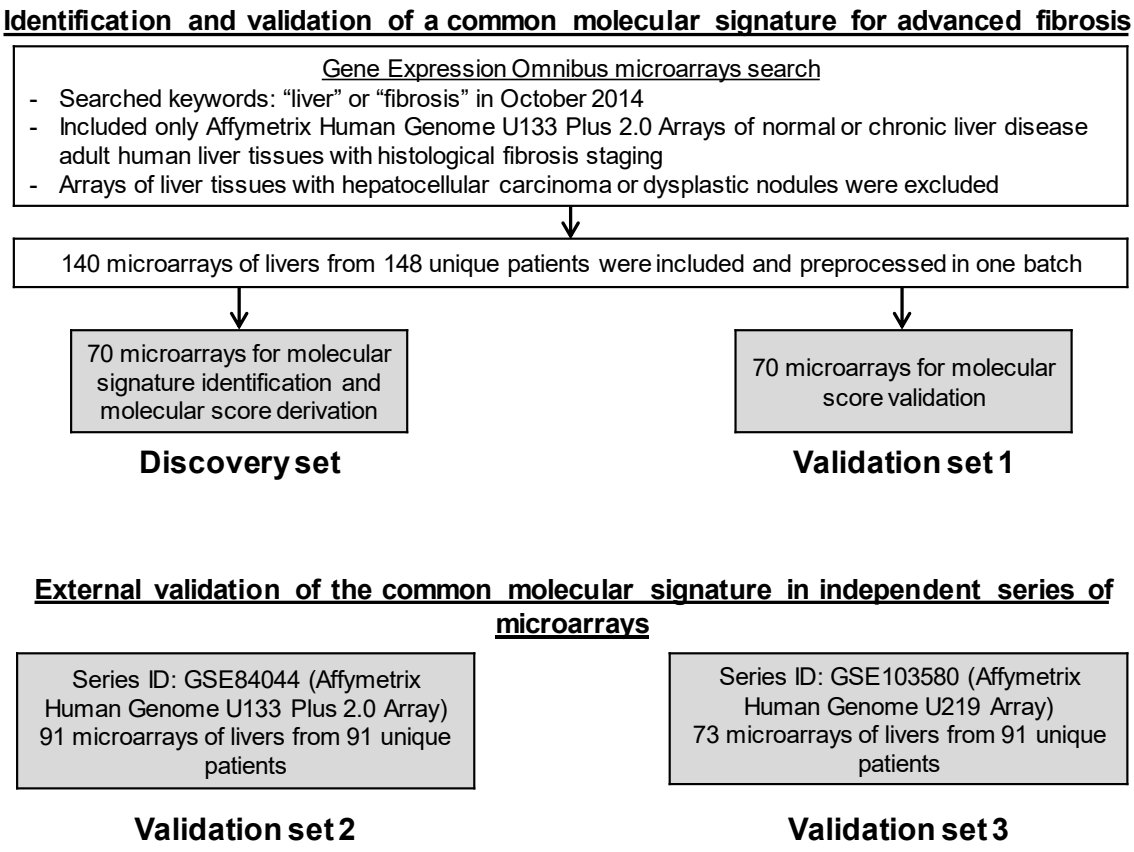

Figure 2.1. Identification and validation of the common fibrosis gene signature.

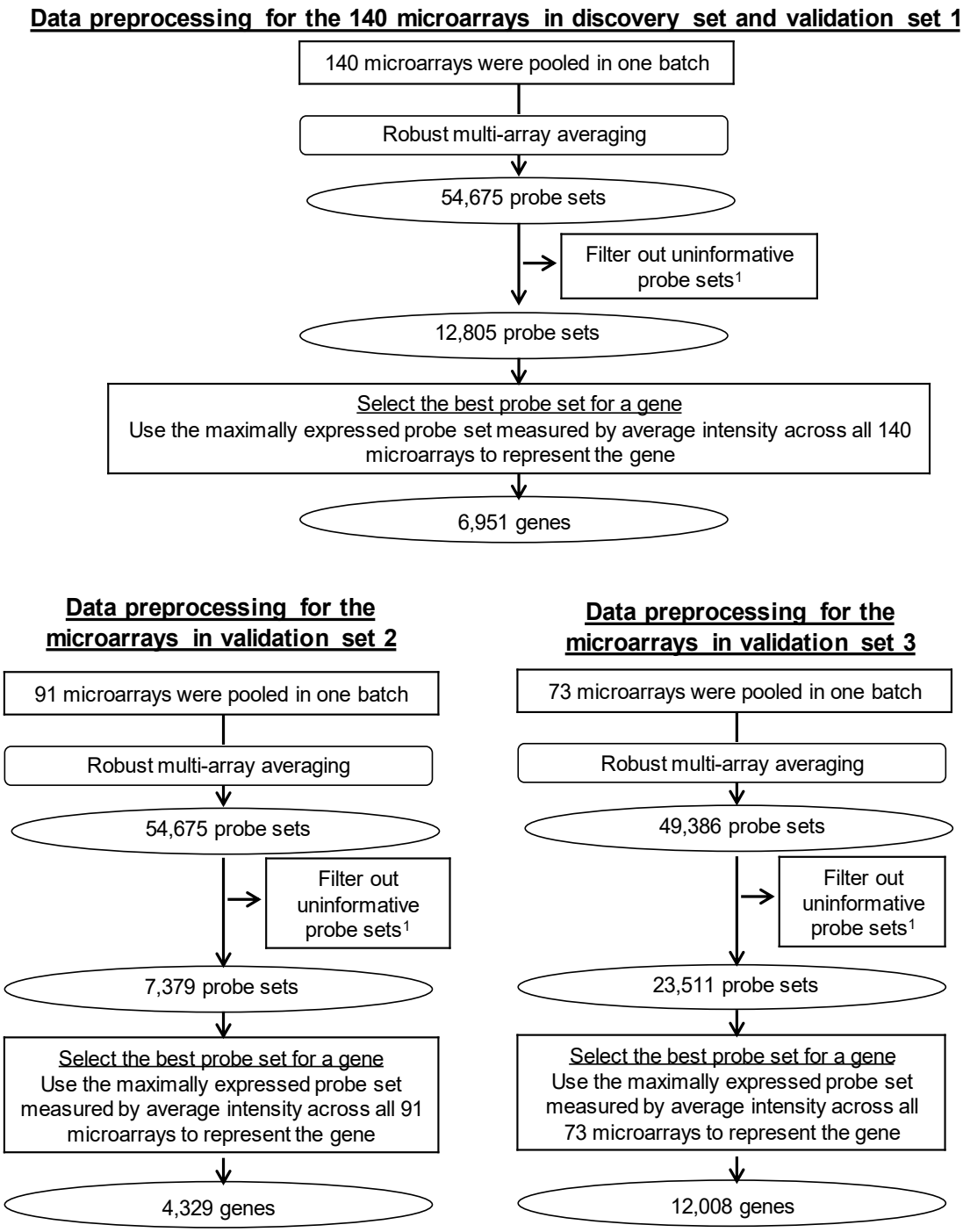

Figure 2.2. Data preprocessing flowchart.

[1]Uninformative probe sets were removed using the procedure as follows: 1. Calculate the median expression value of each probe set in each batch. 2. Divide each probe set expression value by the median expression value to obtain a fold-change value. 3. If less than 20% microarrays have a >1.5 or <-1.5 fold-change value, the probe set is excluded.

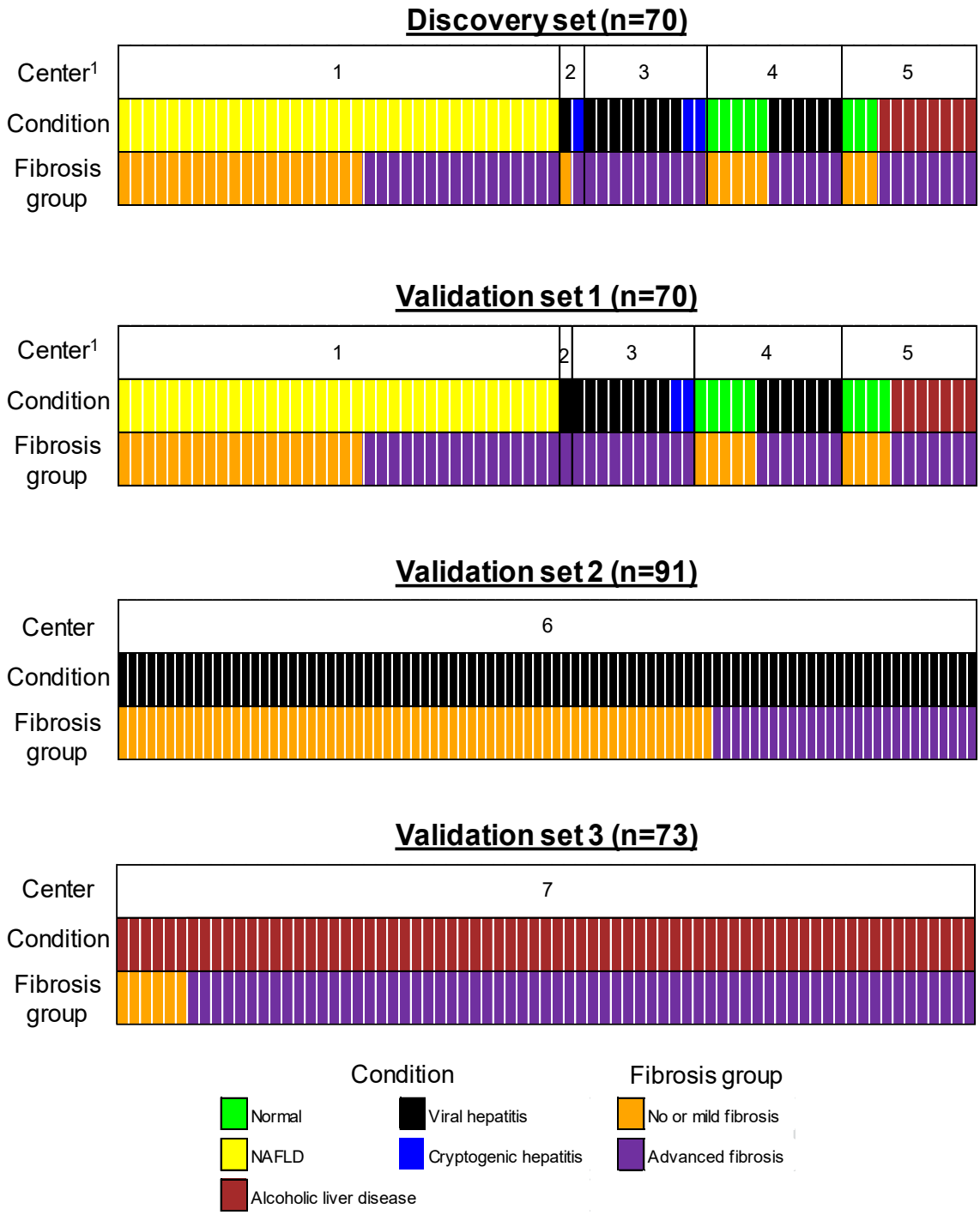

Figure 2.3. Condition of the microarrays.
[1]For the three microarrays from center 2, two were hybridized with a pool of liver RNA samples from four patients and one was hybridized with a pool of liver RNA samples from three patients. The liver tissues that were pooled together were in the same histological fibrosis group. NAFLD, non-alcoholic fatty liver disease.

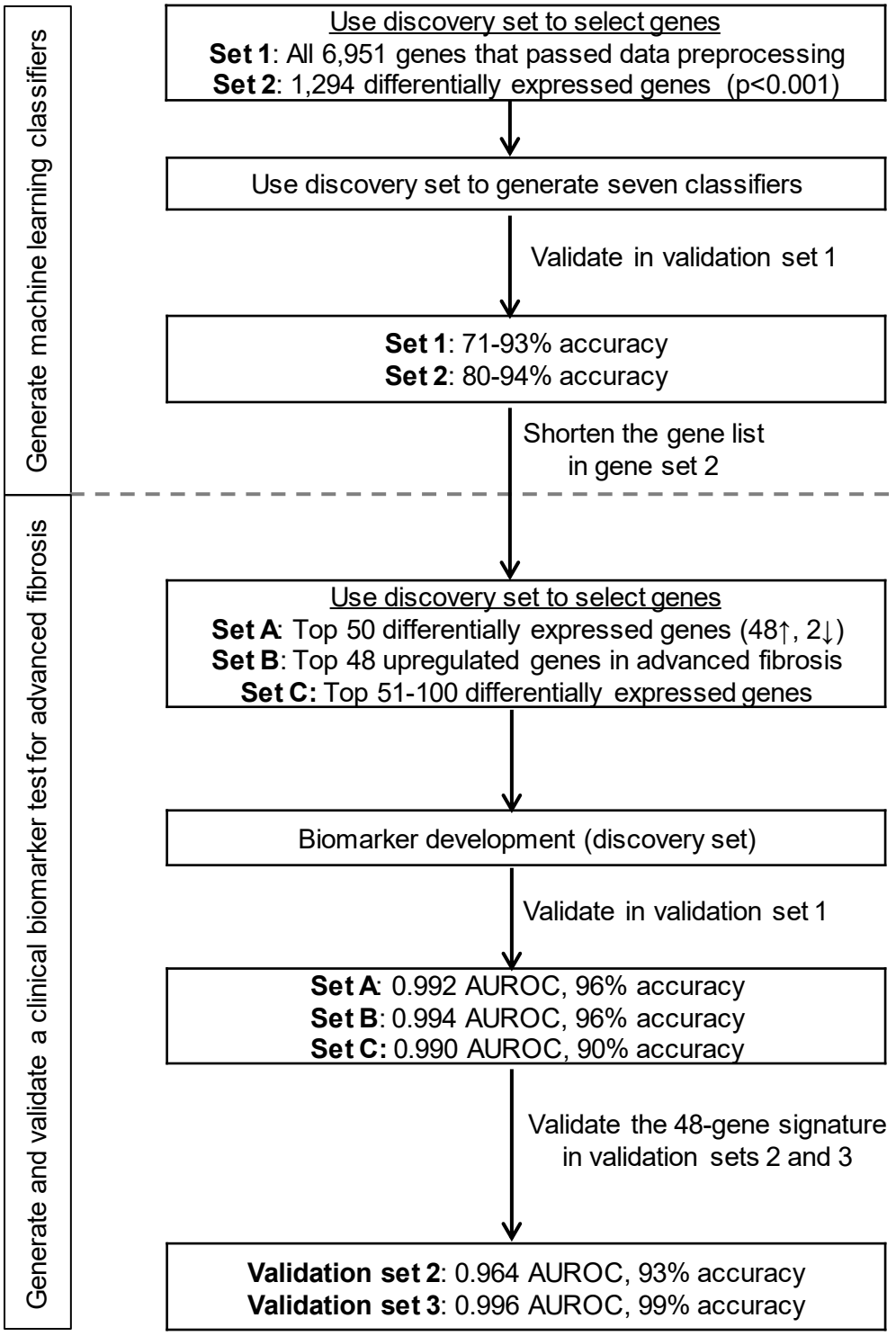

Figure 2.4. Data analysis flowchart.
The upward pointing arrow represented up-regulated in advanced fibrosis, whereas downward pointing arrow represented down-regulated in advanced fibrosis. AUROC, area under the receiver operating characteristic curve.

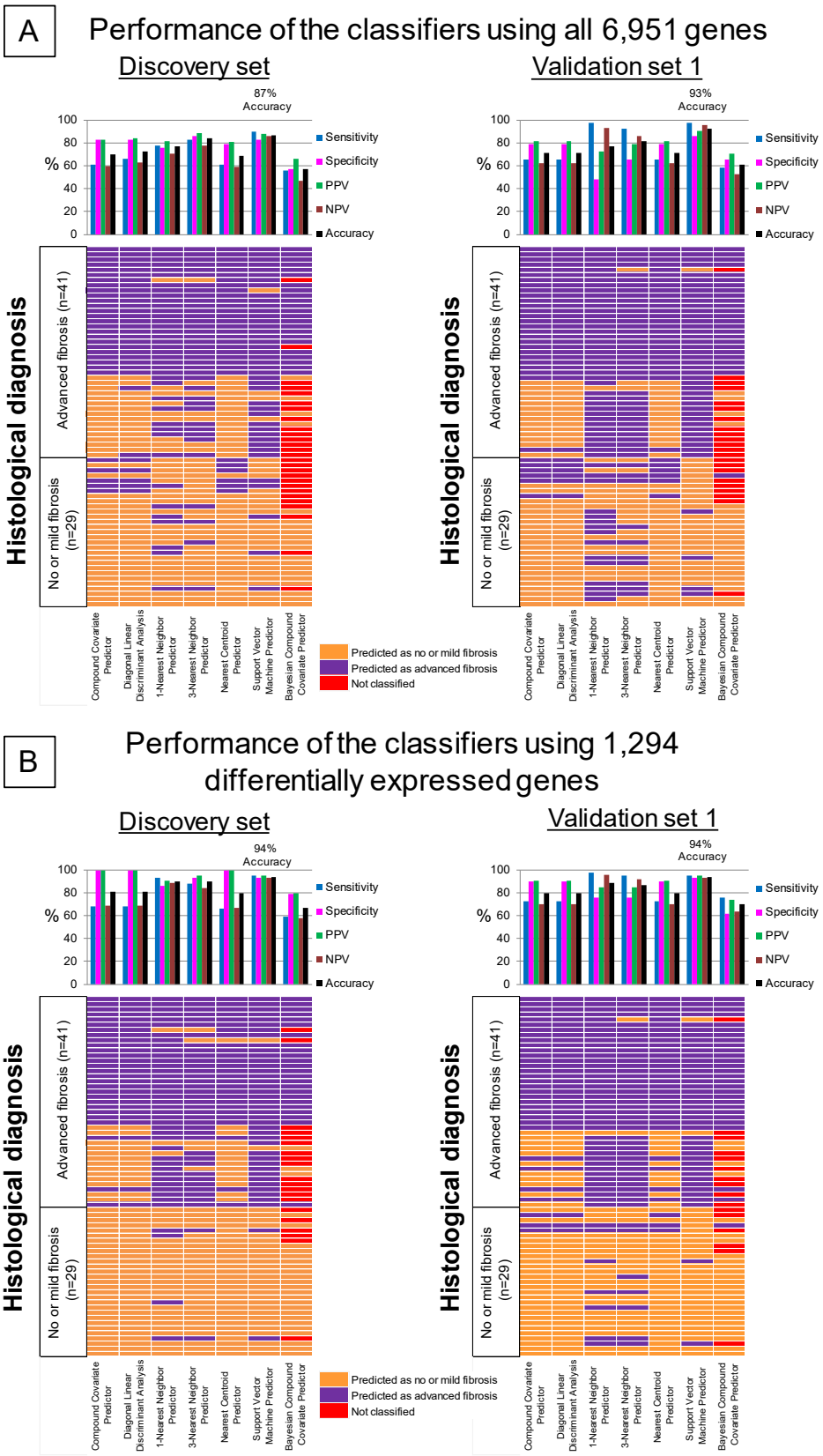

Figure 2.5. Development and validation of machine learning classifiers for identifying advanced liver fibrosis.

(Figure 2.5 continued) I used (A) all 6,951 genes that passed data preprocessing and (B) 1,294 differentially expressed genes ($p<0.001$) between advanced and no or mild fibrosis in the discovery set. The bar graph showed the sensitivity, specificity, positive predictive value (PPV), negative predictive value (NPV), and accuracy of each classifier for histology-proven advanced fibrosis. The performance of the classifiers in the discovery set was obtained using 10-fold cross-validation. The predicted fibrosis group for each sample was demonstrated on the heatmap. Of the seven classifiers, the Support Vector Machine Predictor had the best accuracy for advanced fibrosis when using 1,294 differentially expressed genes in both discovery set (94%) and validation set 1 (94%).

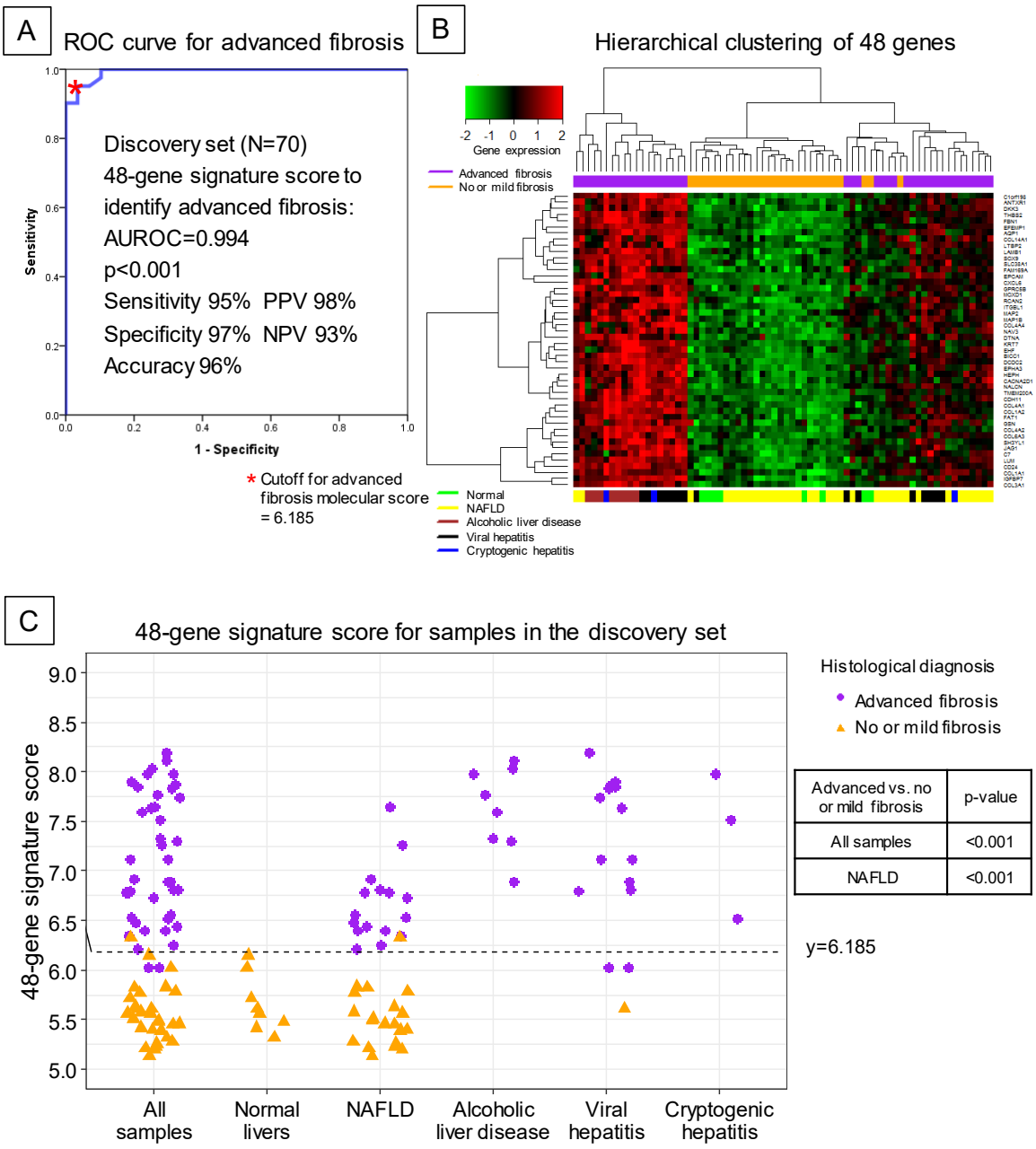

Figure 2.6. The performance of the 48-gene signature for advanced fibrosis in the discovery set.

(A) A 48-gene signature score cutoff (6.185) was derived using the Youden index from the receiver operating characteristic (ROC) curve analysis. (B) Unsupervised hierarchical clustering of the 48 genes showed samples in the same fibrosis group were mostly clustered together. Red was used to denote genes that were up-regulated, and green for genes that were down-regulated. The cluster was created using the Euclidean distance method. (C) The relationship between the 48-gene signature score and the histological diagnosis of each sample. The black dashed line is the molecular score cutoff (6.185) derived from the ROC curve for advanced fibrosis. PPV, positive predictive value; NPV, negative predictive value.

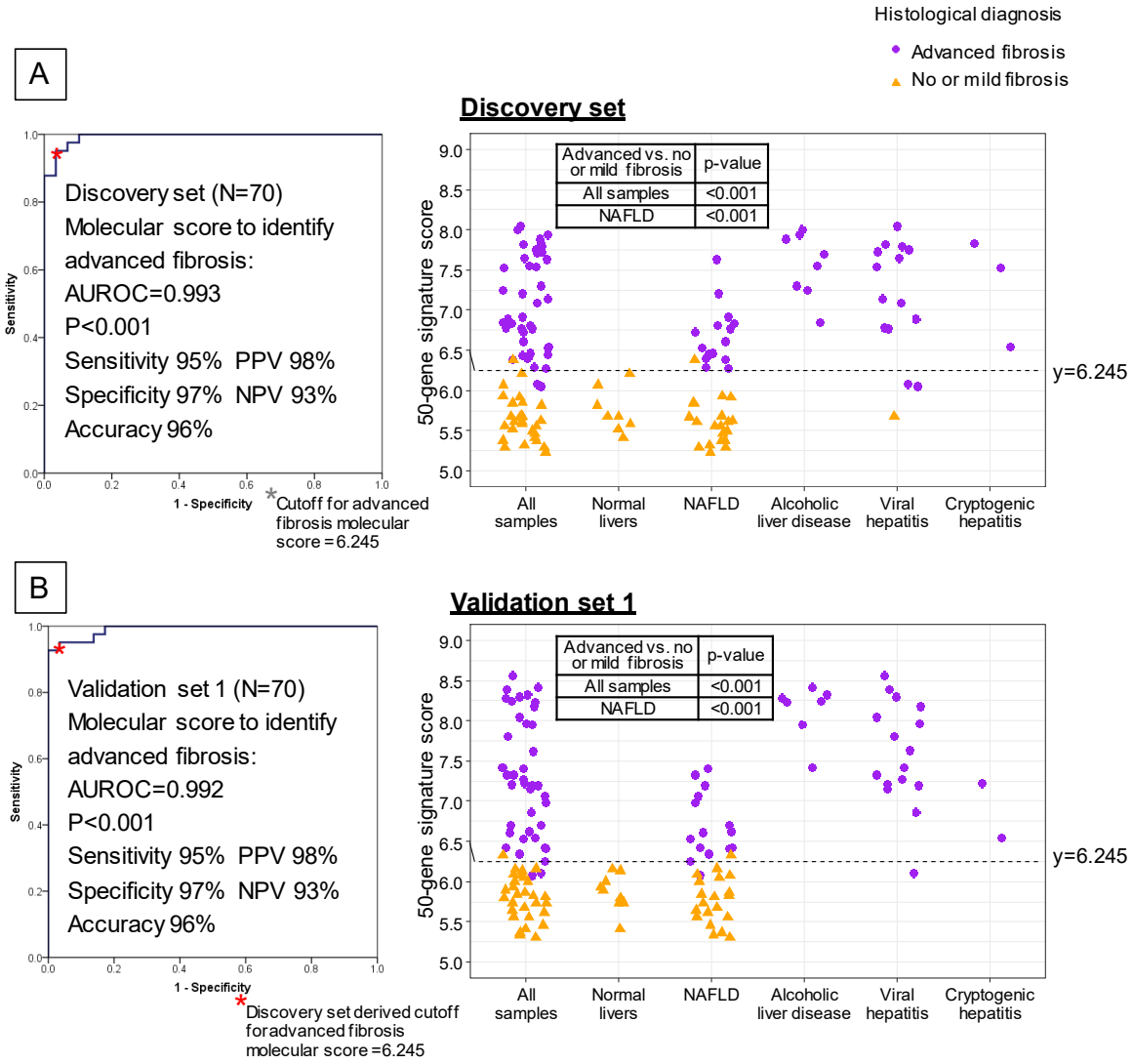

Figure 2.7. The performance of top 50 differentially expressed genes for advanced fibrosis in the (A) discovery set and (B) validation set 1.

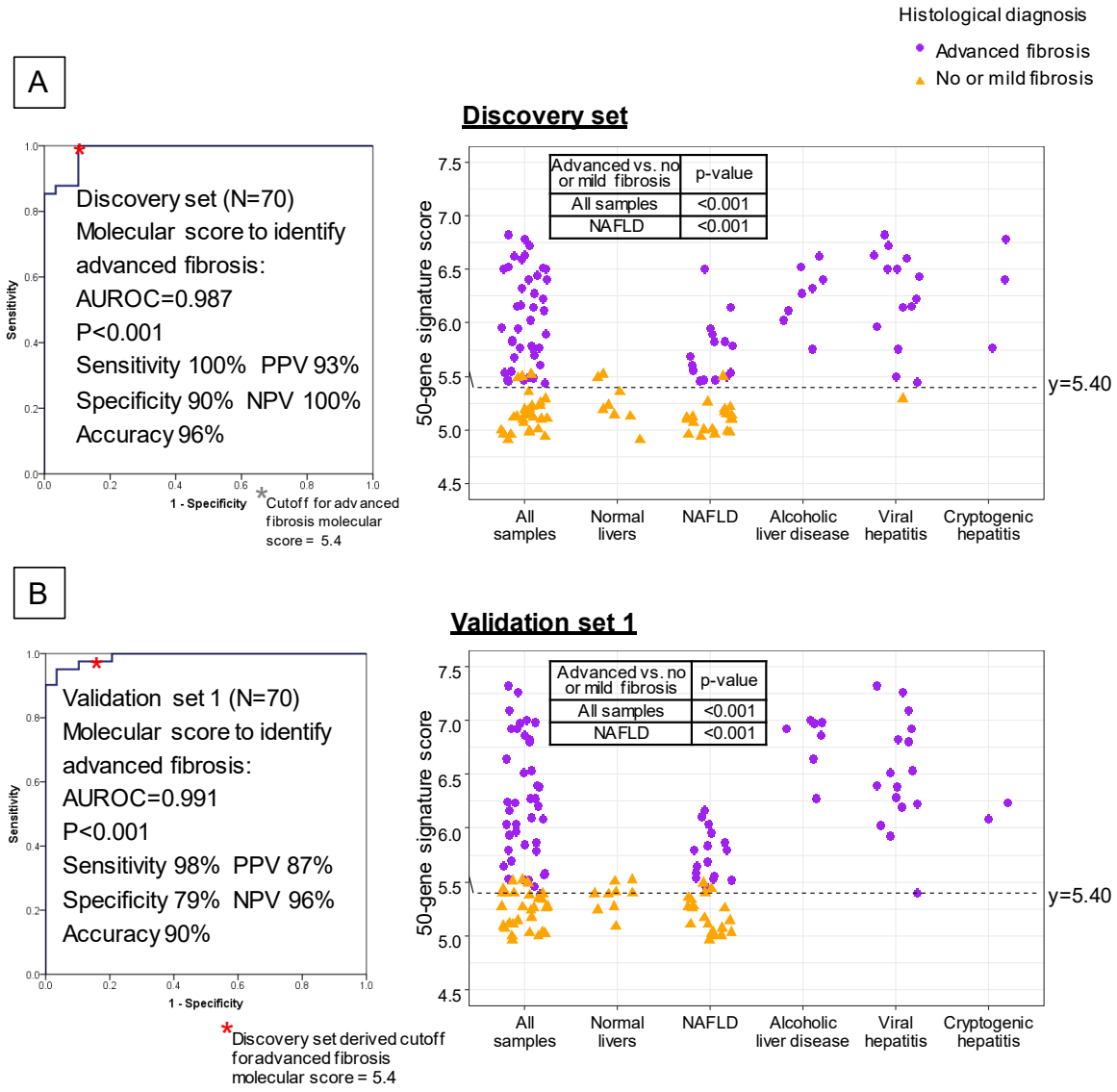

Figure 2.8. The performance of top 51-100 differentially expressed genes for advanced fibrosis in the (A) discovery set and (B) validation set 1.

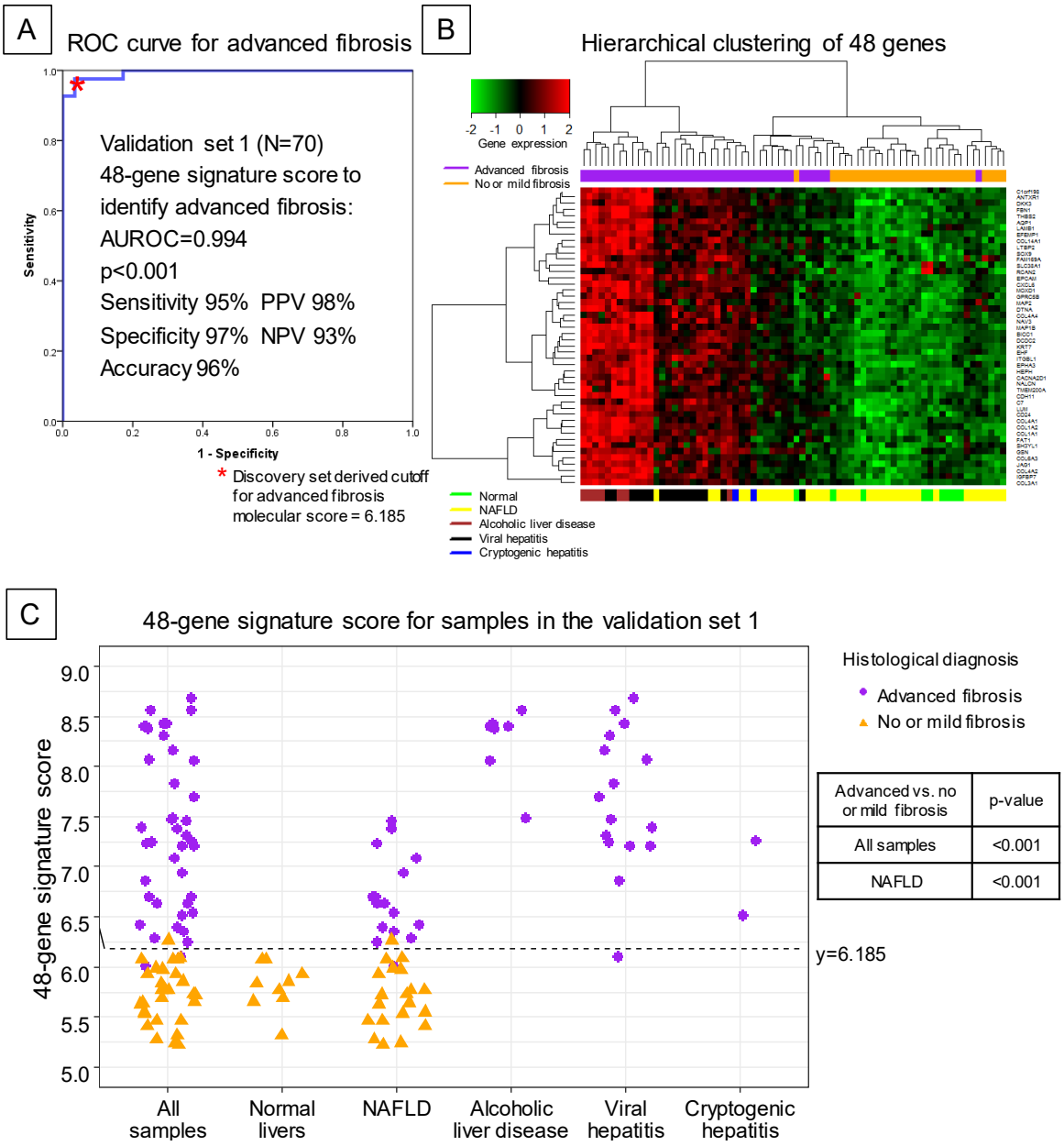

Figure 2.9. External validation of the 48-gene signature for advanced fibrosis in validation set 1.

(A) Application of the discovery set derived cutoff (6.185) in receiver operating characteristic (ROC) curve analysis showed 96% of accuracy and 0.994 of AUROC for advanced fibrosis. (B) Unsupervised hierarchical clustering of the 48 genes showed samples in the same fibrosis group were mostly clustered together. Red was used to denote genes that were up-regulated, and green for genes that were down-regulated. The cluster was created using the Euclidean distance method. (C) The relationship between the 48-gene signature and histological diagnosis of each sample. The black dashed line is the 48-gene signature score cutoff (6.185) derived from the discovery set for advanced fibrosis. PPV, positive predictive value; NPV, negative predictive value.

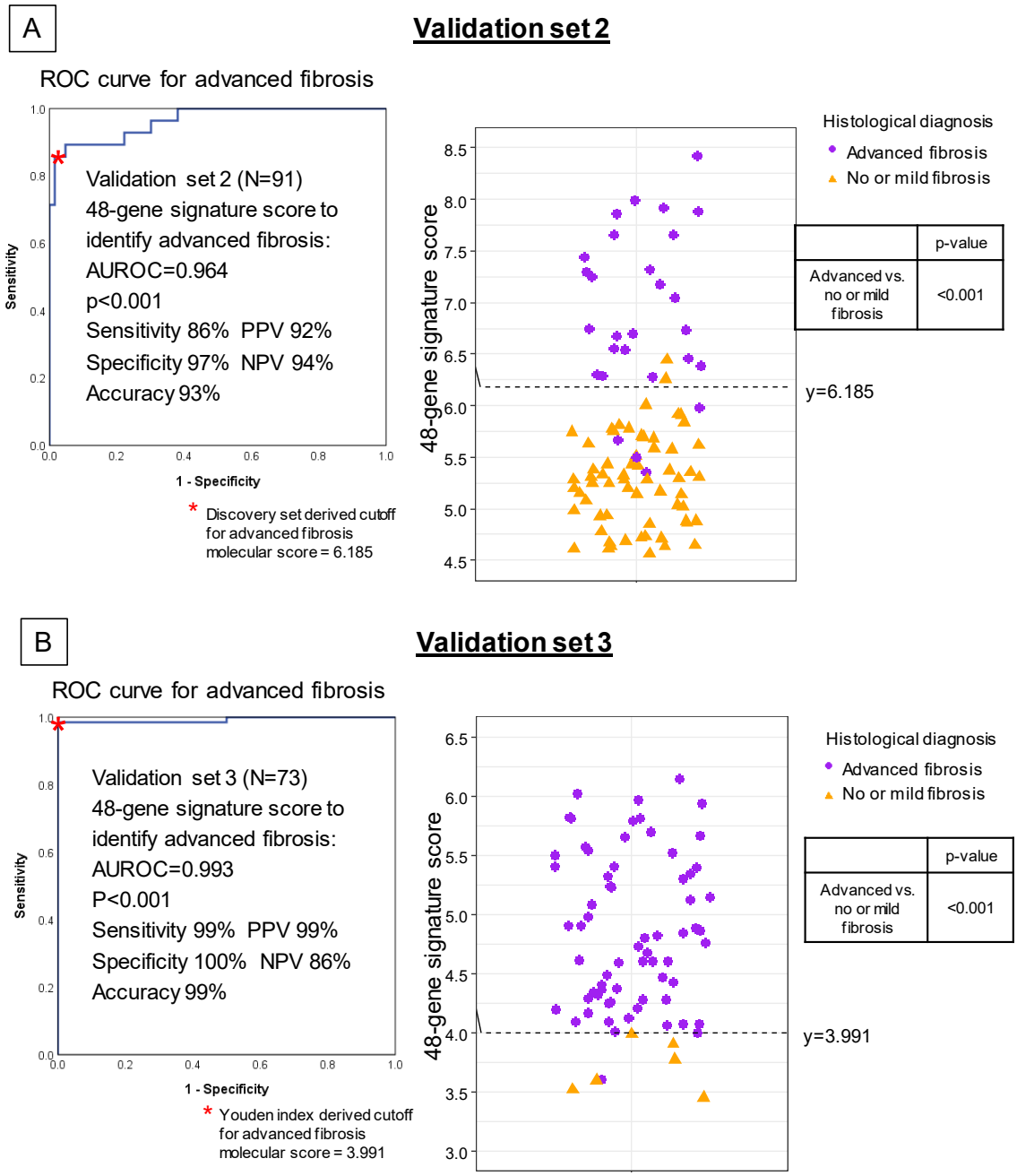

Figure 2.10. External validation of the 48-gene signature for advanced fibrosis in (A) validation set 2 and (B) validation set 3.

Validation set 3 was analyzed on a different microarray platform (Affymetrix Human Genome U219 Array). Thus, the cutoff derived in the discovery set was not applied to validation set 3. Despite different microarray platforms, the 48-gene signature was still significantly upregulated in advanced fibrosis with excellent performance to discriminate advanced and no or mild fibrosis in validation set 3. This showed the 48-gene signature was capable to identify advanced fibrosis across different microarray platforms. PPV, positive predictive value; NPV, negative predictive value. ROC, receiver operating characteristic.

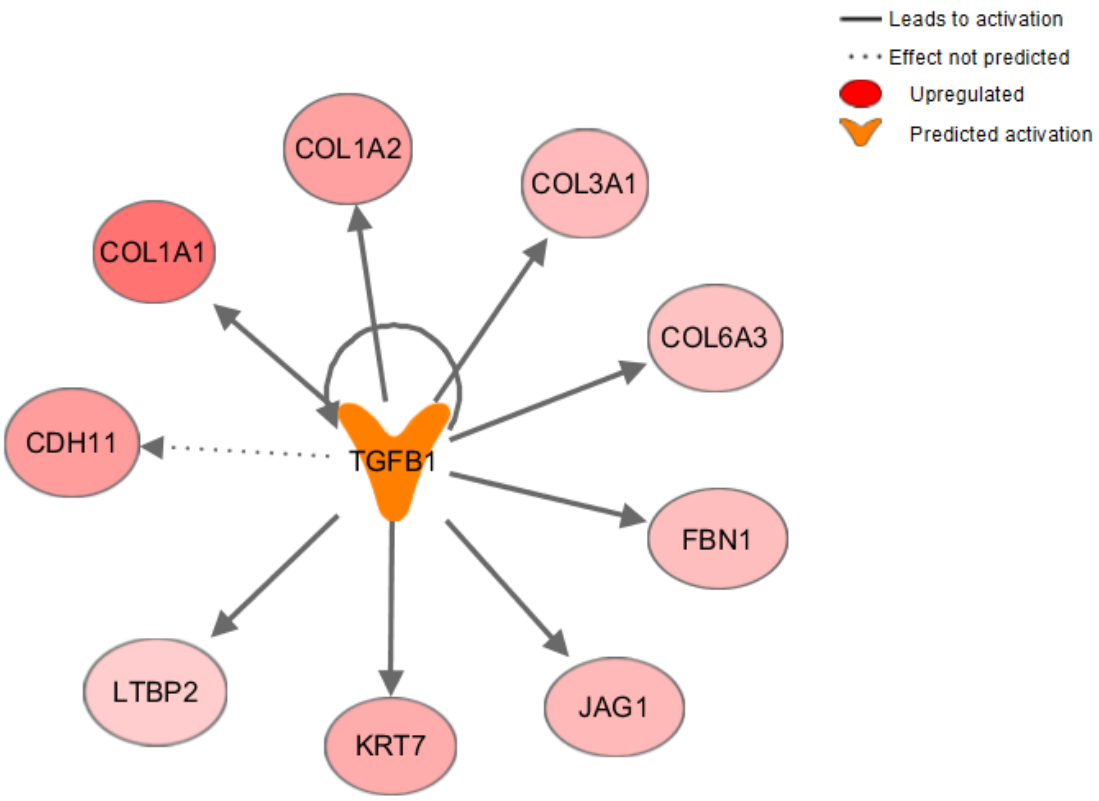

Figure 2.11. TGFβ1 was a significant upstream regulator in the 48-gene signature.

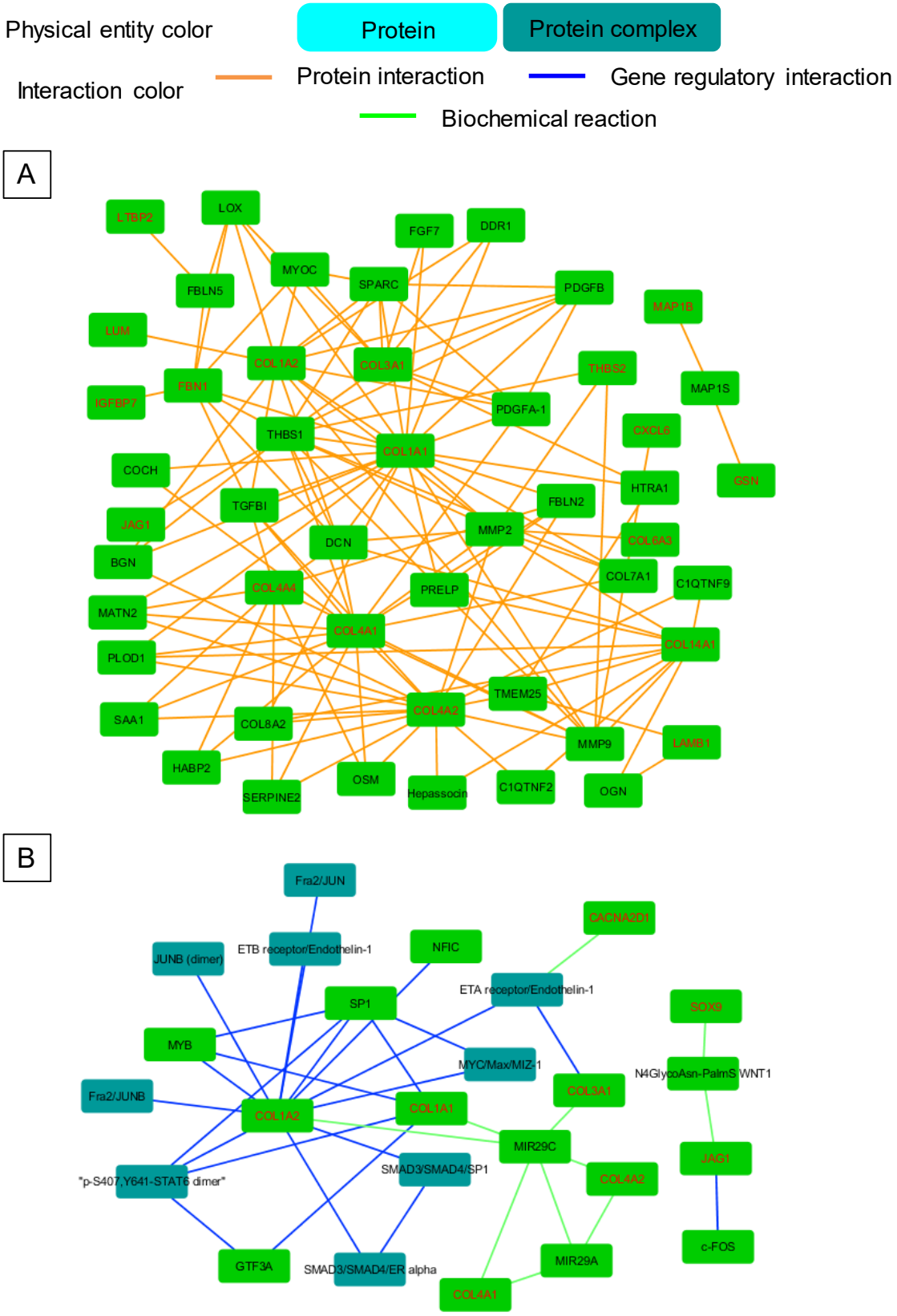

Figure 2.12. Molecular interaction analysis.

(Figure 2.12 continued) Red node labels denote genes in the 48-gene signature and black node labels denote intermediate nodes (potential upstream regulators and specific participants in pathways that interacts with the 48-gene signature). (A) Protein-protein interaction information of the 48-gene signature. The analysis was carried out using only high-confidence binary interactions and a default intermediate nodes z-score threshold of 20. (B) Biochemical reaction and gene regulatory interaction of the 48-gene signature. This analysis was carried out using a default intermediate nodes z-score threshold of 20.

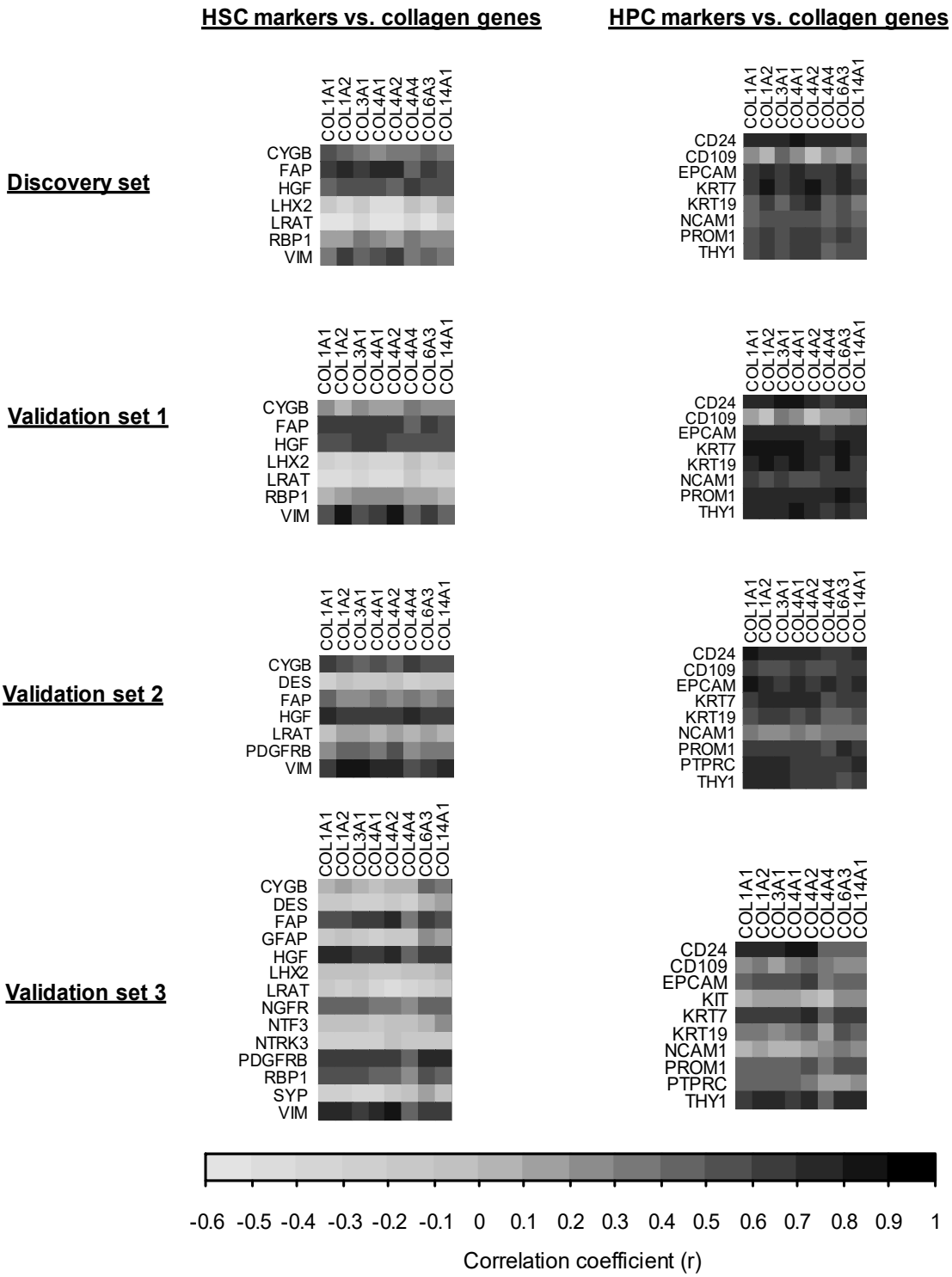

Figure 2.13. Correlation heatmap of the expression of hepatic stellate cell (HSC) markers vs. collagen genes and the expression of hepatic progenitor cell (HPC) markers vs. collagen genes.

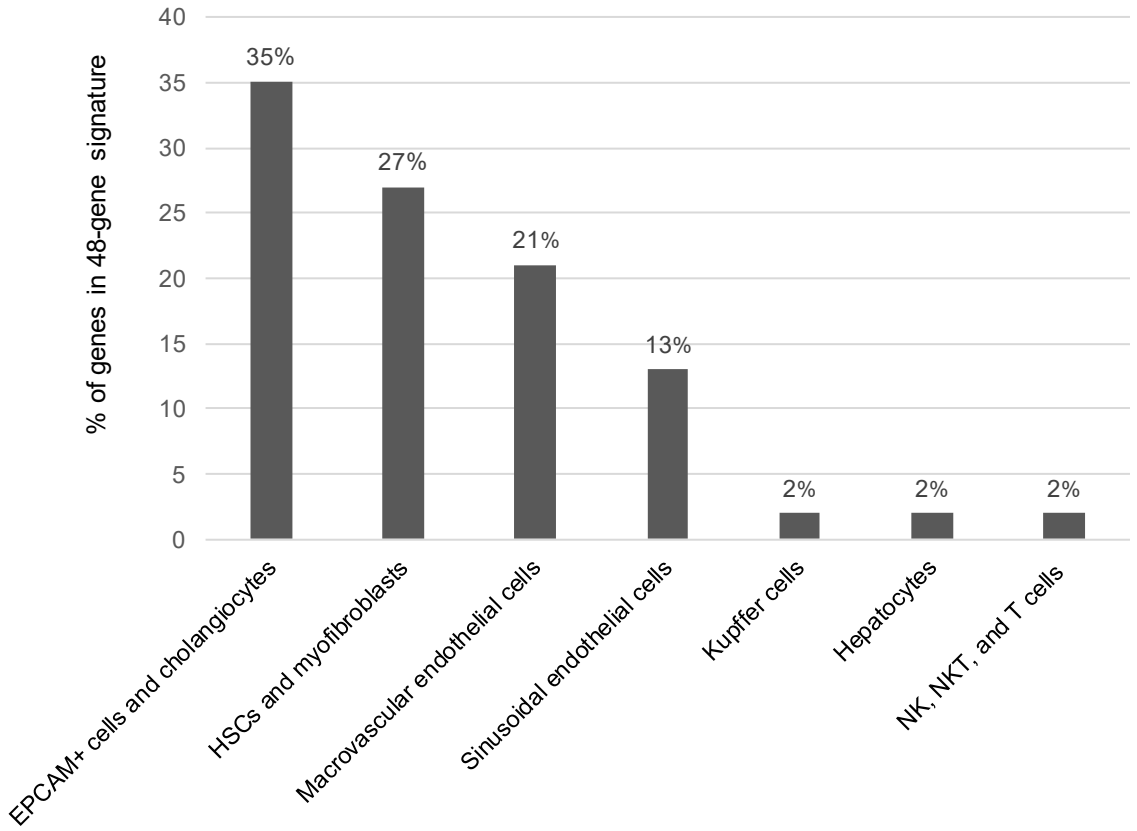

Figure 2.14. The percentage of genes in the 48-gene signature that were up-regulated in a specific cell type when compared to other cell types in normal livers.

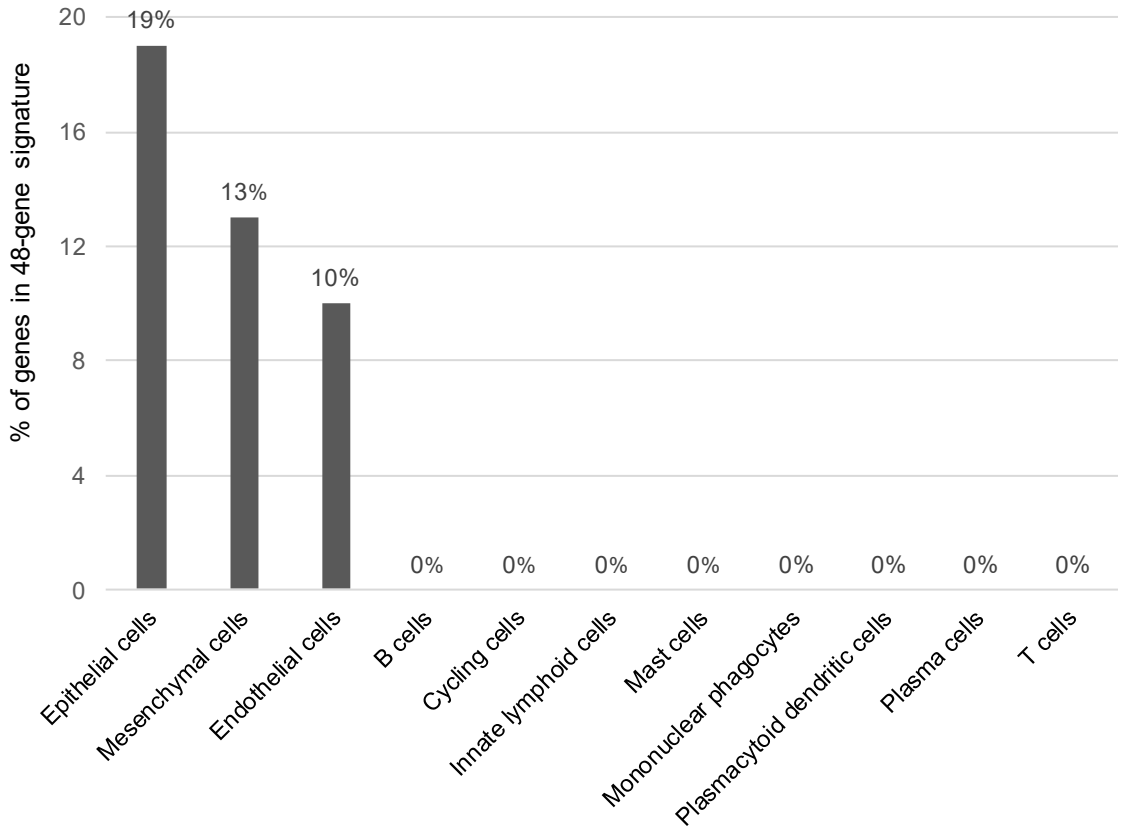

Figure 2.15. The percentage of genes in the 48-gene signature that were significantly up-regulated in a specific cell type in cirrhotic livers when compared to normal livers.

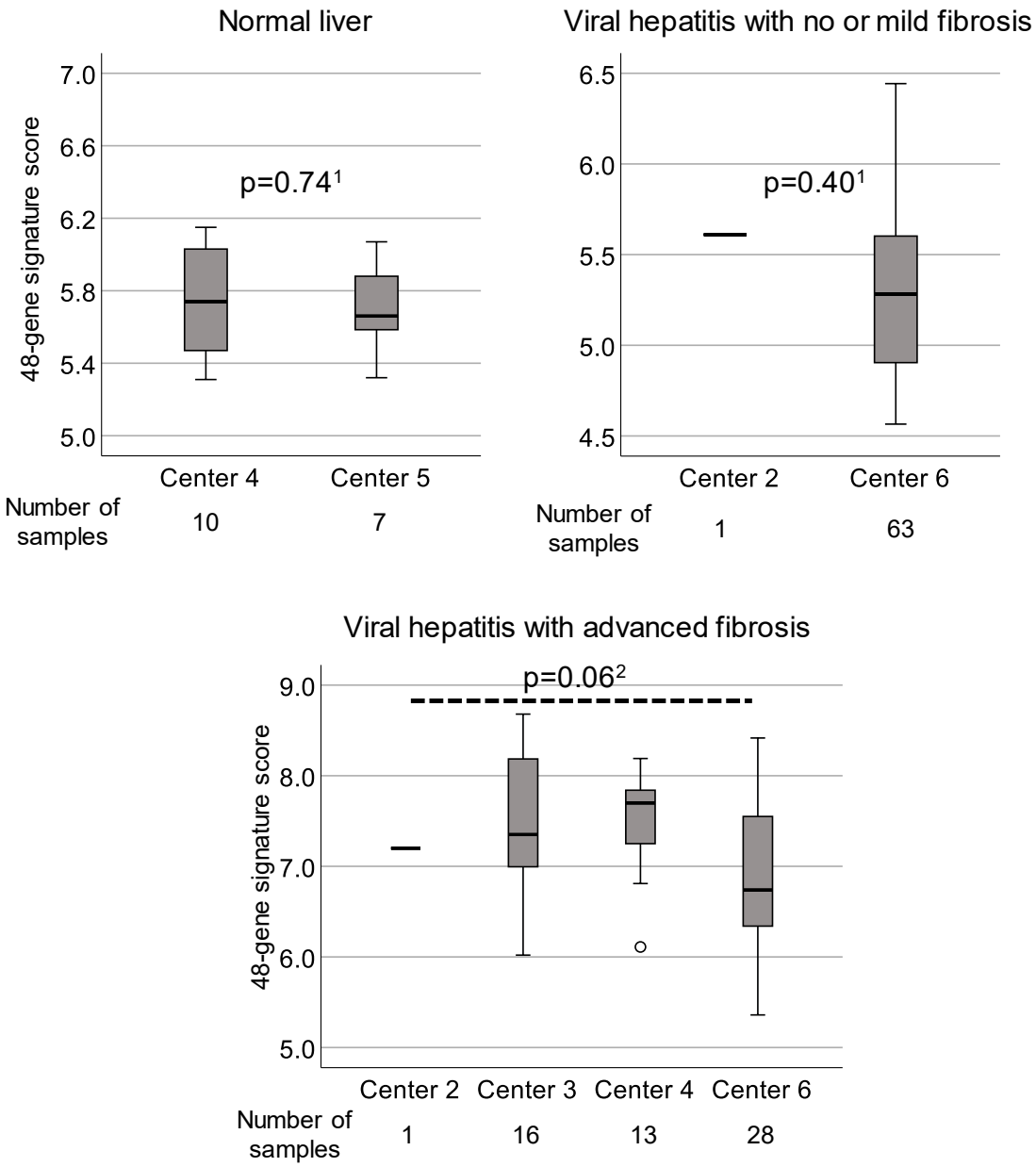

Figure 2.16. The 48-gene signature in samples with the same liver disease and fibrosis group had no significant difference among different centers.
NAFLD samples were not shown because all NAFLD samples were from single center (center 1). Alcoholic liver disease samples were not shown because the samples from center 5 and 7 were analyzed by different microarray platforms. Data for cryptogenic hepatitis were not shown because these samples are heterogeneous and the sample size (n=5) is too small to make an interpretation. [1]Mann-Whitney test. [2]Kruskal-Wallis test.

2.5 – References

1. Younossi ZM, Koenig AB, Abdelatif D, Fazel Y, Henry L, Wymer M. Global epidemiology of nonalcoholic fatty liver disease-Meta-analytic assessment of prevalence, incidence, and outcomes. Hepatology 2016 Jul;64(1):73-84.
2. El-Serag HB. Epidemiology of viral hepatitis and hepatocellular carcinoma. Gastroenterology 2012 May;142(6):1264-1273.
3. Schweitzer A, Horn J, Mikolajczyk RT, Krause G, Ott JJ. Estimations of worldwide prevalence of chronic hepatitis B virus infection: a systematic review of data published between 1965 and 2013. Lancet 2015 Oct 17;386(10003):1546-1555.
4. Younossi ZM, Stepanova M, Afendy M, Fang Y, Younossi Y, Mir H, et al. Changes in the prevalence of the most common causes of chronic liver diseases in the United States from 1988 to 2008. Clin Gastroenterol Hepatol 2011 Jun;9(6):524-530.
5. Bataller R, Brenner DA. Liver fibrosis. J Clin Invest 2005 Feb;115(2):209-218.
6. Khalid SS, Hamid S, Siddiqui AA, Qureshi A, Qureshi N. Gene profiling of early and advanced liver disease in chronic hepatitis C patients. Hepatol Int 2011 Sep;5(3):782-788.
7. Moylan CA, Pang H, Dellinger A, Suzuki A, Garrett ME, Guy CD, et al. Hepatic gene expression profiles differentiate presymptomatic patients with mild versus severe nonalcoholic fatty liver disease. Hepatology 2014 Feb;59(2):471-482.
8. Ahmad W, Ijaz B, Hassan S. Gene expression profiling of HCV genotype 3a initial liver fibrosis and cirrhosis patients using microarray. J Transl Med 2012;10:41.

9. Wang M, Gong Q, Zhang J, Chen L, Zhang Z, Lu L, et al. Characterization of gene expression profiles in HBV-related liver fibrosis patients and identification of ITGBL1 as a key regulator of fibrogenesis. Sci Rep 2017 Mar 6;7:43446.

10. Ramnath D, Irvine KM, Lukowski SW, Horsfall LU, Loh Z, Clouston AD, et al. Hepatic expression profiling identifies steatosis-independent and steatosis-driven advanced fibrosis genes. JCI Insight 2018 Jul 26;3(14).

11. Sanyal AJ, Friedman SL, McCullough AJ, Dimick-Santos L. Challenges and opportunities in drug and biomarker development for nonalcoholic steatohepatitis: findings and recommendations from an American Association for the Study of Liver Diseases-U.S. Food and Drug Administration Joint Workshop. Hepatology 2015 Apr;61(4):1392-1405.

12. Orman ES, Odena G, Bataller R. Alcoholic liver disease: pathogenesis, management, and novel targets for therapy. J Gastroenterol Hepatol 2013 Aug;28 Suppl 1:77-84.

13. Westbrook RH, Dusheiko G. Natural history of hepatitis C. J Hepatol 2014 Nov;61(1 Suppl):S58-S68.

14. Tsochatzis EA, Bosch J, Burroughs AK. Liver cirrhosis. Lancet 2014 May 17;383(9930):1749-1761.

15. EASL-EASD-EASO Clinical Practice Guidelines for the management of non-alcoholic fatty liver disease. J Hepatol 2016 Jun;64(6):1388-1402.

16. Sanyal AJ. Past, present and future perspectives in nonalcoholic fatty liver disease. Nat Rev Gastroenterol Hepatol 2019 Jun;16(6):377-386.

17. Affo S, Dominguez M, Lozano JJ, Sancho-Bru P, Rodrigo-Torres D, Morales-Ibanez O, et al. Transcriptome analysis identifies TNF superfamily receptors as potential therapeutic targets in alcoholic hepatitis. Gut 2013 Mar;62(3):452-460.

18. Yildiz G, Arslan-Ergul A, Bagislar S, Konu O, Yuzugullu H, Gursoy-Yuzugullu O, et al. Genome-wide transcriptional reorganization associated with senescence-to-immortality switch during human hepatocellular carcinogenesis. PLoS One 2013;8(5):e64016.

19. Wurmbach E, Chen YB, Khitrov G, Zhang W, Roayaie S, Schwartz M, et al. Genome-wide molecular profiles of HCV-induced dysplasia and hepatocellular carcinoma. Hepatology 2007 Apr;45(4):938-947.

20. Trepo E, Goossens N, Fujiwara N, Song WM, Colaprico A, Marot A, et al. Combination of Gene Expression Signature and Model for End-Stage Liver Disease Score Predicts Survival of Patients With Severe Alcoholic Hepatitis. Gastroenterology 2018 Mar;154(4):965-975.

21. Gillet JP, Calcagno AM, Varma S, Marino M, Green LJ, Vora MI, et al. Redefining the relevance of established cancer cell lines to the study of mechanisms of clinical anti-cancer drug resistance. Proc Natl Acad Sci U S A 2011 Nov 15;108(46):18708-18713.

22. Andersen JB, Spee B, Blechacz BR, Avital I, Komuta M, Barbour A, et al. Genomic and genetic characterization of cholangiocarcinoma identifies therapeutic targets for tyrosine kinase inhibitors. Gastroenterology 2012 Apr;142(4):1021-1031.

23. Pineau P, Volinia S, McJunkin K, Marchio A, Battiston C, Terris B, et al. miR-221 overexpression contributes to liver tumorigenesis. Proc Natl Acad Sci U S A 2010 Jan 5;107(1):264-269.

24. Aizarani N, Saviano A, Sagar, Mailly L, Durand S, Herman JS, et al. A human liver cell atlas reveals heterogeneity and epithelial progenitors. Nature 2019 Aug;572(7768):199-204.

25. Ramachandran P, Dobie R, Wilson-Kanamori JR, Dora EF, Henderson BEP, Luu NT, et al. Resolving the fibrotic niche of human liver cirrhosis at single-cell level. Nature 2019 Oct 9.

26. Siegmund SV, Schlosser M, Schildberg FA, Seki E, De MS, Uchinami H, et al. Serum Amyloid A Induces Inflammation, Proliferation and Cell Death in Activated Hepatic Stellate Cells. PLoS One 2016;11(3):e0150893.

27. Roderfeld M, Weiskirchen R, Atanasova S, Gressner AM, Preissner KT, Roeb E, et al. Altered factor VII activating protease expression in murine hepatic fibrosis and its influence on hepatic stellate cells. Liver Int 2009 May;29(5):686-691.

28. Levy MT, Trojanowska M, Reuben A. Oncostatin M: a cytokine upregulated in human cirrhosis, increases collagen production by human hepatic stellate cells. J Hepatol 2000 Feb;32(2):218-226.

29. Inoue T, Ohbayashi T, Fujikawa Y, Yoshida H, Akama TO, Noda K, et al. Latent TGF-beta binding protein-2 is essential for the development of ciliary zonule microfibrils. Hum Mol Genet 2014 Nov 1;23(21):5672-5682.

30. Kagan HM, Li W. Lysyl oxidase: properties, specificity, and biological roles inside and outside of the cell. J Cell Biochem 2003 Mar 1;88(4):660-672.

31. Hara H, Uchida S, Yoshimura H, Aoki M, Toyoda Y, Sakai Y, et al. Isolation and characterization of a novel liver-specific gene, hepassocin, upregulated during liver regeneration. Biochim Biophys Acta 2000 Jun 21;1492(1):31-44.

32. Roderburg C, Urban GW, Bettermann K, Vucur M, Zimmermann H, Schmidt S, et al. Micro-RNA profiling reveals a role for miR-29 in human and murine liver fibrosis. Hepatology 2011 Jan;53(1):209-218.

33. Williams MJ, Clouston AD, Forbes SJ. Links between hepatic fibrosis, ductular reaction, and progenitor cell expansion. Gastroenterology 2014 Feb;146(2):349-356.

34. Friedman SL. Hepatic stellate cells: protean, multifunctional, and enigmatic cells of the liver. Physiol Rev 2008 Jan;88(1):125-172.

35. Zhang DY, Goossens N, Guo J, Tsai MC, Chou HI, Altunkaynak C, et al. A hepatic stellate cell gene expression signature associated with outcomes in hepatitis C cirrhosis and hepatocellular carcinoma after curative resection. Gut 2016 Oct;65(10):1754-1764.

36. Meissner EG, McLaughlin M, Matthews L, Gharib AM, Wood BJ, Levy E, et al. Simtuzumab treatment of advanced liver fibrosis in HIV and HCV-infected adults: results of a 6-month open-label safety trial. Liver Int 2016 Dec;36(12):1783-1792.

37. Harrison SA, Abdelmalek MF, Caldwell S, Shiffman ML, Diehl AM, Ghalib R, et al. Simtuzumab Is Ineffective for Patients With Bridging Fibrosis or Compensated

Cirrhosis Caused by Nonalcoholic Steatohepatitis. Gastroenterology 2018 Oct;155(4):1140-1153.

38. Munshaw S, Hwang HS, Torbenson M, Quinn J, Hansen KD, Astemborski J, et al. Laser captured hepatocytes show association of butyrylcholinesterase gene loss and fibrosis progression in hepatitis C-infected drug users. Hepatology 2012 Aug;56(2):544-554.

39. Ahrens M, Ammerpohl O, von SW, Kolarova J, Bens S, Itzel T, et al. DNA methylation analysis in nonalcoholic fatty liver disease suggests distinct disease-specific and remodeling signatures after bariatric surgery. Cell Metab 2013 Aug 6;18(2):296-302.

40. Bourd-Boittin K, Bonnier D, Leyme A, Mari B, Tuffery P, Samson M, et al. Protease profiling of liver fibrosis reveals the ADAM metallopeptidase with thrombospondin type 1 motif, 1 as a central activator of transforming growth factor beta. Hepatology 2011 Dec;54(6):2173-2184.

41. Caillot F, Hiron M, Goria O, Gueudin M, Francois A, Scotte M, et al. Novel serum markers of fibrosis progression for the follow-up of hepatitis C virus-infected patients. Am J Pathol 2009 Jul;175(1):46-53.

42. Caillot F, Derambure C, Bioulac-Sage P, Francois A, Scotte M, Goria O, et al. Transient and etiology-related transcription regulation in cirrhosis prior to hepatocellular carcinoma occurrence. World J Gastroenterol 2009 Jan 21;15(3):300-309.

43. Neuschwander-Tetri BA, Loomba R, Sanyal AJ, Lavine JE, Van Natta ML, Abdelmalek MF, et al. Farnesoid X nuclear receptor ligand obeticholic acid for non-cirrhotic, non-alcoholic steatohepatitis (FLINT): a multicentre, randomised, placebo-controlled trial. Lancet 2015 Mar 14;385(9972):956-965.

44. Loomba R, Lawitz E, Mantry PS, Jayakumar S, Caldwell SH, Arnold H, et al. The ASK1 inhibitor selonsertib in patients with nonalcoholic steatohepatitis: A randomized, phase 2 trial. Hepatology 2017 Sep 11.

45. Muir AJ, Levy C, Janssen HLA, Montano-Loza AJ, Shiffman ML, Caldwell S, et al. Simtuzumab for Primary Sclerosing Cholangitis: Phase 2 Study Results With Insights on the Natural History of the Disease. Hepatology 2018 Aug 28.

46. Torok J, Dranoff JA, Schuppan D, Friedman SL. Strategies and endpoints of antifibrotic drug trials: Summary and recommendations from the AASLD Emerging Trends Conference, Chicago, June 2014. Hepatology 2015 Jan 27.

47. Xu X, Li YM, Ji H, Hou CZ, Cheng YB, Ma FP. Changes of ECM and CAM gene expression profile in the cirrhotic liver after HCV infection: analysis by cDNA expression array. World J Gastroenterol 2005 Apr 14;11(14):2184-2187.

48. Shang L, Hosseini M, Liu X, Kisseleva T, Brenner DA. Human hepatic stellate cell isolation and characterization. J Gastroenterol 2018 Jan;53(1):6-17.

49. Yin C, Evason KJ, Asahina K, Stainier DY. Hepatic stellate cells in liver development, regeneration, and cancer. J Clin Invest 2013 May;123(5):1902-1910.

50. Cassiman D, van PJ, De VR, Van LF, Desmet V, Yap SH, et al. Synaptophysin: A novel marker for human and rat hepatic stellate cells. Am J Pathol 1999 Dec;155(6):1831-1839.

51. Qiu Q, Hernandez JC, Dean AM, Rao PH, Darlington GJ. CD24-positive cells from normal adult mouse liver are hepatocyte progenitor cells. Stem Cells Dev 2011 Dec;20(12):2177-2188.

52. Li J, Xin J, Zhang L, Wu J, Jiang L, Zhou Q, et al. Human hepatic progenitor cells express hematopoietic cell markers CD45 and CD109. Int J Med Sci 2014;11(1):65-79.

53. Yoon SM, Gerasimidou D, Kuwahara R, Hytiroglou P, Yoo JE, Park YN, et al. Epithelial cell adhesion molecule (EpCAM) marks hepatocytes newly derived from stem/progenitor cells in humans. Hepatology 2011 Mar;53(3):964-973.

54. Bateman AC, Hubscher SG. Cytokeratin expression as an aid to diagnosis in medical liver biopsies. Histopathology 2010 Mar;56(4):415-425.

55. Sancho-Bru P, Altamirano J, Rodrigo-Torres D, Coll M, Millan C, Jose LJ, et al. Liver progenitor cell markers correlate with liver damage and predict short-term mortality in patients with alcoholic hepatitis. Hepatology 2012 Jun;55(6):1931-1941.

56. Kim MY, Cho MY, Baik SK, Jeong PH, Suk KT, Jang YO, et al. Beneficial effects of candesartan, an angiotensin-blocking agent, on compensated alcoholic liver fibrosis - a randomized open-label controlled study. Liver Int 2012 Jul;32(6):977-987.

57. McPherson S, Wilkinson N, Tiniakos D, Wilkinson J, Burt AD, McColl E, et al. A randomised controlled trial of losartan as an anti-fibrotic agent in non-alcoholic steatohepatitis. PLoS One 2017;12(4):e0175717.

58. Colmenero J, Bataller R, Sancho-Bru P, Dominguez M, Moreno M, Forns X, et al. Effects of losartan on hepatic expression of nonphagocytic NADPH oxidase and fibrogenic genes in patients with chronic hepatitis C. Am J Physiol Gastrointest Liver Physiol 2009 Oct;297(4):G726-G734.

59. Kim SG, Kim YM, Choi JY, Han JY, Jang JW, Cho SH, et al. Oltipraz therapy in patients with liver fibrosis or cirrhosis: a randomized, double-blind, placebo-controlled phase II trial. J Pharm Pharmacol 2011 May;63(5):627-635.

60. McHutchison J, Goodman Z, Patel K, Makhlouf H, Rodriguez-Torres M, Shiffman M, et al. Farglitazar lacks antifibrotic activity in patients with chronic hepatitis C infection. Gastroenterology 2010 Apr;138(4):1365-73, 1373.

Chapter 3: A Robust and Reproducible Method for Quantitative Measurement of Multigene Signatures in Clinical Liver Biopsies

3.1 – Introduction

Advanced liver fibrosis is the common final pathway of all chronic liver diseases, leading to cirrhosis and poor clinical outcomes (liver decompensation, need for liver transplantation, or premature death) (1). Histopathological assessment of a liver biopsy is a cornerstone in the evaluation and management of patients with chronic liver disease, but it lacks predictive ability for fibrosis progression and clinical outcomes (2, 3). Clinically available imaging- and laboratory test- based approaches also cannot predict fibrosis progression (4). Gene signature studies of clinical liver biopsies with chronic liver disease may allow us to gain more insights into the biology of disease heterogeneity.

Previous researchers reported that gene expression signatures in fresh human livers, compared with histopathology, could provide better prediction of prognosis including fibrosis progression and poor clinical outcomes in patients with chronic liver disease (5-11). However, translating these multiplex gene expression profiling into clinical practice is a challenging task. The major obstacle is the limited availability of fresh clinical specimens to analyze these gene signatures (12). All clinical liver biopsies are processed as formalin-fixed, paraffin-embedded (FFPE) specimens since this is the best standard for histopathology assessment. It is well known that RNA degradation is common in FFPE specimens due to formalin fixation and thus most methods of multiplex gene expression analysis (e.g. microarrays) do not reliably work in FFPE tissue specimens (12, 13). Moreover, there is usually limited amount of needle biopsy specimens left for gene expression analysis after paraffin sectioning for histological diagnostic purposes. To take these gene expression signatures into clinical application, clinical laboratories require a reliable and feasible

method for multiplexed gene expression quantification from miniscule leftover clinical liver biopsy specimens.

Recently, a high-throughput digital system to measure the expression of a large number genes, called NanoString nCounter Analysis System (NanoString Technologies, Seattle, WA), has become available for digital quantification of multiplexed target molecules (14). It uses color-coded molecular barcodes (each barcode corresponds to a gene of interest) and microscopic imaging to capture and count up to 800 individual mRNA transcripts in one hybridization reaction without the need for amplification of the cellular RNA or the need for reverse transcription reactions (14). Several peer-reviewed publications have shown NanoString nCounter Analysis System is more sensitive (smaller limit of detection) than microarrays and similar in sensitivity to quantitative polymerase chain reaction of mRNA detection (14-18). Gene expression measured by NanoString is highly consistent across matched fresh, frozen, and FFPE tissues (15, 17, 19). As an example of its potential for clinical application, the NanoString system has been Food and Drug Administration (FDA)-cleared for gene expression-based risk stratification and treatment planning in breast cancer patients using clinical FFPE breast tumor specimens (20). Despite the robustness of the NanoString technology for multiplex gene expression analysis using FFPE specimens in previous studies, to the best of my knowledge, no study has evaluated the robustness of NanoString nCounter Analysis System when analyzing clinical liver biopsies and how much of tissue is needed.

This chapter aims to establish a method for multiplex gene expression quantification for clinical liver biopsy using NanoString technology and evaluate how much clinical liver biopsy is needed for NanoString gene expression assay. To evaluate the methodological

robustness and feasibility of NanoString nCounter Analysis System, 68 hepatic fibrosis-associated genes (48 fibrosis genes from Chapter 2, 16 literature-selected fibrosis genes, and four housekeeping genes) were analyzed in 348 clinical liver biopsies and 15 explanted liver tissues from 15 patients. Each explanted liver tissue was divided into two pieces: one piece was placed in RNAlater (fresh tissue) and the other in formalin and paraffin embedded (FFPE tissue). Transcript counts in paired fresh vs. FFPE explant livers were analyzed to evaluate if transcript counts measured in FFPE tissues using NanoString are reliable. The results supported that NanoString nCounter Analysis System is favorable for multiplex gene expression quantification using clinical liver biopsies based upon reproducibility, robustness, ease of use, experimental hands-on time, and utility for clinical application.

3.2 – Material and methods

3.2.1 – Sample collection

Single core needle biopsies were obtained under ultrasound guidance by 18-gauge spring-loaded needles. The NanoString assay was used to analyze 348 clinical liver biopsies with different liver diseases, which include 78 autoimmune hepatitis (AIH), 94 non-alcoholic fatty liver disease (NAFLD), 149 post-transplant recurrent viral hepatitis C (HCV), and 27 normal livers (Table 3.1). The 27 normal livers were composed of 15 allograft livers with no significant histological abnormality and 12 native livers, of which three were donor livers and nine were livers with no significant histological abnormality. A core tissue from 15 explanted livers (total hepatectomy specimens) was collected and each core tissue was divided into two pieces: one piece was immediately stabilized in RNAlater (Thermo Fisher Scientific, Waltham, MA), kept at −4°C for 24 hours and stored at −20°C until processing

and one piece fixed in 10% neutral buffered formalin and embedded in paraffin (Figure 3.1). Each piece had a size of approximately 1 cm x 1 cm x 1 cm. This study was approved by the institutional review board of the University of Alberta.

3.2.2 – Histopathological assessment of clinical liver biopsies

Liver biopsy specimens of normal liver, AIH, and recurrent HCV were staged for fibrosis according to METAVIR classification system (21). Liver biopsy specimens of NAFLD were staged for fibrosis according to Brunt classification system (22).

3.2.3 – RNA isolation from fresh samples

Following homogenization in 2 ml of Trizol reagent (Invitrogen, Carlsbad, CA), total RNA from fresh explant livers was isolated and purified using the RNeasy Mini Kit (Qiagen, Ontario, Canada) according to manufacturer recommendation. Precipitated and dried RNA was dissolved in DNase/RNase-free distilled water and the concentration and quality were measured by NanoDrop 2000 spectrophotometer (Thermo Fisher Scientific, Waltham, MA).

3.2.4 – RNA isolation from FFPE samples

Reeda Gill assisted with the RNA isolation from FFPE samples. The length of clinical liver biopsy in FFPE block was measured before cutting sections for RNA isolation. Three to eight consecutive 20-µm thick sections were obtained from each FFPE block with equipment sterilization with RNase away reagent (Ambion, Carlsbad, CA) and microtome blade replacement between blocks. Sections were immediately put into sterile 1.5-mL DNase/RNase free microcentrifuge tubes for RNA isolation using a RecoverAll Total Nucleic Acid Isolation Kit (Ambion, Carlsbad, CA). Precipitated and dried RNA was

dissolved in DNase/RNase-free distilled water. The concentration and quality of RNA was measured by NanoDrop 2000 spectrophotometer (Thermo Fisher Scientific, Waltham, MA). RNA integrity was assessed on an Agilent 2100 Bioanalyzer (Agilent, Palo Alto, CA). Detailed protocols for DNA/RNA free preparation of FFPE tissue sectioning and RNA isolation are available in Appendix A and Appendix B, respectively. Reeda Gill assisted with completing Appendix A and Appendix B.

3.2.5 – Gene expression quantification using NanoString nCounter System

I analyzed 68 hepatic fibrosis-associated genes (48 fibrosis genes from Chapter 2, 16 literature-selected fibrosis genes, and four housekeeping genes) in this chapter (Table 3.2). The 16 literature-selected fibrosis genes were selected by gene expression profiling in microarray datasets in Chapter 2 and genes with an area under the receiver operating characteristic curve ≥ 0.7 for advanced liver fibrosis in the discovery set and validation set 1 (23-27). Gene expression was quantified using a nCounter Elements assay (NanoString Technologies). Oligonucleotide probe sequences (Table 3.3) were designed and synthesized by Integrated DNA Technologies (Coralville, IA). Each probe contained a probe A and a probe B and were designed to hybridize specifically to each mRNA target (Figure 3.2). Probe A contained a capture tag attached to a biotin that enables to capture on streptavidin-coated surface in a cartridge and probe B contained a reporter tag linked to a color-coded molecular signature that was specific to each gene. mRNAs were hybridized (without amplification) to the probes for the measured genes. Hybridizations were carried out in a single tube for each sample for 18 hours at 67 °C. After hybridization, excess probes were removed and hybridized probes were immobilized and aligned on the cartridge by the nCounter Prep Station (NanoString Technologies, Seattle, WA). Transcript counts were quantified by the

nCounter Digital Analyzer (NanoString Technologies, Seattle, WA).

3.2.6 – NanoString quality control and data preprocessing

Quality control and preprocessing of raw NanoString data were performed using nSolver Analysis Software version 4.0 (NanoString Technologies, Seattle, WA) with manufacturer-recommended default parameters for quality control and normalization flagging. The parameters for quality control flagging include imaging (field of view <75%), binding density (<0.05 or >2.25), positive control linearity (R^2 value <0.95), and positive control limit of detection (0.5fM positive control ≤2 standard deviations above the mean of the negative controls). Background noise was adjusted by subtracting the geometric mean transcript counts of six internal negative controls of each sample. mRNA with transcript counts less than the geometric mean transcript counts of the six internal negative controls were floored to a value of 1. Next, to adjust the variations in hybridization and purification efficiency, a positive normalization factor for each sample was calculated from the geometric mean transcript counts of the six internal positive controls (spike-in oligos) across all samples divided by the geometric mean transcript counts of the six internal positive controls of each sample. The positive normalization factor for each sample was multiplied to each mRNA transcript counts after background noise correction (with default flagging of positive normalization factors <0.3 or >3.0). After positive control normalization, to adjust the variations in different RNA input quantities, a housekeeping gene normalization factor for each sample was calculated from the geometric mean transcript counts of the four housekeeping genes across all samples divided by the geometric mean transcript counts of the four housekeeping genes in each sample. The housekeeping gene normalization factor for each sample was multiplied to the measured mRNA transcript counts after positive

control normalization (with default flagging of housekeeping gene normalization factors <0.1 or >10.0).

3.2.7 – NanoString reproducibility experiments

RNA titration experiment was performed with repeat runs of four RNA samples from four unique clinical liver biopsies with four different RNA quantities: 50, 100, 200, and 400 ng. Intra-operator reproducibility experiment was performed with repeat runs of six RNA samples from six unique clinical liver biopsies in different days. Inter-operator reproducibility experiment was performed with repeat runs of four RNA samples from four unique clinical liver biopsies by two different operators: a molecular pathology technologist (Shalawny Miller) and a graduate student (me). Inter-lot reproducibility experiment was performed with repeat runs of two RNA samples from two unique clinical liver biopsies in three different lots of nCounter Elements reagents.

3.2.8 – Statistical analysis

Continuous variables were presented as mean ± standard deviation and categorical variables were presented as number and percentage. Mann-Whitney U-test was used for continuous data compared between two groups. Fisher's exact test was used for categorical variables compared between groups. A Welch's ANOVA followed by the Games-Howell post hoc test was used to determine differences among historical fibrosis stages (F0-F4) vs. molecular gene signature. Correlations between variables were evaluated using Spearman's rank correlation coefficient. All tests with a two-sided p-value <0.05 were considered significant. All analyses and figures were performed and generated using SPSS 25 statistical software (IBM, Armonk, NY, USA), Excel 2010 (Microsoft Corporation, Redmond, WA),

or R-program (version 3.3.2; http://www.r-project.org) with the following packages: corrplot and ggplot2.

3.3 – Results

3.3.1 – The quantity and quality of RNA isolated from clinical liver biopsies

Table 3.1 summarized the characteristics of 348 clinical liver biopsies that were analyzed. Adequate RNA (≥50 ng) was isolated from 99% (348 of 350) of clinical liver biopsies. The 348 successfully isolated clinical liver biopsies yielded a mean of 1703 ng (range: 68 - 8176 ng) with a mean A_{260}/A_{280} spectrophotometry ratio of 1.84 (1.65-2.05). The RNA yield for the two samples < 50 ng were 40.6 and 47.5 ng and the A_{260}/A_{280} were 2.05 and 1.97, respectively. Figure 3.3 showed the RNA integrity number of four representative clinical liver biopsies.

3.3.2 – The quantity and quality of RNA isolated from explant liver tissues

Adequate RNA was isolated from all 15 paired explanted liver tissues for NanoString gene expression assay. The mean A_{260}/A_{280} spectrophotometry ratio was 2.04 (range: 2.00-2.08) for 15 fresh liver tissues and 1.86 (1.72-2.03) for 15 FFPE liver tissues.

3.3.3 – Significant positive correlation between length of the core biopsy and the amount of total RNA

I had a 99% (348 of 350) success rate to isolate enough RNA (≥50 ng) for NanoString gene expression assay with a minimum of 1 mm core tissue length (mean: 17 mm, range: 1 - 40 mm) in the paraffin block before cutting sections (Figure 3.4A). This demonstrated only

very little amount of tissue is required for the NanoString gene expression assay. There was a significant positive correlation between the length of the core biopsy and the amount of total RNA ($r=0.281$, $p<0.001$).

To understand how much tissue is needed for the NanoString gene expression assay, the amount of total RNA was compared to number of sections obtained from the paraffin block. Although NanoString gene expression assay requires minimum 50 ng input of total RNA, here, 100 ng was used as a threshold to ensure enough total RNA for NanoString gene expression assay after RNA quality and quantity assessment. The success rate of isolating >100 ng of RNA with a core biopsy length > 5 mm was similar when obtaining three 20-µm thick sections compared to four to eight 20-µm thick sections (99% vs. 100%, $p=1$) (Table 3.4). However, if the core biopsy length is ≤5 mm, the success rate of isolating >100 ng of RNA was significantly lower when obtaining only three 20-µm thick sections compared to four to eight 20-µm thick sections (62.5% vs. 100%, $p=0.015$) (Table 3.4). Therefore, if there was >5 mm of core biopsy in the block, obtaining three 20-µm thick sections would be enough to isolate enough RNA for the NanoString assay. If there was ≤5 mm of core biopsy, four to eight 20-µm thick sections would be needed.

3.3.4 – No correlation between age of the biopsy and the amount of total RNA

I had a 99% (348 of 350) success rate to isolate enough RNA (≥50 ng) for NanoString gene expression assay with paraffin blocks up to 18 years old (mean: 4.79, range: 0.05-18.42) (Figure 3.4B). There was no correlation between age of the paraffin block and the total RNA yield ($r=-0.046$, $p=0.395$). This showed clinical liver biopsies ≤18 years old were suitable for NanoString gene expression assay; however, this should not be considered as an upper

limit since FFPE specimens older than 18 years were not examined for their suitability for NanoString gene expression assays.

3.3.5 – NanoString gene expression analysis

A total of 378 RNA samples (348 clinical liver biopsies and 30 explant liver samples) were analyzed using NanoString gene expression assay (Figure 3.1). Gene expression quantitation was successful for all 68 hepatic fibrosis-associated genes and all samples passed quality and normalization controls except for 10 (2.6%) samples from clinical liver biopsies. These 10 samples were flagged because of having a housekeeping gene normalization factor >10, which represented these RNA samples were seriously degraded and considered as having poor-quality gene expression profile. These poor-quality samples were removed and only the samples with high-quality gene expression profiles were used in further analysis.

3.3.6 – Transcript counts measured by NanoString gene expression assay were strongly correlated between paired fresh and FFPE samples

To test if the transcript counts of FFPE samples measured by NanoString gene expression assay were reliable, the transcript counts of the 68 hepatic fibrosis-associated genes were measured in 15 paired fresh and FFPE explant livers. Normalized transcript counts of 15 paired fresh and FFPE samples were normally distributed and strongly correlated ($r=0.944$, $p<0.001$, Figure 3.5A and 3.5B). Correlation heatmap of all-pairwise combinations of fresh vs. FFPE samples also revealed strong correlation (Figure 3.5C). To determine if the transcript counts measured in each individual FFPE sample was reliable, I

compared the correlation coefficients between normalized transcript counts for each paired fresh vs. FFPE sample (sample-by-sample comparison). The mean correlation coefficient was 0.956, with a minimum correlation coefficient of 0.900 ($p<0.001$) and a maximum correlation coefficient of 0.984 ($p<0.001$) (Table 3.5). This showed the transcript counts measured in FFPE samples by NanoString gene expression assay were reliable.

3.3.7 – The reproducibility of NanoString gene expression assay

NanoString gene expression assay had robust reproducibility across different RNA input quantities

To understand if different RNA input quantities affect mRNA transcript counts, I performed a titration experiment on four RNA samples from four unique clinical liver biopsies with different RNA input quantities (50 ng, 100 ng, 200 ng, and 400 ng). Normalized transcript counts were strongly correlated among different RNA input quantities for all four samples ($r=0.946$-0.995, $p<0.001$, Figure 3.6). Moreover, all normalized transcript counts with different RNA input quantities were almost identical with fold-change (slope) values near to 1. This demonstrated normalized transcript counts with different RNA input quantities were comparable after normalization.

To show the NanoString gene expression assay was capable to detect fractional fold-changes of different RNA input quantities, the transcript counts of 68 hepatic fibrosis-associated genes of the same four samples on Figure 3.6 were preprocessed without housekeeping gene normalization, which was used to adjust RNA input quantities (Figure 3.7). The slopes for all four samples were correlated closely with the expected fold-change values of 0.5 (100 ng input vs. 50 ng input), 2 (100 ng input vs. 200 ng input), and 4 (100 ng

input vs. 400 ng input). This indicated NanoString gene expression assay had a linear response to different amount of RNA inputs in up to five orders of magnitude (from 1 to 10^5 transcript counts).

NanoString gene expression assay had robust reproducibility with repeat runs by one operator

To assess intra-operator reproducibility of the NanoString gene expression assay, six RNA samples from six unique clinical liver biopsies were analyzed twice on two different days by the same operator (Figure 3.8). Normalized transcript counts of repeat runs of all six samples were strongly correlated to each other ($r=0.950$-0.990, $p<0.001$). This demonstrated the methodological robustness of the NanoString nCounter Analysis System.

To understand the precision of NanoString gene expression assay, I evaluated how many hepatic fibrosis-associated genes were within the 95% confidence interval of the regression line in the six samples on Figure 3.8. Overall, the precision increased with expression levels, with 100% (47 of 47) of highly expressed genes (transcript counts >1000) and 99% (299 of 304) of moderately expressed genes (transcript counts between 10 and 1000), were within the 95% confidence interval (Figure 3.8). However, only 71% (41 of 58) of lowly expressed genes (transcript counts <10) were within the 95% confidence interval. This showed genes with transcripts counts less than 10 might not be reliably quantitated by the NanoString gene expression assay.

NanoString gene expression assay had robust reproducibility with repeat runs by different operators of varying technical expertise

To assess the inter-operator reproducibility of the NanoString gene expression assay,

four RNA samples from four unique clinical liver biopsies were analyzed twice on two different days by two different operators (a graduate student and a molecular pathology technologist) of varying technical expertise (Figure 3.9). Normalized transcript counts of repeat runs of all four samples were strongly correlated to each other ($r=0.949$-0.992, $p<0.001$). This demonstrated the technical replicability of the NanoString nCounter Analysis System.

NanoString gene expression assay had robust reproducibility with repeat runs using different lots of reagents

To assess if different lots of NanoString reagents would affect gene expression measurements, two RNA samples of two unique clinical liver biopsies were analyzed on three different days by the same operator across three different lots of reagents (Figure 3.10). Normalized transcript counts of repeat runs showed nearly prefect correlation ($r=0.998$-0.999, $p<0.001$). This demonstrated different lot of reagents did not affect the mRNA transcript counts.

3.3.8 – The expression levels of the fibrosis genes grouped by biological function increased progressively with histological fibrosis stages

The fibrosis genes were annotated based on their biological functions from literature (Table 3.6). Most of the fibrosis genes were involved in extracellular matrix synthesis or cross-linking (23 genes), inducing fibroblast or myofibroblast or hepatic stellate cell activation (17 genes), collagen genes (8 genes), inflammation genes (6 genes), and hepatic progenitor cell markers (7 genes) (Table 3.7). I compared the geometric mean expression of the gene set in each biological function with different histological fibrosis stages (Figure

3.11A-E). The expression of each gene set increased progressively with histological fibrosis stages. Interestingly, patients within the same histological fibrosis stage had a heterogeneous gene set expression even in F0 and F1 fibrosis. This may suggest developing molecular fibrogenesis in some of the early stage patients and may predict future fibrosis progression. To test this, I analyzed all diseased biopsies without advanced fibrosis (F0-F2) and with follow-up outcome data available to understand if the expression of fibrosis genes can predict progression to advanced fibrosis (fibrosis stage 0-2 in the initial biopsy and fibrosis stage 3 or 4 in any follow-up biopsies or Fibroscan >10.9 kPa in follow-up clinical visit) or progression to poor outcomes (liver decompensation, need for liver transplantation, or liver-related death) (28). Patients who progressed to advanced fibrosis or poor outcomes had significantly higher fibrosis gene signature in initial biopsy with F1 or F2 fibrosis compared to the patients who did not progress (both $p<0.001$, Figure 3.11F). Even patients who progressed to advanced fibrosis or poor outcomes had a marginally significant higher fibrosis gene signature in initial biopsy with F0 fibrosis compared to the patients who did not progress ($p=0.057$, Figure 3.11F). This showed these fibrosis genes may have the potential to serve as prognostic markers for predicting progressive fibrosis and poor outcomes.

3.4 – Discussion

This chapter showed NanoString gene expression assay is technically simple and methodologically robust for multiplex gene expression profiling of clinical liver biopsies that were up to 18 years old with a minimum of 1 mm core tissue. The NanoString nCounter Analysis System meets the requirements of evaluating multiplex gene expression signatures using clinical liver biopsies in the local pathology lab setting.

I successfully isolated enough RNA for NanoString gene expression assay from paraffin blocks with a minimum of 1 mm of liver tissue. Compared with liver resection samples, clinical liver biopsies are extremely valuable as only a small core of tissue was obtained. Moreover, there is usually very limited tissue left after staining of histological sections for clinical diagnosis. Due to these limitations, I evaluated the amount of liver tissue that is needed for NanoString gene expression assay. I had a 99% (348 of 350) success rate to isolate enough RNA from clinical liver biopsies. The two samples without enough RNA had minimal core biopsy (0 and 1 mm) and not enough sections were obtained (only three 20-µm thick sections). To optimize the RNA isolation protocol, despite the length of the core biopsy, only three 20-µm thick sections were obtained for the initial 168 paraffin blocks. The two samples that failed to yield enough RNA were in these initially processed samples. After the RNA isolation protocol is optimized, in the subsequent procedure, I cut four to eight sections 20-µm thick sections from the paraffin blocks with a shorter length of core biopsy. Based on the finalized RNA isolation protocol (Appendix B), I had a 100% success rate to isolate enough RNA for the NanoString gene expression assay from the remaining 182 samples with the length of core biopsy range from 1 mm to 40 mm. I showed almost all routine clinical liver biopsies had enough tissue for NanoString gene expression assay after paraffin sectioning for histological diagnostic purposes.

NanoString gene expression assay is a highly reliable method for multiplexed gene expression quantification when analyzing archived, clinical liver biopsies. There was no correlation between age of clinical liver biopsies (up to 18 years old) and the RNA yield. This demonstrated use of clinical liver biopsies from archival specimens can be applied to NanoString gene expression assay to develop diagnostic and prognostic tests. I also

compared normalized transcript counts between paired fresh vs. FFPE samples and found a strong positive correlation (r=0.944). Other techniques such as Affymetrix microarray and quantitative polymerase chain reaction have lower correlation between paired fresh and FFPE samples (r=0.75, 0.50, respectively) (17, 29). NanoString gene expression assay had a stronger correlation between paired fresh and FFPE samples compared to microarray and quantitative polymerase chain reaction as NanoString method does not need amplification of input RNA and thus eliminates potential artefacts inherent to amplification techniques in a scenario wherein FFPE derived RNAs are smaller in size due to degradation in the fixation protocols. It was well documented that RNA isolated from FFPE tissue suffer from strand breaking and cross-linking. Therefore, the amplification procedure might lose amplifiable templates. Moreover, both microarray and quantitative polymerase chain reaction is not very quantitative (measure relative fluorescence signal intensity and quantification cycle, respectively), whereas NanoString gives a digital readout of the transcript counts in a sample using molecular barcodes (14). These advantages made NanoString one of the most reliable platforms for multiplexed gene expression quantification when analyzing archived clinical liver biopsies.

A clinical assay needs to provide reproducible results when samples are repeated analyzed in different days, by different operators, and use of different lots of reagents (30). This chapter showed NanoString gene expression assay is highly reproducible when performed by the same operator and different operators of varying technical experience (r=0.950-0.990, 0.949-0.992, respectively). Transcript counts in repeat runs using different lots of reagents were almost perfectly correlated (r=0.998-0.999). These results indicated NanoString gene expression assay can provide reproducible results by the same and different

operators and use of different lots of reagents, thus meeting the requirements for clinical implementation.

The fibrosis gene signature increased progressively with histological fibrosis stages and quantitatively differed between histological stages of liver fibrosis (Figure 3.11). Interestingly, some samples with no or mild fibrosis (F0-F1) showed a relatively high fibrosis gene signature. This may represent these patients are at high risk for fibrosis progression with molecular fibrogenesis which cannot be yet identified by histology (31). Future studies will have to be performed in a patient cohort with follow-up data to further establish the usefulness of the fibrosis gene signature to predict fibrosis progression. This is covered in Chapters 4, 5, and 6.

This is the first study that showed NanoString nCounter Analysis System is a methodologically robust and feasible platform for multiplex gene expression quantification when analyzing archived clinical liver biopsies. This research illustrated how much tissue is needed to isolate enough RNA for NanoString gene expression assay. The low amount of tissue requirement will allow an expanded scope of molecular pathology through retrospective analysis of archival clinical liver biopsies that have been annotated with varied information on disease states and outcomes, such as disease progression and prognostic/survival data. Several human liver studies used genome-wide microarrays to identify a set of genes, which their expression pattern can predict disease progression in patients with chronic liver disease (5-11). The NanoString nCounter Analysis System will be the ideal platform for validating and translating these gene signatures for clinical application by analyzing archived clinical liver biopsies and correlate the gene expression with patient outcomes. Moreover, the NanoString nCounter Analysis System could be

seamlessly integrated into existing FFPE-based pathology workflow and could offer the ability to apply molecular diagnostics to the same biopsy core reviewed under the microscope by pathologists. This could provide personalized prognostic risk stratification, which could not be obtained by histopathology alone.

Table 3.1. Characteristics of the clinical liver biopsies analyzed by NanoString

Biopsy characteristics	All samples	Normal livers	Non-alcoholic fatty liver disease	Autoimmune hepatitis	Recurrent viral hepatitis C
Number of biopsies	348	27	94	78	149
Number of biopsies with high-quality gene expression profile	338	26	91	76	145
Number of patients	257	27	92	78	66
Age at biopsy (y), mean ± SD	50.4 ± 14.1[A]	40.4 ± 21.5[B]	51.4 ± 13.6[C]	42.4 ± 17.7	55.8 ± 5.3
Length of tissue (mm), mean ± SD	17.1 ± 7.2	15.26 ± 8.2	17.8 ± 6.6	14.7 ± 8.2	18.27 ± 6.6
Age of tissue (y), mean ± SD	4.8 ± 3.7	3.8 ± 2.4	2.5 ± 2.4	7.9 ± 4.8	4.8 ± 2.6
Fibrosis stage[D], n (%)					
0	83 (24)	21 (78)	26 (28)	6 (8)	30 (20)
1	114 (33)	6 (22)	24 (26)	21 (27)	63 (42)
2	69 (20)	0 (0)	7 (7)	19 (24)	43 (29)
3	53 (15)	0 (0)	21 (22)	21 (27)	11 (7)
4	29 (8)	0 (0)	16 (17)	11 (14)	2 (1)

[A] Missing data from five biopsies.
[B] Missing data from two biopsies.
[C] Missing data from three biopsies.
[D] Non-alcoholic fatty liver disease biopsies were assessed using Brunet staging classification (22). Normal livers, autoimmune hepatitis, and recurrent hepatitis biopsies were assessed using Metavir fibrosis staging classification (21).
Abbreviation: SD, standard deviation.

Table 3.2. The list of the 68-fibrosis associated genes

Gene symbol	Gene full name	Gene symbol	Gene full name
ANTXR1	Anthrax toxin receptor 1	GSN	Gelsolin
AQP1	Aquaporin 1 (Colton blood group)	HEPH	Hephaestin
B2M[B]	Beta-2-microglobulin	IGFBP7	Insulin-like growth factor binding protein 7
BICC1	BicC family RNA binding protein 1	ITGBL1	Integrin, beta-like 1 (with EGF-like repeat domains)
C1orf198	Chromosome 1 open reading frame 198	JAG1	Jagged 1
C7	Complement component 7	KRT7	Keratin 7, type II
CACNA2D1	Calcium channel, voltage-dependent, alpha 2/delta subunit 1	KRT8[A]	Keratin 8, type II
CCL2[A]	Chemokine (C-C motif) ligand 2	LAMB1	Laminin, beta 1
CCR5[A]	Chemokine (C-C motif) receptor 5 (gene/pseudogene)	LDHA[B]	Lactate dehydrogenase A
CD24	CD24 molecule	LGALS3[A]	Lectin, galactoside-binding, soluble, 3
CDH11	Cadherin 11, type 2, OB-cadherin (osteoblast)	LOX[A]	Lysyl oxidase
CHI3L1[A]	Chitinase 3-like 1 (cartilage glycoprotein-39)	LPAR1[A]	Lysophosphatidic acid receptor 1
COL14A1	Collagen, type XIV, alpha 1	LTBP2	Latent transforming growth factor beta binding protein 2
COL1A1	Collagen, type I, alpha 1	LUM	Lumican
COL1A2	Collagen, type I, alpha 2	MAP1B	Microtubule-associated protein 1B
COL3A1	Collagen, type III, alpha 1	MAP2	Microtubule-associated protein 2
COL4A1	Collagen, type IV, alpha 1	MMP2[A]	Matrix metallopeptidase 2
COL4A2	Collagen, type IV, alpha 2	MMP7[A]	Matrix metallopeptidase 7
COL4A4	Collagen, type IV, alpha 4	MOXD1	Monooxygenase, DBH-like 1
COL6A3	Collagen, type VI, alpha 3	NALCN	Sodium leak channel, non-selective
CTGF[A]	Connective tissue growth factor	NAV3	Neuron navigator 3

CXCL6	Chemokine (C-X-C motif) ligand 6	RCAN2	Regulator of calcineurin 2
CXCR4[A]	Chemokine (C-X-C motif) receptor 4	SH3YL1	SH3 and SYLF domain containing 1
DCDC2	Doublecortin domain containing 2	SLC38A1	Solute carrier family 38, member 1
DKK3	Dickkopf WNT signaling pathway inhibitor 3	SNX17[B]	Sorting nexin 17
DTNA	Dystrobrevin, alpha	SOX9	SRY (sex determining region Y)-box 9
EFEMP1	EGF containing fibulin-like extracellular matrix protein 1	SPP1[A]	Secreted phosphoprotein 1
EHF	Ets homologous factor	TAP2[A]	Transporter 2, ATP-binding cassette, sub-family B (MDR/TAP)
EPCAM	Epithelial cell adhesion molecule	TBP[B]	TATA box binding protein
EPHA3	EPH receptor A3	TGFB1[A]	Transforming growth factor, beta 1
FAM169A	Family with sequence similarity 169, member A	THBS2	Thrombospondin 2
FAT1	FAT atypical cadherin 1	TIMP1[A]	TIMP metallopeptidase inhibitor 1
FBN1	Fibrillin 1	TMEM200A	Transmembrane protein 200A
GPRC5B	G protein-coupled receptor, class C, group 5, member B	VWF[A]	Von Willebrand factor

[A] Literature selected fibrosis genes.
[B] Housekeeping gene.

Table 3.3. NanoString probe sequences

Gene symbol	Accession number	NanoString probe sequence
ANTXR1	NM_018153.3	GATGGGGGTCCAGCCTGCTACGGCGGATTTGACCTGTACTTCATTTTGGACAAA TCAGGAAGTGTGCTGCACCACTGGAATGAAATCTATTACTTTGTGG
AQP1	NM_198098.1	CTGGGATTCTACCGTAATTGCTTTGTGCCTTTGGGCACGGCCCTCCTTCTTTTCC TAACATGCACCTTGCTCCCAATGGTGCTTGGAGGGGGAAGAGATC
B2M	NM_004048.2	CGGGCATTCCTGAAGCTGACAGCATTCGGGCCGAGATGTCTCGCTCCGTGGCCT TAGCTGTGCTCGCGCTACTCTCTCTTTCTGGCCTGGAGGCTATCCA
BICC1	NM_001080512.1	CACGGTCATCATATGTCAACATGCAGGCATTTGACTATGAACAGAAGAAGCTAT TAGCCACCAAAGCTATGTTAAAGAAACCAGTGGTGACGGAGGTCAG
C1orf198	NM_001136495.1	CTCAACAAGCCCAATATTCCCTCCAAGTTCTTCTTGGTGCTGAGGGCTGTAGGA ATTATTGAAAGCTTCTGCCTCACTTAGTATCGTCTGGGGCCCAGCA
C7	NM_000587.2	ATGCTTTTGAAACACAGTCCTGTGAACCTACAAGAGGATGTCCAACAGAGGAG GGATGTGGAGAGCGTTTCAGGTGCTTTTCAGGTCAGTGCATCAGCAA
CACNA2D1	NM_000722.2	TCTTATGATTATCAGTCAGTATGTGAGCCCGGTGCTGCACCAAAACAAGGAGCA GGACATCGCTCAGCATATGTGCCATCAGTAGCAGACATATTACAAA
CCL2	NM_002982.3	GAGGAACCGAGAGGCTGAGACTAACCCAGAAACATCCAATTCTCAAACTGAAG CTCGCACTCTCGCCTCCAGCATGAAAGTCTCTGCCGCCCTTCTGTGC
CCR5	NM_000579.1	TAGGAACATACTTCAGCTCACACATGAGATCTAGGTGAGGATTGATTACCTAGT AGTCATTTCATGGGTTGTTGGGAGGATTCTATGAGGCAACCACAGG
CD24	NM_013230.2	ATAGACACTCCCCGAAGTCTTTTGTTCGCATGGTCACACACTGATGCTTAGATG TTCCAGTAATCTAATATGGCCACAGTAGTCTTGATGACCAAAGTCC
CDH11	NM_001797.2	CAGGAAGCCAAAGTCCCAGTGGCCATTAGGGTCCTTGATGTCAACGATAATGCT CCCAAGTTTGCTGCCCCTTATGAAGGTTTCATCTGTGAGAGTGATC
CHI3L1	NM_001276.2	GGTCTCAAAGATTTTCCAAGATAGCCTCCAACACCCAGAGTCGCCGGACTTTCA TCAAGTCAGTACCGCCATTTCTGCGCACCCATGGCTTTGATGGGCT

COL14A1	NM_021110.1	CTTTAAGTCCACCAAGAAACCTGAGAATCTCCAATGTTGGCTCTAACAGTGCTC GATTAACCTGGGACCCAACTTCAAGACAGATCAATGGTTATCGAAT
COL1A1	NM_000088.3	CAGAAACATCGGATTTGGGGAACGCGTGTCAATCCCTTGTGCCGCAGGGCTGG GCGGGAGAGACTGTTCTGTTCCTTGTGTAACTGTGTTGCTGAAAGAC
COL1A2	NM_000089.3	CCAATGGATTTGCTGGTCCTGCTGGTGCTGCTGGTCAACCTGGTGCTAAAGGAG AAAGAGGAGCCAAAGGGCCTAAGGGTGAAAACGGTGTTGTTGGTCC
COL3A1	NM_000090.3	TTGGCACAACAGGAAGCTGTTGAAGGAGGATGTTCCCATCTTGGTCAGTCCTAT GCGGATAGAGATGTCTGGAAGCCAGAACCATGCCAAATATGTGTCT
COL4A1	NM_001845.4	TGGGCTTAAGTTTTCAAGGACCAAAAGGTGACAAGGGTGACCAAGGGGTCAGT GGGCCTCCAGGAGTACCAGGACAAGCTCAAGTTCAAGAAAAAGGAGA
COL4A2	NM_001846.2	GGCATTTCCTTGAAGGGAGAAGAAGGAATCATGGGCTTTCCTGGACTGAGGGG TTACCCTGGCTTGAGTGGTGAAAAAGGATCACCAGGACAGAAGGGAA
COL4A4	NM_000092.4	TATATGGGAGTGGAAAGAAATACATTGGTCCTTGTGGAGGAAGAGATTGCTCT GTTTGCCACTGTGTTCCTGAAAAGGGGTCTCGGGGTCCACCAGGACC
COL6A3	NM_004369.3	AGAGCAAGCGAGACATTCTGTTCCTCTTTGACGGCTCAGCCAATCTTGTGGGCC AGTTCCCTGTTGTCCGTGACTTTCTCTACAAGATTATCGATGAGCT
CTGF	NM_001901.2	ACCACCCTGCCGGTGGAGTTCAAGTGCCCTGACGGCGAGGTCATGAAGAAGAA CATGATGTTCATCAAGACCTGTGCCTGCCATTACAACTGTCCCGGAG
CXCL6	NM_002993.3	AGTAACAAAAAAGACCATGCATCATAAAATTGCCCAGTCTTCAGCGGAGCAGT TTTCTGGAGATCCCTGGACCCAGTAAGAATAAGAAGGAAGGGTTGGT
CXCR4	NM_003467.2	ATTGATGTGTGTCTAGGCAGGACCTGTGGCCAAGTTCTTAGTTGCTGTATGTCTC GTGGTAGGACTGTAGAAAAGGGAACTGAACATTCCAGAGCGTGTA
DCDC2	NM_016356.3	GTCTGAAACACGGGGGGCAGCAGAAGTCCAAGAAGATGAAGATACTCAGGTTG AGGTTCCAGTCGATCAGAGGCCAGCAGAAATAGTAGACGAGGAAGAA
DKK3	NM_001018057.1	AGTGAACCTGGCAAACTTACCTCCCAGCTATCACAATGAGACCAACACAGACA CGAAGGTTGGAAATAATACCATCCATGTGCACCGAGAAATTCACAAG

DTNA	NM_032981.4	GTTCCCAGATCAGCCTGAGAAGCCACTCAACTTGGCTCACATCGTGCCTCCCAG ACCTGTAACCAGCATGAACGACACCCTGTTCTCCCACTCTGTTCCC
EFEMP1	NM_004105.3	ACCTACGACAAACAAGTCCTGTAAGTGCAATGCTTGTGCTCGTGAAGTCATTAT CAGGACCAAGAGAACATATCGTGGACCTGGAGATGCTGACAGTCAG
EHF	NM_012153.3	ATTTAGAAAAAGGTGATGCATCCTCCTCACATAAGCATCCATATGGCTTCGTCA AGGGAGGTGAACATTGTTGCTGAGTTAAATTCCAGGGTCTCAGATG
EPCAM	NM_002354.1	AGAAGAGCAAAACCTGAAGGGGCCCTCCAGAACAATGATGGGCTTTATGATCC TGACTGCGATGAGAGCGGGCTCTTTAAGGCCAAGCAGTGCAACGGCA
EPHA3	NM_005233.5	GAGGCCGGAAAGATGTTACCTTCAACATCATATGTAAAAAATGTGGGTGGAAT ATAAAACAGTGTGAGCCATGCAGCCCAAATGTCCGCTTCCTCCCTCG
FAM169A	NM_015566.2	AACTTGAAGACGTGCCATTTTCACAGAATGCAGGACAGAAGAATCAGTCAGAG GAGCAGTCTGAAGCATCTTCCGAGCAACTGGATCAGTTTACACAATC
FAT1	NM_005245.3	ACCCAACCAGTGGTGTGATAGTGTTAACTGGTAGACTTGATTACCTAGAGACCA AGCTCTATGAGATGGAAATCCTCGCTGCGGACCGTGGCATGAAGTT
FBN1	NM_000138.3	CACTGAAGGCAGCTTCAAATGTCTGTGTCCAGAAGGGTTTTCCTTGTCCTCCAG TGGAAGAAGGTGCCAAGATTTGCGAATGAGCTACTGTTATGCGAAG
GPRC5B	NM_016235.1	GCCCTCTGGGTGATGAAGTGACCATCACATTTGGAAAGTGATCAACCACTGTTC CTTCTATGGGGCTCTTGCTCTAATGTCTATGGTGAGAACACAGGCC
GSN	NM_000177.4	GATGGGAAAATCTTTGTCTGGAAAGGCAAGCAGGCAAACACGGAGGAGAGGA AGGCTGCCCTCAAAACAGCCTCTGACTTCATCACCAAGATGGACTACC
HEPH	NM_138737.3	CCAGCGTGCCTCACCTGGATCTACCATTCTCATGTAGATGCTCCACGAGACATT GCAACTGGCCTAATTGGGCCTCTCATCACCTGTAAAAGAGGAGCCC
IGFBP7	NM_001553.1	CCCAGAAAAGCATGAAGTAACTGGCTGGGTGCTGGTATCTCCTCTAAGTAAGG AAGATGCTGGAGAATATGAGTGCCATGCATCCAATTCCCAAGGACAG
ITGBL1	NM_004791.1	GGTATATTTCTGGGGAGTTCTGTGACTGTGATGACAGAGACTGCGACAAACATG ATGGTCTCATTTGTACAGGGAATGGAATATGTAGCTGTGGAAACTG

JAG1	NM_000214.2	TTGCTTGTGGAGGCGTGGGATTCCAGTAATGACACCGTTCAACCTGACAGTATT ATTGAAAAGGCTTCTCACTCGGGCATGATCAACCCCAGCCGGCAGT
KRT7	NM_005556.3	GGGAACCATGGGCAGCAATGCCCTGAGCTTCTCCAGCAGTGCGGGTCCTGGGC TCCTGAAGGCTTATTCCATCCGGACCGCATCCGCCAGTCGCAGGAGT
KRT8	NM_002273.3	CCGTGCGCACCCAGGAGAAGGAGCAGATCAAGACCCTCAACAACAAGTTTGCC TCCTTCATAGACAAGGTACGGTTCCTGGAGCAGCAGAACAAGATGCT
LAMB1	NM_002291.2	TTGCCAGGAGCTGCTACCAAGATCCTGTTACTTTACAGCTTGCCTGTGTTTGTGA TCCTGGATACATTGGTTCCAGATGTGACGACTGTGCCTCAGGATA
LDHA	NM_001165414.1	AACTTCCTGGCTCCTTCACTGAACATGCCTAGTCCAACATTTTTTCCCAGTGAGT CACATCCTGGGATCCAGTGTATAAATCCAATATCATGTCTTGTGC
LGALS3	NM_001177388.1	CACGGTGAAGCCCAATGCAAACAGAATTGCTTTAGATTTCCAAAGAGGGAATG ATGTTGCCTTCCACTTTAACCCACGCTTCAATGAGAACAACAGGAGA
LOX	NM_002317.4	CGCTACACAGGACATCATGCGTATGCCTCAGGCTGCACAATTTCACCGTATTAG AAGGCAAAGCAAAACTCCCAATGGATAAATCAGTGCCTGGTGTTCT
LPAR1	NM_001401.3	CCTAATGGCTAATCTGGCTGCTGCAGACTTCTTTGCTGGGTTGGCCTACTTCTAT CTCATGTTCAACACAGGACCCAATACTCGGAGACTGACTGTTAGC
LTBP2	NM_000428.2	CATCTCTCCCAGCTTAGCCTCTGGCTGTAAGCTTCGGTCATTGCCTCCATGCCCT TGCTTGGCTCAAGCACCACCAATCGCTTTAATGCTTCAGCCACCG
LUM	NM_002345.3	GCCATTATCCTACTCCAAGATCAAGCATTTGCGTTTGGATGGCAATCGCATCTC AGAAACCAGTCTTCCACCGGATATGTATGAATGTCTACGTGTTGCT
MAP1B	NM_005909.3	CATATAGGATTATAGATACTTAAAGGAACACGTGGGTGAGCGTGTGTGGGGGT ACTAGAAGCTGATCTGATTGGTCCAACAGTTTGATGCTGAGTCATGC
MAP2	NM_031845.2	TACTCTGTATGCTGGGATTCCGAGGTTCCAACACACTGTTACAAATCTGTGGGG GGTTTCTTTCTTCTGATAATTCTAGAGCCTGTTACCATAGAAAGGC
MMP2	NM_004530.2	CCCGGAGGGGCCTGGCAGCCGTGCCTTCAGCTCTACAGCTAATCAGCATTCTCA CTCCTACCTGGTAATTTAAGATTCCAGAGAGTGGCTCCTCCCGGTG

MMP7	NM_002423.3	GTGCCAGATGTTGCAGAATACTCACTATTTCCAAATAGCCCAAAATGGACTTCC AAAGTGGTCACCTACAGGATCGTATCATATACTCGAGACTTACCGC
MOXD1	NM_001031699.1	GATGCATTCCTCACCTGTGAAACTGTGATTTTTGCCTGGGCTATTGGTGGAGAG GGCTTTTCTTATCCACCTCATGTTGGATTATCCCTTGGCACTCCAT
NALCN	NM_052867.2	TGGACGTGATCGTGGCGGCTAGCAACTACTACAAAGGAGAAAACTTCAGGAGG CAGTACGACGAGTTCTACCTGGCGGAGGTGGCTTTTACAGTACTTTT
NAV3	NM_014903.4	CCAGCACTTCTTCTCTTTACTCTACAGCTGAAGAAAAGGCTCATTCAGAGCAAA TCCATAAACTGCGGAGAGAGCTGGTTGCATCACAAGAAAAAGTTGC
RCAN2	NM_005822.3	GTGTCCTCTAGTGGAAGAAATAGTAGGCTCCGCTATTCAGATGCAGAGCACTGC AGCATCCAGCCTTTCAAAGCTGACTCTTCTCAATCATCTGTGGGTC
SH3YL1	NM_001159597.1	AAAGGCCTTGCAATTCTGTCTGTGATCAAAGCCGGGTTCCTGGTGACTGCCAGA GGAGGCAGCGGGATTGTAGTGGCGCGCCTTCCAGATGGAAAATGGT
SLC38A1	NM_001077484.1	TCTATGACAACGTGCAGTCCGACCTCCTTCACAAATATCAGAGTAAAGATGACA TTCTCATCCTGACAGTGCGGCTGGCTGTCATTGTTGCTGTGATCCT
SNX17	NM_014748.2	CTTTCCTTGTCCCCTGGGCTGGCTGCACAGAGGATTGCCCCTTCTCTTTTCAGAG CTGGCCCTCGATGCCAAATTAGCATTTAGTATTTTGCACAAAGTC
SOX9	NM_000346.2	CAGTGGCCAGGCCAACCTTGGCTAAATGGAGCAGCGAAATCAACGAGAAACTG GACTTTTTAAACCCTCTTCAGAGCAAGCGTGGAGGATGATGGAGAAT
SPP1	NM_000582.2	CGCCTTCTGATTGGGACAGCCGTGGGAAGGACAGTTATGAAACGAGTCAGCTG GATGACCAGAGTGCTGAAACCCACAGCCACAAGCAGTCCAGATTATA
TAP2	NM_000544.3	GGCTTCCTTTAAATGCCAATGTGCTCTTGCGAAGCCTGGTGAAAGTGGTGGGGC TGTATGGCTTCATGCTCAGCATATCGCCTCGACTCACCCTCCTTTC
TBP	NM_001172085.1	ACAGTGAATCTTGGTTGTAAACTTGACCTAAAGACCATTGCACTTCGTGCCCGA AACGCCGAATATAATCCCAAGCGGTTTGCTGCGGTAATCATGAGGA
TGFB1	NM_000660.3	TATATGTTCTTCAACACATCAGAGCTCCGAGAAGCGGTACCTGAACCCGTGTTG CTCTCCCGGGCAGAGCTGCGTCTGCTGAGGCTCAAGTTAAAAGTGG

THBS2	NM_003247.2	AAACATCCTTGCAAATGGGTGTGACGCGGTTCCAGATGTGGATTTGGCAAAACC TCATTTAAGTAAAAGGTTAGCAGAGCAAAGTGCGGTGCTTTAGCTG
TIMP1	NM_003254.2	CGTGGGGACACCAGAAGTCAACCAGACCACCTTATACCAGCGTTATGAGATCA AGATGACCAAGATGTATAAAGGGTTCCAAGCCTTAGGGGATGCCGCT
TMEM200A	NM_052913.2	CCTTGTGGTTCCTTTGCCCAACACCAGTGAATCCTTCCAGCCCGTCAGCACAGT GCTACCAAGGAATAATTCCATTGGGGAGTCGTTGTCGAGTCAGTAC
VWF	NM_000552.3	CACCTGCAACCCCTGCCCCCTGGGTTACAAGGAAGAAAATAACACAGGTGAAT GTTGTGGGAGATGTTTGCCTACGGCTTGCACCATTCAGCTAAGAGGA

Table 3.4. Three 20-µm sections were enough to isolate at least 100 ng of RNA from blocks with more than 5 mm of core biopsy

Length of core biopsy in the block	Number of 20-µm sections obtained		p-value
	3	4-8	
0-5 mm	62.5% (5/8)	100% (21/21)	0.015
> 5 mm	99% (298/301)	100% (20/20)	1

Table 3.5. Transcript counts of 68 fibrosis-associated genes were strongly correlated between paired fresh and FFPE livers

Paired fresh and FFPE sample ID	Correlation coefficient	p-value	Paired fresh and FFPE sample ID	Correlation coefficient	p-value
Explant 1	0.934	<0.001	Explant 9	0.971	<0.001
Explant 2	0.984	<0.001	Explant 10	0.982	<0.001
Explant 3	0.969	<0.001	Explant 11	0.900	<0.001
Explant 4	0.924	<0.001	Explant 12	0.962	<0.001
Explant 5	0.964	<0.001	Explant 13	0.964	<0.001
Explant 6	0.969	<0.001	Explant 14	0.912	<0.001
Explant 7	0.954	<0.001	Explant 15	0.975	<0.001
Explant 8	0.974	<0.001			

Table 3.6. Biological annotation of the fibrosis genes

Gene symbol	Biological annotation	Ref	Gene symbol	Biological annotation	Ref
ANTXR1	Induce extracellular matrix synthesis or cross-linking	(32)	GPRC5B	Signal transduction	(33)
AQP1	Expressed in hepatic progenitor cell	(34)	GSN	Expressed in fibroblast or myofibroblast	(35)
BICC1	Wnt signaling pathway	(36)	HEPH	Ion or amino acid transporter	(37)
C1orf198	Unknown		IGFBP7	Induce extracellular matrix synthesis or cross-linking	(38)
C7	Inflammation	(39)	ITGBL1	Induce fibroblast or myofibroblast activation	(40)
CACNA2D1	Ion or amino acid transporter	(41)	JAG1	Expressed in fibroblast or myofibroblast	(42)
CCL2	Inflammation	(43)	KRT7	Expressed in hepatic progenitor cell	(44)
CCR5	Inflammation	(45)	KRT8	Expressed in hepatic progenitor cell	(46)
CD24	Expressed in hepatic progenitor cell	(47)	LAMB1	Induce extracellular matrix synthesis or cross-linking	(48)
CDH11	Induce fibroblast or myofibroblast activation	(49)	LGALS3	Induce fibroblast or myofibroblast activation	(50)
CHI3L1	Inflammation	(43)	LOX	Induce extracellular matrix synthesis or cross-linking	(51)
COL14A1	Induce extracellular matrix synthesis or cross-linking, HSC activation	(9, 52)	LPAR1	Induce fibroblast or myofibroblast activation	(53)
COL1A1	Induce extracellular matrix synthesis or cross-linking, HSC activation	(9, 52)	LTBP2	Induce extracellular matrix synthesis or cross-linking	(54)
COL1A2	Induce extracellular matrix synthesis or cross-linking, HSC activation	(9, 52)	LUM	Induce extracellular matrix synthesis or cross-linking	(55)
COL3A1	Induce extracellular matrix synthesis or cross-linking, HSC activation	(9, 52)	MAP1B	Expressed in hepatic progenitor cell, microtubule binding	(56)

COL4A1	Induce extracellular matrix synthesis or cross-linking, HSC activation	(9, 52)	MAP2	Expressed in fibroblast or myofibroblast, microtubule binding	(57)
COL4A2	Induce extracellular matrix synthesis or cross-linking, HSC activation	(9, 52)	MMP2	Extracellular matrix degradation, HSC, extracellular matrix remodeling	(9, 58)
COL4A4	Induce extracellular matrix synthesis or cross-linking, HSC activation	(9, 52)	MMP7	Extracellular matrix degradation, HSC, extracellular matrix remodeling	(9, 58)
COL6A3	Induce extracellular matrix synthesis or cross-linking, HSC activation	(9, 52)	MOXD1	Ion binding	(59)
CTGF	Induce extracellular matrix synthesis or cross-linking, HSC activation	(9, 60)	NALCN	Ion or amino acid transporter	(61)
CXCL6	Inflammation	(43)	NAV3	Microtubule binding	(62)
CXCR4	Induce fibroblast or myofibroblast activation	(43)	RCAN2	Expressed in fibroblast or myofibroblast, nucleic acid binding	(63)
DCDC2	Wnt signaling	(64)	SH3YL1	Induce fibroblast or myofibroblast activation, regulation of ruffle assembly	(65)
DKK3	Wnt signaling	(66)	SLC38A1	Ion or amino acid transporter	(67)
DTNA	Dystrophin	(68)	SOX9	Induce extracellular matrix synthesis or cross-linking, expressed in hepatic progenitor cell	(69)
EFEMP1	Induce extracellular matrix synthesis or cross-linking	(70)	SPP1	Induce extracellular matrix synthesis or cross-linking	(71)
EHF	Epithelial-mesenchymal transition	(72)	TAP2	Ion or amino acid transport	(73)
EPCAM	Expressed in hepatic progenitor cell	(74)	TGFB1	Induce extracellular matrix synthesis or cross-linking, HSC	(75)
EPHA3	Inflammation	(76)	THBS2	Induce extracellular matrix synthesis or cross-linking	(77)
FAM169A	Unknown		TIMP1	Induce extracellular matrix synthesis or cross-linking, HSC, extracellular matrix remodeling	(9, 58)
FAT1	Epithelial-mesenchymal transition	(78)	TMEM200A	Unknown	

FBN1	Induce extracellular matrix synthesis or cross-linking	(79)	VWF	Induce extracellular matrix synthesis or cross-linking	(80)

HSC, hepatic stellate cell; Ref, reference.

Table 3.7. Biological functions of the fibrosis genes

Biological function	Genes
ECM synthesis or cross-linking	ANTXR1, COL1A1, COL1A2, COL3A1, COL4A1, COL4A2, COL4A4, COL6A3, COL14A1, CTGF, EFEMP1, FBN1, IGFBP7, LAMB1, LOX, LTBP2, LUM, SOX9, SPP1, TGFB1, THBS2, TIMP1, VWF
Fibroblast or myofibroblast or HSC activation	CDH11, COL1A1, COL1A2, COL3A1, COL4A1, COL4A2, COL4A4, COL6A3, CTGF, CXCR4, ITGBL1, LGALS3, LPAR1, MMP2, MMP7, SH3YL1, TIMP1
Collagen	COL1A1, COL1A2, COL3A1, COL4A1, COL4A2, COL4A4, COL6A3, COL14A1
Inflammation	C7, CCL2, CCR5, CHI3L1, CXCL6, EPHA3
Hepatic progenitor cell	AQP1, CD24, EPCAM, KRT7, KRT8, MAP1B, SOX9

ECM, extracellular matrix. HSC, hepatic stellate cell.

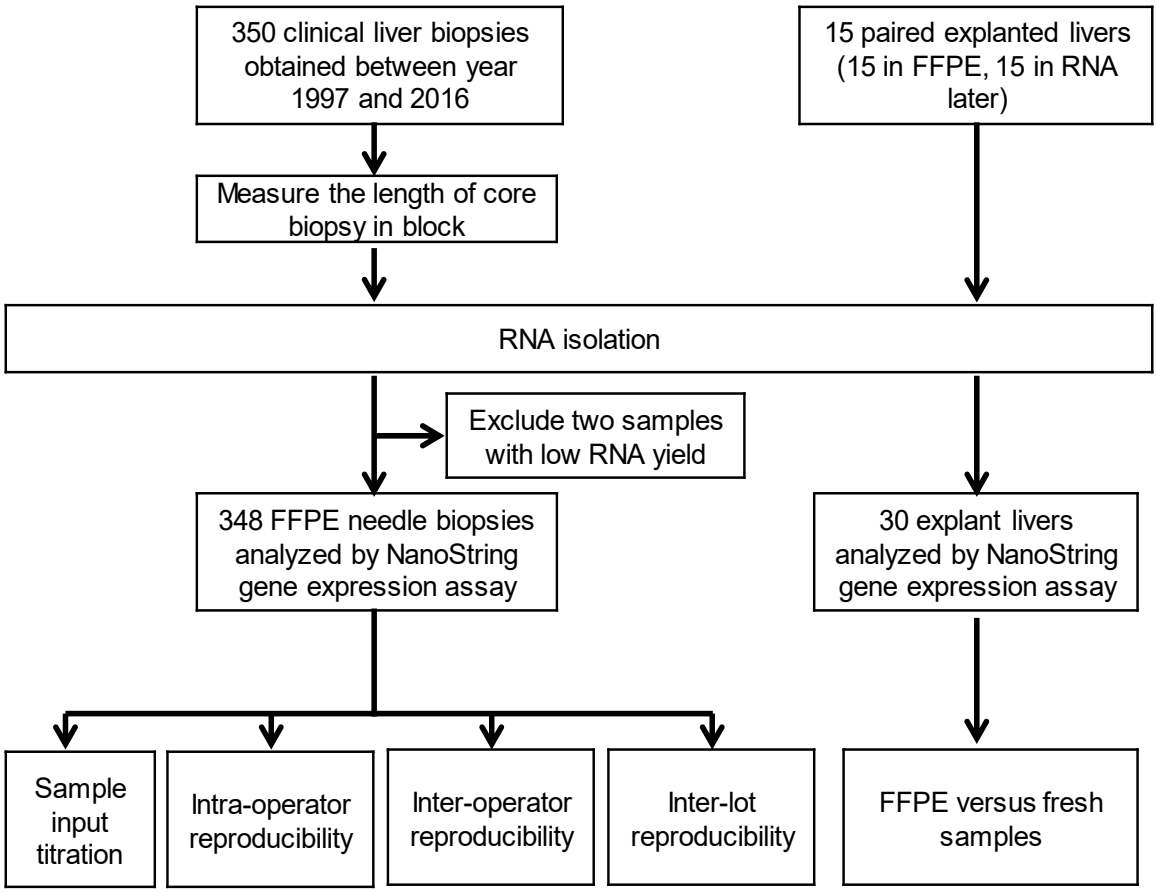

Figure 3.1. Study design.
FFPE, formalin-fixed paraffin-embedded.

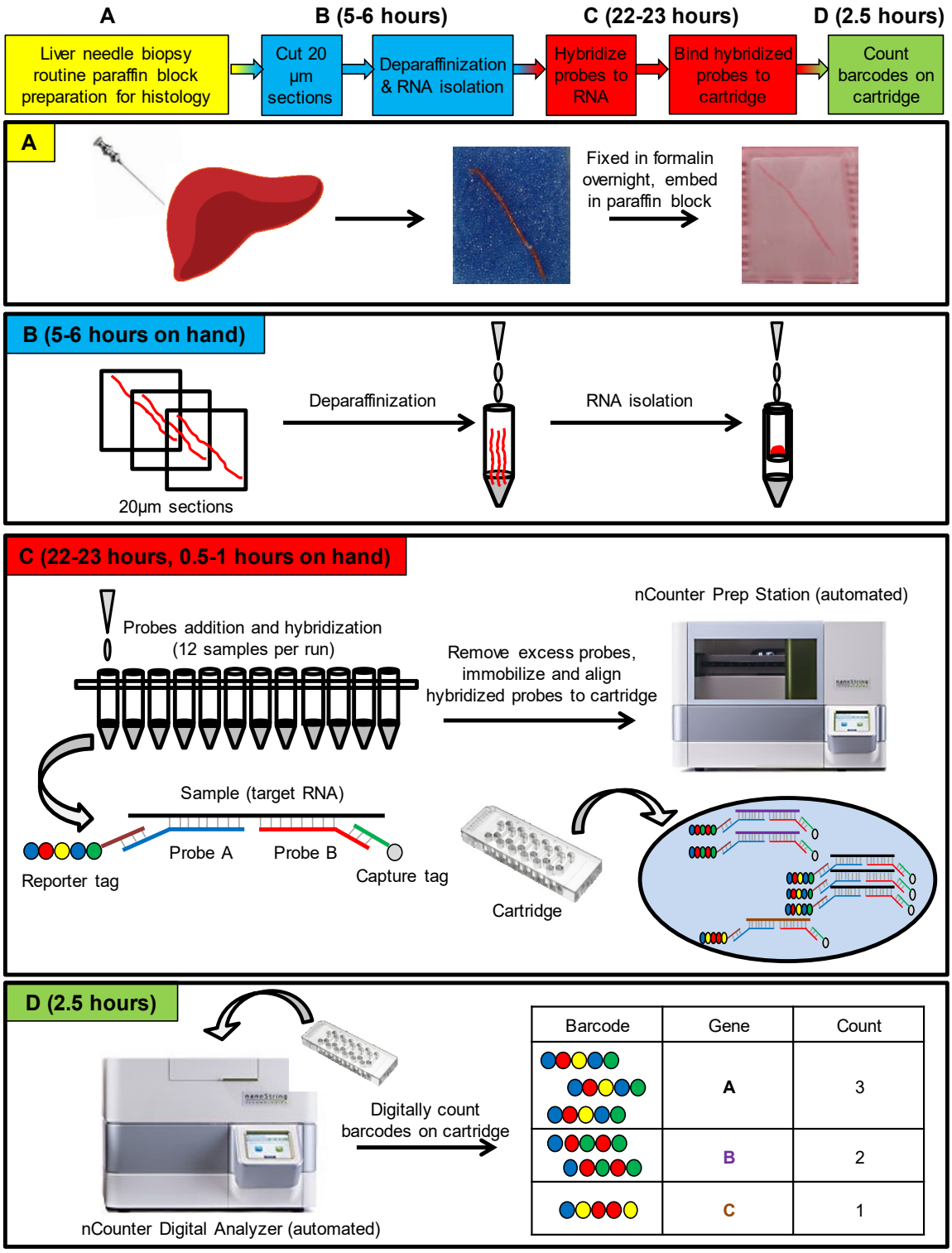

Figure 3.2. NanoString gene expression assay workflow.
From the time of clinical biopsy procurement, NanoString gene expression results can be obtained within 1.5 days and only 7 hours hands-on time.

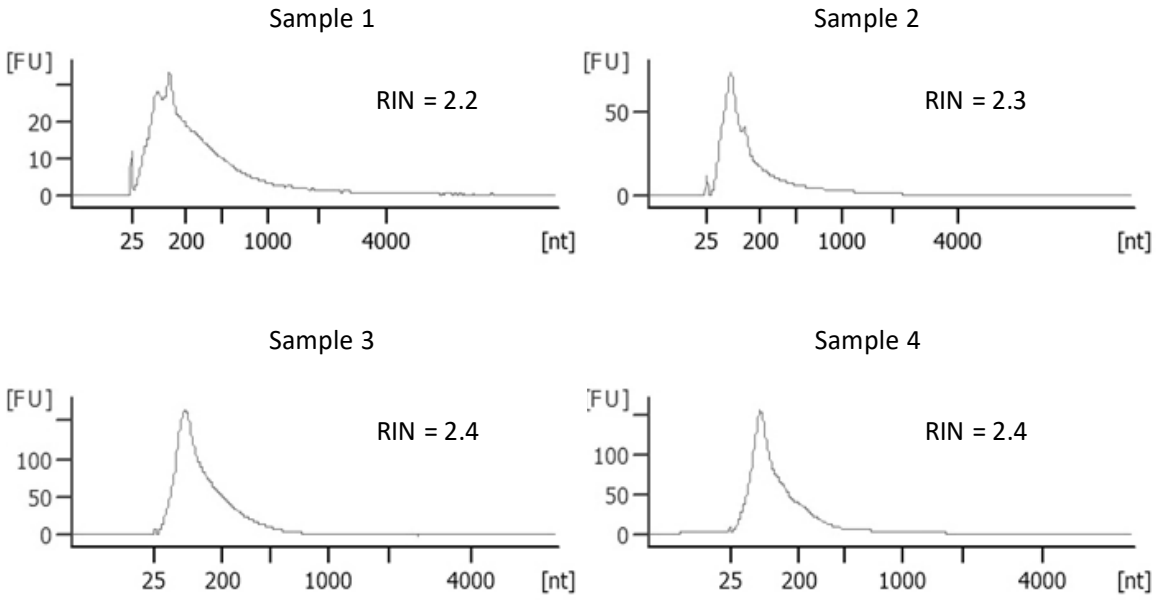

Figure 3.3. Representative chromatogram for four RNA samples from four unique clinical liver biopsies with respective RNA integrity number (RIN).

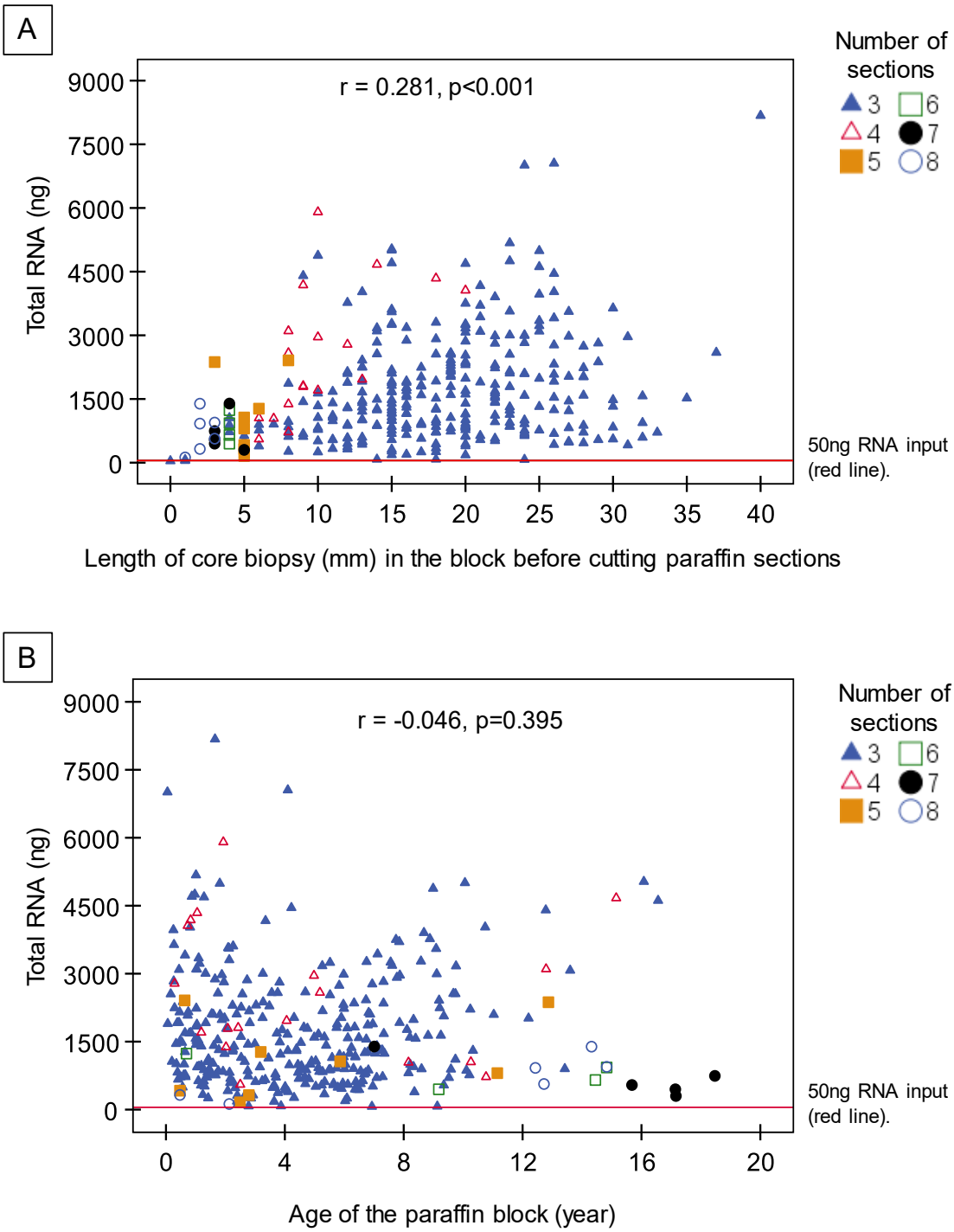

Figure 3.4. Total RNA yield was significantly correlated with the length of core biopsy, but not with the age of paraffin block.
(A) There was a significant correlation between the length of clinical liver biopsy and the total RNA yield. (B) Age of the paraffin block did not correlate with the total RNA yield.

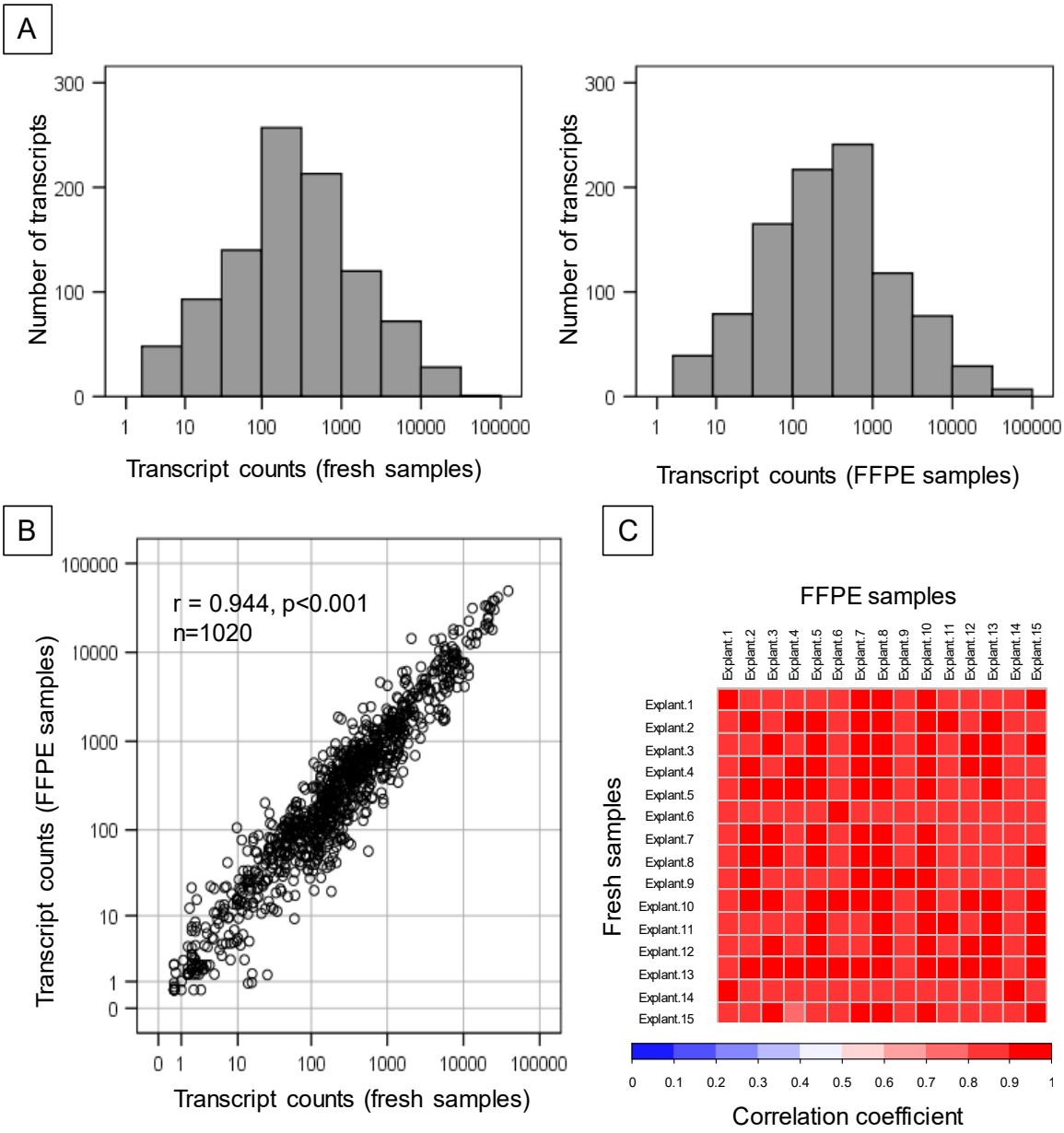

Figure 3.5. Normalized transcript counts of 68 fibrosis-associated genes in fresh biopsies were strongly correlated with 15 paired FFPE biopsies.
(A) Normalized mRNA transcript counts in paired fresh and FFPE samples were normally distributed. (B) Scatter plot of the normalized transcript counts of 68 fibrosis-associated genes obtained from 15 paired fresh vs. FFPE samples. Normalized transcript counts in fresh samples had a strong correlation with paired FFPE samples ($r=0.944$, $p<0.001$). (C) Correlation heatmap of the normalized transcript counts of 68 hepatic fibrosis-associated genes in 15 paired fresh and FFPE samples.

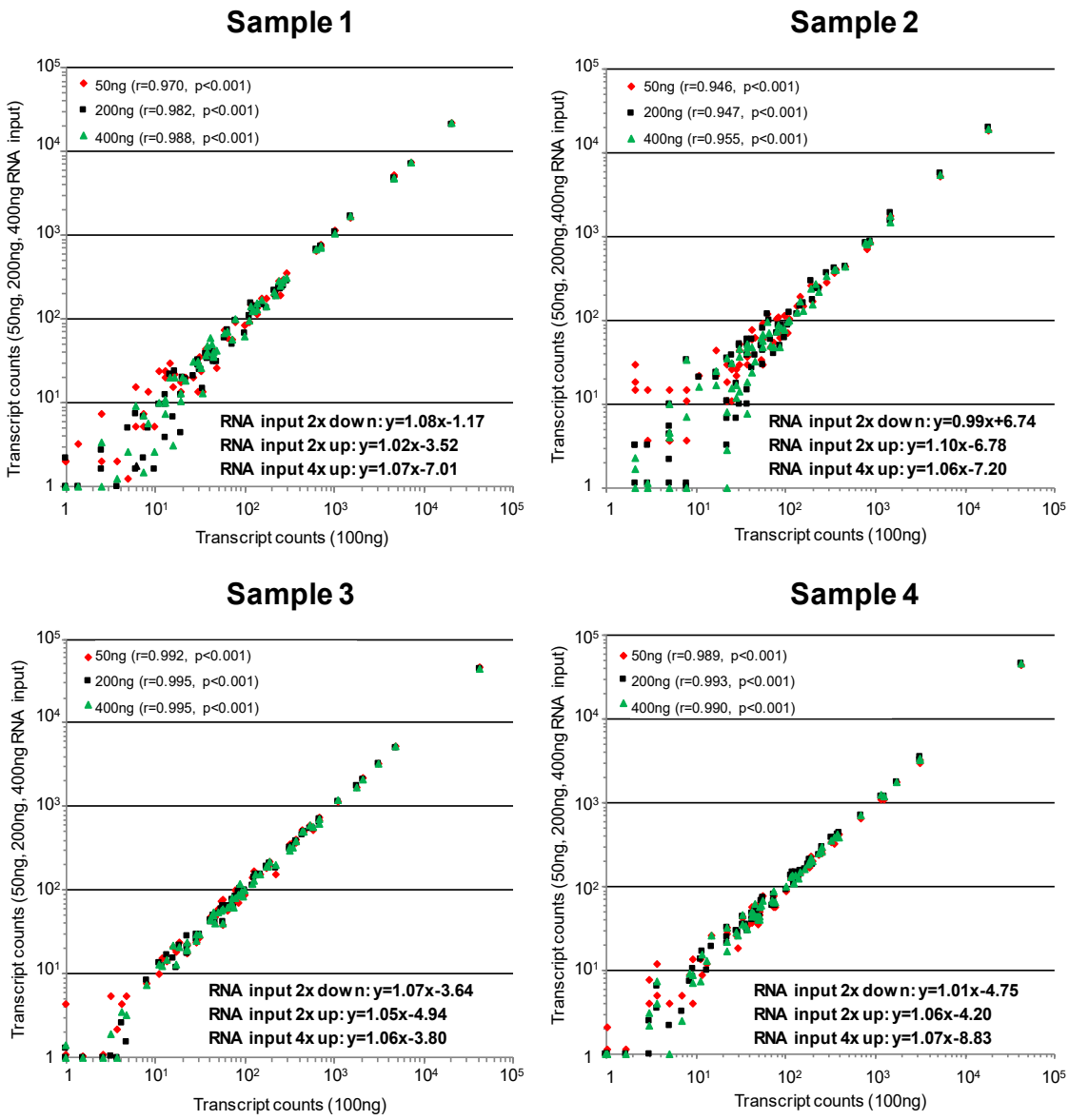

Figure 3.6. NanoString gene expression assay had robust reproducibility across different RNA input quantities.

Four RNA samples from four unique clinical liver biopsies were analyzed using NanoString with different RNA input quantities (50, 100, 200, 400 ng). The results for 50 (red diamond), 200 (black square), and 400 (green triangle) ng of RNA input quantities were represented on the y-axis in relation to corresponding results along the x-axis for the amount of 100 ng. The scatter plot demonstrated normalized transcript counts of 68 hepatic fibrosis-associated genes were strongly correlated in repeat runs with different RNA input quantities.

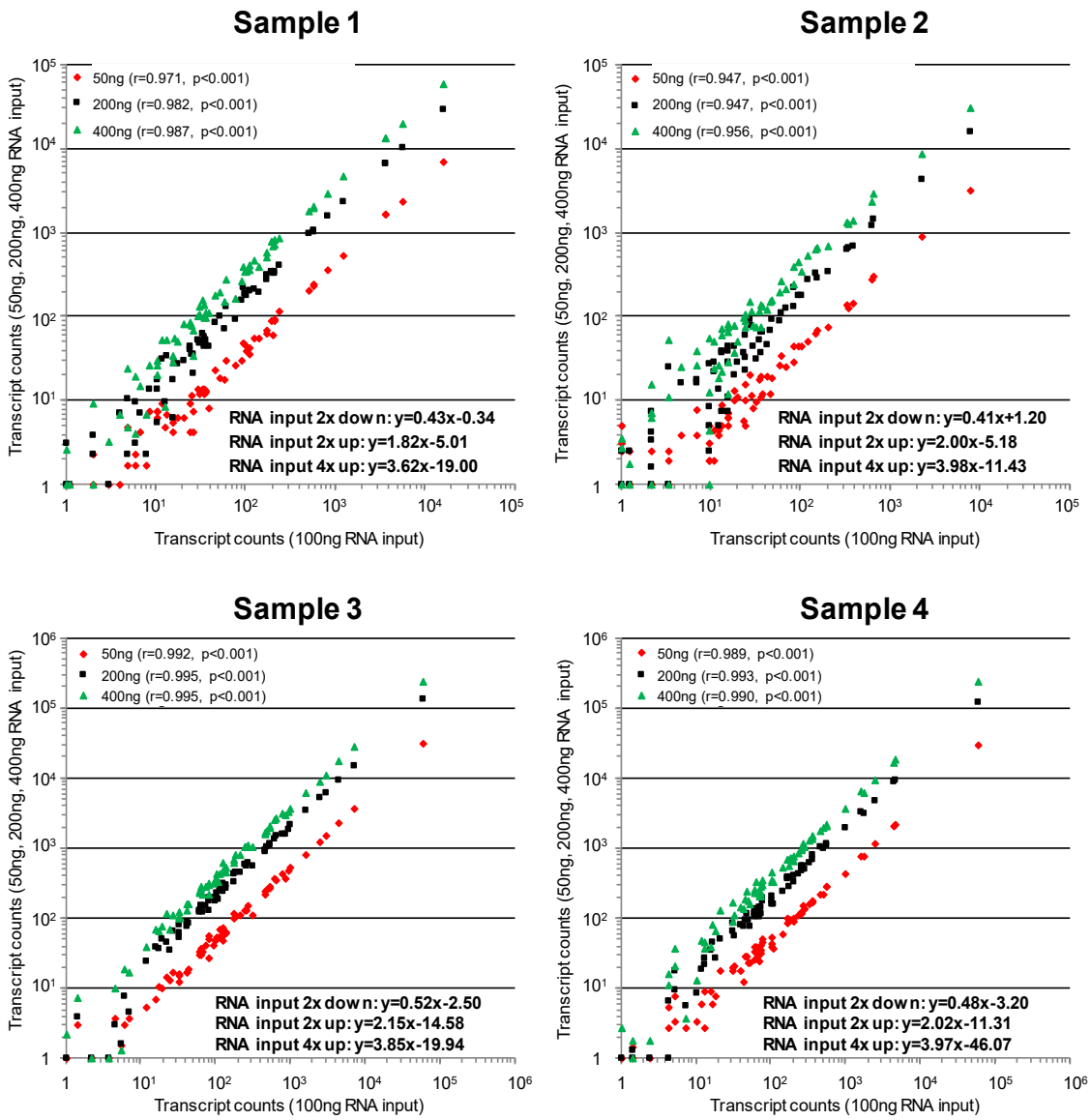

Figure 3.7. NanoString gene expression assay could detect fractional fold-changes across different RNA input quantities.

To show the fractional fold-changes of different RNA input quantities, the transcript counts of the four samples in Figure 3.6 were preprocessed without housekeeping gene normalization. The slopes correlated closely with the expected fold-change values of 0.5 (100ng input vs. 50ng input), 2 (100ng input vs. 200ng input), and 4 (100ng input vs. 400ng input).

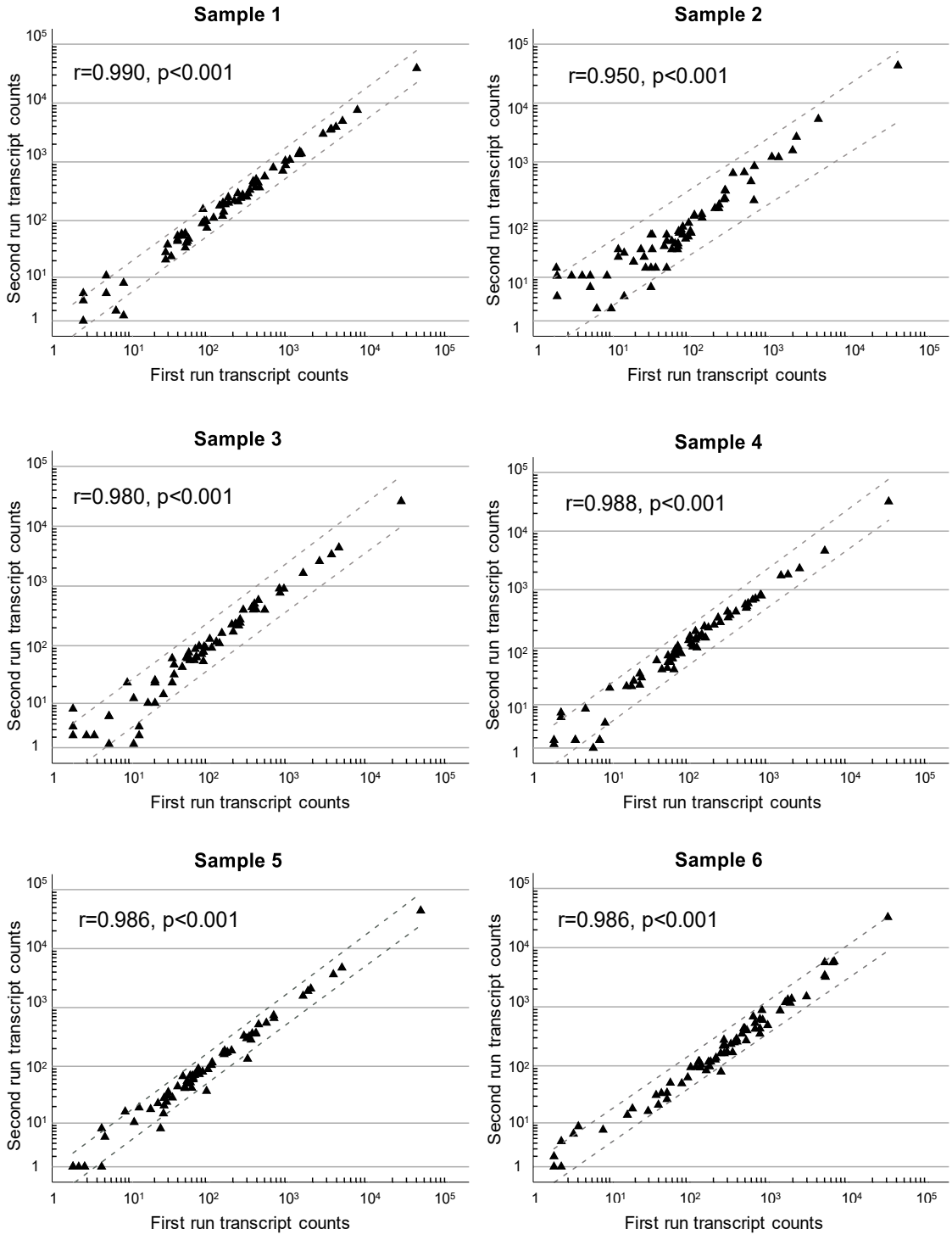

Figure 3.8. NanoString gene expression assay had robust intra-operator reproducibility.

Six RNA samples from six unique clinical liver biopsies were analyzed twice by one operator in different days. The scatter plot showed normalized transcript counts of 68 hepatic fibrosis-associated genes were strongly correlated in repeat runs by the same operator. The gray dashed lines represented 95% confidence interval of the regression line.

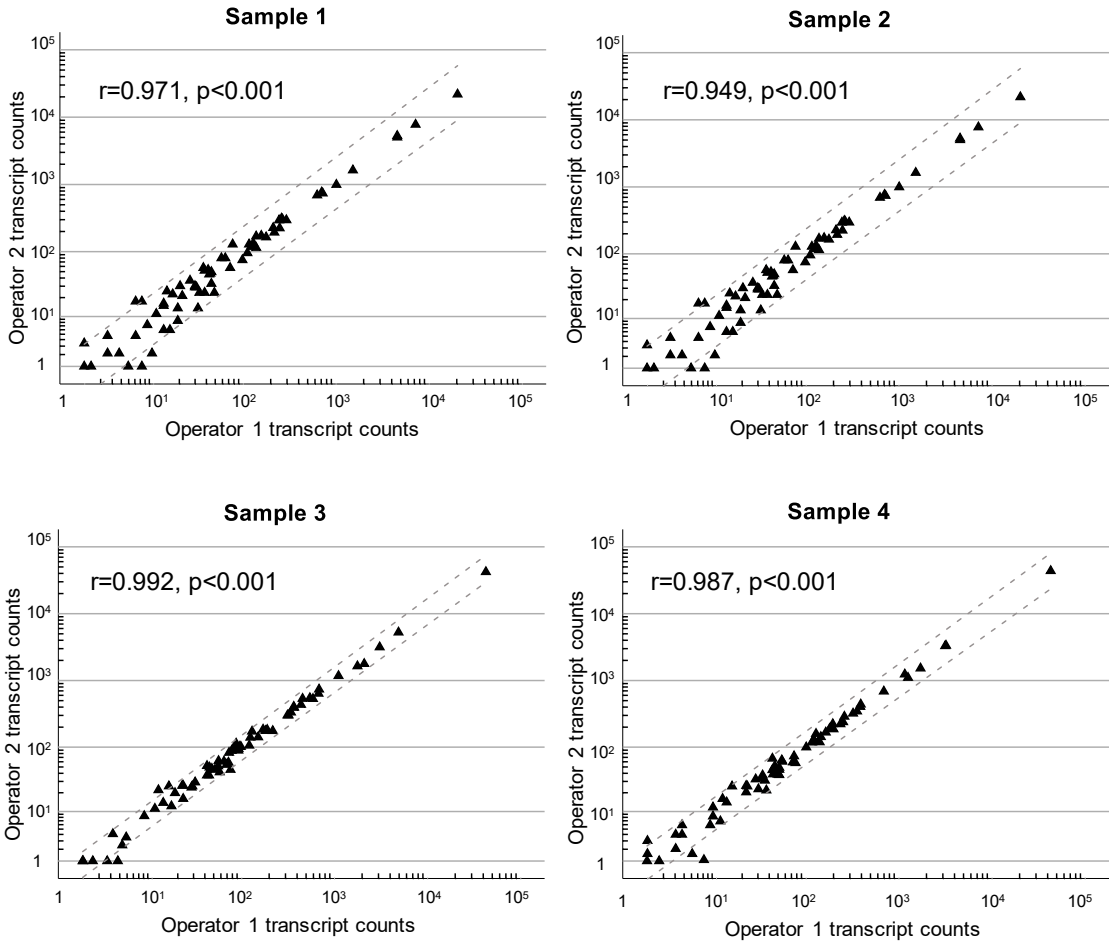

Figure 3.9. NanoString gene expression assay had robust inter-operator reproducibility.

Four RNA samples from four unique clinical liver biopsies were analyzed twice by two operators with different technical experience in different days. The scatter plot showed normalized transcript counts of 68 hepatic fibrosis-associated genes were strongly correlated in repeat runs by different operators. The normalized transcript counts produced by operator 1 (graduate student) were represented on the x-axis in relation to corresponding normalized transcript counts along the y-axis produced by operator 2 (molecular pathology technologist). The gray dashed lines represented 95% confidence interval of the regression line.

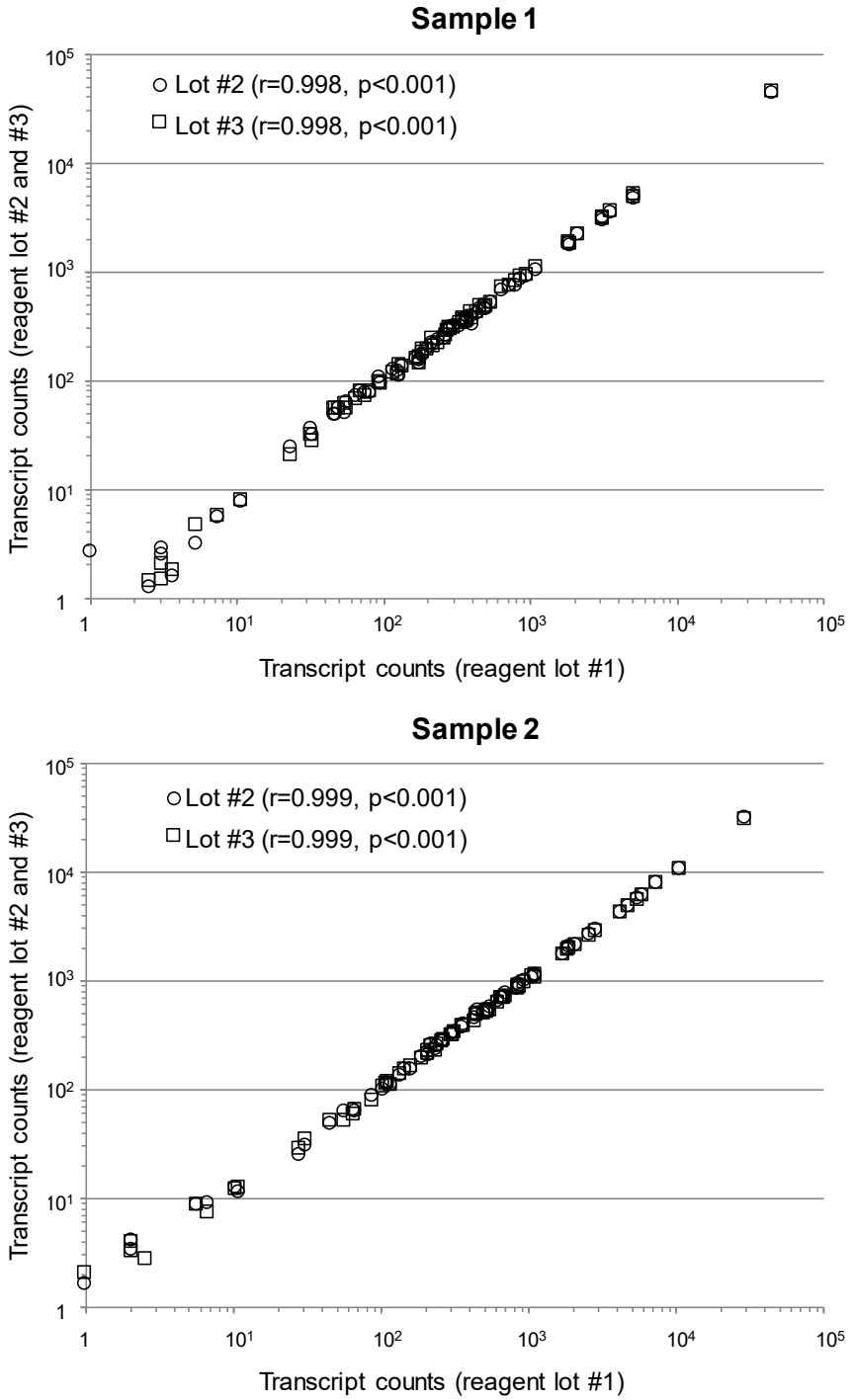

Figure 3.10. NanoString gene expression assay had robust inter-lot reagents reproducibility.

Two RNA samples from two unique clinical liver biopsies were analyzed across three different lots of reagents by the same operator in different days. The scatter plot showed normalized transcript counts of 68 hepatic fibrosis-associated genes were strongly correlated in repeat runs using different lots of reagents.

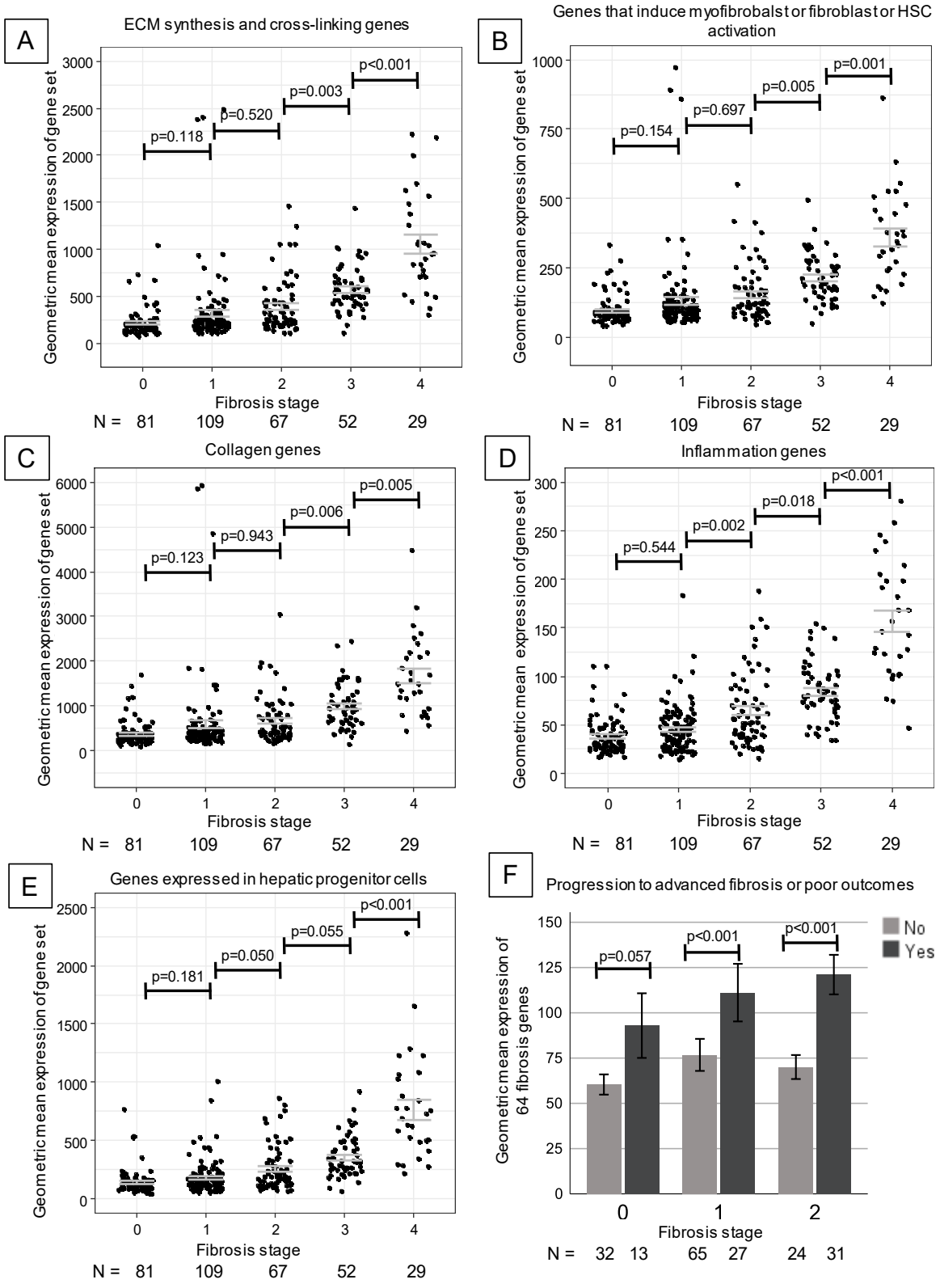

Figure 3.11. The fibrosis gene signature increased progressively with histological fibrosis stage.

(Figure 3.11 continued). The fibrosis gene sets were grouped based on biological function, including (A) extracellular matrix synthesis or cross-linking (23 genes), (B) inducing hepatic stellate cell and/or fibroblast and/or myofibroblast activation (17 genes), (C) collagen genes (8 genes), (D) inflammation genes (6 genes), and (E) hepatic progenitor cell markers (7 genes). (F) The expression of fibrosis genes predicts progression to advanced fibrosis and poor outcomes. Error bars represented mean ± standard error of mean.

3.5 – References

1. Bataller R, Brenner DA. Liver fibrosis. J Clin Invest 2005 Feb;115(2):209-218.
2. Rockey DC, Caldwell SH, Goodman ZD, Nelson RC, Smith AD. Liver biopsy. Hepatology 2009 Mar;49(3):1017-1044.
3. Standish RA, Cholongitas E, Dhillon A, Burroughs AK, Dhillon AP. An appraisal of the histopathological assessment of liver fibrosis. Gut 2006 Apr;55(4):569-578.
4. EASL-ALEH Clinical Practice Guidelines: Non-invasive tests for evaluation of liver disease severity and prognosis. J Hepatol 2015 Jul;63(1):237-264.
5. Hoshida Y, Villanueva A, Sangiovanni A, Sole M, Hur C, Andersson KL, et al. Prognostic gene expression signature for patients with hepatitis C-related early-stage cirrhosis. Gastroenterology 2013 May;144(5):1024-1030.
6. Kim JH, Sohn BH, Lee HS, Kim SB, Yoo JE, Park YY, et al. Genomic predictors for recurrence patterns of hepatocellular carcinoma: model derivation and validation. PLoS Med 2014 Dec;11(12):e1001770.
7. Ji J, Eggert T, Budhu A, Forgues M, Takai A, Dang H, et al. Hepatic stellate cell and monocyte interaction contributes to poor prognosis in hepatocellular carcinoma. Hepatology 2015 Aug;62(2):481-495.
8. King LY, Canasto-Chibuque C, Johnson KB, Yip S, Chen X, Kojima K, et al. A genomic and clinical prognostic index for hepatitis C-related early-stage cirrhosis that predicts clinical deterioration. Gut 2015 Aug;64(8):1296-1302.

9. Zhang DY, Goossens N, Guo J, Tsai MC, Chou HI, Altunkaynak C, et al. A hepatic stellate cell gene expression signature associated with outcomes in hepatitis C cirrhosis and hepatocellular carcinoma after curative resection. Gut 2016 Oct;65(10):1754-1764.

10. Trepo E, Goossens N, Fujiwara N, Song WM, Colaprico A, Marot A, et al. Combination of Gene Expression Signature and Model for End-Stage Liver Disease Score Predicts Survival of Patients With Severe Alcoholic Hepatitis. Gastroenterology 2018 Mar;154(4):965-975.

11. Smith MW, Walters KA, Korth MJ, Fitzgibbon M, Proll S, Thompson JC, et al. Gene expression patterns that correlate with hepatitis C and early progression to fibrosis in liver transplant recipients. Gastroenterology 2006 Jan;130(1):179-187.

12. Penland SK, Keku TO, Torrice C, He X, Krishnamurthy J, Hoadley KA, et al. RNA expression analysis of formalin-fixed paraffin-embedded tumors. Lab Invest 2007 Apr;87(4):383-391.

13. Karsten SL, Van Deerlin VM, Sabatti C, Gill LH, Geschwind DH. An evaluation of tyramide signal amplification and archived fixed and frozen tissue in microarray gene expression analysis. Nucleic Acids Res 2002 Jan 15;30(2):E4.

14. Geiss GK, Bumgarner RE, Birditt B, Dahl T, Dowidar N, Dunaway DL, et al. Direct multiplexed measurement of gene expression with color-coded probe pairs. Nat Biotechnol 2008 Mar;26(3):317-325.

15. Tyekucheva S, Martin NE, Stack EC, Wei W, Vathipadiekal V, Waldron L, et al. Comparing Platforms for Messenger RNA Expression Profiling of Archival Formalin-Fixed, Paraffin-Embedded Tissues. J Mol Diagn 2015 Jul;17(4):374-381.

16. Veldman-Jones MH, Lai Z, Wappett M, Harbron CG, Barrett JC, Harrington EA, et al. Reproducible, Quantitative, and Flexible Molecular Subtyping of Clinical DLBCL Samples Using the NanoString nCounter System. Clin Cancer Res 2015 May 15;21(10):2367-2378.

17. Reis PP, Waldron L, Goswami RS, Xu W, Xuan Y, Perez-Ordonez B, et al. mRNA transcript quantification in archival samples using multiplexed, color-coded probes. BMC Biotechnol 2011;11:46.

18. Richard AC, Lyons PA, Peters JE, Biasci D, Flint SM, Lee JC, et al. Comparison of gene expression microarray data with count-based RNA measurements informs microarray interpretation. BMC Genomics 2014;15:649.

19. Veldman-Jones MH, Brant R, Rooney C, Geh C, Emery H, Harbron CG, et al. Evaluating Robustness and Sensitivity of the NanoString Technologies nCounter Platform to Enable Multiplexed Gene Expression Analysis of Clinical Samples. Cancer Res 2015 Jul 1;75(13):2587-2593.

20. Nielsen T, Wallden B, Schaper C, Ferree S, Liu S, Gao D, et al. Analytical validation of the PAM50-based Prosigna Breast Cancer Prognostic Gene Signature Assay and nCounter Analysis System using formalin-fixed paraffin-embedded breast tumor specimens. BMC Cancer 2014 Mar 13;14:177.

21. Goodman ZD. Grading and staging systems for inflammation and fibrosis in chronic liver diseases. J Hepatol 2007 Oct;47(4):598-607.

22. Brunt EM, Janney CG, Di Bisceglie AM, Neuschwander-Tetri BA, Bacon BR. Nonalcoholic steatohepatitis: a proposal for grading and staging the histological lesions. Am J Gastroenterol 1999 Sep;94(9):2467-2474.

23. Affo S, Dominguez M, Lozano JJ, Sancho-Bru P, Rodrigo-Torres D, Morales-Ibanez O, et al. Transcriptome analysis identifies TNF superfamily receptors as potential therapeutic targets in alcoholic hepatitis. Gut 2013 Mar;62(3):452-460.

24. Yildiz G, Arslan-Ergul A, Bagislar S, Konu O, Yuzugullu H, Gursoy-Yuzugullu O, et al. Genome-wide transcriptional reorganization associated with senescence-to-immortality switch during human hepatocellular carcinogenesis. PLoS One 2013;8(5):e64016.

25. Moylan CA, Pang H, Dellinger A, Suzuki A, Garrett ME, Guy CD, et al. Hepatic gene expression profiles differentiate presymptomatic patients with mild versus severe nonalcoholic fatty liver disease. Hepatology 2014 Feb;59(2):471-482.

26. Khalid SS, Hamid S, Siddiqui AA, Qureshi A, Qureshi N. Gene profiling of early and advanced liver disease in chronic hepatitis C patients. Hepatol Int 2011 Sep;5(3):782-788.

27. Wurmbach E, Chen YB, Khitrov G, Zhang W, Roayaie S, Schwartz M, et al. Genome-wide molecular profiles of HCV-induced dysplasia and hepatocellular carcinoma. Hepatology 2007 Apr;45(4):938-947.

28. Beckebaum S, Iacob S, Klein CG, Dechene A, Varghese J, Baba HA, et al. Assessment of allograft fibrosis by transient elastography and noninvasive biomarker scoring systems in liver transplant patients. Transplantation 2010 Apr 27;89(8):983-993.

29. Abdueva D, Wing M, Schaub B, Triche T, Davicioni E. Quantitative expression profiling in formalin-fixed paraffin-embedded samples by affymetrix microarrays. J Mol Diagn 2010 Jul;12(4):409-417.

30. Schilsky RL, Doroshow JH, Leblanc M, Conley BA. Development and use of integral assays in clinical trials. Clin Cancer Res 2012 Mar 15;18(6):1540-1546.

31. Friedman SL. Evolving challenges in hepatic fibrosis. Nat Rev Gastroenterol Hepatol 2010 Aug;7(8):425-436.

32. Hu K, Olsen BR, Besschetnova TY. Cell autonomous ANTXR1-mediated regulation of extracellular matrix components in primary fibroblasts. Matrix Biol 2017 Oct;62:105-114.

33. Kim YJ, Sano T, Nabetani T, Asano Y, Hirabayashi Y. GPRC5B activates obesity-associated inflammatory signaling in adipocytes. Sci Signal 2012 Nov 20;5(251):ra85.

34. Xian ZH, Cong WM, Wang YH, Wang B, Wu MC. Expression and localization of aquaporin-1 in human cirrhotic liver. Pathol Res Pract 2009;205(11):774-780.

35. Neubauer K, Baruch Y, Lindhorst A, Saile B, Ramadori G. Gelsolin gene expression is upregulated in damaged rat and human livers within non-parenchymal cells and not in hepatocytes. Histochem Cell Biol 2003 Oct;120(4):265-275.

36. Kraus MR, Clauin S, Pfister Y, Di MM, Ulinski T, Constam D, et al. Two mutations in human BICC1 resulting in Wnt pathway hyperactivity associated with cystic renal dysplasia. Hum Mutat 2012 Jan;33(1):86-90.

37. Vashchenko G, Macgillivray RT. Functional role of the putative iron ligands in the ferroxidase activity of recombinant human hephaestin. J Biol Inorg Chem 2012 Dec;17(8):1187-1195.

38. Liu LX, Huang S, Zhang QQ, Liu Y, Zhang DM, Guo XH, et al. Insulin-like growth factor binding protein-7 induces activation and transdifferentiation of hepatic stellate cells in vitro. World J Gastroenterol 2009 Jul 14;15(26):3246-3253.

39. Liaskou E, Wilson DV, Oo YH. Innate immune cells in liver inflammation. Mediators Inflamm 2012;2012:949157.

40. Henderson NC, Arnold TD, Katamura Y, Giacomini MM, Rodriguez JD, McCarty JH, et al. Targeting of alphav integrin identifies a core molecular pathway that regulates fibrosis in several organs. Nat Med 2013 Dec;19(12):1617-1624.

41. Heyes S, Pratt WS, Rees E, Dahimene S, Ferron L, Owen MJ, et al. Genetic disruption of voltage-gated calcium channels in psychiatric and neurological disorders. Prog Neurobiol 2015 Nov;134:36-54.

42. Boulter L, Govaere O, Bird TG, Radulescu S, Ramachandran P, Pellicoro A, et al. Macrophage-derived Wnt opposes Notch signaling to specify hepatic progenitor cell fate in chronic liver disease. Nat Med 2012 Mar 4;18(4):572-579.

43. Marra F, Tacke F. Roles for chemokines in liver disease. Gastroenterology 2014 Sep;147(3):577-594.

44. Sancho-Bru P, Altamirano J, Rodrigo-Torres D, Coll M, Millan C, Jose LJ, et al. Liver progenitor cell markers correlate with liver damage and predict short-term mortality in patients with alcoholic hepatitis. Hepatology 2012 Jun;55(6):1931-1941.

45. Ajuebor MN, Carey JA, Swain MG. CCR5 in T cell-mediated liver diseases: what's going on? J Immunol 2006 Aug 15;177(4):2039-2045.

46. Liu C, Schreiter T, Dirsch O, Gerken G, Oldhafer KJ, Broelsch CE, et al. Presence of markers for liver progenitor cells in human-derived intrahepatic biliary epithelial cells. Liver Int 2004 Dec;24(6):669-678.

47. Yovchev MI, Grozdanov PN, Joseph B, Gupta S, Dabeva MD. Novel hepatic progenitor cell surface markers in the adult rat liver. Hepatology 2007 Jan;45(1):139-149.

48. Xu X, Li YM, Ji H, Hou CZ, Cheng YB, Ma FP. Changes of ECM and CAM gene expression profile in the cirrhotic liver after HCV infection: analysis by cDNA expression array. World J Gastroenterol 2005 Apr 14;11(14):2184-2187.

49. Chang SK, Noss EH, Chen M, Gu Z, Townsend K, Grenha R, et al. Cadherin-11 regulates fibroblast inflammation. Proc Natl Acad Sci U S A 2011 May 17;108(20):8402-8407.

50. Henderson NC, Mackinnon AC, Farnworth SL, Poirier F, Russo FP, Iredale JP, et al. Galectin-3 regulates myofibroblast activation and hepatic fibrosis. Proc Natl Acad Sci U S A 2006 Mar 28;103(13):5060-5065.

51. Liu SB, Ikenaga N, Peng ZW, Sverdlov DY, Greenstein A, Smith V, et al. Lysyl oxidase activity contributes to collagen stabilization during liver fibrosis progression

and limits spontaneous fibrosis reversal in mice. FASEB J 2016 Apr;30(4):1599-1609.

52. Ruehl M, Erben U, Schuppan D, Wagner C, Zeller A, Freise C, et al. The elongated first fibronectin type III domain of collagen XIV is an inducer of quiescence and differentiation in fibroblasts and preadipocytes. J Biol Chem 2005 Nov 18;280(46):38537-38543.

53. Sakai N, Chun J, Duffield JS, Wada T, Luster AD, Tager AM. LPA1-induced cytoskeleton reorganization drives fibrosis through CTGF-dependent fibroblast proliferation. FASEB J 2013 May;27(5):1830-1846.

54. Vehvilainen P, Hyytiainen M, Keski-Oja J. Matrix association of latent TGF-beta binding protein-2 (LTBP-2) is dependent on fibrillin-1. J Cell Physiol 2009 Dec;221(3):586-593.

55. Krishnan A, Li X, Kao WY, Viker K, Butters K, Masuoka H, et al. Lumican, an extracellular matrix proteoglycan, is a novel requisite for hepatic fibrosis. Lab Invest 2012 Dec;92(12):1712-1725.

56. Li J, Xin J, Zhang L, Wu J, Jiang L, Zhou Q, et al. Human hepatic progenitor cells express hematopoietic cell markers CD45 and CD109. Int J Med Sci 2014;11(1):65-79.

57. Pfisterer U, Kirkeby A, Torper O, Wood J, Nelander J, Dufour A, et al. Direct conversion of human fibroblasts to dopaminergic neurons. Proc Natl Acad Sci U S A 2011 Jun 21;108(25):10343-10348.

58. Duarte S, Baber J, Fujii T, Coito AJ. Matrix metalloproteinases in liver injury, repair and fibrosis. Matrix Biol 2015 May;44-46:147-156.

59. Xin X, Mains RE, Eipper BA. Monooxygenase X, a member of the copper-dependent monooxygenase family localized to the endoplasmic reticulum. J Biol Chem 2004 Nov 12;279(46):48159-48167.

60. Gressner OA, Gressner AM. Connective tissue growth factor: a fibrogenic master switch in fibrotic liver diseases. Liver Int 2008 Sep;28(8):1065-1079.

61. Cochet-Bissuel M, Lory P, Monteil A. The sodium leak channel, NALCN, in health and disease. Front Cell Neurosci 2014;8:132.

62. Cohen-Dvashi H, Ben-Chetrit N, Russell R, Carvalho S, Lauriola M, Nisani S, et al. Navigator-3, a modulator of cell migration, may act as a suppressor of breast cancer progression. EMBO Mol Med 2015 Mar;7(3):299-314.

63. Miyazaki T, Kanou Y, Murata Y, Ohmori S, Niwa T, Maeda K, et al. Molecular cloning of a novel thyroid hormone-responsive gene, ZAKI-4, in human skin fibroblasts. J Biol Chem 1996 Jun 14;271(24):14567-14571.

64. Schueler M, Braun DA, Chandrasekar G, Gee HY, Klasson TD, Halbritter J, et al. DCDC2 mutations cause a renal-hepatic ciliopathy by disrupting Wnt signaling. Am J Hum Genet 2015 Jan 8;96(1):81-92.

65. Kobayashi M, Harada K, Negishi M, Katoh H. Dock4 forms a complex with SH3YL1 and regulates cancer cell migration. Cell Signal 2014 May;26(5):1082-1088.

66. Zhou S, Zhu Y, Mashrah M, Zhang X, He Z, Yao Z, et al. Expression pattern of DKK3, dickkopf WNT signaling pathway inhibitor 3, in the malignant progression of oral submucous fibrosis. Oncol Rep 2017 Feb;37(2):979-985.

67. Kondoh N, Imazeki N, Arai M, Hada A, Hatsuse K, Matsuo H, et al. Activation of a system A amino acid transporter, ATA1/SLC38A1, in human hepatocellular carcinoma and preneoplastic liver tissues. Int J Oncol 2007 Jul;31(1):81-87.

68. Blake DJ, Weir A, Newey SE, Davies KE. Function and genetics of dystrophin and dystrophin-related proteins in muscle. Physiol Rev 2002 Apr;82(2):291-329.

69. Hanley KP, Oakley F, Sugden S, Wilson DI, Mann DA, Hanley NA. Ectopic SOX9 mediates extracellular matrix deposition characteristic of organ fibrosis. J Biol Chem 2008 May 16;283(20):14063-14071.

70. Baiocchini A, Montaldo C, Conigliaro A, Grimaldi A, Correani V, Mura F, et al. Extracellular Matrix Molecular Remodeling in Human Liver Fibrosis Evolution. PLoS One 2016;11(3):e0151736.

71. Matsue Y, Tsutsumi M, Hayashi N, Saito T, Tsuchishima M, Toshikuni N, et al. Serum osteopontin predicts degree of hepatic fibrosis and serves as a biomarker in patients with hepatitis C virus infection. PLoS One 2015;10(3):e0118744.

72. Albino D, Longoni N, Curti L, Mello-Grand M, Pinton S, Civenni G, et al. ESE3/EHF controls epithelial cell differentiation and its loss leads to prostate tumors with mesenchymal and stem-like features. Cancer Res 2012 Jun 1;72(11):2889-2900.

73. Chen M, Tabaczewski P, Truscott SM, Van KL, Stroynowski I. Hepatocytes express abundant surface class I MHC and efficiently use transporter associated with antigen

processing, tapasin, and low molecular weight polypeptide proteasome subunit components of antigen processing and presentation pathway. J Immunol 2005 Jul 15;175(2):1047-1055.

74. Dolle L, Theise ND, Schmelzer E, Boulter L, Gires O, van Grunsven LA. EpCAM and the biology of hepatic stem/progenitor cells. Am J Physiol Gastrointest Liver Physiol 2015 Feb 15;308(4):G233-G250.

75. Rockey DC, Bell PD, Hill JA. Fibrosis--a common pathway to organ injury and failure. N Engl J Med 2015 Mar 19;372(12):1138-1149.

76. Ivanov AI, Romanovsky AA. Putative dual role of ephrin-Eph receptor interactions in inflammation. IUBMB Life 2006 Jul;58(7):389-394.

77. Calabro NE, Kristofik NJ, Kyriakides TR. Thrombospondin-2 and extracellular matrix assembly. Biochim Biophys Acta 2014 Aug;1840(8):2396-2402.

78. Kalluri R, Weinberg RA. The basics of epithelial-mesenchymal transition. J Clin Invest 2009 Jun;119(6):1420-1428.

79. Lorena D, Darby IA, Reinhardt DP, Sapin V, Rosenbaum J, Desmouliere A. Fibrillin-1 expression in normal and fibrotic rat liver and in cultured hepatic fibroblastic cells: modulation by mechanical stress and role in cell adhesion. Lab Invest 2004 Feb;84(2):203-212.

80. Matsui T, Kunishima S, Hamako J, Katayama M, Kamiya T, Naoe T, et al. Interaction of von Willebrand factor with the extracellular matrix and glycocalicin under static conditions. J Biochem 1997 Feb;121(2):376-381.

Chapter 4: A 48-gene Signature in Clinical Liver Biopsies with Recurrent Viral Hepatitis C Predicts Progression to Advanced Fibrosis and Poor Clinical Outcomes

4.1 – Introduction

Currently, there are more than two billion patients worldwide who suffer from chronic liver disease. The most common causes are non-alcoholic fatty liver disease (NAFLD), viral hepatitis B, alcoholic liver disease, and viral hepatitis C (HCV) with prevalence rates of 25.24%, 3.61%, 2.05%, and 1.00% worldwide, respectively (1-4). Patients with chronic liver disease can behave as rapid or slow/no progressors, with time progression to advanced fibrosis ranging from a few years to several decades (5, 6). As advanced fibrosis is the common final pathway that leads to poor clinical outcomes (liver decompensation, need for liver transplantation, and premature death), recent clinical guidelines strongly recommend that not only patients with advanced fibrosis should be considered for lifestyle changes or pharmacotherapy, but also patients with early fibrosis (F0 or F1) who are at high-risk of progressing to advanced fibrosis (7, 8). Previous studies identified several common risk factors of fibrosis progression in chronic liver diseases, such as older age, excessive alcohol consumption, and obesity (9-11). However, no single clinical variable can reliably predict high-risk for progression to advanced fibrosis and poor clinical outcomes in individual patients especially when the patient is at early stage.

Histopathology assessment of liver biopsy remains the gold standard for staging liver fibrosis that provides clinically important diagnostic information; but it cannot provide risk stratification for progressing to advanced fibrosis or poor clinical outcomes (12). This is because liver fibrosis is a heterogeneous condition, with intervals of progression and regression, and thus patients with the same histological fibrosis stage could present different histopathological changes and clinical outcomes over time. The inherent limitations of

histopathology have led to the development of non-invasive diagnostic tests (imaging methods, serum biomarkers), but these tests can only detect fibrosis if present at the time of diagnostic tests but cannot predict disease progression (13). Therefore, there is an urgent clinical need for a surrogate biomarker to predict fibrosis progression and poor clinical outcomes in patients with early stage chronic liver disease.

Increasing evidence indicated that genetic factors have a major influence on fibrosis progression, but less is known of the relationship between fibrosis progression and gene expression alterations (14). Previous studies showed that mRNA expression of several fibrosis genes can predict fibrosis progression in early fibrosis stages (15, 16). However, these findings were conducted in small cohorts of patients, thus remain unreplicated and also it is unknown if these genes can predict clinical outcomes (15, 16). In Chapter 2, I identified and validated a common 48-gene signature with over 93% of accuracy for advanced liver fibrosis, independent of etiologies, by microarray based whole genome transcriptomics. However, the prognostic value of the 48-gene signature is unknown. Patients with recurrent HCV after liver transplantation are known to have accelerated fibrosis progression, thus sequential biopsies from recurrent HCV can serve as a human model for progressive liver fibrosis. In this chapter, using post-transplant patients with recurrent HCV before the era of new direct-acting antiviral treatments, I aim to analyze if the 48-gene signature can predict progression to advanced fibrosis, liver decompensation, and liver-related death.

4.2 – Materials and methods

4.2.1 – Patients

This research used post-transplant patients with recurrent HCV as a human disease

model for fibrosis progression. Post-transplant patients with HCV recurrence from Edmonton and Toronto between 2004 and 2014 were identified (Figure 4.1). Patients were retrospectively included if they had an early (median: 6-months) and late (median: 2-3 years) liver biopsy post-transplantation with leftover archived formalin-fixed paraffin-embedded (FFPE) tissue. A total of 62 Edmonton patients and 60 Toronto patients were included in the study. The study was approved by the institutional review board of the University of Alberta and University of Toronto.

4.2.2 – Treatment of recurrent viral hepatitis C

Recurrent HCV infection was defined as the detection of HCV RNA in the serum and/or liver after liver transplantation. Prior to April 2014, recurrent HCV patients were treated with Peginterferon and/or Ribavirin with or without Boceprevir. After April 2014, recurrent HCV patients were treated with Sofosbuvir-containing regimens. Sustained virologic response (SVR) was defined as undetectable serum HCV RNA at 24 weeks after completion of Peginterferon and/or Ribavirin with or without Boceprevir therapy (17). For patients who were treated with Sofosbuvir-containing regimens, SVR was defined as undetectable serum HCV RNA at 12 weeks after completion of therapy (17).

4.2.3 – Histopathological assessment

Histopathological evaluation of representative stained slides was independently performed by liver pathologists according to the Metavir classification system to grade and stage recurrent HCV disease (18). Scores that were not provided as an integer were rounded in the analysis to a higher grade or stage (e.g., stage 0-1 was rounded to 1 and stage 1-2 was rounded to 2) (19). All histopathological evaluations were blinded to the clinical and

molecular data.

4.2.4 – RNA isolation

Reeda Gill assisted with the RNA isolation. One to three consecutive 20-µm sections were obtained from each clinical liver biopsy with equipment sterilization with RNase away reagent (Ambion, Carlsbad, CA) and microtome blade replacement between blocks. Sections were then taken immediately into a sterile 1.5-mL DNase/RNase free microcentrifuge tube for subsequent RNA extraction using a RecoverAll Total Nucleic Acid Isolation Kit (Ambion, Carlsbad, CA). Precipitated and dried RNA was dissolved in DNase/RNase-free distilled water and the concentration and quality were measured by NanoDrop 2000 spectrophotometer (Thermo Fisher Scientific, Waltham, MA).

4.2.5 – NanoString gene expression quantification

This chapter analyzed 52 genes. Of the 52 genes, 48 were up-regulated in advanced liver fibrosis (discovered in Chapter 2) and four were housekeeping genes (Table 4.1). Oligonucleotide probe sequences of 52 genes were designed and synthesized by Integrated DNA Technologies (Coralville, IA) (Table 4.1). Probes were hybridized to 60-100 ng of total RNA for 18 hours at 67 degrees. After hybridization, excess probes were removed and hybridized probes were immobilized and aligned on the streptavidin-coated cartridge by the nCounter Prep Station (NanoString Technologies, Seattle, WA). Gene expression was quantified by the nCounter Digital Analyzer (NanoString Technologies, Seattle, WA).

4.2.6 – NanoString data preprocessing

Quality control and normalization of raw NanoString transcript counts were

performed by nSolver Analysis Software version 4.0 (NanoString Technologies, Seattle, WA). Background noise was adjusted by subtracting the geometric mean of six internal negative controls of each sample. Genes with transcript counts less than the geometric mean of the negative controls were floored to a value of 1. After background noise adjustment, transcript counts were normalized with the geometric mean of the six internal positive controls, followed by normalization to the geometric mean of four housekeeping genes in each sample. Two lots of NanoString reagents were utilized during the study. Thus, two consistent reference samples were analyzed in each lot for lot-to-lot normalization.

4.2.7 – Study endpoint

The study endpoint was progression to adverse outcomes, defined as progressed to any one of the following: advanced fibrosis, liver decompensation, need for liver transplantation, or liver-related death. Progression to advanced fibrosis was defined as Metavir fibrosis stage 3 or 4 in late or any other follow-up biopsies or Fibroscan >10.9 kPa in follow-up clinical visits (20). Liver decompensation was defined as diagnosis of any of the following: ascites, hepatic encephalopathy, variceal bleeding, or hepatorenal syndrome (21). Liver-related death was defined as death caused by liver failure: nearest liver function test with total bilirubin > 50 umol/L and international normalized ratio (INR) > 1.7 before death (22, 23). The time to endpoint was calculated using the date of biopsy to an event.

4.2.8 – Statistical analysis

Aggregate gene set expression was determined for each biopsy by calculating the geometric mean of the normalized transcript counts of 48 fibrosis genes (48-gene signature). Continuous variables were presented as median and interquartile range (IQR) and categorical

variables were presented as number and percentage. All data were compared between groups using Mann-Whitney U-test for continuous variables and Fisher's exact test for categorical variables. Survival analyses were performed after biopsies with the Kaplan–Meier method using a log-rank test and univariate and multivariate models with Cox regression method. The assumption of proportional hazards over time was verified using the log–log graphic method and met by all covariates. Potential linearity of covariates was investigated by collinearity diagnostics before multivariate survival analysis. All tests with a two-sided p-value <0.05 were considered significant. All analyses and figures were performed and generated using the SPSS 25 statistical software (IBM, Armonk, NY, USA), Excel 2010 (Microsoft Corporation, Redmond, WA), or R-program (version 3.3.2; http://www.r-project.org) with the ggplot2 package.

4.3 – Results

4.3.1 – Patient characteristics

This study analyzed 62 Edmonton and 60 Toronto patients with recurrent HCV after liver transplantation (Figure 4.1). Table 4.2 summarized the clinical characteristics of Edmonton and Toronto patients. Median age at transplantation was 54.9 and 58.1 years old for the Edmonton and Toronto patients, respectively. Fifty (80.6%) Edmonton patients had no or mild fibrosis (F0 or F1) and 12 (19.4%) had moderate fibrosis (F2) in early biopsy. Fifty-five (91.7%) Toronto patients had no or mild fibrosis, 4 (6.7%) had moderate fibrosis, and 1 (1.7%) had advanced fibrosis (F3) in early biopsy. There were no significant differences between Edmonton and Toronto patients with respect to fibrosis stage in both early and late biopsies (p=0.12, 0.09, respectively). However, Edmonton patients had

significantly longer follow-up period than Toronto patients (median 8.4 vs. 3.1 years, $p<0.001$), and this resulted in more Edmonton patients with progression to adverse outcomes compared to Toronto patients (41.9% vs. 13.3%, $p=0.001$). In this chapter, progressed to adverse outcomes refer to development of any of the following during follow-up: progression to advanced fibrosis, liver decompensation, need for liver transplantation, or liver-related death. There was also heterogeneity between patients from two centers with respect to immunosuppressive therapy and HCV genotype (Table 4.2). These heterogeneities may help to ensure that the 48-gene signature has real-world applicability across heterogeneous populations of recipients with different drug treatments and HCV genotype.

4.3.2 – RNA quantity, quality and NanoString quality control

Adequate RNA was isolated from all 184 liver tissues for NanoString gene expression assay. The quality (A_{260}/A_{280} spectrophotometry ratio) of the isolated RNA was between 1.65 and 2.05, which met manufacturer-recommended specifications. No quality control or normalization flags were encountered during nSolver analysis for any of the samples.

4.3.3 – Distribution of the histological fibrosis stage and the 48-gene signature in Edmonton early biopsies

Of 62 Edmonton patients, 32% (6 of 19) with F0 fibrosis, 35% (11 of 31) with F1 fibrosis, and 75% (9 of 12) with F2 fibrosis in early biopsy progressed to adverse outcomes. Biopsies with a 48-gene signature greater than 64.36 (the median of 48-gene signature in 62 Edmonton early biopsies) were assigned as having a high 48-gene signature (Figure 4.2A).

There were significantly more patients with a high 48-gene signature progressed to adverse outcomes compared to patients with a low 48-gene signature (65% vs. 19%, p=0.001, Figure 4.2B). When only patients with F0 or F1 fibrosis were analyzed, there were also significantly more patients with a high 48-gene signature progressed to adverse outcomes compared to patients with a low 48-gene signature (50% vs. 21%, p=0.040, Figure 4.2B). However, the percentage of patients progressed to adverse outcomes were similar between F0 and F1 fibrosis in early biopsy (32% vs. 35%, p=1.00).

Of 62 Edmonton patients, progressors (patients who progressed to adverse outcomes) had significantly higher 48-gene signature and higher histological fibrosis stage compared to the non-progressors in early biopsy (p=0.003 and 0.048, respectively) (Figure 4.3A and 4.3B). Of the 50 Edmonton patients with F0 or F1 fibrosis in early biopsy, progressors had significantly higher 48-gene signature compared to non-progressors (p=0.013, Figure 4.2C), but similar histological fibrosis stage between progressors and non-progressors (p=0.779, Figure 4.2D). This showed histological fibrosis stage cannot predict adverse outcomes in patients with F0 or F1 fibrosis.

Of the 12 Edmonton patients with F2 fibrosis in early biopsy, there were significantly more patients with a high 48-gene signature progressed to adverse outcomes compared to patients with a low 48-gene signature (100% vs. 0%, p=0.005, Figure 4.2B). Moreover, progressors had significantly higher 48-gene signature compared to non-progressors (p=0.009, Figure 4.4). This showed the 48-gene signature could accurately classify patients with the same histological fibrosis stage into distinct prognostic categories, thus providing additional prognostic information.

4.3.4 – The 48-gene signature in Edmonton early biopsies with F0 or F1 fibrosis predicts adverse outcomes, but histological fibrosis stage cannot

Edmonton patients with a high 48-gene signature and higher fibrosis stage in early biopsy had significantly higher probability of progression to adverse outcomes during the follow-up period while taking time into account in Kaplan-Meier analysis (log-rank $p<0.001$ and 0.001, respectively) (Figure 4.5A and 4.5B). When only the patients with F0 or F1 fibrosis were analyzed, patients with a high 48-gene signature had significantly higher probability of progression to adverse outcomes compared to patients with a low 48-gene signature (50% vs. 21%, log-rank $p=0.030$, Figure 4.6A), but histological assessment comparisons between F0 and F1 fibrosis patients showed no statistically significant differences (32% vs. 35%, log-rank $p=0.482$, Figure 4.6B). This showed the 48-gene signature can predict adverse outcomes earlier than histology.

Of the 12 Edmonton patients with F2 fibrosis in early biopsy, all patients with a high 48-gene signature progressed to adverse outcomes (100% vs. 0%, log-rank $p=0.011$, Figure 4.7).

4.3.5 – Variables associated with progression to adverse outcomes

Univariate and multivariate Cox regression analyses were used to analyze potential variables for progression to adverse outcomes. Univariate analysis revealed Edmonton patients with older age at transplantation, older donor age, higher Metavir fibrosis stage and a high 48-gene signature in early biopsy were significantly associated with increased risk for progression to adverse outcomes, whereas SVR was significantly associated with decreased risk for progression to adverse outcomes (Table 4.3). Histological activity score was not

significantly associated with progression to adverse outcomes (HR=1.87; 95% CI, 0.80-4.38; p=0.15).

Multivariate analyses included all variables with a p-value <0.05 in univariate analysis (recipient age at transplantation, donor age, HCV treatment response, Metavir fibrosis stage in early biopsy, and 48-gene signature in early biopsy). Due to limited number of patients progressed to adverse outcomes (n=26), multivariate models were limited to three variables to avoid model overfitting. To analyze the effect of 48-gene signature predicting progression to adverse outcomes, six models were built: 48-gene signature in early biopsy with recipient age at transplantation and Metavir fibrosis stage in early biopsy (model 1); 48-gene signature in early biopsy with donor age and Metavir fibrosis stage in early biopsy (model 2); 48-gene signature in early biopsy with recipient age at transplantation and donor age (model 3); 48-gene signature in early biopsy with recipient age at transplantation and HCV treatment (model 4); 48-gene signature in early biopsy with donor age and HCV treatment (model 5); 48-gene signature in early biopsy with HCV treatment and Metavir fibrosis stage in early biopsy (model 6) (Table 4.3). A high 48-gene signature was significantly and independently associated with progression to adverse outcomes in all six multivariate models.

Multivariate analysis repeated with all variables with p<0.05 in univariate analysis provided the same conclusions as above. A high 48-gene signature was the most significant independent predictor for progression to adverse outcomes (HR=4.47; 95% CI, 1.70-11.78; p=0.002) (Table 4.4).

4.3.6 – Distribution of the histological fibrosis stage and the 48-gene signature in Edmonton late biopsies

Of the 62 Edmonton patients, 14% (1 of 7) with F0 fibrosis, 19% (4 of 21) with F1 fibrosis, and 43% (10 of 23) with F2 fibrosis in late biopsy had progressed to adverse outcomes. Using the cutoff (48-gene signature = 64.36) derived in Edmonton early biopsies, Edmonton late biopsies with a 48-gene signature greater than 64.36 were assigned as having a high 48-gene signature (Figure 4.8A). There were significantly more patients with a high 48-gene signature progressed to adverse outcomes compared to patients with a low 48-gene signature (62% vs. 12%, $p<0.001$). When only patients with F0, F1, or F2 fibrosis were analyzed, there were also significantly more patients with a high 48-gene signature progressed to adverse outcomes compared to patients with a low 48-gene signature (48% vs. 8%, $p=0.002$). However, the percentage of patients progressed to adverse outcomes were similar across F0, F1, and F2 fibrosis in late biopsy (14%, 19%, and 43%, respectively, $p=0.149$).

Of the 62 Edmonton patients, progressors had significantly higher 48-gene signature and histological fibrosis stage compared to non-progressors in late biopsies (both $p<0.001$, Figure 4.9A and 4.9B). When only patients with F0-F2 fibrosis were analyzed, progressors had significantly higher 48-gene signature compared to non-progressors ($p<0.001$, Figure 4.8B), but progressors only had a marginally significant higher histological fibrosis stage compared to non-progressors ($p=0.052$) (Figure 4.8C). When only patients with F0 or F1 fibrosis were analyzed, progressors had a marginally significant higher 48-gene signature compared to non-progressors ($p=0.051$, Figure 4.8D), but similar histological fibrosis stage between progressors vs. non-progressors ($p=0.780$, Figure 4.8E). These results supported

that the 48-gene signature can predict adverse outcomes earlier than histology.

4.3.7 – The 48-gene signature in Edmonton late biopsies without advanced fibrosis predicts adverse outcomes, but histological fibrosis stage cannot

Here, patients with F0-F2 fibrosis in late biopsy were analyzed because of the small sample size and events if only include patients with F0 or F1 fibrosis (n=28, events=5). Patients with a high 48-gene signature had significantly higher probability of progression to adverse outcomes compared to patients with a low 48-gene signature while taking time into account in Kaplan-Meier analysis (48% vs. 8%, log-rank p=0.003, Figure 4.10A), but histological assessment comparisons between F0, F1, and F2 fibrosis patients showed no statistically significant differences (14%, 19%, and 43%, respectively, log-rank p=0.208, Figure 4.10B). This showed the 48-gene signature can early predict adverse outcomes, but histological fibrosis stage cannot.

4.3.8 – Validation of the 48-gene signature in Toronto early biopsies

Of 60 Toronto patients, 9% (2 of 22) with F0 fibrosis, 15% (5 of 33) with F1 fibrosis, and 0% (0 of 4) with F2 fibrosis in early biopsy progressed to adverse outcomes during follow-up. Using the cutoff (48-gene signature = 64.36) derived in Edmonton early biopsies, Toronto early biopsies with a 48-gene signature greater than 64.36 were assigned as having a high 48-gene signature (Figure 4.11A). There were significantly more patients with a high 48-gene signature progressed to adverse outcomes compared to patients with a low 48-gene signature (27% vs. 3%, p=0.009) (Figure 4.11B). When only patients with F0 or F1 fibrosis were analyzed, there were also significantly more patients with a high 48-gene signature

progressed to adverse outcomes compared to patients with a low 48-gene signature (25% vs. 3%, p=0.035) (Figure 4.11B). However, the percentage of patients progressed to adverse outcomes were similar between F0 and F1 fibrosis (9% vs. 15%, p=0.689).

Of 60 Toronto patients, progressors had significantly higher 48-gene signature compared to the non-progressors in early biopsies (p=0.002, Figure 4.12A), but similar histological fibrosis stage (p=0.404, Figure 4.12B). When only patients with F0 or F1 fibrosis were analyzed, progressors still had significantly higher 48-gene signature compared to non-progressors (p=0.008, Figure 4.11C), but similar histological fibrosis stage between progressors vs. non-progressors (p=0.513, Figure 4.11D). These validated results showed that the 48-gene signature can predict adverse outcomes in patients earlier than histology.

4.4 – Discussion

This chapter showed for the first-time using patients with recurrent HCV after liver transplantation as a disease model for fibrosis progression, a 48-fibrosis gene signature in liver tissue can predict adverse outcomes (development of advanced fibrosis, liver decompensation, need for liver transplantation, or liver-related death) during follow-up. Early prediction of advanced fibrosis has been recognized as an effective strategy to substantially impact prognosis in patients with chronic liver disease (24). However, histopathology assessment of liver biopsy is poorly predictive for advanced fibrosis and liver-related outcomes in early disease stage. This 48-gene signature test can provide personalized risk stratification for fibrosis progression and poor liver-related outcomes that cannot be obtained by histology and the test can be easily implemented into a clinical assay platform.

Early prognostic prediction for patients with chronic liver disease is important in clinical management as patients at high-risk should be considered for lifestyle changes or timely treatment before development of advanced fibrosis. The importance of early diagnosing advanced fibrosis was indicated in a phase II anti-fibrotic drug trial. Simtuzumab, a drug targeting LOXL2 to prevent cross-linkage of collagen, was recently found ineffective in decreasing fibrosis in non-alcoholic steatohepatitis and HCV patients with advanced fibrosis (25, 26). One explanation of the failure is that these patients were too advanced and were not amenable to fibrinolysis after inhibition of collagen cross-linkage. Mauro et al. also reported regression of fibrosis was unlikely in HCV patients with cirrhosis and clinically significant portal hypertension even after successful antiviral therapy (27). These results showed the importance of predicting advanced fibrosis early and timely clinical management before development of advanced fibrosis. The 48-gene signature could serve as a clinical surrogate biomarker test to early identify high-risk patients who may benefit from the upcoming antifibrotic drug treatments to prevent progression to advanced fibrosis and poor liver-related outcomes.

Many previous studies had discovered gene expression profile associated with advanced fibrosis in liver tissue from patients with chronic liver diseases (28-32). However, to the best of my knowledge, only three studies analyzed the gene expression profile in liver tissue with HCV to predict fibrosis progression (15, 33, 34). Using microarray gene expression profiling, Smith et al. found recurrent HCV patients with early progressive fibrosis had up-regulated expression markers of myofibroblasts compared to patients without progressive fibrosis (15). Similarly, Munshaw et al. found the expression of butyrylcholinesterase in hepatocyte decreased before the onset of advanced fibrosis (33).

Marcolongo et al. discovered a score based on seven single-nucleotide polymorphisms can predict fibrosis progression in males with HCV, but not in females (34). A major difference between this study and the earlier ones was the findings in this chapter were validated in an independent cohort of patients from a different center, rather than only a single center study without external validation. This ensured that the 48-gene signature have real-world applicability across heterogeneous populations of patients.

This study had two limitations that were important to acknowledge. First, the follow-up time after transplantation for the Toronto patients is relatively short (median 3.1 years) and this resulted in limited number of events. Validation in another independent data set with longer follow-up period should be performed to assure the confidence in the results. Second, I used patients with recurrent HCV as a disease model because these patients have accelerated fibrosis progression compared to other chronic liver diseases (35). Future studies should assess the 48-gene signature in other liver diseases, especially in NAFLD, as currently there are no baseline clinical, histologic, or biochemical variables that could predict NAFLD progression and the high prevalence of this disease globally (36).

This chapter showed using patients with recurrent HCV after transplantation as a disease model for fibrosis progression, the 48-gene signature was able to predict progression to advanced fibrosis and poor liver-related outcomes earlier than histology. This 48-gene signature may be incorporated and validated into future clinical studies of different chronic liver diseases for early prediction of fibrosis progression.

Table 4.1. The list of 48-gene signature and four housekeeping genes

Gene	Official gene name	Accession number	Probe sequence
ANTXR1	Anthrax toxin receptor 1	NM_018153.3	GATGGGGGTCCAGCCTGCTACGGCGGATTTGACCT GTACTTCATTTTGGACAAATCAGGAAGTGTGCTGC ACCACTGGAATGAAATCTATTACTTTGTGG
AQP1	Aquaporin 1	NM_198098.1	CTGGGATTCTACCGTAATTGCTTTGTGCCTTTGGGC ACGGCCCTCCTTCTTTTCCTAACATGCACCTTGCTC CCAATGGTGCTTGGAGGGGGAAGAGATC
BICC1	BicC family RNA binding protein 1	NM_001080512.1	CACGGTCATCATATGTCAACATGCAGGCATTTGAC TATGAACAGAAGAAGCTATTAGCCACCAAAGCTAT GTTAAAGAAACCAGTGGTGACGGAGGTCAG
C1orf198	Chromosome 1 open reading frame 198	NM_001136495.1	CTCAACAAGCCCAATATTCCCTCCAAGTTCTTCTTG GTGCTGAGGGCTGTAGGAATTATTGAAAGCTTCTG CCTCACTTAGTATCGTCTGGGGCCCAGCA
C7	Complement component 7	NM_000587.2	ATGCTTTTGAAACACAGTCCTGTGAACCTACAAGA GGATGTCCAACAGAGGAGGGATGTGGAGAGCGTT TCAGGTGCTTTTCAGGTCAGTGCATCAGCAA
CACNA2D1	Calcium channel, voltage-dependent, alpha 2/delta subunit 1	NM_000722.2	TCTTATGATTATCAGTCAGTATGTGAGCCCGGTGCT GCACCAAAACAAGGAGCAGGACATCGCTCAGCAT ATGTGCCATCAGTAGCAGACATATTACAAA
CD24	CD24 molecule	NM_013230.2	ATAGACACTCCCCGAAGTCTTTTGTTCGCATGGTCA CACACTGATGCTTAGATGTTCCAGTAATCTAATAT GGCCACAGTAGTCTTGATGACCAAAGTCC
CDH11	Cadherin 11, type 2, OB-cadherin	NM_001797.2	CAGGAAGCCAAAGTCCCAGTGGCCATTAGGGTCCT TGATGTCAACGATAATGCTCCCAAGTTTGCTGCCC CTTATGAAGGTTTCATCTGTGAGAGTGATC
COL14A1	Collagen, type XIV, alpha 1	NM_021110.1	CTTTAAGTCCACCAAGAAACCTGAGAATCTCCAAT GTTGGCTCTAACAGTGCTCGATTAACCTGGGACCC AACTTCAAGACAGATCAATGGTTATCGAAT
COL1A1	Collagen, type I, alpha 1	NM_000088.3	CAGAAACATCGGATTTGGGGAACGCGTGTCAATCC CTTGTGCCGCAGGGCTGGGCGGGAGAGACTGTTCT GTTCCTTGTGTAACTGTGTTGCTGAAAGAC

COL1A2	Collagen, type I, alpha 2	NM_000089.3	CCAATGGATTTGCTGGTCCTGCTGGTGCTGCTGGTC AACCTGGTGCTAAAGGAGAAAGAGGAGCCAAAGG GCCTAAGGGTGAAAACGGTGTTGTTGGTCC
COL3A1	Collagen, type III, alpha 1	NM_000090.3	TTGGCACAACAGGAAGCTGTTGAAGGAGGATGTTC CCATCTTGGTCAGTCCTATGCGGATAGAGATGTCT GGAAGCCAGAACCATGCCAAATATGTGTCT
COL4A1	Collagen, type IV, alpha 1	NM_001845.4	TGGGCTTAAGTTTTCAAGGACCAAAAGGTGACAAG GGTGACCAAGGGGTCAGTGGGCCTCCAGGAGTACC AGGACAAGCTCAAGTTCAAGAAAAAGGAGA
COL4A2	Collagen, type IV, alpha 2	NM_001846.2	GGCATTTCCTTGAAGGGAGAAGAAGGAATCATGG GCTTTCCTGGACTGAGGGGTTACCCTGGCTTGAGT GGTGAAAAAGGATCACCAGGACAGAAGGGAA
COL4A4	Collagen, type IV, alpha 4	NM_000092.4	TATATGGGAGTGGAAAGAAATACATTGGTCCTTGT GGAGGAAGAGATTGCTCTGTTTGCCACTGTGTTCC TGAAAAGGGGTCTCGGGGTCCACCAGGACC
COL6A3	Collagen, type VI, alpha 3	NM_004369.3	AGAGCAAGCGAGACATTCTGTTCCTCTTTGACGGC TCAGCCAATCTTGTGGGCCAGTTCCCTGTTGTCCGT GACTTTCTCTACAAGATTATCGATGAGCT
CXCL6	Chemokine ligand 6	NM_002993.3	AGTAACAAAAAAGACCATGCATCATAAAATTGCCC AGTCTTCAGCGGAGCAGTTTTCTGGAGATCCCTGG ACCCAGTAAGAATAAGAAGGAAGGGTTGGT
DCDC2	Doublecortin domain containing 2	NM_016356.3	GTCTGAAACACGGGGGGCAGCAGAAGTCCAAGAA GATGAAGATACTCAGGTTGAGGTTCCAGTCGATCA GAGGCCAGCAGAAATAGTAGACGAGGAAGAA
DKK3	Dickkopf WNT signaling pathway inhibitor 3	NM_001018057.1	AGTGAACCTGGCAAACTTACCTCCCAGCTATCACA ATGAGACCAACACAGACACGAAGGTTGGAAATAA TACCATCCATGTGCACCGAGAAATTCACAAG
DTNA	Dystrobrevin, alpha	NM_032981.4	GTTCCCAGATCAGCCTGAGAAGCCACTCAACTTGG CTCACATCGTGCCTCCCAGACCTGTAACCAGCATG AACGACACCCTGTTCTCCCACTCTGTTCCC
EFEMP1	EGF containing fibulin-like extracellular matrix protein 1	NM_004105.3	ACCTACGACAAACAAGTCCTGTAAGTGCAATGCTT GTGCTCGTGAAGTCATTATCAGGACCAAGAGAACA TATCGTGGACCTGGAGATGCTGACAGTCAG

EHF	Ets homologous factor	NM_012153.3	ATTTAGAAAAAGGTGATGCATCCTCCTCACATAAG CATCCATATGGCTTCGTCAAGGGAGGTGAACATTG TTGCTGAGTTAAATTCCAGGGTCTCAGATG
EPCAM	Epithelial cell adhesion molecule	NM_002354.1	AGAAGAGCAAAACCTGAAGGGGCCCTCCAGAACA ATGATGGGCTTTATGATCCTGACTGCGATGAGAGC GGGCTCTTTAAGGCCAAGCAGTGCAACGGCA
EPHA3	EPH receptor A3	NM_005233.5	GAGGCCGGAAAGATGTTACCTTCAACATCATATGT AAAAAATGTGGGTGGAATATAAAACAGTGTGAGC CATGCAGCCCAAATGTCCGCTTCCTCCCTCG
FAM169A	Family with sequence similarity 169, member A	NM_015566.2	AACTTGAAGACGTGCCATTTTCACAGAATGCAGGA CAGAAGAATCAGTCAGAGGAGCAGTCTGAAGCAT CTTCCGAGCAACTGGATCAGTTTACACAATC
FAT1	FAT atypical cadherin 1	NM_005245.3	ACCCAACCAGTGGTGTGATAGTGTTAACTGGTAGA CTTGATTACCTAGAGACCAAGCTCTATGAGATGGA AATCCTCGCTGCGGACCGTGGCATGAAGTT
FBN1	Fibrillin 1	NM_000138.3	CACTGAAGGCAGCTTCAAATGTCTGTGTCCAGAAG GGTTTTCCTTGTCCTCCAGTGGAAGAAGGTGCCAA GATTTGCGAATGAGCTACTGTTATGCGAAG
GPRC5B	G protein-coupled receptor, class C, group 5, member B	NM_016235.1	GCCCTCTGGGTGATGAAGTGACCATCACATTTGGA AAGTGATCAACCACTGTTCCTTCTATGGGGCTCTTG CTCTAATGTCTATGGTGAGAACACAGGCC
GSN	Gelsolin	NM_000177.4	GATGGGAAAATCTTTGTCTGGAAAGGCAAGCAGGC AAACACGGAGGAGAGGAAGGCTGCCCTCAAAACA GCCTCTGACTTCATCACCAAGATGGACTACC
HEPH	Hephaestin	NM_138737.3	CCAGCGTGCCTCACCTGGATCTACCATTCTCATGTA GATGCTCCACGAGACATTGCAACTGGCCTAATTGG GCCTCTCATCACCTGTAAAAGAGGAGCCC
IGFBP7	Insulin-like growth factor binding protein 7	NM_001553.1	CCCAGAAAAGCATGAAGTAACTGGCTGGGTGCTGG TATCTCCTCTAAGTAAGGAAGATGCTGGAGAATAT GAGTGCCATGCATCCAATTCCCAAGGACAG
ITGBL1	Integrin, beta-like 1	NM_004791.1	GGTATATTTCTGGGGAGTTCTGTGACTGTGATGAC AGAGACTGCGACAAACATGATGGTCTCATTTGTAC AGGGAATGGAATATGTAGCTGTGGAAACTG

JAG1	Jagged 1	NM_000214.2	TTGCTTGTGGAGGCGTGGGATTCCAGTAATGACAC CGTTCAACCTGACAGTATTATTGAAAAGGCTTCTC ACTCGGGCATGATCAACCCCAGCCGGCAGT
KRT7	Keratin 7	NM_005556.3	GGGAACCATGGGCAGCAATGCCCTGAGCTTCTCCA GCAGTGCGGGTCCTGGGCTCCTGAAGGCTTATTCC ATCCGGACCGCATCCGCCAGTCGCAGGAGT
LAMB1	Laminin, beta 1	NM_002291.2	TTGCCAGGAGCTGCTACCAAGATCCTGTTACTTTAC AGCTTGCCTGTGTTTGTGATCCTGGATACATTGGTT CCAGATGTGACGACTGTGCCTCAGGATA
LTBP2	Latent transforming growth factor beta binding protein 2	NM_001401.3	CCTAATGGCTAATCTGGCTGCTGCAGACTTCTTTGC TGGGTTGGCCTACTTCTATCTCATGTTCAACACAGG ACCCAATACTCGGAGACTGACTGTTAGC
LUM	Lumican	NM_000428.2	CATCTCTCCCAGCTTAGCCTCTGGCTGTAAGCTTCG GTCATTGCCTCCATGCCCTTGCTTGGCTCAAGCACC ACCAATCGCTTTAATGCTTCAGCCACCG
MAP1B	Microtubule-associated protein 1B	NM_002345.3	GCCATTATCCTACTCCAAGATCAAGCATTTGCGTTT GGATGGCAATCGCATCTCAGAAACCAGTCTTCCAC CGGATATGTATGAATGTCTACGTGTTGCT
MAP2	Microtubule-associated protein 2	NM_005909.3	CATATAGGATTATAGATACTTAAAGGAACACGTGG GTGAGCGTGTGTGGGGGTACTAGAAGCTGATCTGA TTGGTCCAACAGTTTGATGCTGAGTCATGC
MOXD1	Monooxygenase, DBH-like 1	NM_001031699.1	GATGCATTCCTCACCTGTGAAACTGTGATTTTTGCC TGGGCTATTGGTGGAGAGGGCTTTTCTTATCCACCT CATGTTGGATTATCCCTTGGCACTCCAT
NALCN	Sodium leak channel, non-selective	NM_052867.2	TGGACGTGATCGTGGCGGCTAGCAACTACTACAAA GGAGAAAACTTCAGGAGGCAGTACGACGAGTTCT ACCTGGCGGAGGTGGCTTTTACAGTACTTTT
NAV3	Neuron navigator 3	NM_014903.4	CCAGCACTTCTTCTCTTTACTCTACAGCTGAAGAAA AGGCTCATTCAGAGCAAATCCATAAACTGCGGAGA GAGCTGGTTGCATCACAAGAAAAAGTTGC
RCAN2	Regulator of calcineurin 2	NM_005822.3	GTGTCCTCTAGTGGAAGAAATAGTAGGCTCCGCTA TTCAGATGCAGAGCACTGCAGCATCCAGCCTTTCA AAGCTGACTCTTCTCAATCATCTGTGGGTC

SH3YL1	SH3 and SYLF domain containing 1	NM_001159597.1	AAAGGCCTTGCAATTCTGTCTGTGATCAAAGCCGG GTTCCTGGTGACTGCCAGAGGAGGCAGCGGGATTG TAGTGGCGCGCCTTCCAGATGGAAAATGGT
SLC38A1	Solute carrier family 38, member 1	NM_001077484.1	TCTATGACAACGTGCAGTCCGACCTCCTTCACAAA TATCAGAGTAAAGATGACATTCTCATCCTGACAGT GCGGCTGGCTGTCATTGTTGCTGTGATCCT
SOX9	SRY (sex determining region Y)-box 9	NM_000346.2	CAGTGGCCAGGCCAACCTTGGCTAAATGGAGCAGC GAAATCAACGAGAAACTGGACTTTTTAAACCCTCT TCAGAGCAAGCGTGGAGGATGATGGAGAAT
THBS2	Thrombospondin 2	NM_003247.2	AAACATCCTTGCAAATGGGTGTGACGCGGTTCCAG ATGTGGATTTGGCAAAACCTCATTTAAGTAAAAGG TTAGCAGAGCAAAGTGCGGTGCTTTAGCTG
TMEM200A	Transmembrane protein 200A	NM_052913.2	CCTTGTGGTTCCTTTGCCCAACACCAGTGAATCCTT CCAGCCCGTCAGCACAGTGCTACCAAGGAATAATT CCATTGGGGAGTCGTTGTCGAGTCAGTAC
B2M*	Beta-2-microglobulin	NM_004048.2	CGGGCATTCCTGAAGCTGACAGCATTCGGGCCGAG ATGTCTCGCTCCGTGGCCTTAGCTGTGCTCGCGCTA CTCTCTCTTTCTGGCCTGGAGGCTATCCA
LDHA*	Lactate dehydrogenase A	NM_001165414.1	AACTTCCTGGCTCCTTCACTGAACATGCCTAGTCCA ACATTTTTTCCCAGTGAGTCACATCCTGGGATCCAG TGTATAAATCCAATATCATGTCTTGTGC
SNX17*	Sorting nexin 17	NM_014748.2	CTTTCCTTGTCCCCTGGGCTGGCTGCACAGAGGATT GCCCCTTCTCTTTTCAGAGCTGGCCCTCGATGCCAA ATTAGCATTTAGTATTTTGCACAAAGTC
TBP*	TATA box binding protein	NM_001172085.1	ACAGTGAATCTTGGTTGTAAACTTGACCTAAAGAC CATTGCACTTCGTGCCCGAAACGCCGAATATAATC CCAAGCGGTTTGCTGCGGTAATCATGAGGA

* Housekeeping gene.

Table 4.2. Patient characteristics

Characteristics	Edmonton (n=62)	Toronto (n=60)	p-value
Recipient age at transplantation (year), median (IQR)	54.9 (50.9-58.2)	58.1 (51.7-60.8)	0.10
Recipient male, n (%)	47 (75.8)	43 (71.7)	0.68
Donor age (year), median (IQR)	45.3 (27.3-53.8)	39.8 (25.1-54.0)[A]	0.42
Donor male, n (%)	32 (51.6)	32 (55.2)[B]	0.86
Early biopsy			
Time from transplantation (day), median (IQR)	183 (143-256)	182 (171-187)	0.59
Log10 HCV RNA at biopsy (IU/mL), median (IQR)	6.8 (6.2-7.3)[C]	NA	NA
Acute cellular rejection, n (%)	13 (21.0)	NA	NA
Metavir activity score, n (%)		NA	NA
0	5 (8.1)		
1	41 (66.1)		
2	15 (24.2)		
3	1 (1.6)		
Metavir fibrosis stage, n (%)			0.12
0	19 (30.6)	22 (36.7)	
1	31 (50.0)	33 (55.0)	
2	12 (19.4)	4 (6.7)	
3	0 (0)	1 (1.7)	
4	0 (0)	0 (0)	
Late biopsy			
Time from transplantation (day), median (IQR)	727 (441-1208)	1141 (737-1454)	<0.001
Log10 HCV RNA at biopsy (IU/mL), median (IQR)	5.5 (0.0-6.8)[D]	NA	NA
Acute cellular rejection, n (%)	6 (9.7)	NA	NA
Metavir activity score, n (%)		NA	NA
0	6 (9.7)		
1	37 (59.7)		
2	14 (22.6)		
3	5 (8.1)		

Metavir fibrosis stage, n (%)			0.09
0	8 (12.9)	1 (1.7)	
1	21 (33.9)	23 (38.3)	
2	23 (37.1)	28 (46.7)	
3	8 (12.9)	4 (6.7)	
4	2 (3.2)	4 (6.7)	
Progress to adverse outcomes, n (%)	26 (41.9)	8 (13.3)	0.001
Follow-up period (year), median (IQR)	8.4 (5.2-11.7)	3.1 (2.0-4.0)	<0.001
Immunosuppressive therapy, n (%)			
Tacrolimus	54 (87.1)	17 (28.8)[A]	<0.001
Prednisone	28 (45.2)	60 (100)	<0.001
Mycophenolate	60 (96.8)	51 (85.0)	0.03
HCV genotype, n (%)			0.01
1	54 (87.0)	39 (65.0)	
Other	4 (6.5)	14 (23.3)	
Unknown	4 (6.5)	7 (11.7)	
HCV treatment, n (%)		NA	NA
Ribavirin	36 (58.1)		
Peginterferon	33 (53.2)		
Boceprevir	5 (8.1)		
Sofosbuvir and ledipasvir	25 (40.3)		
Response to HCV treatment, n (%)		NA	NA
Sustained virologic response	45 (72.6)		
Non-response	4 (6.5)		
Not treated	13 (21.0)		

IQR, interquartile range. NA, not available. Percentage might not add up to 100% because of rounding.
[A] Data was not available for 1 patient.
[B] Data was not available for 2 patients.
[C] Data was not available for 29 patients.
[D] Data was not available for 23 patients.

Table 4.3. Univariate and multivariate analyses of progression to adverse outcomes in 62 Edmonton patients (n=26 events)

Variable	HR	95% CI	p-value
Univariate analysis			
Recipient age at transplantation, year	1.09	1.00-1.19	**0.04**
Recipient gender			
Female (reference)	1.00		
Male	0.94	0.43-2.51	0.94
Donor age, year	1.06	1.03-1.09	**<0.001**
Donor gender			
Female (reference)	1.00		
Male	0.92	0.42-2.00	0.83
Tacrolimus			
No (reference)	1.00		
Yes	1.03	0.31-3.46	0.96
Prednisone			
No (reference)	1.00		
Yes	1.32	0.61-2.88	0.48
Mycophenolate			
No (reference)	1.00		
Yes	2.45	0.30-20.00	0.40
HCV genotype			
Other (reference)	1.00		
Genotype 1	0.56	0.13-2.43	0.44
Log10 HCV RNA at early biopsy[1]	1.16	0.66-2.03	0.60
HCV treatment			
No treatment (reference)	1.00		
Non-response	1.79	0.44-7.25	0.41
Sustained virologic response	0.37	0.14-0.995	**0.049**
Acute cellular rejection (early biopsy)			
No (reference)	1.00		
Yes	1.51	0.55-4.09	0.42

Metavir activity score (early biopsy)			
A0-A1 (reference)	1.00		
A2-A3	1.87	0.80-4.38	0.15
Metavir fibrosis stage (early biopsy)			
F0-F1 (reference)	1.00		
F2	4.40	1.89-10.20	**0.001**
48-gene signature (early biopsy)			
Low 48-gene signature (reference)	1.00		
High 48-gene signature	4.90	1.96-12.25	**0.001**
Multivariate analysis			
Model 1			
Recipient age at transplantation, year	1.07	0.99-1.14	0.08
Metavir fibrosis stage (early biopsy)			
F0-F1 (reference)	1.00		
F2	3.80	1.60-9.01	**0.002**
48-gene signature (early biopsy)			
Low 48-gene signature (reference)	1.00		
High 48-gene signature	4.83	1.91-12.20	**0.001**
Model 2			
Donor age, year	1.04	1.01-1.07	**0.005**
Metavir fibrosis stage (early biopsy)			
F0-F1 (reference)	1.00		
F2	2.31	0.91-5.85	0.08
48-gene signature (early biopsy)			
Low 48-gene signature (reference)	1.00		
High 48-gene signature	4.29	1.68-10.95	**0.002**
Model 3			
Recipient age at transplantation, year	1.07	0.99-1.15	0.08
Donor age, year	1.05	1.03-1.09	**<0.001**
48-gene signature (early biopsy)			
Low 48-gene signature (reference)	1.00		

High 48-gene signature	5.38	2.11-13.70	**<0.001**
Model 4			
Recipient age at transplantation, year	1.06	0.99-1.14	0.09
HCV treatment			
No treatment (reference)	1.00		
Non-response	1.17	0.29-4.77	0.82
Sustained virologic response	0.59	0.23-1.53	0.28
48-gene signature (early biopsy)			
Low 48-gene signature (reference)	1.00		
High 48-gene signature	4.45	1.74-11.40	**0.002**
Model 5			
Donor age, year	1.05	1.02-1.08	**0.001**
HCV treatment			
No treatment (reference)	1.00		
Non-response	1.13	0.28-4.58	0.87
Sustained virologic response	0.82	0.31-2.16	0.69
48-gene signature (early biopsy)			
Low 48-gene signature (reference)	1.00		
High 48-gene signature	4.53	1.75-11.70	**0.002**
Model 6			
HCV treatment			
No treatment (reference)	1.00		
Non-response	1.32	0.32-5.48	0.70
Sustained virologic response	0.69	0.26-1.81	0.44
Metavir fibrosis stage (early biopsy)			
F0-F1 (reference)	1.00		
F2	3.59	1.51-8.56	**0.004**
48-gene signature (early biopsy)			
Low 48-gene signature (reference)	1.00		
High 48-gene signature	4.12	1.60-10.64	**0.003**

[1] Analyzed in 33 patients with available data.

To avoid model over fitting, multivariate models were limited to three variables (number of events=26). In the multivariate analyses, the 48-gene signature was analyzed with all other significant variables in the univariate analyses.

Table 4.4. Multivariate analysis of progression to adverse outcomes including all variables with p<0.05 in univariate analyses

Variable	Multivariate analysis		
	HR	95% CI	p-value
Recipient age at transplantation, year	1.08	1.00-1.16	**0.048**
Donor age, year	1.05	1.01-1.08	**0.005**
HCV treatment			
No treatment (reference)	1.00		
Non-response	1.09	0.26-4.60	0.32
Sustained virologic response	0.61	0.23-1.62	0.91
Metavir fibrosis stage (early biopsy)			
F0-F1 (reference)	1.00		
F2	2.61	1.05-6.50	**0.04**
48-gene signature (early biopsy)			
Low 48-gene signature (reference)	1.00		
High 48-gene signature	4.47	1.70-11.78	**0.002**

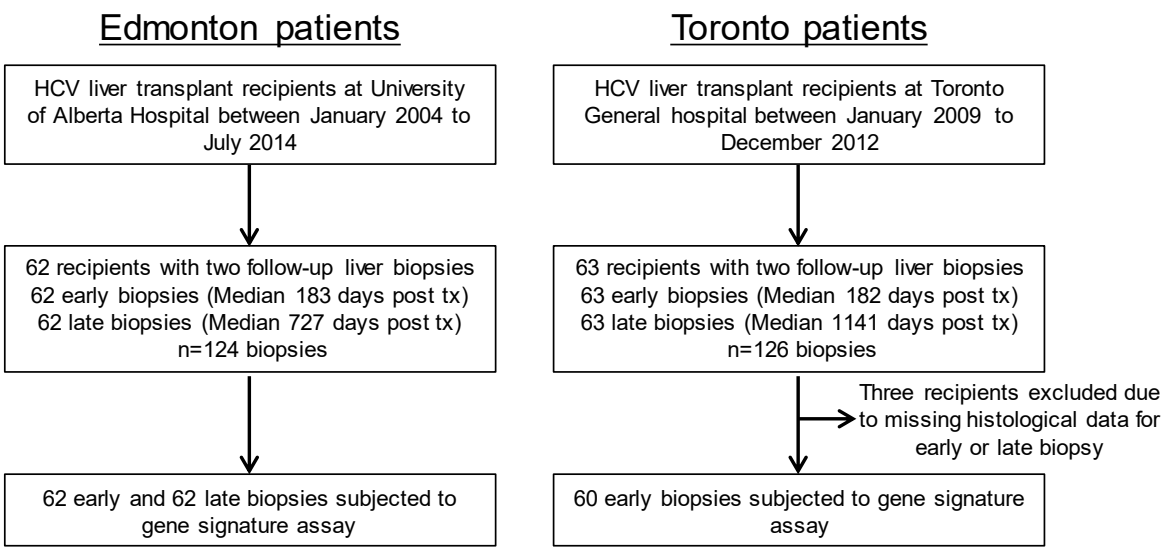

Figure 4.1. Study design.
Tx, transplant.

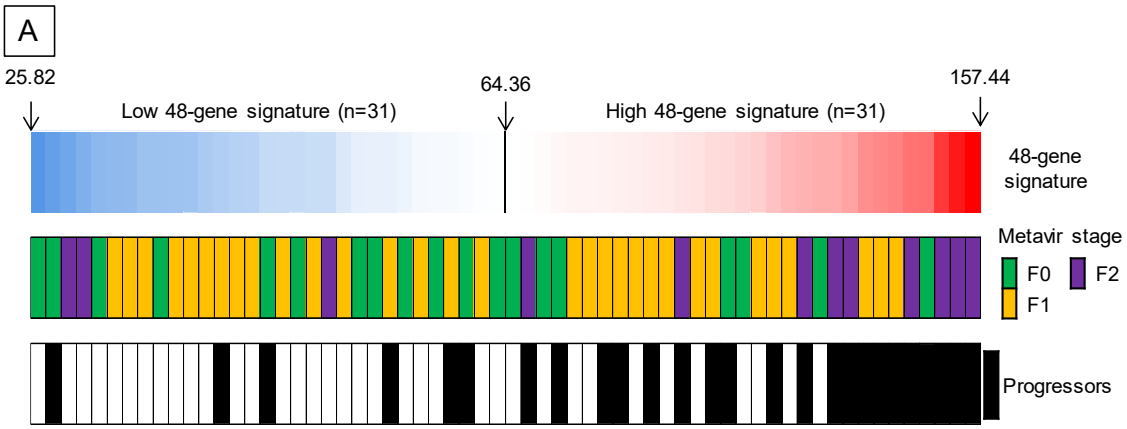

B

Fibrosis stage	48-gene signature	N of patients	N of non-progressors	N of progressors	P-value (Fisher exact test)
F0-F1	Low	28	22 (79%)	6 (21%)	0.040
	High	22	11 (50%)	11 (50%)	
F2	Low	3	3 (100%)	0 (0%)	0.005
	High	9	0 (0%)	9 (100%)	
F0-F2	Low	31	25 (81%)	6 (19%)	0.001
	High	31	11 (35%)	20 (65%)	

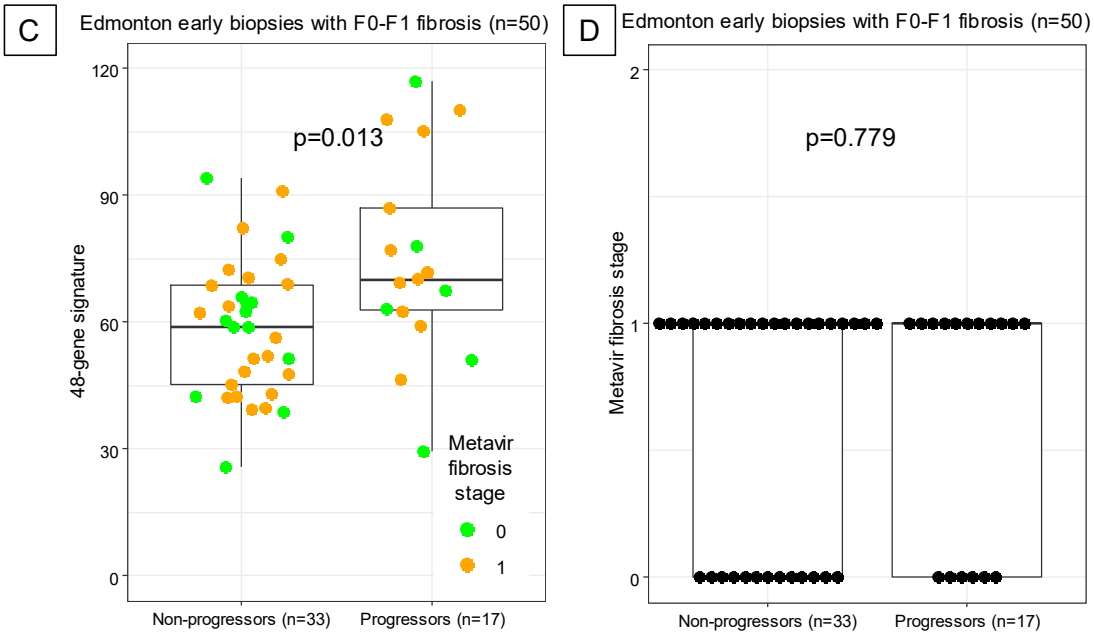

Figure 4.2. The distribution of the 48-gene signature and histological fibrosis stage in Edmonton early biopsies.

(A) Edmonton early biopsies were sorted based on the 48-gene signature from low (blue) to high (red). (B) Patients with high 48-gene signature had significantly higher probability of progression to adverse outcomes. (C) Progressors had significantly higher 48-gene signature compared to non-progressors in patients with F0 or F1 fibrosis. (D) Histological fibrosis stage was similar between progressors and non-progressors in patients with F0 or F1 fibrosis.

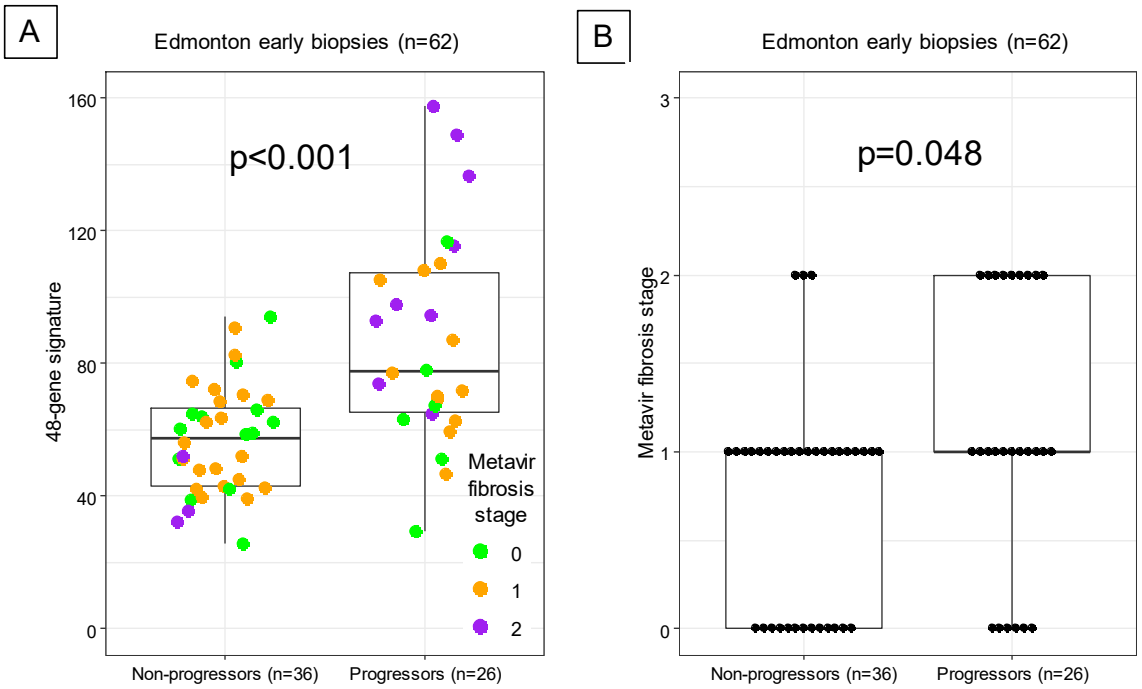

Figure 4.3. Edmonton progressors had significantly higher (A) 48-gene signature and (B) histological fibrosis stage in early biopsy compared to non-progressors.

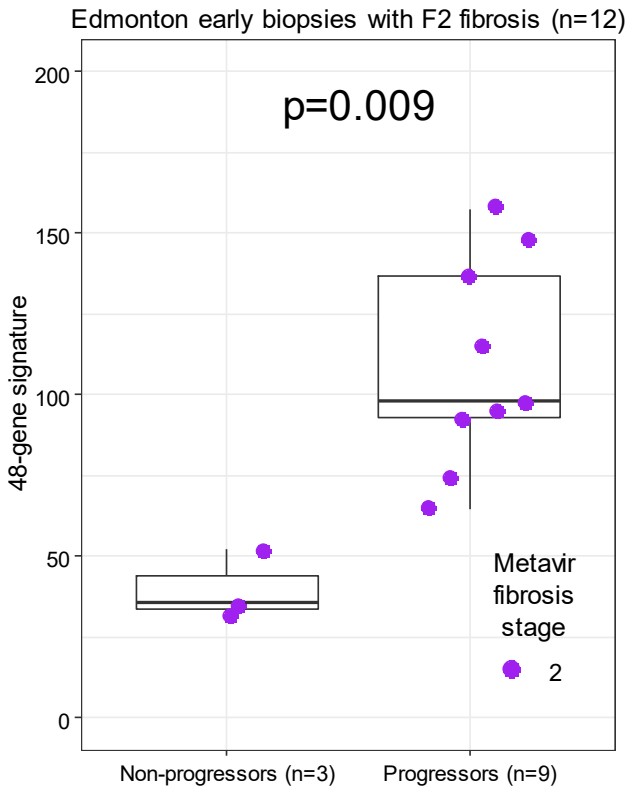

Figure 4.4. Of Edmonton patients with F2 fibrosis in early biopsy, progressors had significantly higher 48-gene signature compared to non-progressors.

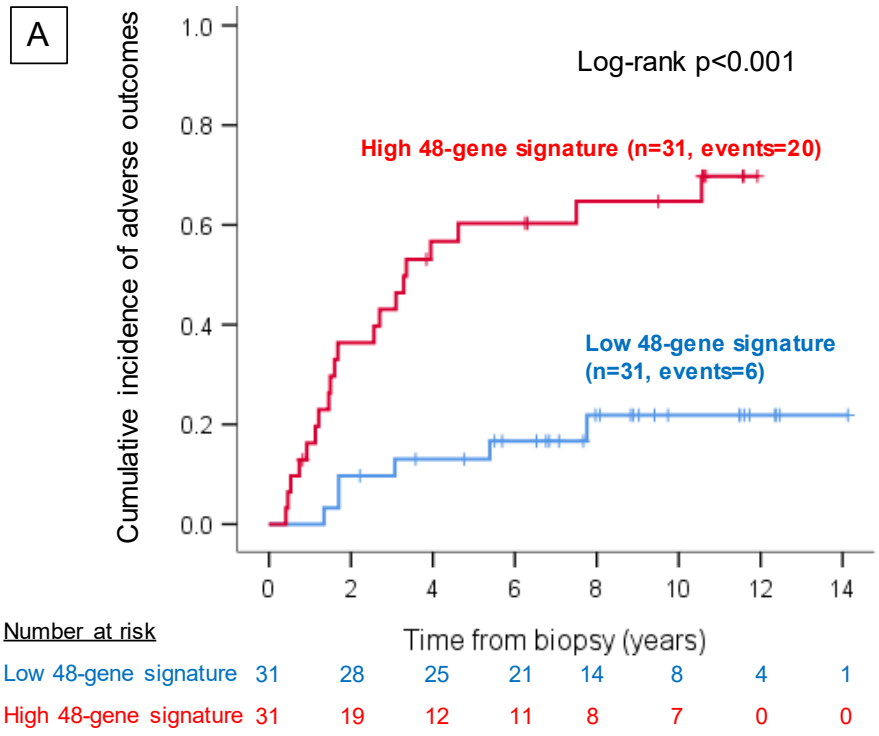

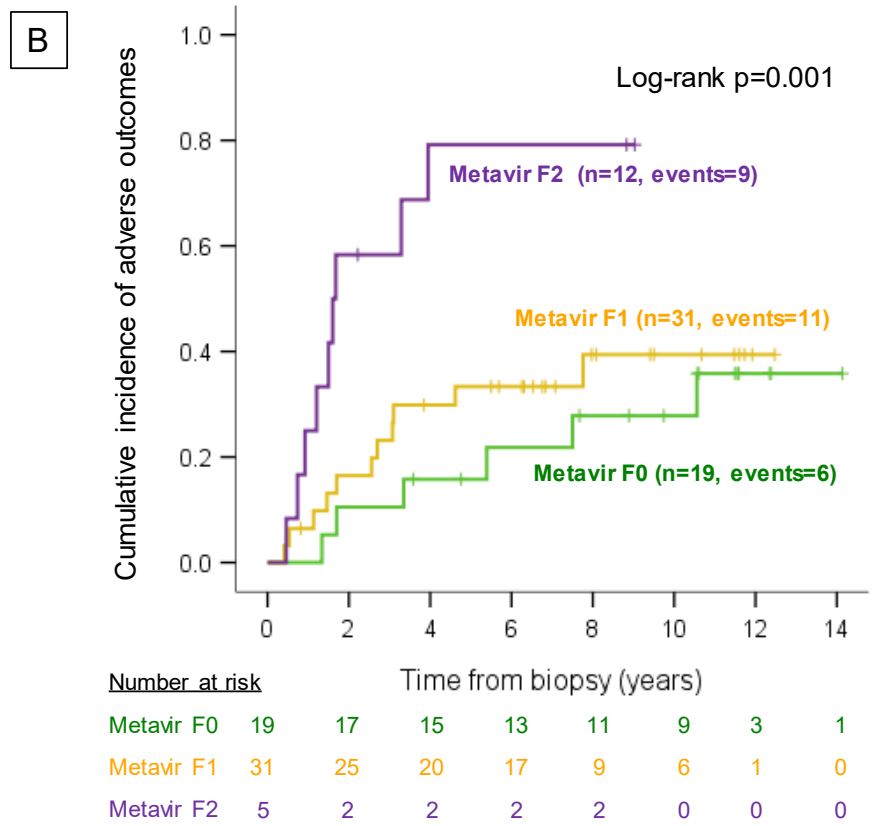

Figure 4.5. Cumulative incidence of adverse outcomes in Edmonton patients stratified by (A) the 48-gene signature and (B) histological fibrosis stage in early biopsy.

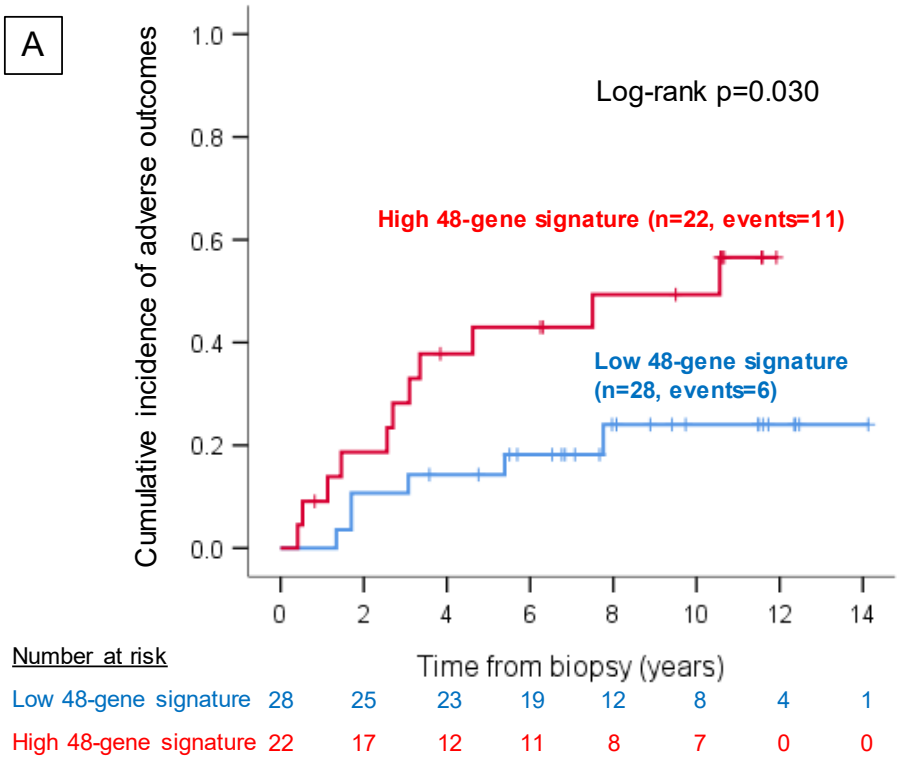

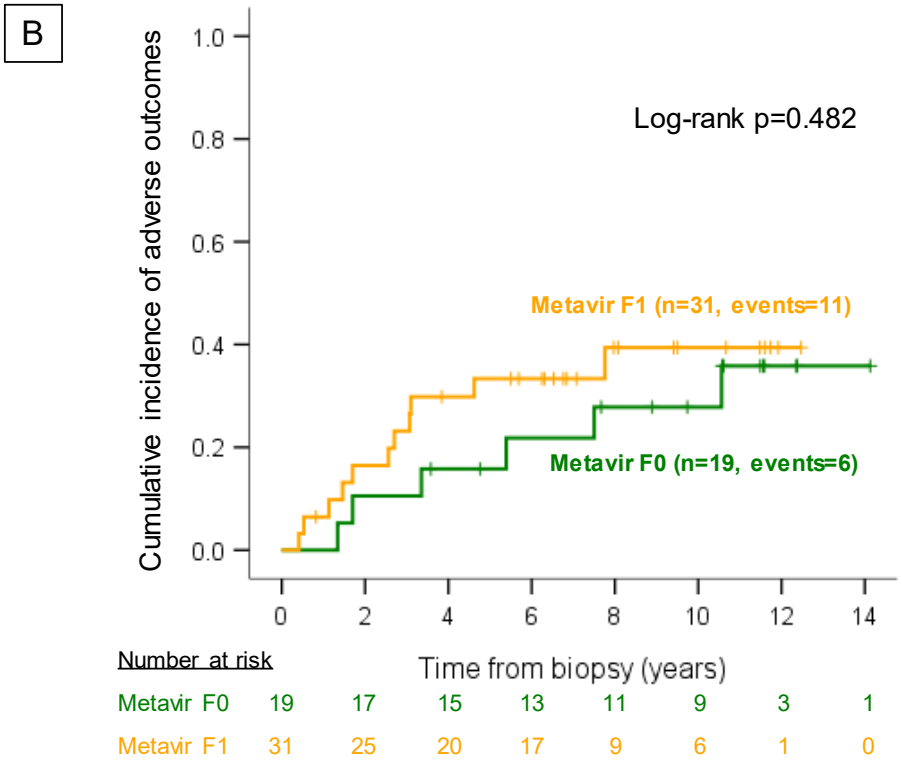

Figure 4.6. Cumulative incidence of adverse outcomes in Edmonton patients stratified by (A) the 48-gene signature and (B) histological fibrosis stage in early biopsy with F0 or F1 fibrosis.

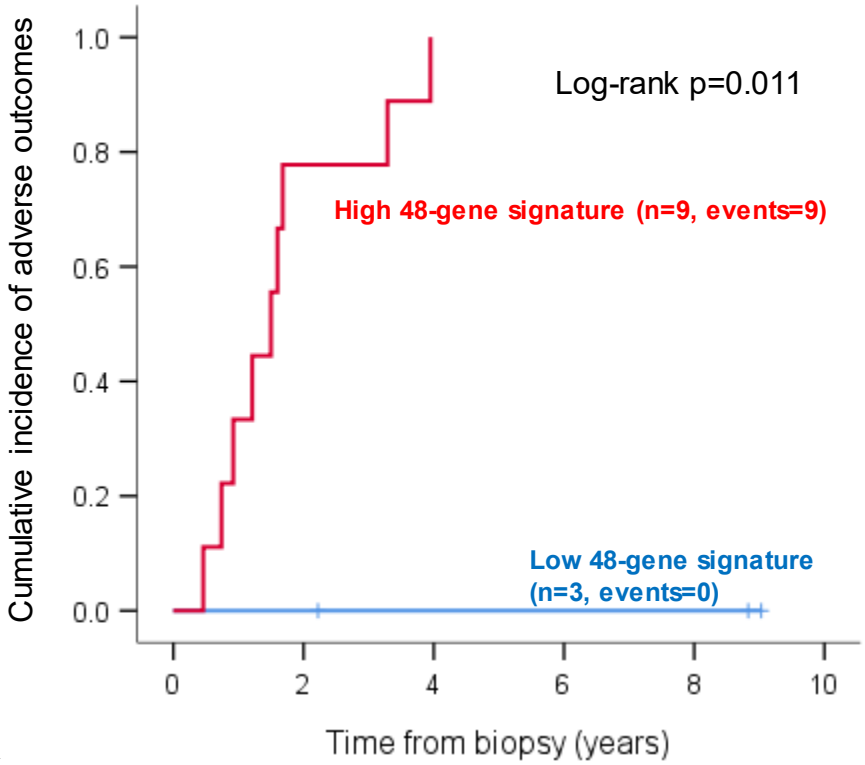

Number at risk						
Low 48-gene signature	3	3	2	2	2	0
High 48-gene signature	9	2	0	0	0	0

Figure 4.7. Cumulative incidence of adverse outcomes in Edmonton patients stratified by the 48-gene signature in early biopsy with F2 fibrosis.

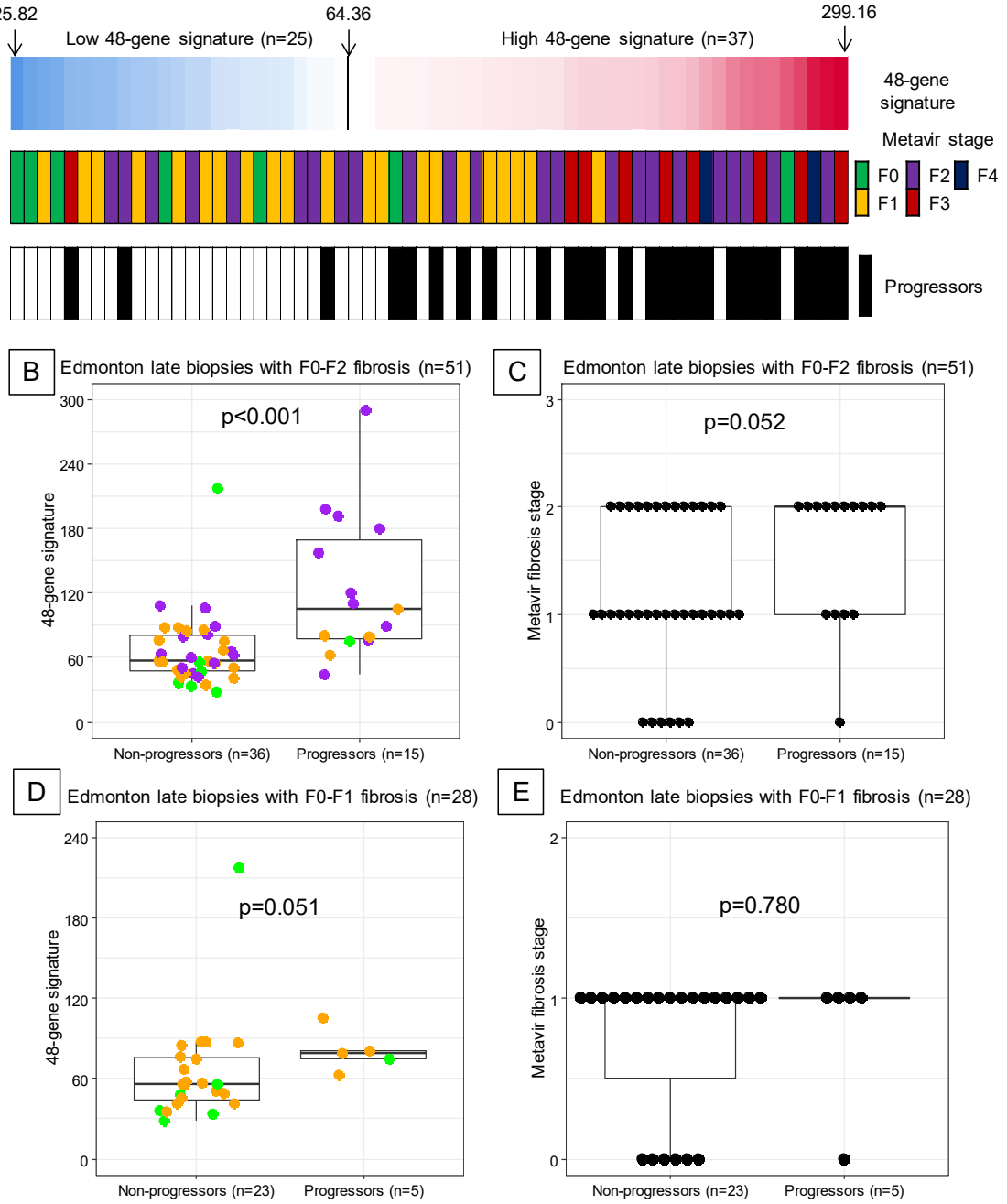

Figure 4.8. The distribution of the 48-gene signature and histological fibrosis stage in Edmonton late biopsies.

(A) Edmonton late biopsies were sorted based on the 48-gene signature from low (blue) to high (red). (B) Progressors had significantly higher 48-gene signature compared to non-progressors in patients with F0, F1, or F2 fibrosis. (C) Progressors had a marginally significantly higher histological fibrosis stage than non-progressors in patients with F0, F1, or F2 fibrosis. (D) Progressors had a maraginally significantly higher 48-gene signature compared to non-progressors in patients with F0 or F1 fibrosis. (E) Histological fibrosis stage was similar between progressors and non-progressors in patients with F0 or F1 fibrosis.

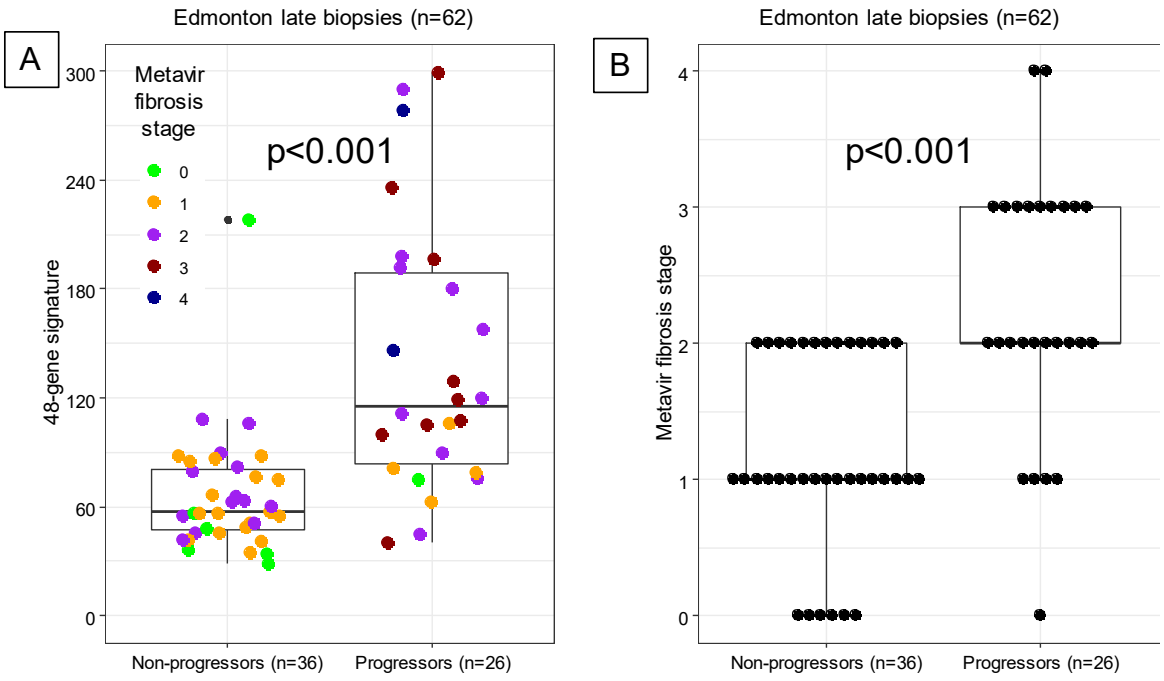

Figure 4.9. Edmonton progressors had significantly higher (A) 48-gene signature and (B) histological fibrosis stage in late biopsy compared to non-progressors.

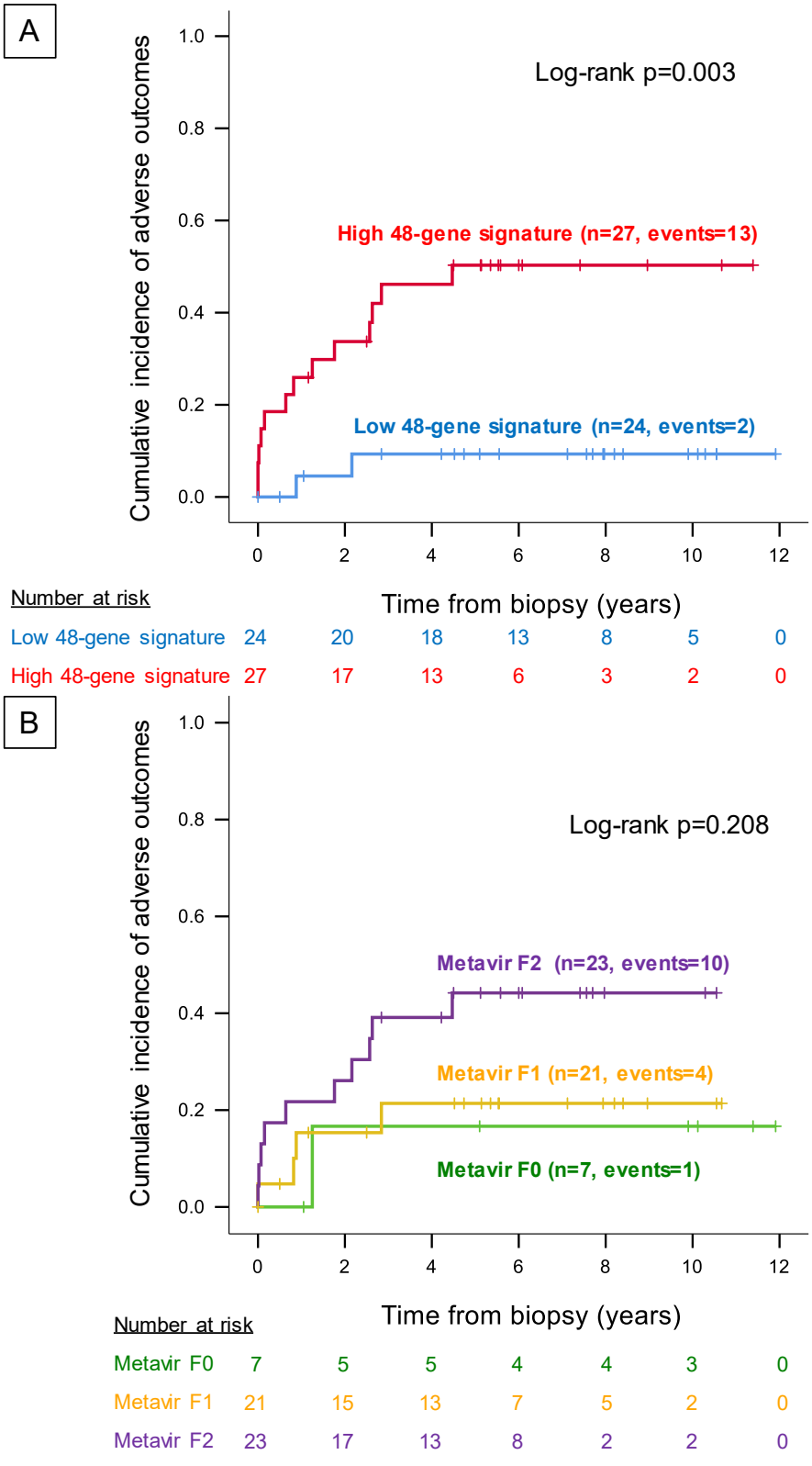

Figure 4.10. Cumulative incidence of adverse outcomes in Edmonton patients stratified by (A) the 48-gene signature and (B) histological fibrosis stage in late biopsy without advanced fibrosis.

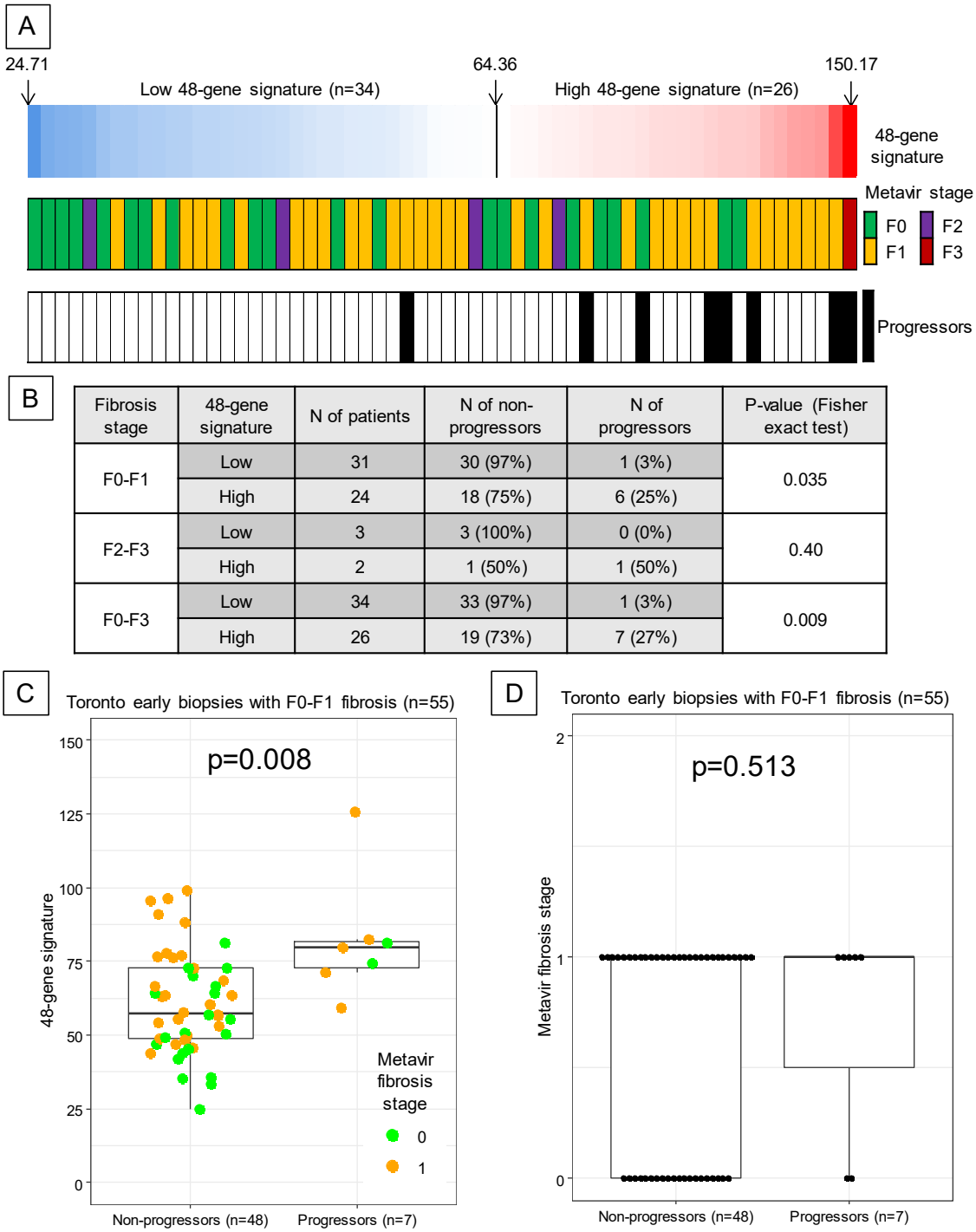

Fibrosis stage	48-gene signature	N of patients	N of non-progressors	N of progressors	P-value (Fisher exact test)
F0-F1	Low	31	30 (97%)	1 (3%)	0.035
	High	24	18 (75%)	6 (25%)	
F2-F3	Low	3	3 (100%)	0 (0%)	0.40
	High	2	1 (50%)	1 (50%)	
F0-F3	Low	34	33 (97%)	1 (3%)	0.009
	High	26	19 (73%)	7 (27%)	

Figure 4.11. The distribution of the 48-gene signature and histological fibrosis stage in Toronto early biopsies.

(A) Toronto early biopsies were sorted based on the 48-gene signature from low (blue) to high (red). (B) Patients with high 48-gene signature had significantly higher probability of progression to adverse outcomes. (C) Progressors had significantly higher 48-gene signature compared to non-progressors in patients with F0 or F1 fibrosis. (D) Histological fibrosis stage was similar between progressors and non-progressors in patients with F0 or F1 fibrosis.

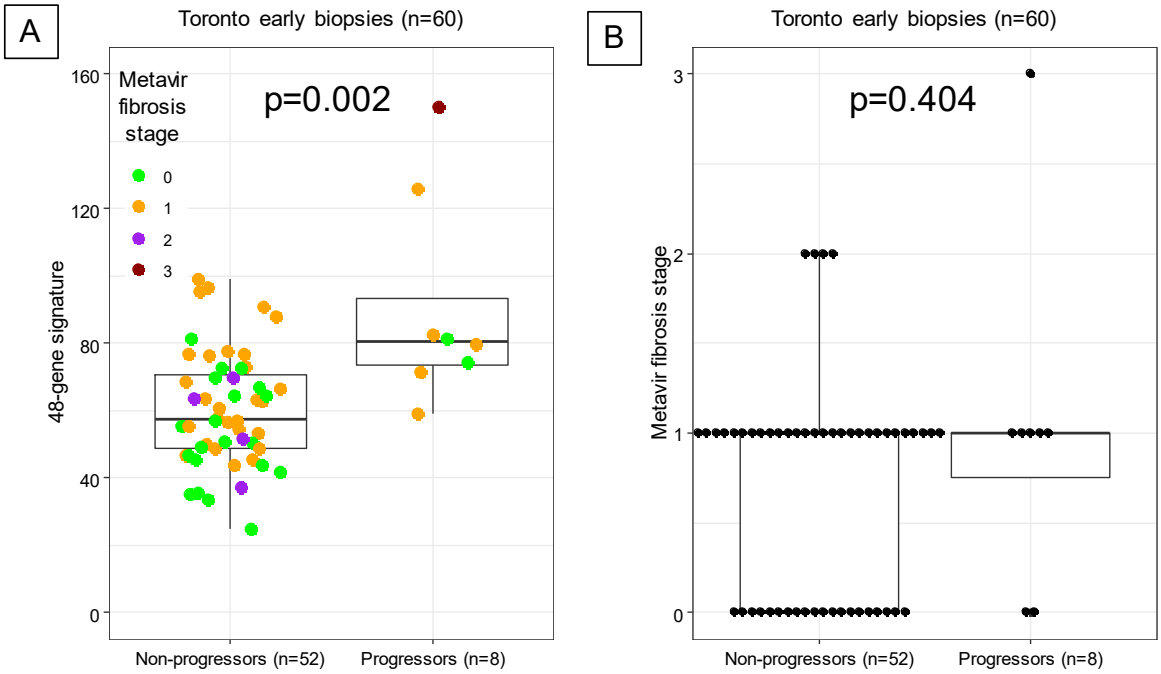

Figure 4.12. Toronto progressors had significantly higher (A) 48-gene signature, but similar (B) histological fibrosis stage in early biopsy compared to non-progressors.

4.5 – References

1. Younossi ZM, Koenig AB, Abdelatif D, Fazel Y, Henry L, Wymer M. Global epidemiology of nonalcoholic fatty liver disease-Meta-analytic assessment of prevalence, incidence, and outcomes. Hepatology 2016 Jul;64(1):73-84.
2. Schweitzer A, Horn J, Mikolajczyk RT, Krause G, Ott JJ. Estimations of worldwide prevalence of chronic hepatitis B virus infection: a systematic review of data published between 1965 and 2013. Lancet 2015 Oct 17;386(10003):1546-1555.
3. El-Serag HB. Epidemiology of viral hepatitis and hepatocellular carcinoma. Gastroenterology 2012 May;142(6):1264-1273.
4. Younossi ZM, Stepanova M, Afendy M, Fang Y, Younossi Y, Mir H, et al. Changes in the prevalence of the most common causes of chronic liver diseases in the United States from 1988 to 2008. Clin Gastroenterol Hepatol 2011 Jun;9(6):524-530.
5. Pellicoro A, Ramachandran P, Iredale JP, Fallowfield JA. Liver fibrosis and repair: immune regulation of wound healing in a solid organ. Nat Rev Immunol 2014 Mar;14(3):181-194.
6. Bataller R, Brenner DA. Liver fibrosis. J Clin Invest 2005 Feb;115(2):209-218.
7. Chalasani N, Younossi Z, Lavine JE, Charlton M, Cusi K, Rinella M, et al. The diagnosis and management of nonalcoholic fatty liver disease: Practice guidance from the American Association for the Study of Liver Diseases. Hepatology 2018 Jan;67(1):328-357.

8. Williams R, Aspinall R, Bellis M, Camps-Walsh G, Cramp M, Dhawan A, et al. Addressing liver disease in the UK: a blueprint for attaining excellence in health care and reducing premature mortality from lifestyle issues of excess consumption of alcohol, obesity, and viral hepatitis. Lancet 2014 Nov 29;384(9958):1953-1997.

9. Poynard T, Mathurin P, Lai CL, Guyader D, Poupon R, Tainturier MH, et al. A comparison of fibrosis progression in chronic liver diseases. J Hepatol 2003 Mar;38(3):257-265.

10. EASL Clinical Practice Guidelines: Management of alcohol-related liver disease. J Hepatol 2018 Jul;69(1):154-181.

11. Calzadilla BL, Adams LA. The Natural Course of Non-Alcoholic Fatty Liver Disease. Int J Mol Sci 2016 May 20;17(5).

12. Berenguer J, Zamora FX, Aldamiz-Echevarria T, Von Wichmann MA, Crespo M, Lopez-Aldeguer J, et al. Comparison of the prognostic value of liver biopsy and FIB-4 index in patients coinfected with HIV and hepatitis C virus. Clin Infect Dis 2015 Mar 15;60(6):950-958.

13. EASL-ALEH Clinical Practice Guidelines: Non-invasive tests for evaluation of liver disease severity and prognosis. J Hepatol 2015 Jul;63(1):237-264.

14. Hold GL, Untiveros P, Saunders KA, El-Omar EM. Role of host genetics in fibrosis. Fibrogenesis Tissue Repair 2009 Dec 4;2(1):6.

15. Smith MW, Walters KA, Korth MJ, Fitzgibbon M, Proll S, Thompson JC, et al. Gene expression patterns that correlate with hepatitis C and early progression to fibrosis in liver transplant recipients. Gastroenterology 2006 Jan;130(1):179-187.

16. Asselah T, Bieche I, Laurendeau I, Paradis V, Vidaud D, Degott C, et al. Liver gene expression signature of mild fibrosis in patients with chronic hepatitis C. Gastroenterology 2005 Dec;129(6):2064-2075.

17. Yoshida EM, Sulkowski MS, Gane EJ, Herring RW, Jr., Ratziu V, Ding X, et al. Concordance of sustained virological response 4, 12, and 24 weeks post-treatment with sofosbuvir-containing regimens for hepatitis C virus. Hepatology 2015 Jan;61(1):41-45.

18. Bedossa P, Poynard T. An algorithm for the grading of activity in chronic hepatitis C. The METAVIR Cooperative Study Group. Hepatology 1996 Aug;24(2):289-293.

19. Zeremski M, Dimova RB, Pillardy J, de Jong YP, Jacobson IM, Talal AH. Fibrosis Progression in Patients With Chronic Hepatitis C Virus Infection. J Infect Dis 2016 Oct 15;214(8):1164-1170.

20. Beckebaum S, Iacob S, Klein CG, Dechene A, Varghese J, Baba HA, et al. Assessment of allograft fibrosis by transient elastography and noninvasive biomarker scoring systems in liver transplant patients. Transplantation 2010 Apr 27;89(8):983-993.

21. Lens S, Torres F, Puigvehi M, Marino Z, Londono MC, Martinez SM, et al. Predicting the development of liver cirrhosis by simple modelling in patients with chronic hepatitis C. Aliment Pharmacol Ther 2016 Feb;43(3):364-374.

22. Manousou P, Burroughs AK, Tsochatzis E, Isgro G, Hall A, Green A, et al. Digital image analysis of collagen assessment of progression of fibrosis in recurrent HCV after liver transplantation. J Hepatol 2013 May;58(5):962-968.

23. Friedman LS. Surgery in the patient with liver disease. Trans Am Clin Climatol Assoc 2010;121:192-204.

24. Angulo P, Kleiner DE, Dam-Larsen S, Adams LA, Bjornsson ES, Charatcharoenwitthaya P, et al. Liver Fibrosis, but No Other Histologic Features, Is Associated With Long-term Outcomes of Patients With Nonalcoholic Fatty Liver Disease. Gastroenterology 2015 Aug;149(2):389-397.

25. Harrison SA, Abdelmalek MF, Caldwell S, Shiffman ML, Diehl AM, Ghalib R, et al. Simtuzumab Is Ineffective for Patients With Bridging Fibrosis or Compensated Cirrhosis Caused by Nonalcoholic Steatohepatitis. Gastroenterology 2018 Oct;155(4):1140-1153.

26. Meissner EG, McLaughlin M, Matthews L, Gharib AM, Wood BJ, Levy E, et al. Simtuzumab treatment of advanced liver fibrosis in HIV and HCV-infected adults: results of a 6-month open-label safety trial. Liver Int 2016 Dec;36(12):1783-1792.

27. Mauro E, Crespo G, Montironi C, Londono MC, Hernandez-Gea V, Ruiz P, et al. Portal pressure and liver stiffness measurements in the prediction of fibrosis regression after sustained virological response in recurrent hepatitis C. Hepatology 2018 May;67(5):1683-1694.

28. Caillot F, Hiron M, Goria O, Gueudin M, Francois A, Scotte M, et al. Novel serum markers of fibrosis progression for the follow-up of hepatitis C virus-infected patients. Am J Pathol 2009 Jul;175(1):46-53.

29. Caillot F, Derambure C, Bioulac-Sage P, Francois A, Scotte M, Goria O, et al. Transient and etiology-related transcription regulation in cirrhosis prior to

hepatocellular carcinoma occurrence. World J Gastroenterol 2009 Jan 21;15(3):300-309.

30. Moylan CA, Pang H, Dellinger A, Suzuki A, Garrett ME, Guy CD, et al. Hepatic gene expression profiles differentiate presymptomatic patients with mild versus severe nonalcoholic fatty liver disease. Hepatology 2014 Feb;59(2):471-482.

31. Bourd-Boittin K, Bonnier D, Leyme A, Mari B, Tuffery P, Samson M, et al. Protease profiling of liver fibrosis reveals the ADAM metallopeptidase with thrombospondin type 1 motif, 1 as a central activator of transforming growth factor beta. Hepatology 2011 Dec;54(6):2173-2184.

32. Ahmad W, Ijaz B, Hassan S. Gene expression profiling of HCV genotype 3a initial liver fibrosis and cirrhosis patients using microarray. J Transl Med 2012;10:41.

33. Munshaw S, Hwang HS, Torbenson M, Quinn J, Hansen KD, Astemborski J, et al. Laser captured hepatocytes show association of butyrylcholinesterase gene loss and fibrosis progression in hepatitis C-infected drug users. Hepatology 2012 Aug;56(2):544-554.

34. Marcolongo M, Young B, Dal PF, Fattovich G, Peraro L, Guido M, et al. A seven-gene signature (cirrhosis risk score) predicts liver fibrosis progression in patients with initially mild chronic hepatitis C. Hepatology 2009 Oct;50(4):1038-1044.

35. Berenguer M, Schuppan D. Progression of liver fibrosis in post-transplant hepatitis C: mechanisms, assessment and treatment. J Hepatol 2013 May;58(5):1028-1041.

36. Nasr P, Ignatova S, Kechagias S, Ekstedt M. Natural history of nonalcoholic fatty liver disease: A prospective follow-up study with serial biopsies. Hepatol Commun 2018 Feb;2(2):199-210.

Chapter 5: A 48-gene Signature in Clinical Liver Biopsies Enables Early Prediction of Progression to Cirrhosis in Patients with Autoimmune Hepatitis at Disease Onset

5.1 – Introduction

Autoimmune hepatitis (AIH) is a complex and heterogeneous chronic inflammatory liver disease characterized by high serum immunoglobulin G (IgG) level, positivity for circulating autoantibodies, interface hepatitis on liver histology, and response to immunosuppressive treatment (1). Despite immunosuppressive treatment induce clinical, laboratory, and histological improvement for most patients, cirrhosis still develops in up to 40% of treated patients (2). As cirrhosis leads to poor clinical outcomes, early diagnosis and prevention of cirrhosis is important (3). Previous research identified risk factors of fibrosis progression in AIH, such as presence of human leukocyte antigen DR3 and higher histology activity index (4). However, no single clinical variable can reliably predict who is at high-risk for progression to cirrhosis and poor clinical outcomes at disease onset.

Histopathology assessment of liver biopsy at disease onset is considered prerequisite to assess AIH disease severity in order to guide treatment decisions, but it cannot provide risk stratification for progression to cirrhosis (5). Since AIH had a huge disease heterogeneity, this limitation made identifying high-risk patients for tailored treatment challenging and caused a wide variation of immunosuppressive treatment regimens in clinical practice (1, 6, 7). Progression to cirrhosis is present in 3% of patients with treatment per year and even happens in patients with complete treatment response (4, 8, 9). This indicated that currently there is no confident clinical indices to identify patients who are at high-risk for progression to cirrhosis. Moreover, the benefits of treatment for mild, asymptomatic AIH (alanine aminotransferase [ALT] < 3x upper limit of normal [ULN], histological activity index <4, and absence of advanced fibrosis) are currently debated, as the risk vs. benefit of

immunosuppression treatment for these patients is not clear (1, 7, 10). Due to these circumstances, there is an urgent clinical need for a surrogate biomarker to identify high-risk patients for progression to cirrhosis. The surrogate biomarker can help guide personalized treatment regimens that is of greatest efficacy and lowest burden to patients.

Increasing evidence indicates that genetic factors have a major influence on fibrosis progression, but less is known of the relationship between fibrosis progression and gene expression alterations in patients with AIH (11). Previous studies showed mRNA expression of several fibrosis genes can predict fibrosis progression (12, 13). However, these findings were mostly conducted in other chronic liver diseases and have not been confirmed if these genes were applicable in patients with AIH (12, 13). In Chapter 2, I identified and validated a common 48-gene signature that had over 93% of accuracy for advanced liver fibrosis, independent of etiologies, by microarray based whole genome transcriptomics. In this chapter, I aim to analyze if the 48-gene signature can predict progression to cirrhosis, liver decompensation, and liver-related death.

5.2 – Materials and Methods

5.2.1 – Patients

This chapter retrospectively included 78 patients diagnosed with probable or definitive AIH (defined by the International Autoimmune Hepatitis Group) and had a liver biopsy at disease onset between 1997 and 2016 at University of Alberta, Edmonton, Canada (Figure 5.1) (14). This study was approved by the institutional review board of the University of Alberta.

5.2.2 – Clinical and laboratory assessments

Baseline factors evaluated in this chapter include gender, age, biochemical and serological markers, body mass index (BMI), liver enzymes, albumin levels, bilirubin levels, platelet counts, IgG levels, international normalized ratio (INR), and model of end-stage liver disease (MELD) score.

5.2.3 – Histopathological assessment

Histopathological assessment of representative stained slides were scored according to the Metavir classification system for activity grading (scale 0-3) and fibrosis staging (scale 0-4) (15).

5.2.4 – Treatment and response

Patients were treated with prednisone or a combination of prednisone and azathioprine according to the international guidelines (1). Treatment responses were assessed every month until laboratory resolution, and then at 6-month interval. Complete response was defined as normalization of serum ALT, AST, and IgG levels. Incomplete response was defined as improvement of serum ALT or AST levels to 1–3 ULN or worsening serum ALT and AST during treatment. Relapse was defined as an increase in serum AST level to more than three-fold ULN with or without the reappearance of symptoms after discontinuation of the medication.

5.2.5 – RNA isolation

Three to eight consecutive 20-µm sections were obtained from each FFPE block with

equipment sterilization with RNase away reagent (Ambion, Carlsbad, CA) and microtome blade replacement between blocks. Sections were then immediately placed into sterile 1.5-mL DNase/RNase free microcentrifuge tubes for later RNA extraction using a RecoverAll Total Nucleic Acid Isolation Kit (Ambion, Carlsbad, CA). Total RNA was dissolved in RNase-free water and the concentration and quality were measured by NanoDrop 2000 spectrophotometer (Thermo Fisher Scientific, Waltham, MA).

5.2.6 – NanoString gene expression quantification

Details of NanoString gene expression quantification were previously described in Chapter 4.2.5.

5.2.7 – NanoString data preprocessing

All 78 samples were preprocessed and normalized in one batch. Details of NanoString data preprocessing and normalization were previously described in Chapter 4.2.6.

5.2.8 – Study endpoint

The primary study endpoint was progression to cirrhosis, defined as absence of cirrhosis in the initial biopsy and had Metavir fibrosis stage 4 in follow-up biopsies or Fibroscan >14 kPa in follow-up clinical visits (16). The secondary study endpoint was progression to poor outcomes, defined as development of any one of the following: liver decompensation, need for liver transplantation, or liver-related death. Liver decompensation was defined as diagnosis of any of the followings: ascites, hepatic encephalopathy, variceal bleeding, or hepatorenal syndrome (17). Liver-related death was defined as death caused by

liver failure: nearest liver function test with total bilirubin > 50 umol/L and INR > 1.7 before deceased (18, 19). The time to endpoint was calculated using the date of biopsy to an event.

5.2.9 – Statistical analysis

Aggregate gene set expression was determined for each biopsy by calculating the geometric mean of the normalized counts of 48 fibrosis genes (48-gene signature). Continuous variables were presented as median and interquartile range (IQR) and categorical variables were presented as number and percentage. All data were compared between groups using Mann-Whitney U-test for continuous variables and Fisher's exact test for categorical variables. Correlation coefficients were analyzed using Spearman rank-order correlation. The receiver operating curve was used to analyze the diagnostic performance of the 48-gene signature to predict progression to cirrhosis. The best cutoff of the curve was determined by Youden index. Survival analyses were performed after biopsies with the Kaplan–Meier method using a log-rank test and univariate and multivariate models with Cox regression method. The assumption of proportional hazards over time was verified using the log–log graphic method and met by all covariates. Potential linearity of covariates was investigated by collinearity diagnostics before multivariate survival analysis. All tests with two-sided p-value <0.05 were considered significant. All analyses and figures were performed and generated using the SPSS 25 statistical software (IBM, Armonk, NY, USA), Excel 2010 (Microsoft Corporation, Redmond, WA), or R-program (version 3.3.2; http://www.r-project.org) with the following packages: ggplot2 and pROC.

5.3 – Results

5.3.1 – Patient characteristics

Of 78 RNA samples from 78 unique patients, two were excluded due to low-quality gene expression profiles (Figure 5.1). Table 5.1 summarized the clinical and histological characteristics of the 76 patients. One patient was diagnosed with primary sclerosing cholangitis overlap syndrome. Median age at disease onset was 37.3 years old (IQR: 24.9-54.4). Seventy-eight percent patients had positive anti-nuclear antibodies and 66% had positive smooth muscle antibodies. Liver tissue examination at disease onset revealed severe inflammatory (Metavir activity grade=3) in 35 patients (46.1%) and cirrhosis in 11 patients (14.5%). During a median 8.5 years of follow-up (IQR: 4.9-12.5), 13 patients without cirrhosis at disease onset progressed to cirrhosis. Of all 76 patients, 12 (15.8%) progressed to poor outcomes during follow-up. Progressed to poor outcomes refer to development of any one of the following during follow-up: liver decompensation, need for liver transplantation, or liver-related death.

5.3.2 – Treatment and response

All patients were treated initially with prednisone and 64 (84%) were treated with prednisone in combination with azathioprine. Twelve patients developed side effects with the first-line therapies. Of these 12 patients, four were managed with mycophenolate mofetil. After a median 8.5 years of follow-up (IQR: 4.9-12.5), 52 (68.4%) patients had achieved a complete treatment response, 21 (27.6%) with incomplete treatment response, and 3 (3.9%) with relapse.

5.3.3 – RNA quantity and quality

Adequate RNA was isolated from all liver tissues for NanoString gene expression assay. The quality (A_{260}/A_{280} spectrophotometry ratio) of the isolated RNA was between 1.67 and 1.98, which met manufacturer-recommended specifications.

5.3.4 – Comparison of the 48-gene signature with biochemistry and histology parameters

The 48-gene signature was compared with biochemical and histological parameters at disease onset. The levels of the 48-gene signature were significantly correlated with increased histological fibrosis stage ($r=0.467$, $p<0.001$) and activity score ($r=0.266$, $p=0.020$) as well as increased levels of IgG ($r=0.423$, $p<0.001$), INR ($r=0.496$, $p<0.001$), and MELD score ($r=0.421$, $p=0.004$). The levels of the 48-gene signature were also significantly correlated with decreased levels of albumin ($r=-0.389$, $p=0.005$) and platelet counts ($r=-0.377$, $p=0.005$).

5.3.5 – Distribution of the histological fibrosis stage and the 48-gene signature

Figure 5.2A showed the distribution of the 48-gene signature, histological fibrosis stage, and outcomes for all 76 patients. A 48-gene signature cut-off of 113.56 for progression to cirrhosis was derived from receiver operating characteristic curve analysis in patients without cirrhosis at disease onset (Youden index = 113.56, Figure 5.2B). Based on this cutoff, patients with a 48-gene signature greater than 113.56 were assigned as having a high 48-gene signature (Figure 5.2A).

Of the 65 patients without cirrhosis at disease onset, 0% (0 of 5) with F0 fibrosis, 18%

(4 of 22) with F1 fibrosis, 22% (4 of 18) with F2 fibrosis, and 25% (5 of 20) with F3 fibrosis progressed to cirrhosis during follow-up. The probability of progression to cirrhosis was similar across different fibrosis stages (p=0.811). Patients progressed to cirrhosis had significantly higher 48-gene signature compared to patients who did not progress (p=0.001, Figure 5.3A), but similar histological fibrosis stage (p=0.298, Figure 5.3B) and activity score (p=0.345, Figure 5.4A). Patients progressed to cirrhosis had similar 48-gene signature compared to patients who had cirrhosis at disease onset (p=0.505, Figure 5.3A).

Of all 76 patients, 0% (0 of 5) with F0 fibrosis, 5% (1 of 22) with F1 fibrosis, 22% (4 of 18) with F2 fibrosis, 15% (3 of 20) with F3 fibrosis, and 36% (4 or 11) with F4 fibrosis progressed to poor outcomes. Patients progressed to poor outcomes had a marginally significant higher 48-gene signature and significantly higher histological fibrosis stage compared to patients who did not progress (p=0.073, 0.027, respectively, Figure 5.3C and 5.3D). Histological activity score was similar between patients who progressed and did not progress to poor outcomes (p=0.289, Figure 5.4B).

5.3.6 – The 48-gene signature predicts progression to cirrhosis, but histological fibrosis stage and activity score cannot

Of the 65 patients without cirrhosis at disease onset, patients with a high 48-gene signature had significantly higher probability of progression to cirrhosis compared to patients with a low 48-gene signature (53% vs. 7%, log-rank p<0.001, Figure 5.5A). However, the probability of progression to cirrhosis was similar between F2-F3 vs. F0-F1 fibrosis (24% vs. 15%, log-rank p=0.420, Figure 5.5B) and A2-A3 vs. A1 (24% vs. 7%, log-rank p=0.133, Figure 5.6A). This showed the 48-gene signature can predict progression to cirrhosis at

disease onset, but histological fibrosis stage and activity score cannot.

5.3.7 – Variables associated with progression to cirrhosis

Univariate Cox regression analyses in 65 patients without cirrhosis at disease onset revealed incomplete treatment response (HR: 4.06, 95% CI: 1.23-13.41, p=0.02), INR >1.2 at disease onset (HR: 13.04, 95% CI: 1.67-101.89, p=0.01) and a high 48-gene signature at disease onset (HR: 7.95, 95% CI: 2.44-25.87, p=0.001) were significantly associated with progression to cirrhosis (Table 5.2). Histological activity grade and fibrosis stage at disease onset were not significantly associated with progression to cirrhosis.

Multivariate analyses included the variables with p<0.05 in univariate analysis (48-gene signature, INR, and treatment response). Due to limited number of patients progressed to cirrhosis (n=13), to avoid model overfitting, multivariate models were limited to two variables. To analyze the effect of 48-gene signature predicting progression to cirrhosis, two models were built: 48-gene signature with treatment response (model 1) and 48-gene signature with INR (model 2) (Table 5.2). In model 1, the risk of progressing to cirrhosis is 7.63-fold higher in patients with a high 48-gene signature compared to patients with a low 48-gene signature after adjustment for treatment response (HR: 7.63, 95% CI: 1.94-30.03, p=0.004). In model 2, the risk of progressing to cirrhosis is 5.65-fold higher in patients with a high 48-gene signature compared to patients with a low 48-gene signature after adjustment for INR (HR: 5.65, 95% CI: 1.51-21.18, p=0.01).

Multivariate analysis repeated with all three variables with p<0.05 in univariate analysis provided the same conclusions as above (Table 5.2).

I further analyzed INR, which was significantly associated with progression to

cirrhosis in model 2 for progression to cirrhosis. Of the 65 patients without cirrhosis at disease onset, 53 (81.5%) had INR measurements. Patients with an INR >1.2 at disease onset had significantly higher probability of progression to cirrhosis compared to patients with an INR ≤ 1.2 (38% vs. 4%, log-rank p=0.002, Figure 5.7).

5.3.8 – Histological parameters and 48-gene signature cannot predict poor outcomes

Of the 65 patients without cirrhosis at disease onset, the probability of progression to poor outcomes was similar between patients with high and low 48-gene signature (21% vs. 9%, log-rank p=0.113) (Figure 5.8A), between F2-F3 and F0-F1 (18% vs. 4%, log-rank p=0.096) (Figure 5.8B), and between A2-A3 and A1 (16% vs. 0%, log-rank p=0.085) (Figure 5.6B).

5.3.9 – Variables associated with progression to poor outcomes

Univariate Cox regression analyses revealed incomplete treatment response (HR: 4.44, 95% CI: 1.24-15.88, p=0.02), decreased platelet counts at disease onset (HR: 0.99, 95% CI: 0.98-1.00, p=0.01), and cirrhosis at disease onset (HR: 3.50, 95% CI: 1.02-11.96, p=0.046) were significantly associated with progression to poor outcomes (Table 5.3).

Due to the limited number of patients that progressed to poor outcomes (n=12), only the top two variables with the most significant p-value in the univariate analysis (treatment response and platelet counts at disease onset) were included in the multivariate analysis. In multivariate analysis, only decreased platelet counts at disease onset (HR: 0.99 95% CI: 0.98-1.00, p=0.03) was significantly associated with poor outcomes after adjusting for treatment

response (Table 5.3).

5.4 – Discussion

Predicting the risk of progression to cirrhosis in patients with AIH at disease onset is an unmet clinical need. This chapter showed for the first time that a 48-fibrosis gene signature in clinical liver biopsies predicts progression to cirrhosis, long before the event, but histology parameters do not offer this level of risk stratification. Patients with a high 48-gene signature had significantly higher probability of progression to cirrhosis compared to patients with a low 48-gene signature (53% vs. 7%, log-rank $p<0.001$). The risk of progression to cirrhosis was 6.78-fold higher in patients with a high 48-gene signature compared to patients with a low 48-gene signature after adjusting for other significant variables in univariate analysis. This finding has a significant clinical relevance because early prediction of cirrhosis can guide physicians to adjust treatment regimens and dosages to substantially impact prognosis for individual patients. Moreover, the 48-gene signature test can be easily applied into a routine clinical assay as it can be analyzed in standard procurement and work-up of diagnostic liver biopsies.

There is an unmet clinical need in predicting and monitoring progression of liver fibrosis at the start and during immunosuppressive therapy (20). Corticosteroids are the first line treatment for AIH and have anti-fibrotic actions. However, they are inconsistency in controlling fibrosis due to corticosteroids are not primarily anti-fibrotic agents and they are lack of site-specific target action that can be monitored reliably (21). Current available non-invasive biomarkers for hepatic fibrosis are limited in predicting fibrosis progression (22). This chapter showed non-cirrhotic patients at disease onset with high 48-gene signature had

significantly higher risk of progression to cirrhosis. Therefore, the 48-gene signature can help to monitor the risk of progression to cirrhosis before or during therapy.

All AIH patients with active disease or advanced fibrosis should be treated; however, there is a debate about whether mild, asymptomatic patients need immunosuppressive regimes or not, as the risk vs. benefit of treatment for these patients is not clear (1). Untreated AIH has heterogeneous disease behavior and a proportion of patients progress to cirrhosis during follow-up (10). As AIH is a lifelong disease, and progression to cirrhosis take years to decades to become clinically apparent, current published observational studies may have too short follow-up to demonstrate the benefit of immunosuppressive treatment in patients with mild AIH. The 48-gene signature may help to early predict mild AIH patients who are at high-risk for developing cirrhosis. This can identify a sub-group of mild patients at disease onset but at high-risk for disease progression that would benefit more from immunosuppressive treatment. Moreover, as progression to cirrhosis usually takes years to decades in these patients, the 48-gene signature may be used as a surrogate endpoint to early predict progression to cirrhosis.

Patients who progressed to cirrhosis had a significantly higher 48-gene signature compared to patients who did not progress, but similar when compared to patients with cirrhosis at disease onset (Figure 5.2A). This showed patients progressed to cirrhosis had a similar molecular phenotype with patients who had cirrhosis at disease onset and suggested the 48-gene signature could distinguish between subgroups of patients based on prognosis (progress to cirrhosis or not), and this cannot be provided by histology alone.

Despite neither histological activity score nor fibrosis stage at disease onset can predict progression to cirrhosis, a high INR (a sign of liver dysfunction) at disease onset was

a significant determinant for progression to cirrhosis (Table 5.2, Figure 5.7). A previous study found INR >1.2 was significantly associated with cirrhosis at disease onset (23). These results showed increased INR was associated with both cirrhosis at disease onset and increased risk for progression to cirrhosis. Of 24 patients with INR ≤1.2 at disease onset in this cohort, only 1 (4%) progressed to cirrhosis during follow-up. This shows INR may be used as a rule-out test for progression to cirrhosis at disease onset.

There were limitations of this study. First, this was a retrospective study with a small number of patients and relatively short follow-up time (median 8.5 years) to detect enough events of poor outcomes. A previous study analyzed 245 AIH patients and found only 9% and 30% developed liver-related death or need for transplantation after 10 and 20 years of follow-up, respectively (24). The small number of patients and relatively short follow-up time may be the reason of why the 48-gene signature was not significantly associated with progression to poor outcomes. Since the 48-gene signature predicts progression to cirrhosis and cirrhosis portends poor prognosis in AIH, the 48-gene signature should also be capable to predict progression to poor outcomes if more patients were included with a longer follow-up time. Second, as AIH is a rare disease, I do not have enough patients to consider splitting of the samples to two or more independent sets to validate the results. Therefore, validation in a second larger, independent cohort with longer follow-up time should be performed to assure confidence in these initial results.

This chapter showed the 48-gene signature in patients with AIH at disease onset early predicts progression to cirrhosis, but histology cannot. Measurement of the 48-gene signature at the time of AIH diagnosis should be considered as it can provide additional prognostic information that cannot be provided by histology. The prognostic information can provide

risk stratification and help physicians to tailor treatment regimen for individual patients.

Table 5.1. Patient characteristics

Characteristics	Patients evaluated, n (%)	Median (IQR) or n (%)
Age at disease onset (year), median (IQR)	76 (100%)	37.3 (24.9-54.4)
Sex female, n (%)	76 (100%)	54 (71.1)
Ethnicity white, n (%)	31 (41%)	26 (83.9)
BMI at disease onset, median (IQR)	61 (80%)	28.8 (25.3-33.8)
Biochemistry at disease onset		
AST, U/L, median (IQR)	58 (76%)	707 (281-1137)
ALT, U/L, median (IQR)	67 (88%)	651 (278-1100)
ALP, U/L, median (IQR)	65 (86%)	166 (138-236)
Albumin, g/L, median (IQR)	50 (66%)	34 (29-40)
Total bilirubin, umol/L, median (IQR)	67 (88%)	46 (17-141)
IgG, g/L, median (IQR)	72 (95%)	26.1 (22.1-35.6)
INR >1.2, n (%)	63 (83%)	34 (54)
MELD, median (IQR)	47 (62%)	17 (10-22)
Platelet, 10^9/L, median (IQR)	65 (86%)	180 (128-249)
Serology at disease onset		
Positive anti-nuclear antibody, n (%)	74 (97%)	58 (78.4)
Positive smooth muscle antibody, n (%)	50 (66%)	33 (66.0)
Histology		
Metavir activity score, n (%)	76 (100%)	
0		0 (0)
1		17 (22.4)
2		24 (31.6)
3		35 (46.1)
Metavir fibrosis stage, n (%)	76 (100%)	
0		5 (6.6)
1		22 (28.9)
2		18 (23.7)
3		20 (26.3)

4		11 (14.5)
Fibrosis outcome	76 (100%)	
Cirrhosis at disease onset, n (%)		11 (14.5)
Progressed to cirrhosis, n (%)		13 (17.1)
Did not progress to cirrhosis, n (%)		52 (68.4)
Treatment response	76 (100%)	
Complete, n (%)		52 (68.4)
Incomplete, n (%)		21 (27.6)
Relapse, n (%)		3 (3.9)
Progressed to poor outcomes, n (%)	76 (100%)	12 (15.8)
Follow-up period after biopsy (year), median (IQR)	76 (100%)	8.5 (4.9-12.5)

Percentage might not add up to 100% because of rounding.

Table 5.2. Univariate and multivariate analyses of progression to cirrhosis in 65 patients without cirrhosis at disease onset (n=13 events)

Variable	HR	95% CI	p-value
Univariate analyses			
Age at disease onset, year	1.01	0.98-1.05	0.38
Gender			
Male (reference)	1.00		
Female	1.24	0.34-4.53	0.74
Treatment response			
Complete (reference)	1.00		
Incomplete	4.06	1.23-13.41	**0.02**
ALT at disease onset	0.999	0.998-1.000	0.13
AST at disease onset	1.00	0.999-1.001	0.91
ALP at disease onset	1.001	0.996-1.006	0.69
Albumin at disease onset	0.93	0.84-1.04	0.22
Total bilirubin at disease onset	1.001	0.997-1.006	0.57
IgG at disease onset	1.02	0.99-1.05	0.29
INR at disease onset			
≤1.2	1.00		
>1.2	13.04	1.67-101.89	**0.01**
MELD at disease onset	1.14	0.98-1.32	0.09
Platelet at disease onset	0.993	0.986-1.000	0.06
Metavir activity score			
A1 (reference)	1.00		
A2-A3	4.24	0.55-32.59	0.17
Metavir fibrosis stage			
F0-F1 (reference)	1.00		
F2-F3	1.15	0.38-3.52	0.81
48-gene signature			
Low (reference)	1.00		
High	7.95	2.44-25.87	**0.001**

Multivariate analyses			
Model 1			
Treatment response			
Complete (reference)	1.00		
Incomplete	2.42	0.71-8.24	0.16
48-gene signature			
Low (reference)	1.00		
High	7.63	1.94-30.03	**0.004**
Model 2			
INR at disease onset			
≤1.2	1.00		
>1.2	9.08	1.14-72.42	**0.04**
48-gene signature			
Low (reference)	1.00		
High	5.65	1.51-21.18	**0.01**
Model with all three significant variables in univariate analysis			
Treatment response			
Complete (reference)	1.00		
Incomplete	1.54	0.42-5.63	0.51
INR at disease onset			
≤1.2	1.00		
>1.2	7.10	0.86-58.43	0.07
48-gene signature			
Low (reference)	1.00		
High	6.78	1.33-34.56	**0.02**

To avoid model over fitting, multivariate model was limited to two variables due to the number of events (n=13). The 48-gene signature was analyzed with all other significant variables in the univariate analyses.

Table 5.3. Univariate and multivariate analyses of progression to poor outcomes (n=76 patients, 12 events)

Variable	Univariate analysis			Multivariate analysis		
	HR	95% CI	p-value	HR	95% CI	p-value
Age at disease onset, year	0.98	0.95-1.01	0.20			
Gender						
Male (reference)	1.00					
Female	1.29	0.35-4.76	0.70			
Treatment response						
Complete (reference)	1.00			1.00		
Incomplete	4.44	1.24-15.88	**0.02**	4.72	0.88-25.22	0.07
ALT at disease onset	0.999	0.998-1.001	0.27			
AST at disease onset	1.000	0.998-1.001	0.64			
ALP at disease onset	1.00	0.99-1.01	0.94			
Albumin at disease onset	0.93	0.82-1.06	0.29			
Total bilirubin at disease onset	0.999	0.993-1.006	0.80			
IgG at disease onset	1.02	0.98-1.05	0.46			
INR at disease onset						
≤1.2	1.00					
>1.2	2.77	0.56-13.73	0.21			
MELD at disease onset	1.04	0.90-1.20	0.64			
Platelet at disease onset	0.99	0.98-1.00	**0.01**	0.99	0.98-1.00	**0.03**
Metavir activity score						
A1 (reference)	1.00					
A2-A3	32.75	0.13-8416	0.22			
Metavir fibrosis stage						
F0-F1 (reference)	1.00					
F2-F4	6.31	0.81-48.90	0.08			
Cirrhosis at disease onset						
No (reference)	1.00					
Yes	3.50	1.02-11.96	**0.046**			

48-gene signature				
Low (reference)	1.00			
High	2.24	0.71-7.12	0.17	

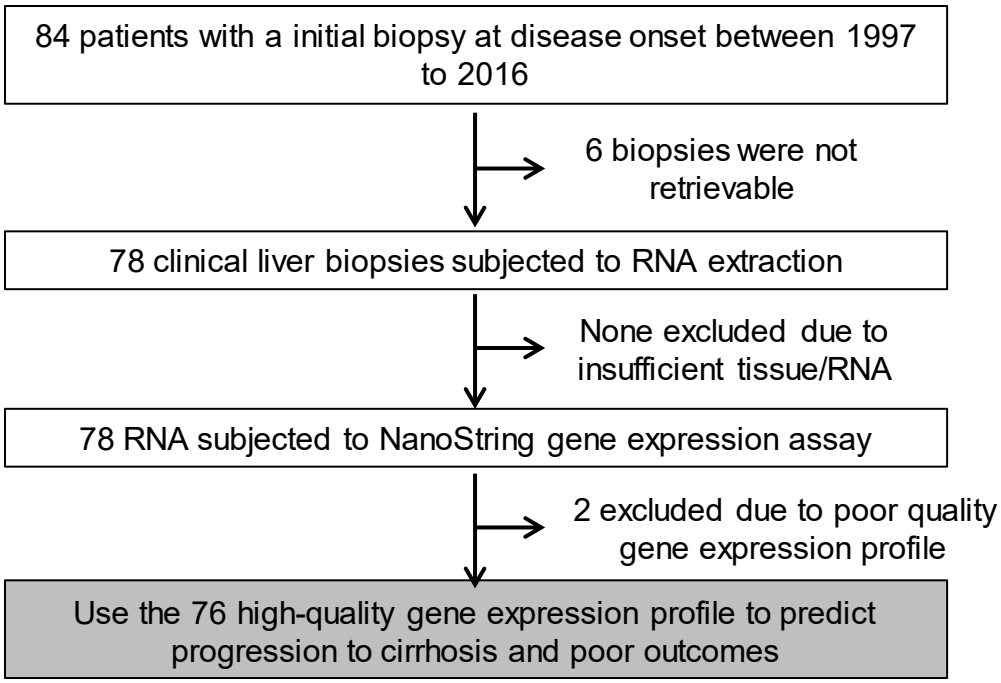

Figure 5.1. Study design.

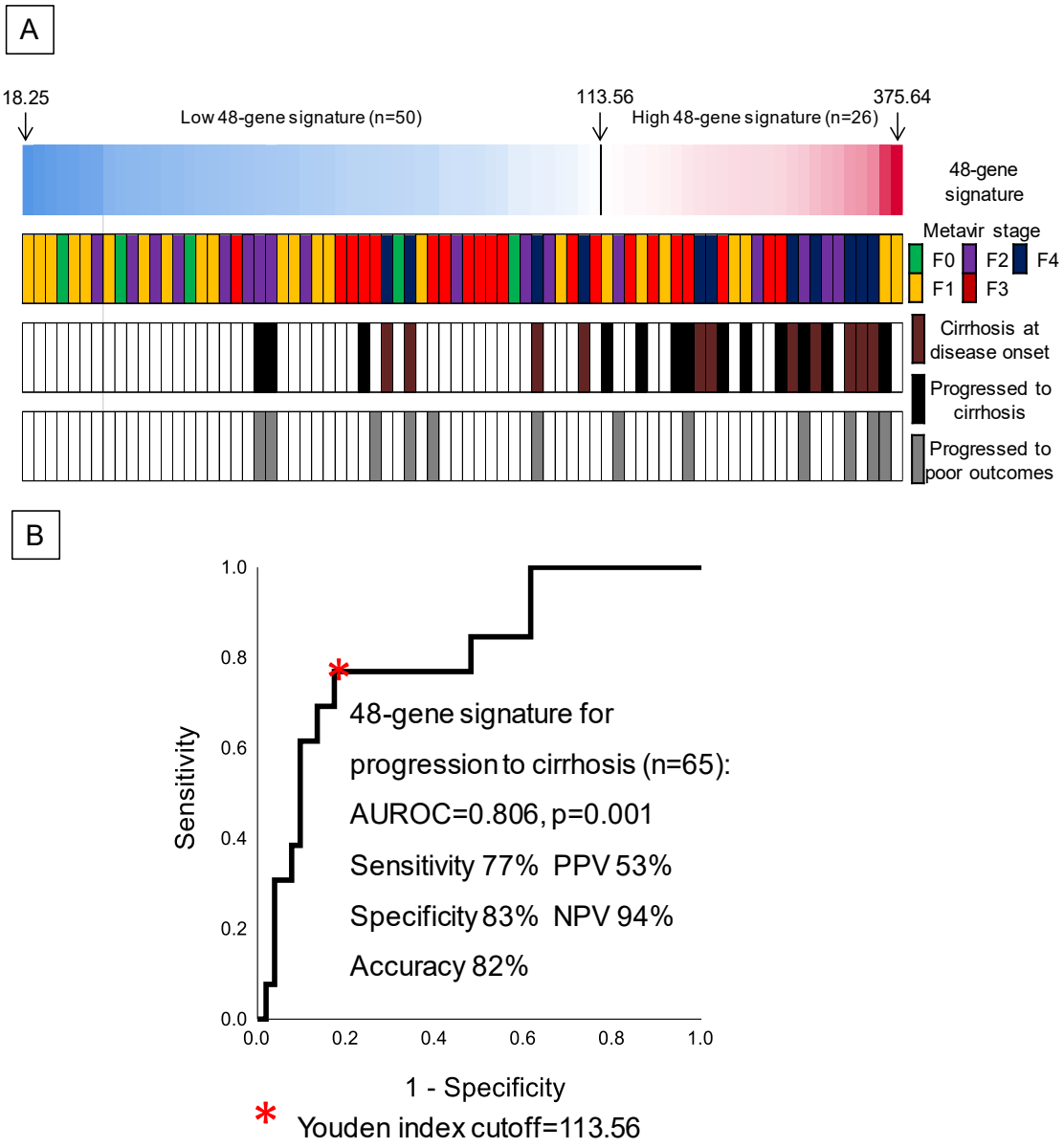

Figure 5.2. The distribution of the 48-gene signature and histological fibrosis stage. (A) The biopsies were sorted based on the 48-gene signature from low (blue) to high (red). (B) The performance of the 48-gene signature predicting progression to cirrhosis in 65 patients without cirrhosis at disease onset.

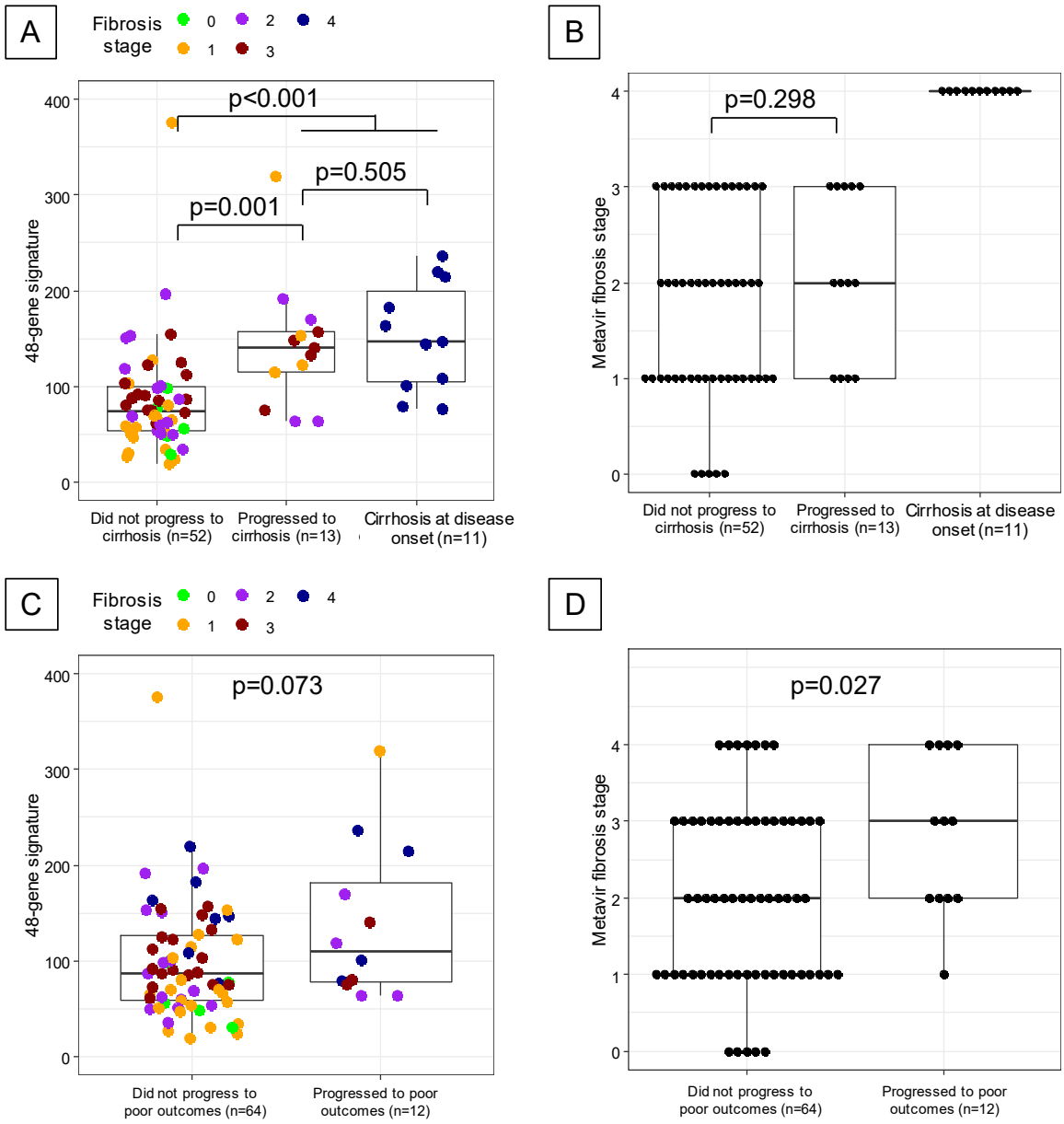

Figure 5.3. The 48-gene signature values and histological fibrosis stage grouped according to different outcomes.

(A) Patients progressed to cirrhosis had significantly higher 48-gene signature compared to patients who did not progress (p=0.001). (B) Patients progressed to cirrhosis had similar histological fibrosis stage compared to patients who did not progress (p=0.298). (C) Patients progressed to poor outcomes had borderline significantly higher 48-gene signature compared to patients who did not progress (p=0.073). (D) Patients progressed to poor outcomes had significantly higher histological fibrosis stage compared to patients who did not progress (p=0.027).

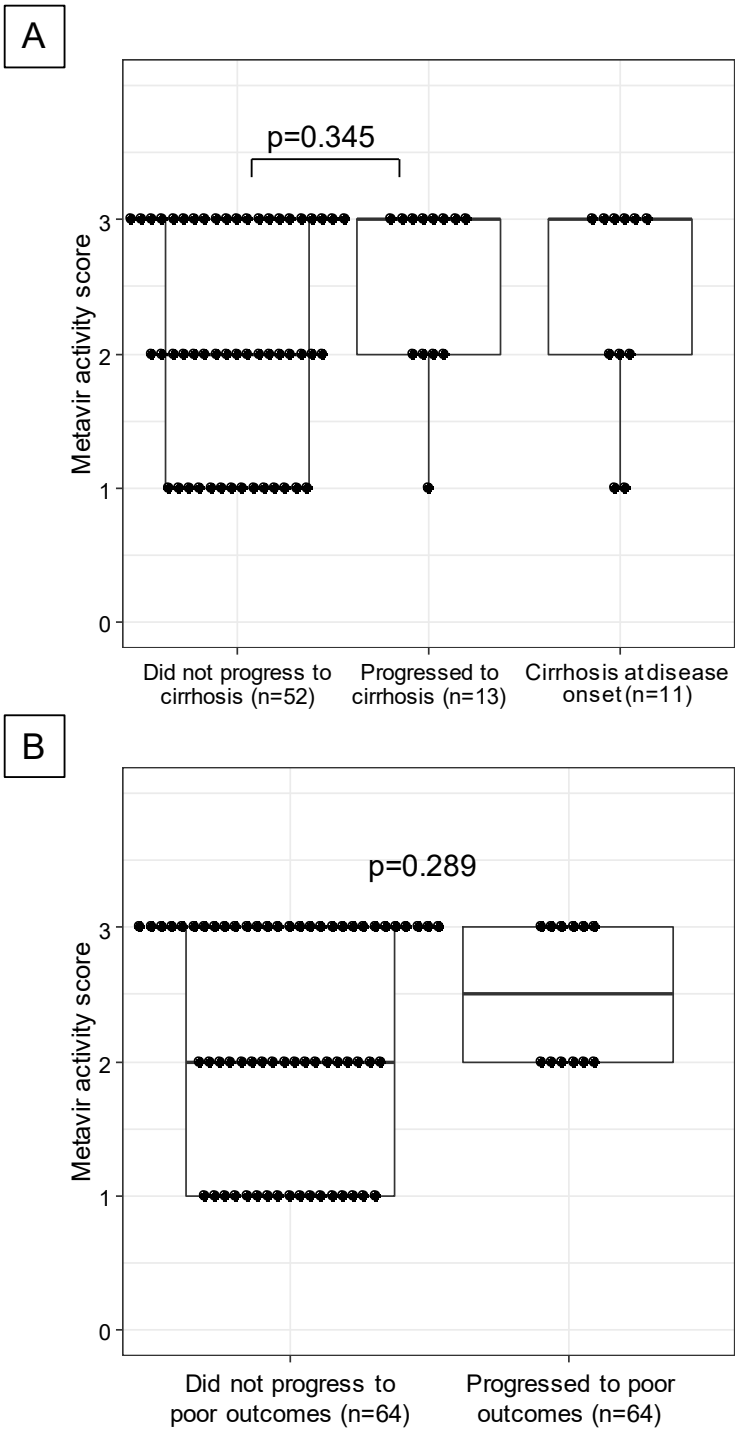

Figure 5.4. The histological activity score grouped according to different outcomes. (A) Patients progressed to cirrhosis had similar activity score at disease onset compared to patients who did not progress (p=0.345). (B) Patients progressed to poor outcomes had similar activity score at disease onset compared to patients who did not progress (p=0.289).

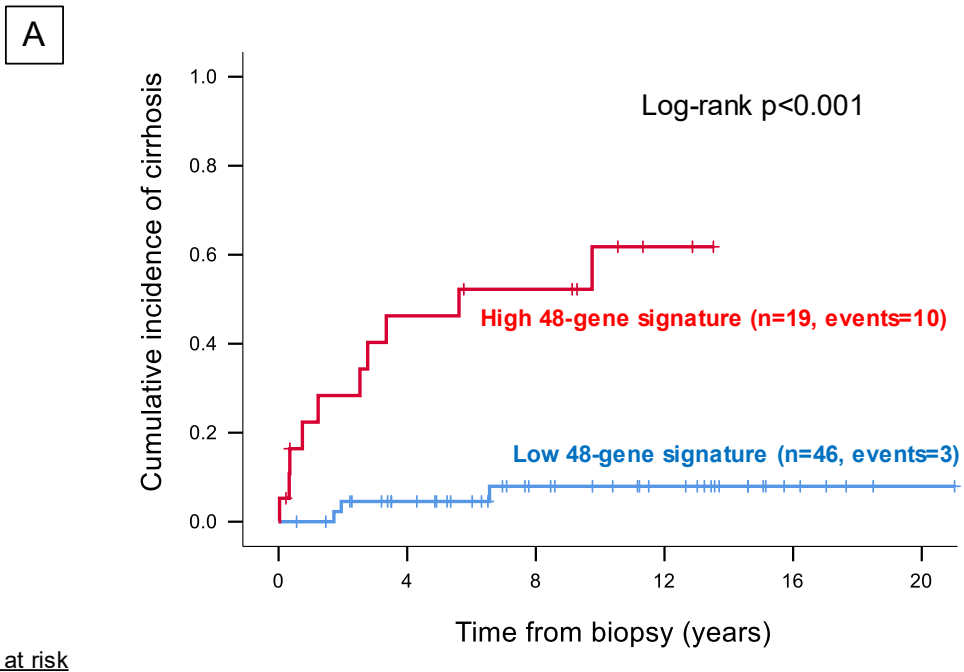

Number at risk						
Low 48-gene signature	46	36	23	16	5	1
High 48-gene signature	19	9	7	2	0	0

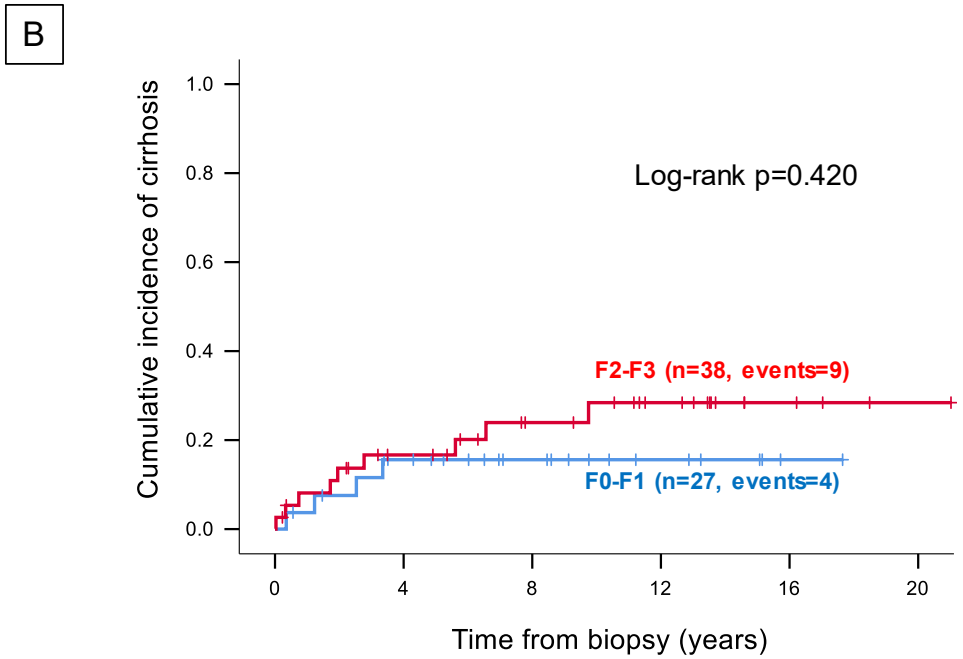

Number at risk						
F0-F1	27	19	12	6	1	0
F2-F3	38	26	18	12	4	1

Figure 5.5. Cumulative incidence of cirrhosis in patients without cirrhosis at disease onset stratified by (A) the 48-gene signature and (B) histological fibrosis stage.

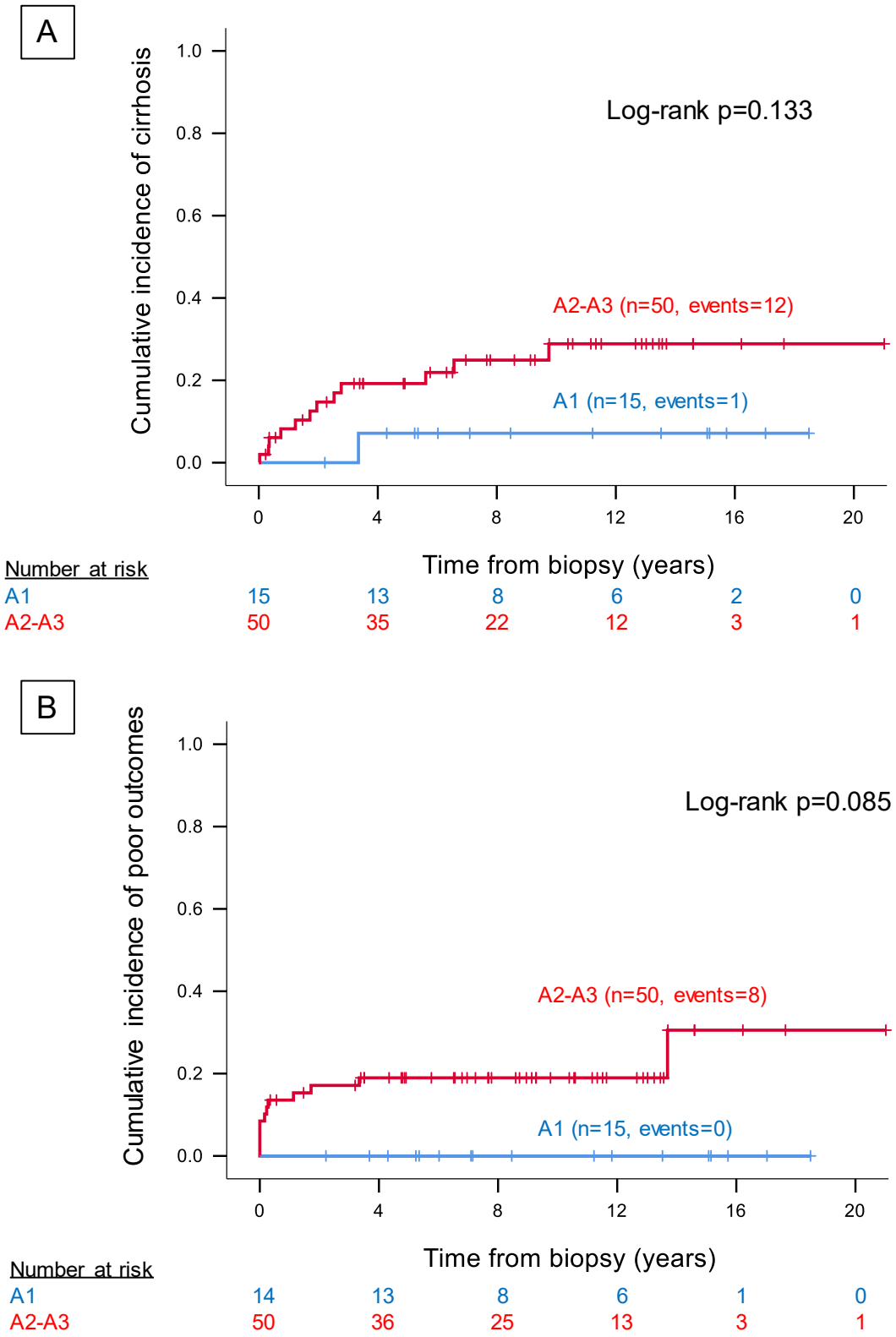

Figure 5.6. Cumulative incidence of (A) cirrhosis and (B) poor outcomes in patients without cirrhosis at disease onset stratified by Metavir activity score.

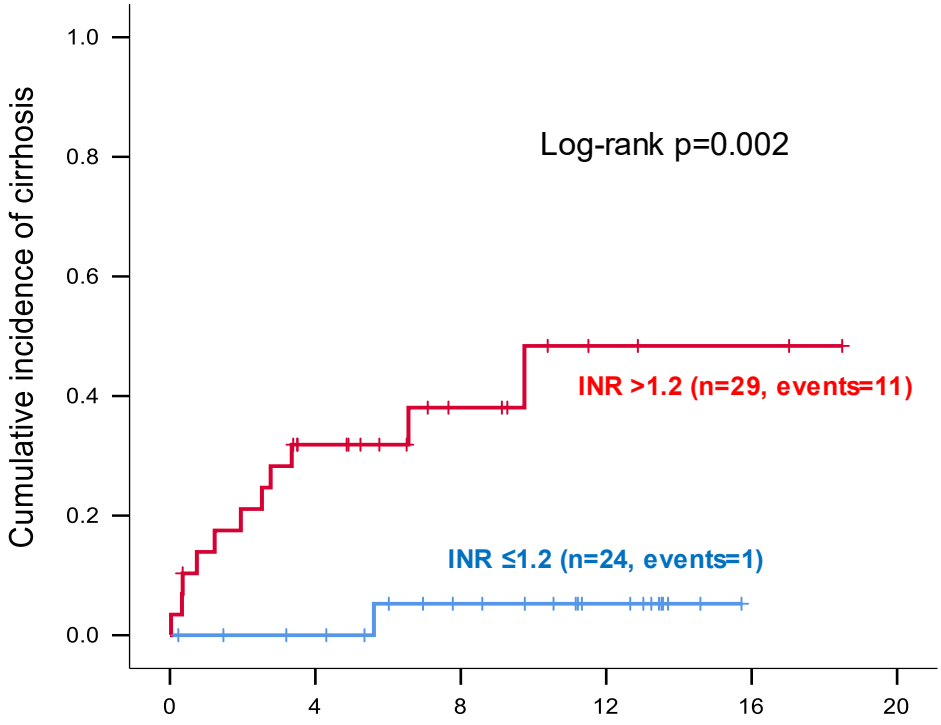

Number at risk						
INR ≤1.2	24	21	15	9	0	0
INR >1.2	29	16	8	3	2	0

Figure 5.7. Cumulative incidence of cirrhosis in patients without cirrhosis at disease onset stratified by INR.

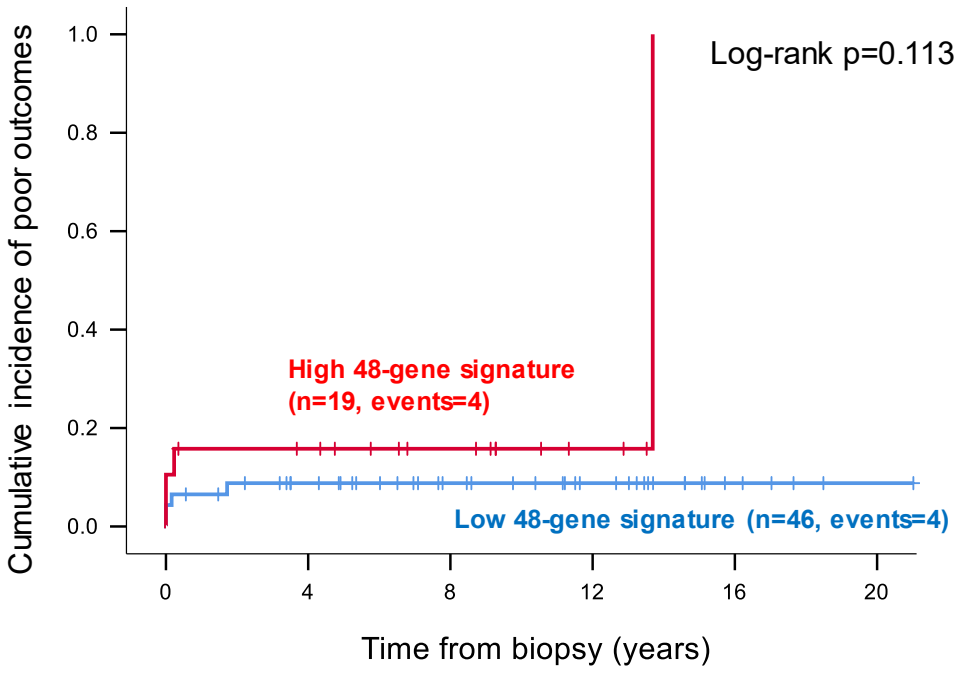

Number at risk						
Low 48-gene signature	46	35	24	16	5	1
High 48-gene signature	19	14	9	3	0	0

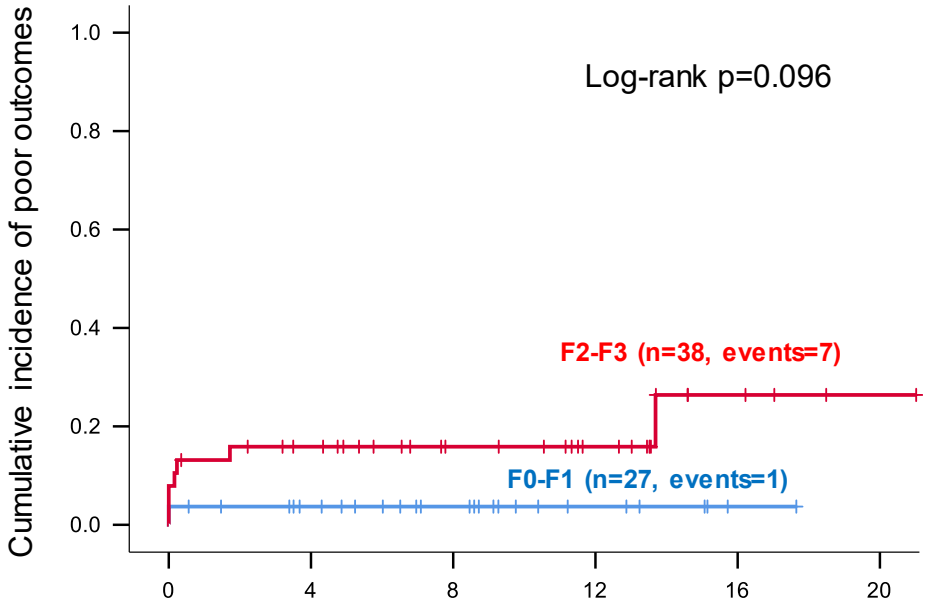

Number at risk						
F0-F1	27	21	14	6	1	0
F2-F4	38	28	19	13	4	1

Figure 5.8. Cumulative incidence of poor outcomes in patients without cirrhosis at disease onset stratified by (A) the 48-gene signature and (B) histological fibrosis stage.

5.5 – References

1. EASL Clinical Practice Guidelines: Autoimmune hepatitis. J Hepatol 2015 Oct;63(4):971-1004.
2. Roberts SK, Therneau TM, Czaja AJ. Prognosis of histological cirrhosis in type 1 autoimmune hepatitis. Gastroenterology 1996 Mar;110(3):848-857.
3. Bataller R, Brenner DA. Liver fibrosis. J Clin Invest 2005 Feb;115(2):209-218.
4. Czaja AJ, Carpenter HA. Progressive fibrosis during corticosteroid therapy of autoimmune hepatitis. Hepatology 2004 Jun;39(6):1631-1638.
5. Berenguer J, Zamora FX, Aldamiz-Echevarria T, Von Wichmann MA, Crespo M, Lopez-Aldeguer J, et al. Comparison of the prognostic value of liver biopsy and FIB-4 index in patients coinfected with HIV and hepatitis C virus. Clin Infect Dis 2015 Mar 15;60(6):950-958.
6. Gleeson D, Heneghan MA. British Society of Gastroenterology (BSG) guidelines for management of autoimmune hepatitis. Gut 2011 Dec;60(12):1611-1629.
7. Trivedi PJ, Hubscher SG, Heneghan M, Gleeson D, Hirschfield GM. Grand round: Autoimmune hepatitis. J Hepatol 2019 Apr;70(4):773-784.
8. Davis GL, Czaja AJ, Ludwig J. Development and prognosis of histologic cirrhosis in corticosteroid-treated hepatitis B surface antigen-negative chronic active hepatitis. Gastroenterology 1984 Dec;87(6):1222-1227.

9. Liberal R, Grant CR. Cirrhosis and autoimmune liver disease: Current understanding. World J Hepatol 2016 Oct 8;8(28):1157-1168.

10. Czaja AJ. Features and consequences of untreated type 1 autoimmune hepatitis. Liver Int 2009 Jul;29(6):816-823.

11. Hold GL, Untiveros P, Saunders KA, El-Omar EM. Role of host genetics in fibrosis. Fibrogenesis Tissue Repair 2009 Dec 4;2(1):6.

12. Smith MW, Walters KA, Korth MJ, Fitzgibbon M, Proll S, Thompson JC, et al. Gene expression patterns that correlate with hepatitis C and early progression to fibrosis in liver transplant recipients. Gastroenterology 2006 Jan;130(1):179-187.

13. Asselah T, Bieche I, Laurendeau I, Paradis V, Vidaud D, Degott C, et al. Liver gene expression signature of mild fibrosis in patients with chronic hepatitis C. Gastroenterology 2005 Dec;129(6):2064-2075.

14. Hennes EM, Zeniya M, Czaja AJ, Pares A, Dalekos GN, Krawitt EL, et al. Simplified criteria for the diagnosis of autoimmune hepatitis. Hepatology 2008 Jul;48(1):169-176.

15. Bedossa P, Poynard T. An algorithm for the grading of activity in chronic hepatitis C. The METAVIR Cooperative Study Group. Hepatology 1996 Aug;24(2):289-293.

16. Ebadi M, Bhanji RA, Mazurak VC, Lytvyak E, Mason A, Czaja AJ, et al. Severe vitamin D deficiency is a prognostic biomarker in autoimmune hepatitis. Aliment Pharmacol Ther 2019 Jan;49(2):173-182.

17. Lens S, Torres F, Puigvehi M, Marino Z, Londono MC, Martinez SM, et al. Predicting the development of liver cirrhosis by simple modelling in patients with chronic hepatitis C. Aliment Pharmacol Ther 2016 Feb;43(3):364-374.

18. Manousou P, Burroughs AK, Tsochatzis E, Isgro G, Hall A, Green A, et al. Digital image analysis of collagen assessment of progression of fibrosis in recurrent HCV after liver transplantation. J Hepatol 2013 May;58(5):962-968.

19. Friedman LS. Surgery in the patient with liver disease. Trans Am Clin Climatol Assoc 2010;121:192-204.

20. Montano-Loza AJ, Thandassery RB, Czaja AJ. Targeting Hepatic Fibrosis in Autoimmune Hepatitis. Dig Dis Sci 2016 Nov;61(11):3118-3139.

21. Czaja AJ. Drug choices in autoimmune hepatitis: part A--Steroids. Expert Rev Gastroenterol Hepatol 2012 Sep;6(5):603-615.

22. EASL-ALEH Clinical Practice Guidelines: Non-invasive tests for evaluation of liver disease severity and prognosis. J Hepatol 2015 Jul;63(1):237-264.

23. Ngu JH, Gearry RB, Frampton CM, Stedman CA. Predictors of poor outcome in patients w ith autoimmune hepatitis: a population-based study. Hepatology 2013 Jun;57(6):2399-2406.

24. Hoeroldt B, McFarlane E, Dube A, Basumani P, Karajeh M, Campbell MJ, et al. Long-term outcomes of patients with autoimmune hepatitis managed at a nontransplant center. Gastroenterology 2011 Jun;140(7):1980-1989.

Chapter 6: A 48-gene Signature in Clinical Liver Biopsies Enables Early Prediction of Progression to Cirrhosis in Patients with Non-alcoholic Fatty Liver Disease

6.1 – Introduction

Non-alcoholic fatty liver disease (NAFLD) is the most common chronic liver disease that affects over 25% of the population worldwide (1). It is a spectrum of liver damage with overlapping histology phenotypes that varies from simple steatosis to non-alcoholic steatohepatitis (NASH) with presence of lobular inflammation and hepatocyte ballooning with or without fibrosis. NAFLD is a heterogeneous disease that has very different rates of disease progression among individuals. About 20-30% of patients with simple steatosis will develop NASH, of whom 20% will progress to cirrhosis (2). Cirrhosis is the final pathway that leads to poor clinical outcomes (liver decompensation, need for liver transplantation, premature death) (3, 4). Therefore, early diagnosis and prevention of cirrhosis is important. Approximately 20% of patients with NAFLD rapidly progress to advanced fibrosis/cirrhosis, but there is no reliable method to identify these rapid progressors (5). The characteristics of subpopulations with rapid or slow fibrosis progression are not well established. Previous research identified several common risk factors of fibrosis progression such as obesity, type 2 diabetes, and genetic predisposition (6). However, currently there is no baseline clinical, histological, or biochemical variables that can predict progression to cirrhosis in early disease stage (7).

Although currently there is no Food and Drug Administration (FDA)-approved drug for treating NASH, several ongoing phase III pivotal trials will likely report initial results around 2021 (8). Currently accepted endpoint by regulatory authorities for an antifibrotic drug is fibrosis regression without worsening NASH, evaluated by paired liver histology, one before treatment and another after treatment (9). However, there is a debate on whether

improvement of fibrosis is a valid surrogate of fibrosis progression (9). A recent phase II NASH therapeutic trial showed more patients had fibrosis improvement on active drug than on placebo, but the proportion of patients with fibrosis progression was similar between the two arms (10). As the impact on the number of patients that progressed to cirrhosis is only driven by the proportion of patients who have worsen fibrosis stage, not the proportion of those that improve, fibrosis regression may not be sufficient to serve as a valid surrogate for progression to cirrhosis (9). Due to the aforementioned circumstance, there is an unmet and urgent clinical need for a molecular biomarker to accurately identify high-risk patients for fibrosis progression who may benefit from upcoming drug treatments to prevent further liver damage. (6).

Increasing evidence indicated that genetic factors have a major influence on fibrosis progression in NAFLD. Previous studies showed mRNAs expression of several fibrosis genes and mutation of patatin-like phospholipase domain containing 3 (PNPLA3) and the transmembrane 6 superfamily 2 (TM6SF2) were associated with advanced fibrosis (11-13). However, the prognostic value of these genes for predicting fibrosis progression is unknown. NAFLD is a complex disease driven by multiple pathways. Therefore, it is unlikely that a variable can accurately predict fibrosis progression in all NAFLD patients. In Chapter 2, I identified and validated a common 48-gene signature that had over 93% of accuracy to predict advanced liver fibrosis, independent of etiologies, by microarray based whole genome transcriptomics. The prognostic value of the 48-gene signature in NAFLD is unknown. In this chapter, I aim to understand if the 48-gene signature can predict progression to cirrhosis, liver decompensation, and liver-related death.

6.2 – Materials and Methods

6.2.1 – Patients

This chapter retrospectively included 105 patients with NAFLD confirmed by liver biopsy at the University of Alberta, Edmonton, Canada (Figure 6.1). In addition, 10 normal livers and 9 explant NASH cirrhotic livers were included as negative and positive controls, respectively. Of the 10 normal livers, two were donor liver biopsies and eight were liver tissues with no histological abnormality. This study was approved by the institutional review board of the University of Alberta.

6.2.2 – Clinical and laboratory assessments

Baseline factors evaluated in this study include gender, age, biochemical markers, body mass index (BMI), presence of metabolic syndrome, liver enzymes, albumin, bilirubin, platelet counts, and HbA1c.

6.2.3 – Histopathological assessment

Histopathological evaluation of representative stained slides were scored according to the Brunt classification system for fibrosis staging (scale 0-4) (14). Simple steatosis was defined as steatosis, but no hepatocyte ballooning or inflammation and NASH was defined as steatosis with hepatocyte ballooning degeneration and inflammation with or without fibrosis (15).

6.2.4 – RNA isolation

Details of RNA isolation were previously described in Chapter 4.2.4.

6.2.5 – NanoString gene expression quantification

Details of NanoString gene expression quantification were previously described in Chapter 4.2.5.

6.2.6 – NanoString data preprocessing

All 105 NAFLD samples and the negative and positive controls were preprocessed and normalized in one batch. Details of NanoString data preprocessing and normalization were previously described in Chapter 4.2.6.

6.2.7 – Study endpoint

The primary study endpoint was progression to cirrhosis, defined as absence of cirrhosis in the initial biopsy and had Metavir fibrosis stage 4 in follow-up biopsies or Fibroscan >10.3 kPa in follow-up clinical visits (16). The secondary study endpoint was progression to poor outcomes, defined as development of any one of the following: liver decompensation, need for liver transplantation, or liver-related death (17). Liver-related death was defined as death caused by liver failure: nearest liver function test with total bilirubin > 50 umol/L and international normalized ratio (INR) > 1.7 before deceased (18, 19). The time to endpoint was calculated using the date of biopsy to event.

6.2.8 – Statistical analysis

Aggregate gene set expression was determined for each biopsy by calculating the geometric mean of the normalized counts of 48 fibrosis genes (48-gene signature). Continuous variables were presented as median and interquartile range (IQR) and categorical variables were presented as number and percentage. Data were compared between groups using Mann-Whitney U-test for continuous variables and Fisher's exact test for categorical variables. The receiver operating characteristic (ROC) curve was used to analyze the diagnostic performance of the 48-gene signature for NASH. The cutoff of the ROC curve for NASH was determined by Youden index. Survival analyses were performed after biopsies with the Kaplan–Meier method using a log-rank test and univariate and multivariate models with Cox regression method. Multivariate model was built using a backward stepwise procedure for selecting variables, retaining those with $p<0.05$. The assumption of proportional hazards over time was verified using the log–log graphic method and met by all covariates. Potential linearity of covariates was investigated by collinearity diagnostics before multivariate survival analysis. All tests with two-sided p-value <0.05 were considered significant. All analyses and figures were performed using the R-program (version 3.3.2; http://www.r-project.org), SPSS 25 statistical software (IBM, Armonk, NY, USA), or Excel 2010 (Microsoft Corporation, Redmond, WA). or R-program (version 3.3.2; http://www.r-project.org) with the pROC package.

6.3 – Results

6.3.1 – Patient characteristics

Among 105 RNA samples from 105 unique patients, four were excluded due to low-quality gene expression profiles (Figure 6.1). Table 6.1 summarized the clinical and histological characteristics of 101 patients analyzed in this chapter. Median age at biopsy was 50.9 years old. Fifty-eight percent had diabetes mellitus and 68% had hypertension. Liver tissue examination revealed cirrhosis in 17 (16.8%) patients at biopsy. During a median of 2.6 years of follow-up (IQR: 1.4-3.4), 10 (9.9%) patients without cirrhosis at biopsy progressed to cirrhosis. Of all 101 patients, 21 (20.8%) progressed to poor outcomes. Progression to poor outcomes refers to development of any one of the following during follow-up: liver decompensation, need for liver transplantation, or liver-related death.

6.3.2 – RNA quantity and quality

Adequate RNA was isolated from all liver tissues for NanoString gene expression assay. The quality (A_{260}/A_{280} spectrophotometry ratio) of the isolated RNA was between 1.73 and 1.99, which met manufacturer-recommended specifications.

6.3.3 – Comparison of the 48-gene signature with biochemical and histological parameters

The 48-gene signature was compared with biochemical and histological parameters at biopsy. The level of 48-gene signature was significantly correlated with an increased histological fibrosis stage ($r=0.801$, $p<0.001$) and increased levels of aspartate

aminotransferase (AST) (r=0.587, p<0.001), gamma-glutamyl transferase (GGT) (r=0.313, p=0.013), total bilirubin (r=0.299, p=0.004), as well as decreased levels of albumin (r=-0.376, p<0.001) and platelet counts (r=-0.565, p=0.01).

6.3.4 – The expression of 48-gene signature increased with disease severity

The 48-gene signature in liver tissues was compared across simple steatosis, NASH without cirrhosis, and NASH with cirrhosis (Figure 6.2). The expression of the 48-gene signature increased significantly with disease severity. The level of 48-gene signature was similar between simple steatosis and normal livers (negative control) and between NASH cirrhosis and explant NASH cirrhosis (positive control). The 48-gene signature had an area under the receiver operator characteristic curve (AUROC) of 0.89 (95% confidence interval, 0.82-0.95, p<0.001) for NASH and at a Youden index cutoff of 69.34, the 48-gene signature had 86% sensitivity, 80% specificity, and 83% of accuracy for NASH (Figure 6.3). Based on the 69.34 cutoff, the 48-gene signature was stratified into two groups, low and high 48-gene signature (Figure 6.4).

6.3.5 – Distribution of the histological fibrosis stage and 48-gene signature

Figure 6.4 showed the distribution of the 48-gene signature, histological fibrosis stage and clinical outcomes for all 101 patients. Seventeen (16.8%) patients had cirrhosis at biopsy. Of the 84 patients without cirrhosis at biopsy, 9% (3 of 33) with F0 fibrosis, 8% (2 of 24) with F1 fibrosis, 14% (1 of 7) with F2 fibrosis, and 20% (4 of 20) with F3 fibrosis progressed to cirrhosis during the follow-up period. The percentage of patients progressed to cirrhosis was similar across different fibrosis stages (p=0.581). Patients progressed to

cirrhosis had a marginally significantly higher 48-gene signature compared to patients who did not progress (p=0.055, Figure 6.5A), but histological fibrosis stage was similar between progressors vs. non-progressors (p=0.269, Figure 6.5B).

Of all 101 patients, 3% (1 of 33) with F0 fibrosis, 0% (0 of 24) with F1 fibrosis, 14% (1 of 7) with F2 fibrosis, 25% (5 of 20) with F3 fibrosis, and 83% (14 or 17) with F4 fibrosis at biopsy progressed to poor outcomes during follow-up. Patients progressed to poor outcomes had significantly higher 48-gene signature and histological fibrosis stage compared to patients who did not progress (both p<0.001, Figure 6.5C and 6.5D).

6.3.6 – The 48-gene signature predicts progression to cirrhosis, but histological fibrosis staging cannot

Of the 84 patients without cirrhosis at biopsy, patients with a high 48-gene signature had a marginally significantly higher probability of progression to cirrhosis compared to patients with a low 48-gene signature (21% vs. 4%, log-rank p=0.05, Figure 6.6A). However, the probability of progression to cirrhosis was similar between F2-F3 vs. F0-F1 (19% vs. 9%, log-rank p=0.172, Figure 6.6B). This supported that the 48-gene signature has a trend that can early predict progression to cirrhosis, but this was not possible by histological fibrosis stage.

6.3.7 – Variables associated with progression to cirrhosis

Univariate Cox regression analysis revealed present of diabetes mellitus (HR: 4.88 95% CI: 1.03-23.17, p=0.046) and increased HbA1c (HR: 1.82, 95% CI: 1.18-2.80, p=0.007) at biopsy were significantly associated with progression to cirrhosis (Table 6.2). There was

a trend that a high 48-gene signature (HR: 4.20 95% CI: 0.89-19.92, p=0.07) and increased BMI (HR: 1.06 95% CI: 1.00-1.12, p=0.07) at biopsy were associated with progression to cirrhosis. Histological fibrosis stage at biopsy was not associated with progression to cirrhosis. Multivariate analysis was not performed due to the small number of patients progressed to cirrhosis within a relatively short follow-up (n=10).

6.3.8 – Both histological fibrosis stage and 48-gene signature predict progression to poor outcomes

The probability of progression to poor outcomes was significantly higher in patients with a high 48-gene signature compared to patients with a low 48-gene signature (46% vs. 0%, respectively, log-rank p<0.001) and patients with higher fibrosis stages compared to patients with lower fibrosis stages (F0-F1: 2%, F2-F3: 22%, and F4: 82%, log-rank p<0.001) (Figure 6.7A and 6.7B).

6.3.9 – Variables associated with progression to poor outcomes

Univariate Cox regression analysis revealed increased levels of AST (HR: 1.01 95% CI: 1.00-1.01, p=0.04), GGT (HR: 1.001, 95% CI: 1.000-1.002, p=0.02), ALP (HR: 1.00, 95% CI: 1.00-1.01, p=0.046), total bilirubin (HR: 1.00, 95% CI: 1.00-1.01, p<0.001), and a higher fibrosis stage (F0-1 vs. F2-3: HR: 16.09, 95% CI: 1.87-138.9, p=0.01) and a high 48-gene signature (HR: 55.71, 95% CI: 1.61-1924, p=0.03), as well as decreased levels of albumin (HR: 0.9, 95% CI: 0.86-0.95, p<0.001) and platelet (HR: 0.99, 95% CI: 0.98-0.99, p<0.001) at biopsy were significantly associated with progression to poor outcomes (Table 6.3).

In a backward stepwise elimination Cox regression model starting with all prognostic factors with $p<0.05$ in univariate analysis as independent covariates, only increased ALT and decreased platelet counts at biopsy remained as significant variables in the final model (Table 6.3).

6.4 – Discussion

In this retrospective cohort study that covered the whole disease spectrum of patients with NAFLD, I showed a 48-gene signature can early predict progression to cirrhosis, but histological fibrosis stage and activity score cannot. This finding has a significant clinical relevance because the 48-gene signature can serve as a surrogate biomarker and provide personalized risk stratification to predict liver cirrhosis at an early time in the disease trajectory, long before the event. Moreover, the 48-gene signature can identify patients who may benefit from upcoming drug treatments to prevent further liver damage. As for clinical application, the 48-gene signature can be easily applied into a routine clinical assay using standard procurement and work-up of diagnostic liver biopsies.

Predicting progressive fibrosis in NAFLD is an unmet clinical need. Currently, NAFLD risk stratification mainly focused on measurement of the disease state at biopsy (histological activity score and fibrosis stage). Despite presence of NASH represents a more advanced disease, a portion of patients with only simple steatosis, behave as rapid progressors. Simple steatosis was initially recognized as a benign course with low-risk of fibrosis progression. However, a previous study found the proportion of patients who had fibrosis progression was not significantly different between simple steatosis and NASH (37% vs. 43%, $p = 0.65$) (20). They found 22% of patients with simple steatosis progressed to

bridging fibrosis or cirrhosis in a median 6.6 years of follow-up. These simple steatosis patients with high-risk of fibrosis progression cannot be identified by current available clinical or histological measurements. The findings in this chapter suggested that the 48-gene signature in liver tissues can overcome this gap by providing personalized risk stratification for progression to cirrhosis.

One of the aim of this chapter is to determine if there were any clinical or biochemical parameters that could predict fibrosis progression among patients with NAFLD. Unfortunately, conventional liver function tests cannot predict progression to cirrhosis. Only presence of diabetes mellitus (HR: 4.88, 95% CI: 1.03-23.17, p=0.046) and increased HbA1c level (HR: 1.82, 95% CI: 1.18-2.80, p=0.007) at biopsy were significantly associated with progression to cirrhosis. Increased BMI (HR: 1.06 95% CI: 1.00-1.12, p=0.07) also had a trend to be associated with progression to cirrhosis. These results matched with a previous study and was expected as the severity of the metabolic syndrome was reported associated with fibrosis progression (20).

This chapter had two major limitations that are important to acknowledge. First, there is a small number of patients that progressed to cirrhosis (n=10) due to a relatively short follow-up period (median 2.6 years). This resulted in the 48-gene signature had a trend, but a marginally significant p-value for progression to cirrhosis in the survival analyses. In a Kaplan-Meier analysis, patients with a high 48-gene signature had higher probability progression to cirrhosis compared to patients with a low 48-gene signature (21% vs. 4%, p=0.05, Figure 6.6A). In a univariate Cox regression analysis, there was also a trend that patients with a high 48-gene signature had a higher probability of progression to cirrhosis (HR: 4.20, 95% CI: 0.89-19.92, p=0.07). Future studies with more patients and longer

follow-up periods should be performed to assure confidence in these initial results. Second, this was not a controlled trial and therefore several potential confounding factors such as glycemic control or medications (e.g. anti-diabetic agents) that could impact fibrosis progression could not be assessed.

In conclusion, the 48-gene signature in routine clinical liver biopsy with NAFLD could identify high-risk patients for progression to cirrhosis. Measurement of the 48-gene signature at the time of biopsy should be considered as it can provide additional prognostic information that cannot be identified by histology. The prognostic information can provide risk stratification and help physicians to tailor upcoming NAFLD treatment regimen for individual patients.

Table 6.1. Patient characteristics

Characteristics	Patients evaluated, n	Median (IQR) or n (%)
Age at biopsy (yr), median (IQR)	93 (92.1%)	50.9 (43.7-58.9)
Sex male, n (%)	92 (91.1%)	48 (52.2)
Ethnicity white, n (%)	91 (90.1%)	84 (92.3)
BMI, median (IQR)	75 (74.3%)	30.9 (27.5-36.0)
Diabetes mellitus, n (%)	89 (88.1%)	52 (58.4)
Hypertension, n (%)	72 (71.3%)	49 (68.1)
Hyperlipidemia, n (%)	86 (85.1%)	80 (93.0)
Biochemistry at biopsy		
AST, U/L, median (IQR)	67 (66.3%)	47 (29.0-104.0)
ALT, U/L, median (IQR)	90 (89.1%)	58 (32.8-99.0)
ALP, U/L, median (IQR)	91 (90.1%)	100 (76.0-145.0)
GGT, U/L, median (IQR)	62 (61.3%)	90 (40.8-257.8)
Total bilirubin, umol/L, median (IQR)	91 (90.1%)	10 (13.0-20.0)
Platelet, 10^9/L, median (IQR)	91 (90.1%)	203 (140.0-252.0)
HbA1c, %, median (IQR)	73 (72.3%)	6.0 (5.3-6.9)
Histology		
Brunt fibrosis stage, n (%)	101 (100%)	
0		33 (32.7)
1		24 (23.8)
2		7 (6.9)
3		20 (19.8)
4		17 (16.8)
Diagnosis, n (%)	101 (100%)	
Simple steatosis		46 (45.5)
NASH without cirrhosis		38 (37.6)
NASH with cirrhosis		17 (16.8)
Follow-up (years), median (IQR)	101 (100%)	2.6 (1.4-3.4)

Fibrosis outcome, n (%)	101 (100%)	
Cirrhosis at biopsy		17 (16.8)
Progressed to cirrhosis		10 (9.9)
Did not progress to cirrhosis		74 (73.3)
Progressed to poor outcomes, n (%)	101 (100%)	21 (20.8)

IQR, interquartile range. Percentage might not add up to 100% because of rounding.

Table 6.2. Variables associated with progression to cirrhosis (n=84 patients, 10 events)

Variable	Univariate analysis		
	HR	95% CI	p-value
Age at biopsy, year	1.00	0.96-1.04	0.97
Gender			
Female (reference)	1.00		
Male	0.88	0.24-3.19	0.88
BMI	1.06	1.00-1.12	0.07
Hypertension			
No (reference)	1.00		
Yes	1.98	0.39-10.07	0.41
Diabetes mellitus			
No (reference)	1.00		
Yes	4.88	1.03-23.17	**0.046**
Hyperlipidemia			
No (reference)	1.00		
Yes	0.76	0.10-6.03	0.76
ALT at biopsy	1.00	0.99-1.01	0.88
AST at biopsy	0.99	0.97-1.01	0.50
GGT at biopsy	1.00	0.99-1.01	0.48
ALP at biopsy	1.00	1.00-1.01	0.55
Albumin at biopsy	0.91	0.80-1.04	0.17
Total bilirubin at biopsy	0.95	0.85-1.05	0.30
Platelet at biopsy	1.01	1.00-1.01	0.28
HbA1c at biopsy	1.82	1.18-2.80	**0.007**
Brunt fibrosis stage			
F0-F1 (reference)	1.00		
F2-F3	2.37	0.66-8.55	0.66
48-gene signature			
Low 48-gene signature	1.00		
High 48-gene signature	4.20	0.89-19.92	0.07

Table 6.3. Variables associated with progression poor outcomes (n=101 patients, 21 events)

Variable	Univariate analysis			Multivariate analysis (backward stepwise elimination)		
	HR	95% CI	p-value	HR	95% CI	p-value
Age at biopsy, year	1.03	1.00-1.07	0.06			
Gender						
Female (reference)	1.00					
Male	0.41	0.17-1.03	0.06			
BMI	1.01	0.95-1.06	0.87			
Hypertension						
No (reference)	1.00					
Yes	1.93	0.54-6.83	0.31			
Diabetes mellitus						
No (reference)	1.00					
Yes	1.97	0.76-5.11	0.17			
Hyperlipidemia						
No (reference)	1.00					
Yes	1.44	0.18-10.32	0.76			
ALT at biopsy	0.99	0.98-1.00	0.06			
AST at biopsy	1.01	1.00-1.01	**0.04**			
GGT at biopsy	1.001	1.000-1.002	**0.02**			
ALP at biopsy	1.00	1.00-1.01	**0.046**	1.004	1.000-1.008	**0.03**
Albumin at biopsy	0.90	0.86-0.95	**<0.001**			
Total bilirubin at biopsy	1.01	1.00-1.01	**<0.001**			
Platelet at biopsy	0.99	0.98-0.99	**<0.001**	0.98	0.97-0.99	**0.003**
HbA1c at biopsy	1.11	0.86-1.43	0.41			
Brunt fibrosis stage						
F0-F1 (reference)	1.00					
F2-F3	16.09	1.87-138.9	**0.01**			
F4	96.25	11.02-840.9	**<0.001**			

48-gene signature				
Low 48-gene signature	1.00			
High 48-gene signature	55.71	1.61-1924	**0.03**	

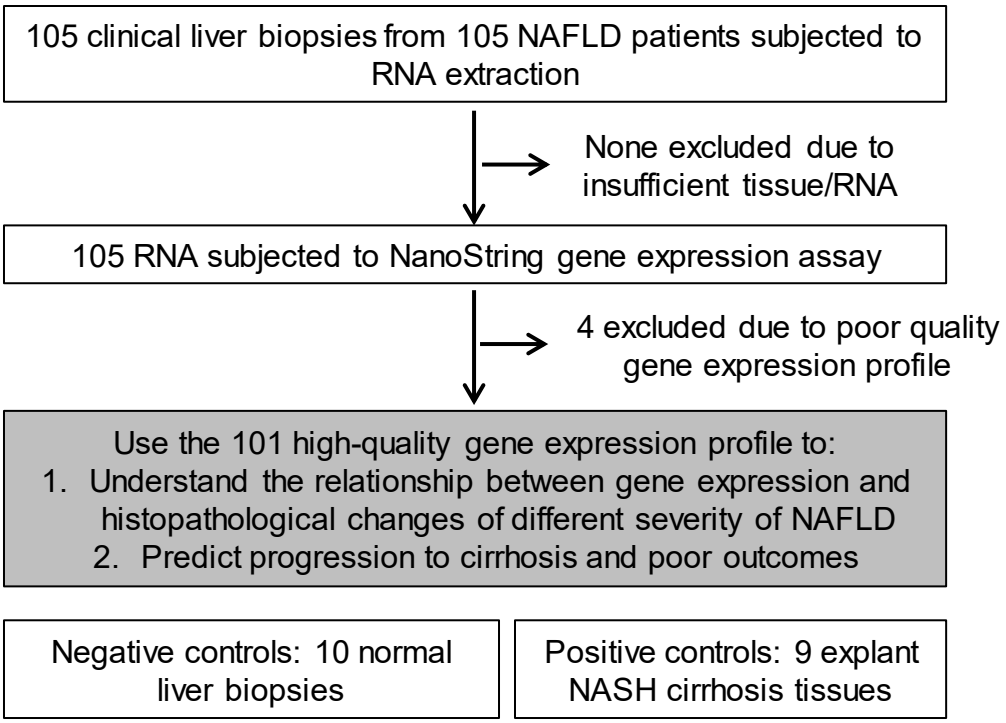

Figure 6.1. Study design.

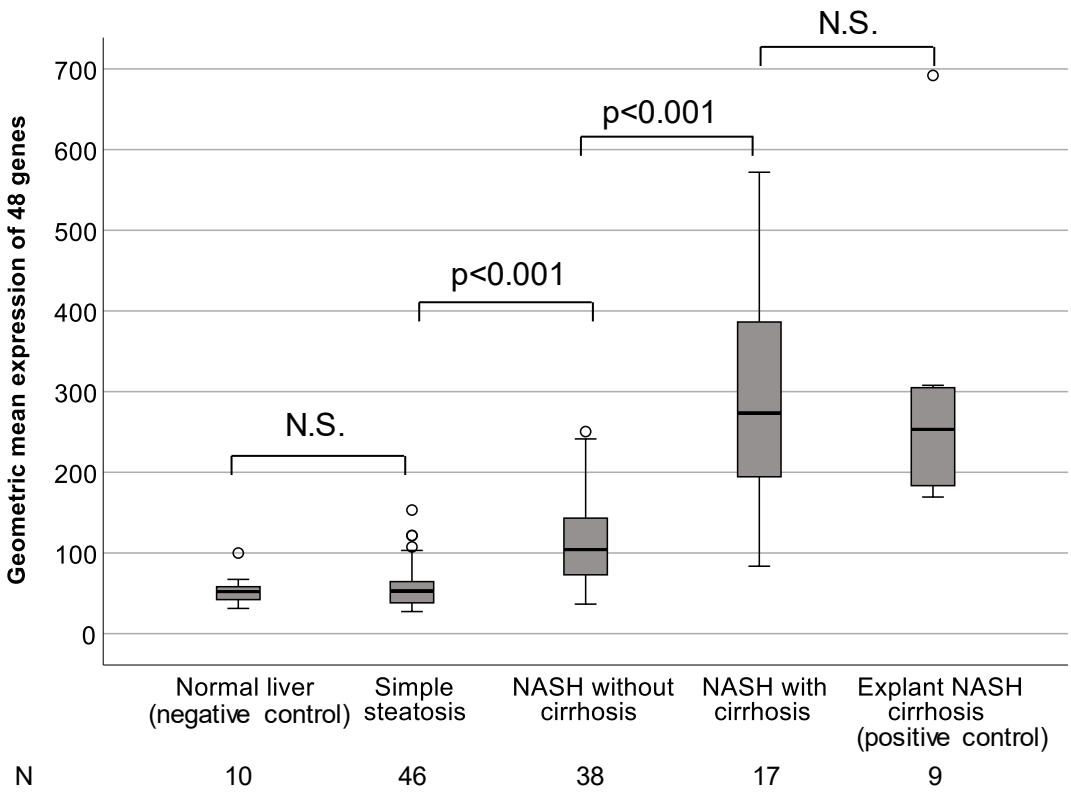

Figure 6.2. The 48-gene signature increased with disease severity.
N.S., non-significant (p>0.05).

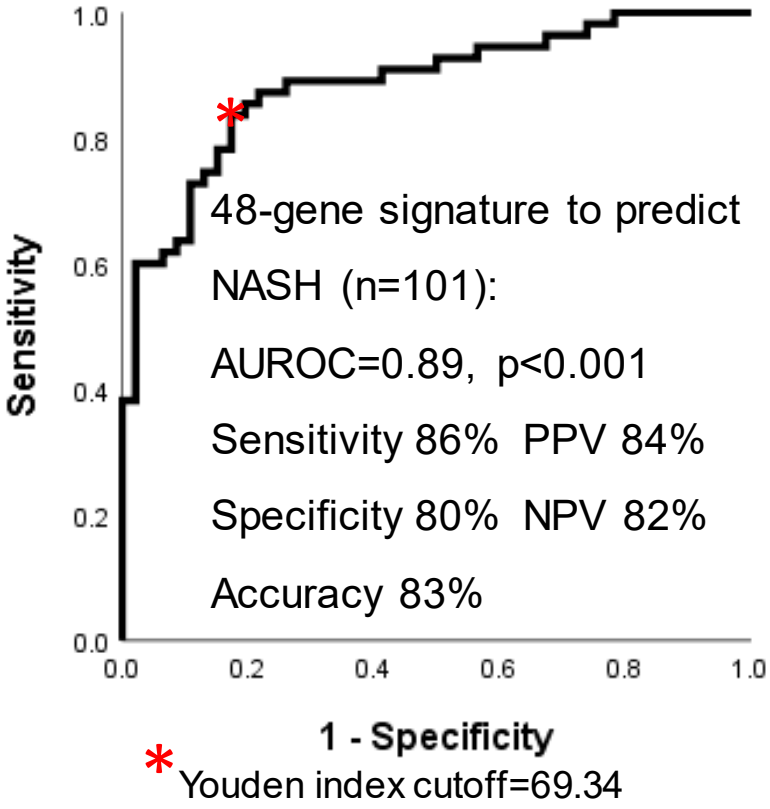

Figure 6.3. The performance of 48-gene signature for NASH.

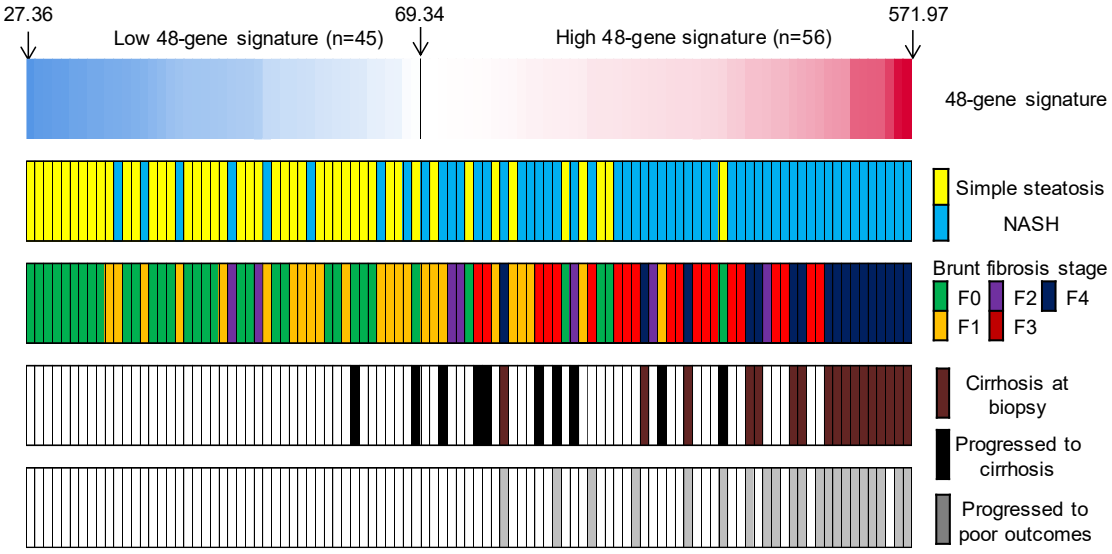

Figure 6.4. The distribution of 48-gene signature, histological fibrosis stage, and outcomes of all 101 NAFLD patients.

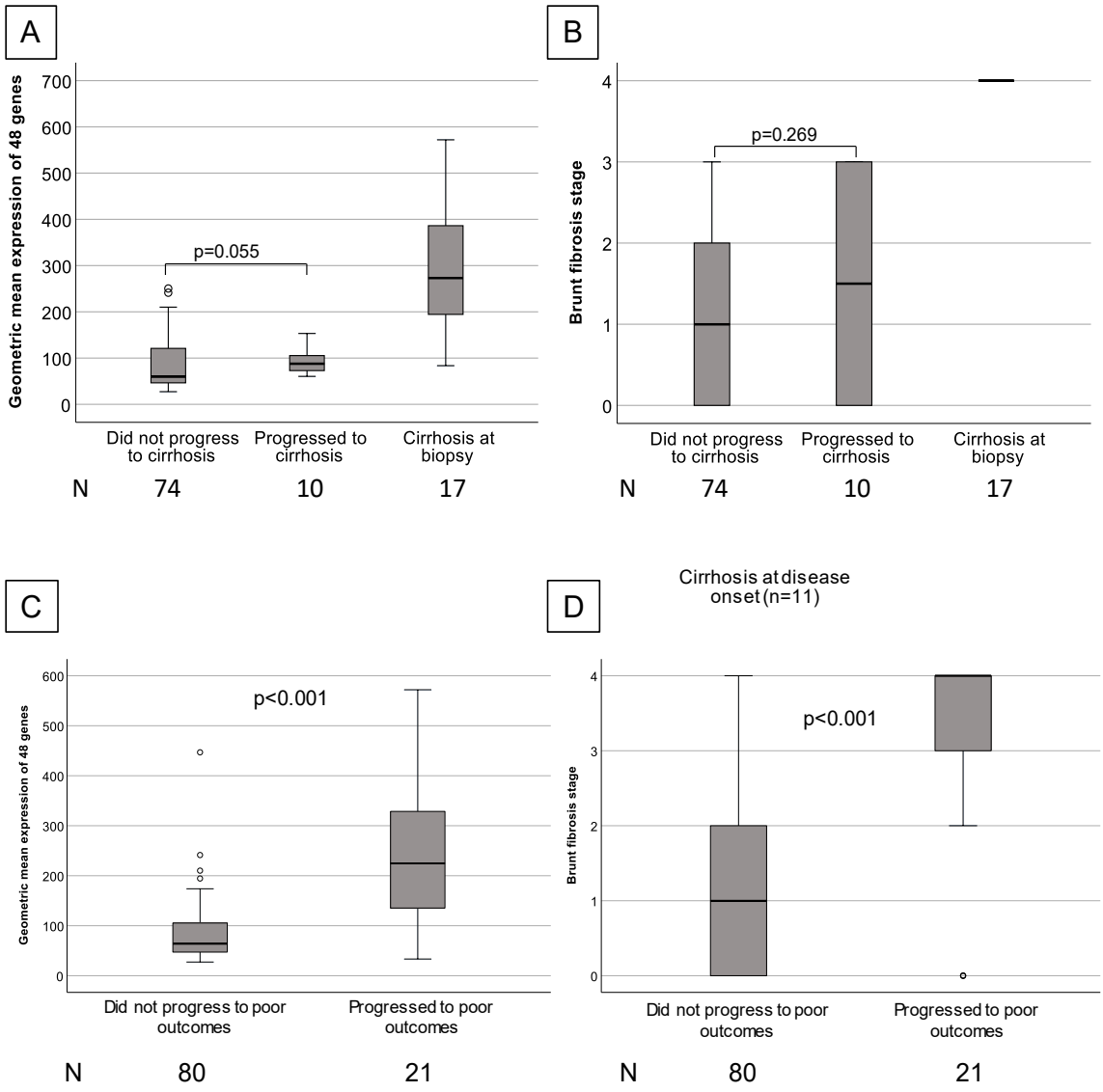

Figure 6.5. The 48-gene signature values and histological fibrosis stages grouped according to different outcomes.

(A) Patients progressed to cirrhosis had a marginally significantly higher 48-gene signature compared to patients who did not progress (p=0.055). (B) Patients progressed to cirrhosis had similar histological fibrosis stage compared to patients who did not progress (p=0.269). (C) Patients progressed to poor outcomes had significantly higher 48-gene signature compared to patients who did not progress (p<0.001). (D) Patients progressed to poor outcomes had significantly higher histological fibrosis stage compared to patients who did not progress (p<0.001).

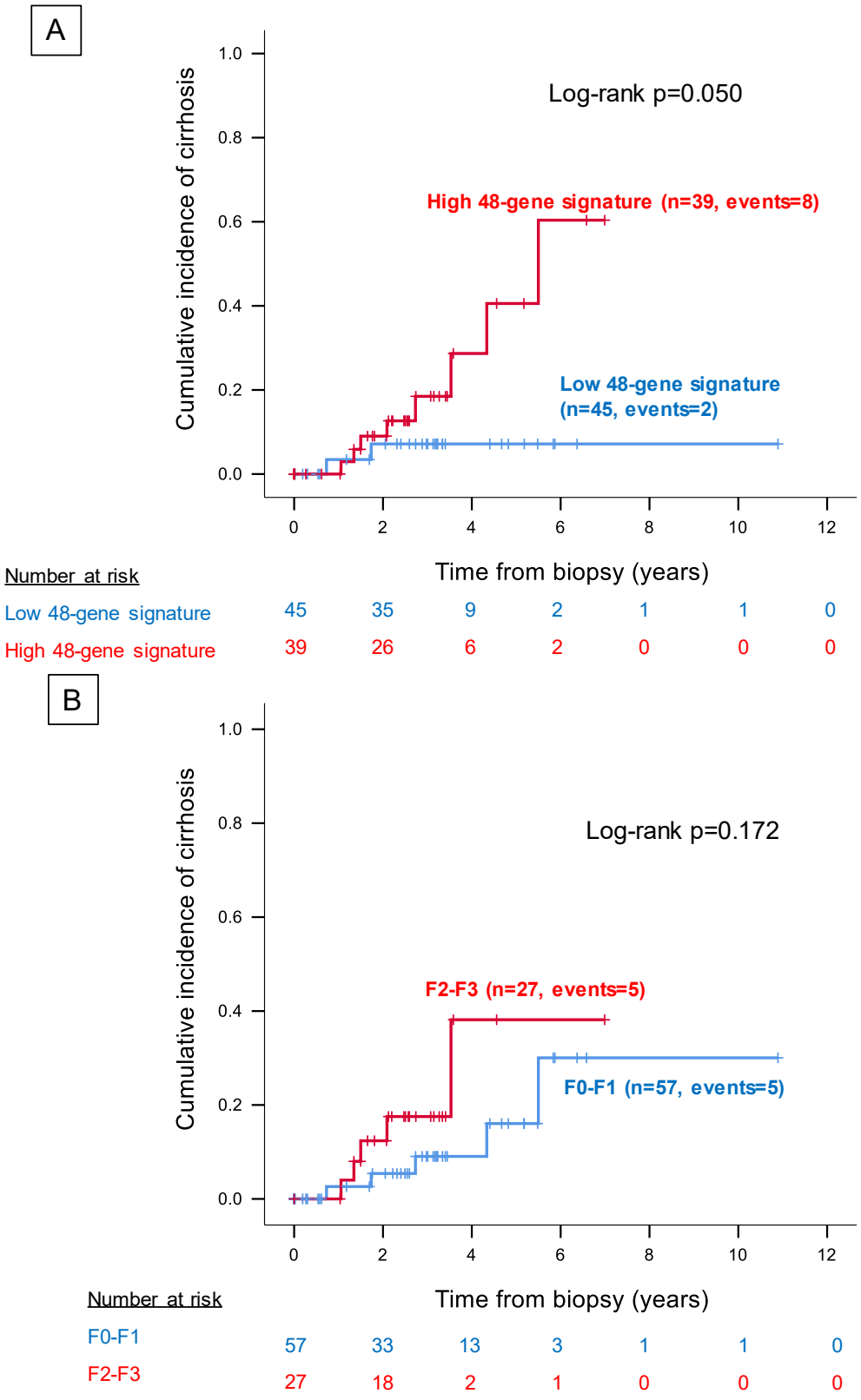

Figure 6.6. Cumulative incidence of cirrhosis in patients without cirrhosis at biopsy stratified by (A) the 48-gene signature and (B) histological fibrosis stage.

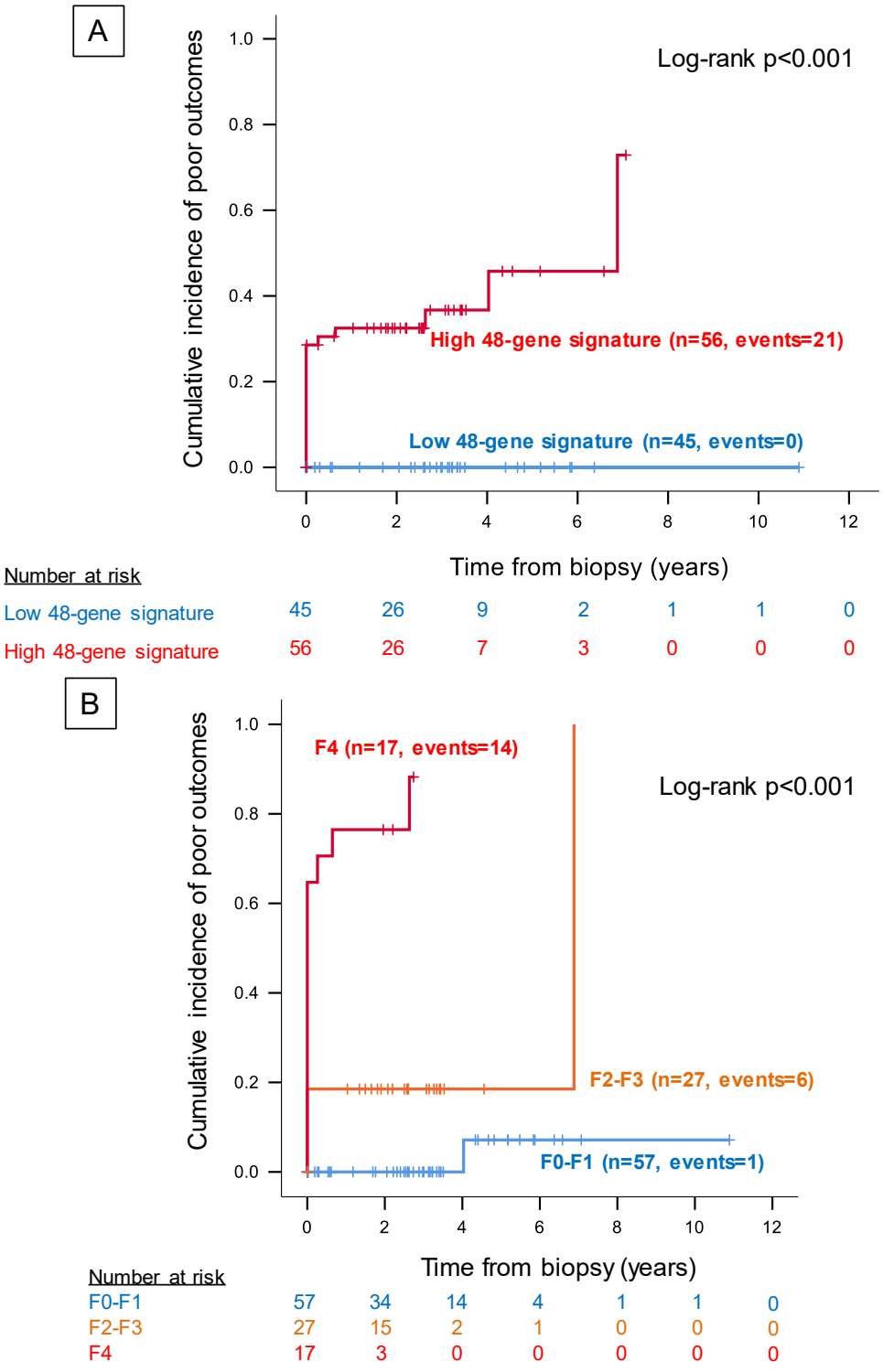

Figure 6.7. Cumulative incidence of poor outcomes in patients stratified by (A) the 48-gene signature and (B) histological fibrosis stage.

6.5 – References

1. Younossi ZM, Koenig AB, Abdelatif D, Fazel Y, Henry L, Wymer M. Global epidemiology of nonalcoholic fatty liver disease-Meta-analytic assessment of prevalence, incidence, and outcomes. Hepatology 2016 Jul;64(1):73-84.
2. Bataller R, Rombouts K, Altamirano J, Marra F. Fibrosis in alcoholic and nonalcoholic steatohepatitis. Best Pract Res Clin Gastroenterol 2011 Apr;25(2):231-244.
3. Bataller R, Brenner DA. Liver fibrosis. J Clin Invest 2005 Feb;115(2):209-218.
4. Ekstedt M, Hagstrom H, Nasr P, Fredrikson M, Stal P, Kechagias S, et al. Fibrosis stage is the strongest predictor for disease-specific mortality in NAFLD after up to 33 years of follow-up. Hepatology 2015 May;61(5):1547-1554.
5. Singh S, Allen AM, Wang Z, Prokop LJ, Murad MH, Loomba R. Fibrosis progression in nonalcoholic fatty liver vs nonalcoholic steatohepatitis: a systematic review and meta-analysis of paired-biopsy studies. Clin Gastroenterol Hepatol 2015 Apr;13(4):643-654.
6. Friedman SL, Neuschwander-Tetri BA, Rinella M, Sanyal AJ. Mechanisms of NAFLD development and therapeutic strategies. Nat Med 2018 Jul;24(7):908-922.
7. Nasr P, Ignatova S, Kechagias S, Ekstedt M. Natural history of nonalcoholic fatty liver disease: A prospective follow-up study with serial biopsies. Hepatol Commun 2018 Feb;2(2):199-210.
8. Sanyal AJ. Past, present and future perspectives in nonalcoholic fatty liver disease. Nat Rev Gastroenterol Hepatol 2019 Jun;16(6):377-386.

9. Ratziu V. A critical review of endpoints for non-cirrhotic NASH therapeutic trials. J Hepatol 2018 Feb;68(2):353-361.

10. Friedman SL, Ratziu V, Harrison SA, Abdelmalek MF, Aithal GP, Caballeria J, et al. A randomized, placebo-controlled trial of cenicriviroc for treatment of nonalcoholic steatohepatitis with fibrosis. Hepatology 2018 May;67(5):1754-1767.

11. Moylan CA, Pang H, Dellinger A, Suzuki A, Garrett ME, Guy CD, et al. Hepatic gene expression profiles differentiate presymptomatic patients with mild versus severe nonalcoholic fatty liver disease. Hepatology 2014 Feb;59(2):471-482.

12. Romeo S, Kozlitina J, Xing C, Pertsemlidis A, Cox D, Pennacchio LA, et al. Genetic variation in PNPLA3 confers susceptibility to nonalcoholic fatty liver disease. Nat Genet 2008 Dec;40(12):1461-1465.

13. Kozlitina J, Smagris E, Stender S, Nordestgaard BG, Zhou HH, Tybjaerg-Hansen A, et al. Exome-wide association study identifies a TM6SF2 variant that confers susceptibility to nonalcoholic fatty liver disease. Nat Genet 2014 Apr;46(4):352-356.

14. Brunt EM, Janney CG, Di Bisceglie AM, Neuschwander-Tetri BA, Bacon BR. Nonalcoholic steatohepatitis: a proposal for grading and staging the histological lesions. Am J Gastroenterol 1999 Sep;94(9):2467-2474.

15. Yeh MM, Brunt EM. Pathological features of fatty liver disease. Gastroenterology 2014 Oct;147(4):754-764.

16. Wong VW, Vergniol J, Wong GL, Foucher J, Chan HL, Le BB, et al. Diagnosis of fibrosis and cirrhosis using liver stiffness measurement in nonalcoholic fatty liver disease. Hepatology 2010 Feb;51(2):454-462.

17. Lens S, Torres F, Puigvehi M, Marino Z, Londono MC, Martinez SM, et al. Predicting the development of liver cirrhosis by simple modelling in patients with chronic hepatitis C. Aliment Pharmacol Ther 2016 Feb;43(3):364-374.

18. Manousou P, Burroughs AK, Tsochatzis E, Isgro G, Hall A, Green A, et al. Digital image analysis of collagen assessment of progression of fibrosis in recurrent HCV after liver transplantation. J Hepatol 2013 May;58(5):962-968.

19. Friedman LS. Surgery in the patient with liver disease. Trans Am Clin Climatol Assoc 2010;121:192-204.

20. McPherson S, Hardy T, Henderson E, Burt AD, Day CP, Anstee QM. Evidence of NAFLD progression from steatosis to fibrosing-steatohepatitis using paired biopsies: implications for prognosis and clinical management. J Hepatol 2015 May;62(5):1148-1155.

Chapter 7: Protein Level Validation of the Fibrosis Gene Signature by Objective Immunostaining Quantification

7.1 – Introduction

In Chapters 4, 5, and 6, I showed a 48-gene signature in clinical liver biopsies can predict fibrosis progression in patients with recurrent viral hepatitis C (HCV), autoimmune hepatitis (AIH), and non-alcoholic fatty liver disease (NAFLD), respectively. However, mRNA levels may or may not correspond to the protein content in the tissues, and as protein is the key molecule that mediates catalytic and enzymatic functions, it is critical to assure that the observed mRNA expression changes were accompanied by changes in expression of the respective proteins. If mRNA levels and protein expression levels in tissues are correlated, this knowledge could potentially be used to develop immunohistochemical analysis of tissue sections and automated quantification of the staining as a diagnostic ancillary test.

Hepatic stellate cells (HSCs) and hepatic progenitor cells (HPCs) are proposed as two main contributors to liver fibrosis in non-biliary diseases (1, 2). Majority of the 48-gene signature were expressed by HPCs, defined as epithelial cell adhesion molecule (EPCAM) positive cells (Table 2.9). During liver injury, quiescent HPCs become activated and cause ductular reaction, characterized by the proliferation of reactive bile ducts (3). The degree of ductular reaction correlated closely with the severity of fibrosis across different chronic liver diseases, including HCV (4), alcoholic hepatitis (5), and NAFLD (3). EPCAM and keratin 7 (KRT7) are well defined HPC markers that marks newly derived hepatocytes and bile ducts from HPCs (6, 7). These two genes were present in the 48-gene signature. A previous study reported that protein expression of EPCAM and KRT7 can predict 90-days mortality in patients with alcoholic hepatitis (8). However, it is totally unknown if HPC markers have a

prognostic value for predicting fibrosis progression in many of the chronic liver diseases.

Immunohistochemistry (IHC) reveals the presence, location and cellular origin of a specific protein in tissue sections. It allows study of the distribution and localization of specific cellular components by providing supplemental information to the routine morphological assessment of tissues. This could provide additional diagnostic and prognostic information relative to disease status and biology. The target protein expression can be quantified by computerized image analysis, which measures the area of staining and the area of remaining liver tissue and produces the proportion of the area of the biopsy occupied by the stain. This technique can be adapted in routine pathology workflow. In this chapter, I used the clinical liver biopsies in Chapters 4, 5, and 6 with available tissue after NanoString gene expression assay and analyzed the protein expression of EPCAM and KRT7 by IHC. This chapter aims to understand the relationship between the mRNA and protein expression of EPCAM and KRT7 as representative markers in clinical liver biopsies and to analyze if protein expression can predict progression to cirrhosis, liver decompensation, and liver-related death, using a simple IHC experiment that can be easily applied into clinical pathology labs.

7.2 – Materials and Methods

7.2.1 – Liver samples and histological examination

I analyzed 94 clinical liver biopsies from 94 patients in Chapters 4, 5, and 6 with available tissue after routine clinical diagnosis and NanoString gene expression assay (Figure 7.1). Additional four cirrhotic explant livers were included as extreme phenotype samples (1 with HCV, 1 with primary biliary cirrhosis, 1 with alcoholic steatohepatitis, and 1 with non-

alcoholic steatohepatitis). The liver biopsy specimens with recurrent HCV and AIH were staged for fibrosis according to Metavir staging system (9) and NAFLD was staged according to Brunt staging system (10).

7.2.2 – Immunohistochemistry

The IHC staining was performed by lab technicians at Alberta Health Services, Edmonton zone, immunohistochemistry lab. Both EPCAM and KRT7 staining were performed on Dako Autostainer Link 48 (Agilent, Santa Clara, CA). Four-µm section of formalin-fixed paraffin-embedded tissue were cut and subsequently mounted onto Leica APEX slides and baked at 60 degrees for 1 hour. The tissue sections were deparaffinized with xylene, rehydrated with graded alcohols, and washed in distilled water. EPCAM slides were retrieved with Envision Flex Target Retrieval Solution, Low pH (Dako, K8005) in the Dako PT Link for 20 minutes at 97 degrees. KRT7 sections were retrieved with Envision Flex Target Retrieval Solution, High pH (Dako, K8000) in the Dako PT Link for 20 minutes at 97 degrees. Tissue sections were then immersed in 3% hydrogen peroxide in methanol to inactivate endogenous peroxidase. After blocking non-specific antibody, EPCAM slides were stained with mouse monoclonal MOC-31 (Dako M3525) at a 1/25 dilution for 20 minutes at room temperature followed by Mouse Linker (Dako, SM804) for 15 minutes and then horseradish peroxidase (Dako, SM802) for 20 minutes and KRT7 slides were stained with mouse monoclonal OV-TL 12/30 (Dako, IR619) pre-dilute applied to slides for 20 minutes at room temperature followed by horseradish peroxidase (Dako, SM802) for 20 minutes. Visualization was performed using Ventana Ultraview 3,3'-diaminobenzidine (DAB) (Dako, SM803) chromogen detection for 10 minutes. The slides were then counterstained on the DAKO Autostainer using Hematoxylin Gill I (Leica, 30801500) for 3

minutes and mounted. A positive and a negative control slide per batch for each stain were included. In each case, bile ducts were used as internal positive controls. Histologically normal livers were used as baseline controls and cirrhotic explant livers as extreme phenotype samples.

7.2.3 – Whole slide image scanning

High-resolution digital whole slide images were generated using Aperio ScanScope CS (Aperio Technologies, Inc., Vista, CA) at 20x magnification (resolution of 0.50 μm/pixel). All slides had a quality factor >90 (range 0-100) and I did manual quality checks of all slides to ensure that the scanned images were faithful to the original glass slide with appropriate background staining and were in-focus. Analysis alterations caused by tissue folds and staining artifacts were eliminated from the analysis boxes with a negative pen tool. The scanned liver tissues were then analyzed by Aperio Imagescope Positive Pixel Count algorithm v9, with a hue value = 0.0 and a hue width = 0.4. The algorithm automatically analyzed the positive DAB staining of the selected regions into three different colored pixels: strong positive (red), positive (orange), and weak positive (yellow) (Figure 7.2). The hematoxylin counterstain was represented by blue negative pixels. The percentage of positive pixels was calculated: positivity (%) = (weak positive + positive + strong positive pixels) / (total number of positive and negative pixels) × 100.

7.2.4 – RNA isolation and NanoString gene expression quantification

Details of RNA isolation and gene expression quantification were previously described in Chapters 3.2.4 and 3.2.5, respectively.

7.2.5 – NanoString quality control and data preprocessing

Details of NanoString quality control and data preprocessing were previously described in Chapter 3.2.6.

7.2.6 – Study endpoint

The primary study endpoint was progression to cirrhosis, defined as absence of cirrhosis in the initial biopsy and had Metavir fibrosis stage 4 in follow-up biopsies or Fibroscan >12.5 kPa (recurrent HCV), >14 kPa (AIH), or >10.3 kPa (NAFLD) in follow-up clinical visits (11-13). The secondary study endpoint was progression to poor outcomes, defined as any one of the following: development of liver decompensation, need for liver transplantation, or liver-related death (14). Liver-related death was defined as death caused by liver failure: nearest liver function test with total bilirubin > 50 umol/L and international normalized ratio (INR) > 1.7 before deceased (15, 16).

7.2.7 – Statistical analysis

Continuous variables were presented as median and interquartile range (IQR) and categorical variables were presented as number and percentage. Correlation coefficients were analyzed using Spearman rank-order correlation. Sensitivity, specificity, positive predictive value, negative predictive value, accuracy, and area under the receiver operating characteristic curve (AUROC) values of EPCAM and KRT7 protein expression for predicting progression to cirrhosis were calculated. Cumulative incidence of progression to cirrhosis or poor outcomes was calculated using Kaplan-Meier method with log-rank test. All tests with two-sided p-value <0.05 were considered significant. All analyses and figures

were performed using SPSS 25 statistical software (IBM, Armonk, NY, USA).

7.3 – Results

7.3.1 – Patient characteristics

The 94 liver biopsy specimens from 94 patients consisted of eight cases of recurrent HCV, 21 AIH, 62 NAFLD, and three livers with normal histology (Table 7.1). Table 7.2 listed the disease and fibrosis stage of 94 liver biopsies. Of 94 patients, 15 (16.0%) had cirrhosis at biopsy and 11 (11.7%) progressed to cirrhosis during follow-up (Table 7.1). Nineteen (20.2%) patients progressed to poor outcomes, which refer to development of any one of the following during follow-up: liver decompensation, need for liver transplantation, or liver-related death.

7.3.2 – Significant positive correlation between mRNA and protein expression of EPCAM and KRT7

There was a significant positive correlation between the mRNA and the protein expression of EPCAM ($r=0.667$, $p<0.001$) as well as between the mRNA and the protein expression of KRT7 ($r=0.788$, $p<0.001$) (Figure 7.3A and 7.3B). This confirms that upregulation of EPCAM and KRT7 mRNA expression led to an increase of the protein expression of EPCAM and KRT7 in most of the biopsy samples.

7.3.3 – EPCAM protein expression predicts progression to cirrhosis and poor outcomes

Of all 94 patients, 15 (16%) had cirrhosis at biopsy. Of the 79 patients without

cirrhosis at biopsy, patients who progressed to cirrhosis had significantly higher EPCAM protein expression compared to patients who did not progress ($p<0.001$, Figure 7.4A). Protein expression of EPCAM had an AUROC of 0.82 (95% confidence interval, 0.67-0.97, $p=0.001$) for predicting progression to cirrhosis (Figure 7.4B). The Youden index cutoff of the ROC curve at 2.55% as an immunostaining cutoff had 73% sensitivity, 91% specificity, and 89% of accuracy for predicting progression to cirrhosis. Based on the 2.55% cutoff, the patients were stratified into two groups, low and high EPCAM expression.

Non-cirrhotic patients at biopsy with a high EPCAM expression had significantly higher probability of progression to cirrhosis compared to patients with a low EPCAM expression (57% vs. 5%, log-rank $p<0.001$, Figure 7.5A).

Patients with a high EPCAM expression at biopsy had significantly higher probability of progression to poor outcomes compared to patients with a low EPCAM expression (45% vs. 13%, log-rank $p<0.001$, Figure 7.5B).

7.3.4 – KRT7 protein expression predicts progression to cirrhosis and poor outcomes

Of the 79 patients without cirrhosis at biopsy, patients who progressed to cirrhosis had significantly higher KRT7 protein expression compared to patients who did not progress ($p<0.001$, Figure 7.6A). Protein expression of KRT7 had an AUROC of 0.82 (95% confidence interval, 0.65-0.99, $p=0.001$) for predicting progression to cirrhosis (Figure 7.6B). The Youden index cutoff of the ROC curve at 1.46% as an immunostaining cutoff had 73% sensitivity, 87% specificity, and 85% of accuracy for predicting progression to cirrhosis. Based on the 1.46% cutoff, patients were stratified into two groups, low and high

KRT7 expression.

Non-cirrhotic patients at biopsy with a high KRT7 expression had significantly higher probability of progression to cirrhosis compared to patients with a low KRT7 expression (47% vs. 5%, log-rank $p<0.001$, Figure 7.7A).

Patients with a high EPCAM expression at biopsy had significantly higher probability of progression to poor outcomes compared to patients with a low KRT7 expression (43% vs. 11%, log-rank $p<0.001$, Figure 7.7B).

7.4 – Discussion

This chapter analyzed the protein expression of two HPC markers (EPCAM and KRT7), which were in the 48-fibrosis gene signature, in liver tissues with different diseases and confirmed that an increase of mRNA expression of EPCAM and KRT7 led to an increase of EPCAM and KRT7 protein expression. The results supported that HPC proliferation is a shared feature of progressive liver disease in different etiologies and the protein expression EPCAM and KRT7 could serve as potential surrogate markers for predicting progression to cirrhosis, liver decompensation, and liver-related death. This surrogate marker and quantification method can be easily applied to routine diagnostic liver biopsies.

This is the first study that showed the protein expression of EPCAM and KRT7 can predict progression to cirrhosis in patients with chronic liver disease of different etiologies. Previous studies only reported that HPC proliferation was associated with the severity of liver fibrosis (3-5), but had not addressed if HPC proliferation was associated with fibrosis progression. A previous study analyzed 59 patients with alcoholic hepatitis and showed increased gene and protein expression of EPCAM and KRT7 in liver biopsies were

associated with 90-days mortality (8). However, most of their patients were cirrhotic (74%) and were in acute-on-chronic condition. Currently little is known about the prognostic value of HPC makers in early stage liver disease. The unique finding of this chapter is HPC proliferation may occur not only in late stage, but also in early stage of chronic liver disease and the degree of HPC proliferation can predict progression to cirrhosis before fibrosis deposit in the liver.

Currently there is a debate on whether fibrosis deposition leads to HPC-associated regenerative response or whether fibrosis is exacerbated by the profibrogenic factors from the HPCs during ductular reaction (17). In this chapter, I found patients in early stage of liver disease with high EPCAM and KRT7 protein expression had significantly higher probability of progression to cirrhosis (Figure 7.5 and 7.7). This result supported that in early stage of liver disease, HPC proliferation might contribute more to fibrosis exacerbation rather than fibrosis regression.

This chapter showed that the protein expression of EPCAM and KRT7 can predict progression to cirrhosis and poor outcomes in early stage of different chronic liver diseases. This suggested that HPC proliferation plays an important role in fibrosis progression and could serve as a prognostic marker for fibrosis progression in routine diagnostic liver biopsies.

Table 7.1. Patient characteristics

Patient characteristics	Patients evaluated, n (%)
Disease	
Normal	3 (3.2)
Recurrent viral hepatitis C	8 (8.5)
Autoimmune hepatitis	21 (22.3)
Non-alcoholic fatty liver disease	62 (66.0)
Fibrosis outcome	
Cirrhosis at biopsy	15 (16.0)
Progressed to cirrhosis	11 (11.7)
Did not progress to cirrhosis	68 (72.3)
Progressed to poor outcomes	19 (20.2)

Table 7.2. Biopsy characteristics

Disease	F0	F1	F2	F3	F4	Total
Normal, n	3	0	0	0	0	3
Recurrent viral hepatitis C, n	2	3	2	1	0	8
Autoimmune hepatitis, n	3	6	4	5	3	21
Simple steatosis, n	12	10	1	0	0	23
Non-alcoholic steatohepatitis, n	0	10	5	12	12	39
Total, n	20	29	12	18	15	94

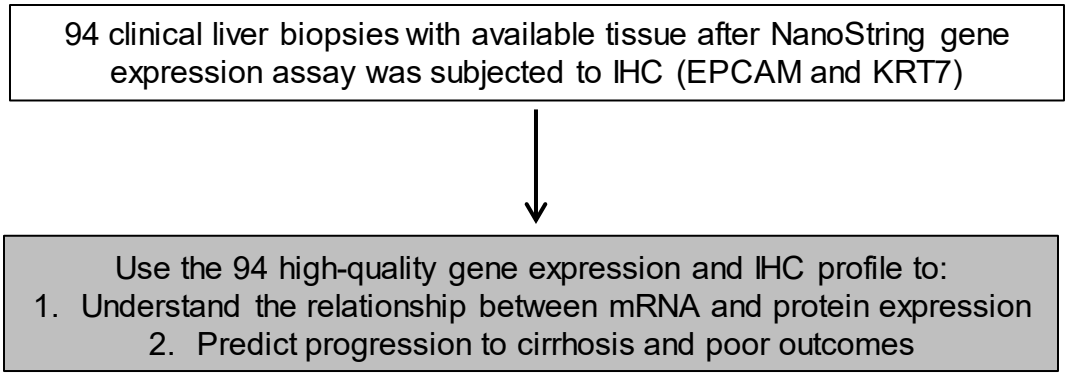

Figure 7.1 Study design.

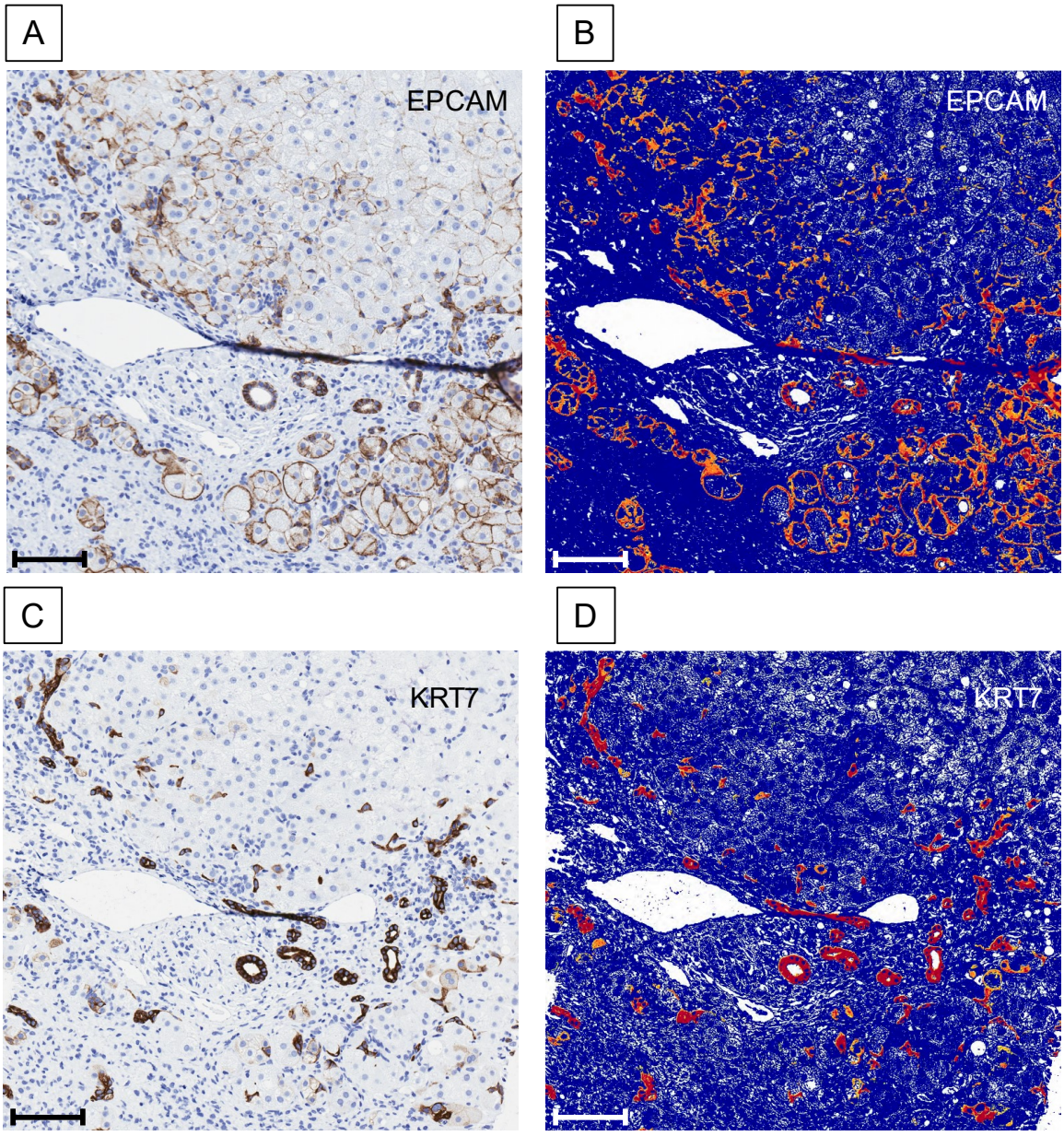

Figure 7.2. Imaging analysis using Aperio Imagescope Positive Pixel Count algorithm.

(A) Digital image of EPCAM-stained liver biopsy slide and (B) corresponding analysis mark-up image (Aperio ImageScope Positive Pixel Count algorithm, hue value 0.0, hue width 0.4, original 20x magnification, 100 µm measurement bar). (C) Digital image of KRT7-stained liver biopsy slide and (D) corresponding analysis mark-up image (Aperio ImageScope Positive Pixel Count algorithm, hue value 0.0, hue width 0.4, original 20x magnification, 100 µm measurement bar).

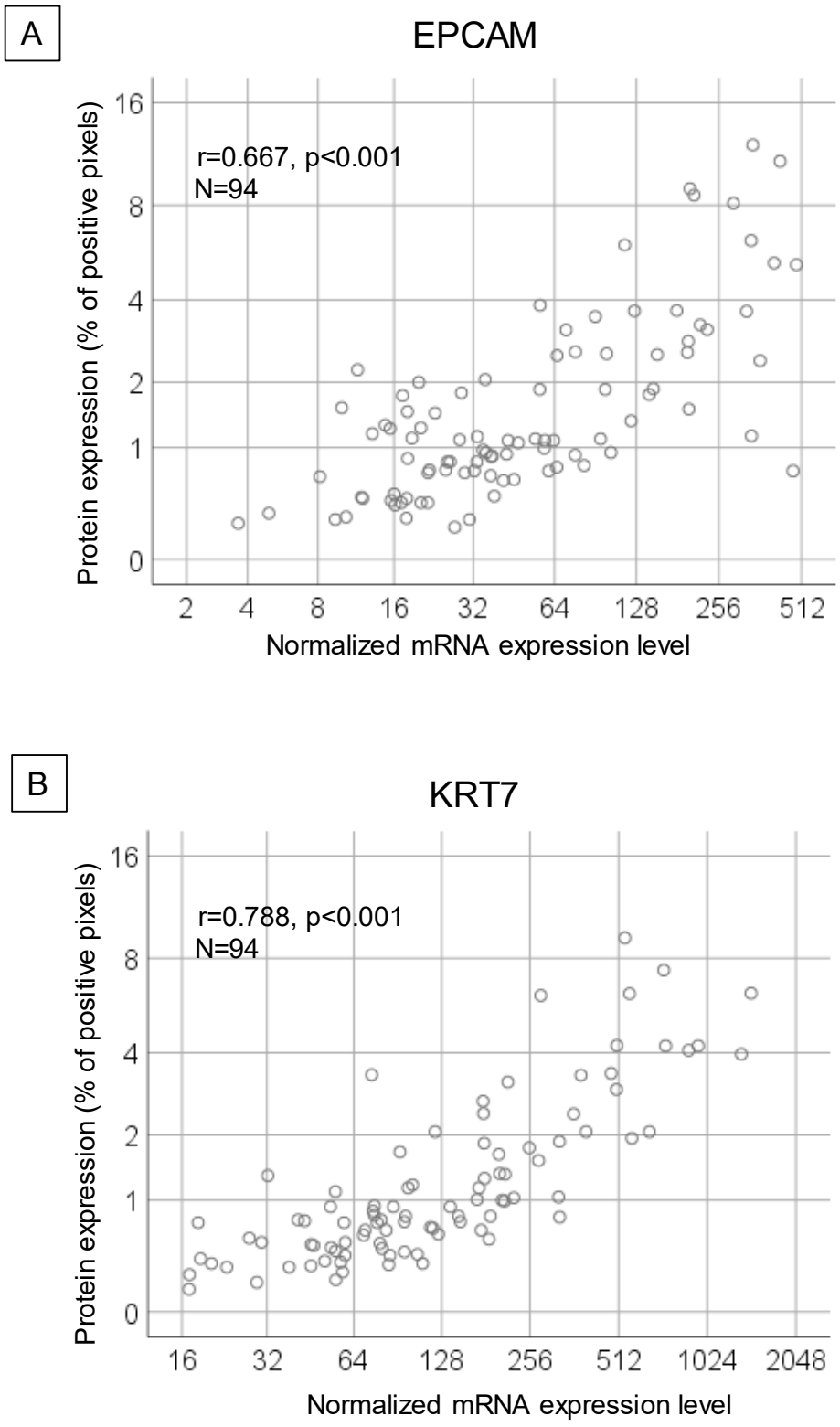

Figure 7.3. There was a significant positive correlation between the mRNA and the protein expression of (A) EPCAM and (B) KRT7.

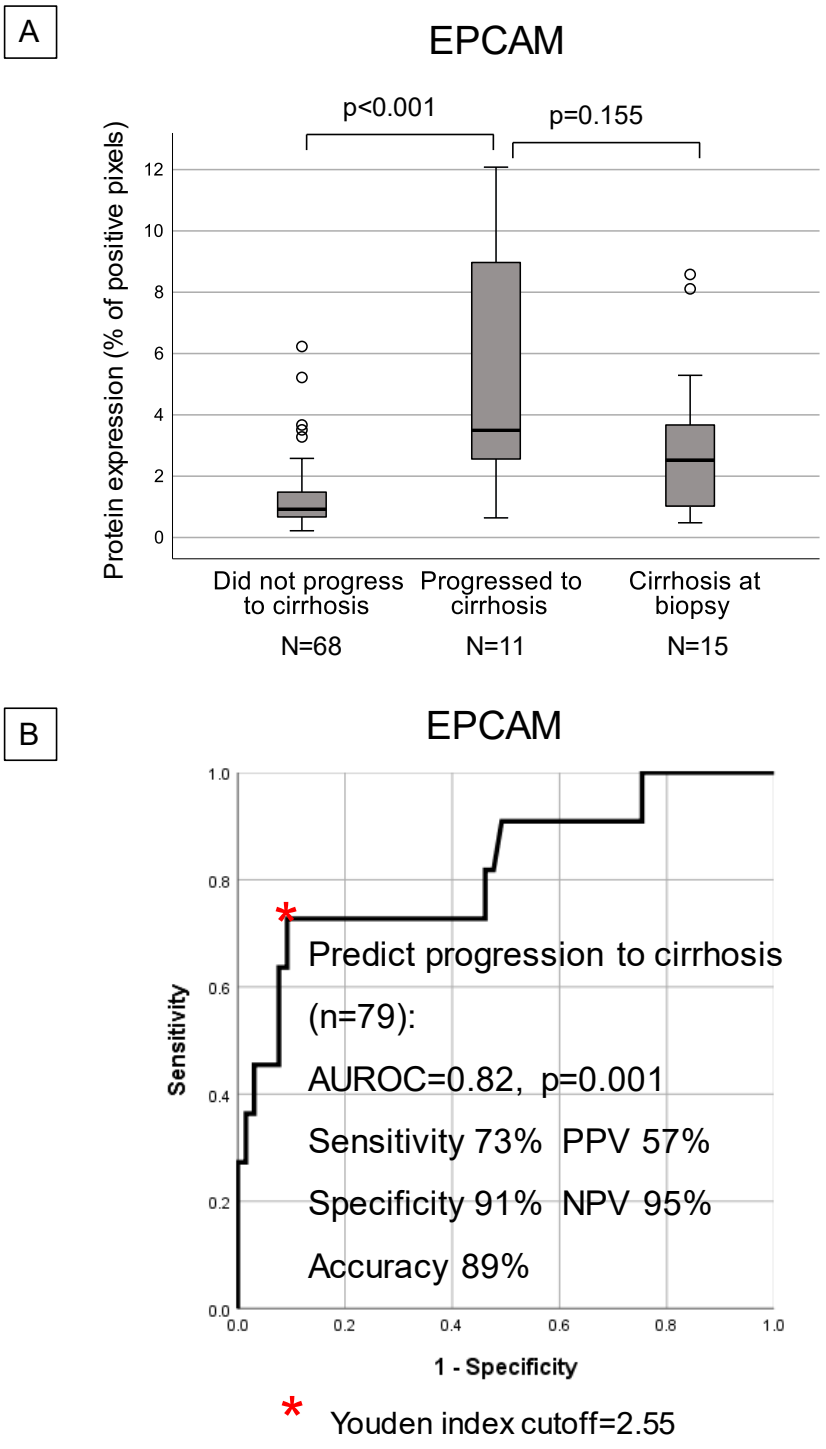

Figure 7.4. EPCAM protein expression predicts progression to cirrhosis.
(A) Patients progressed to cirrhosis had significantly higher EPCAM expression compared to patients who did not progress ($p<0.001$). (B) EPCAM had an area under the receiver operating characteristic curve (AUROC) of 0.82 to predict progression to cirrhosis.

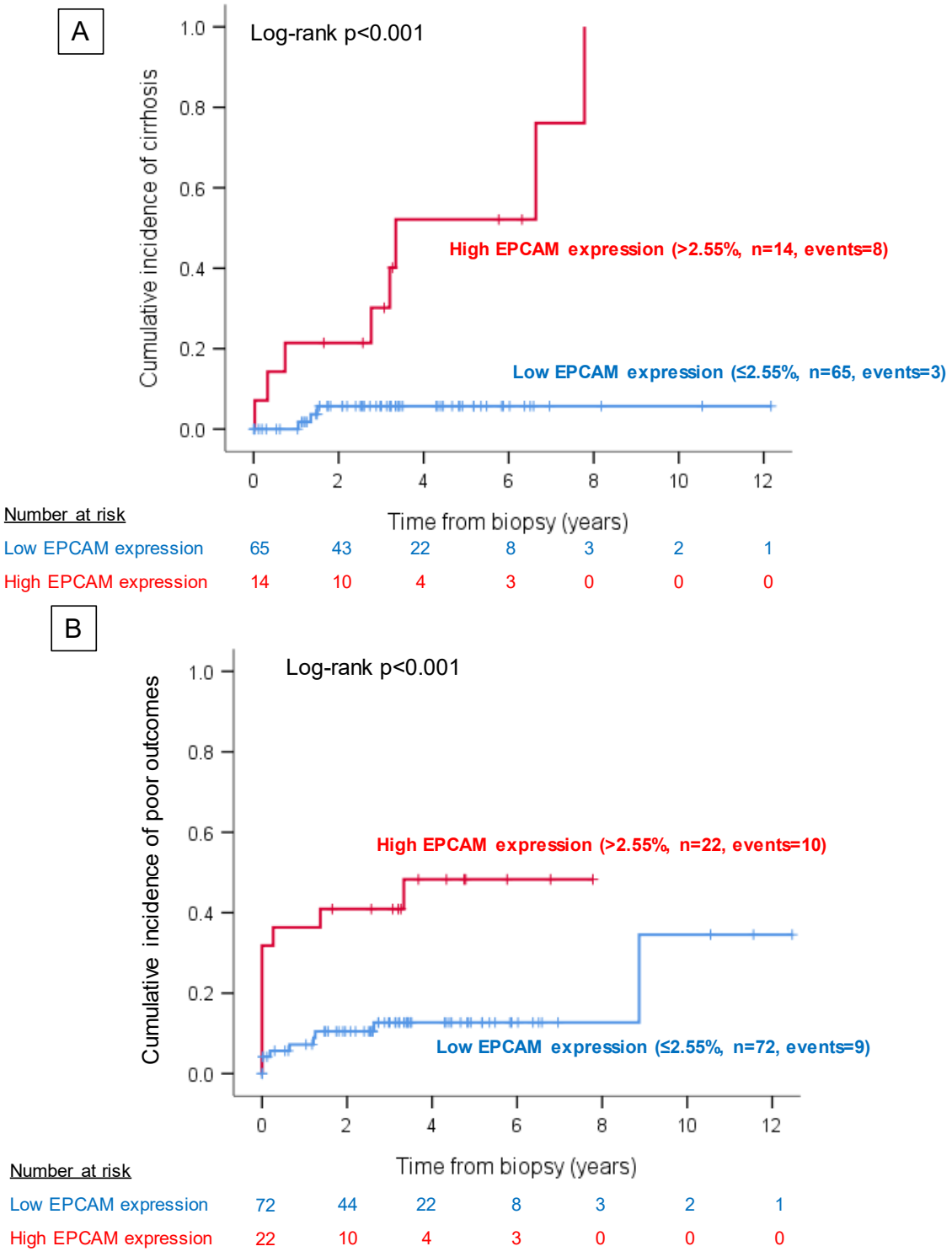

Figure 7.5. Cumulative incidence of (A) cirrhosis and (B) poor outcomes stratified by EPCAM protein expression.

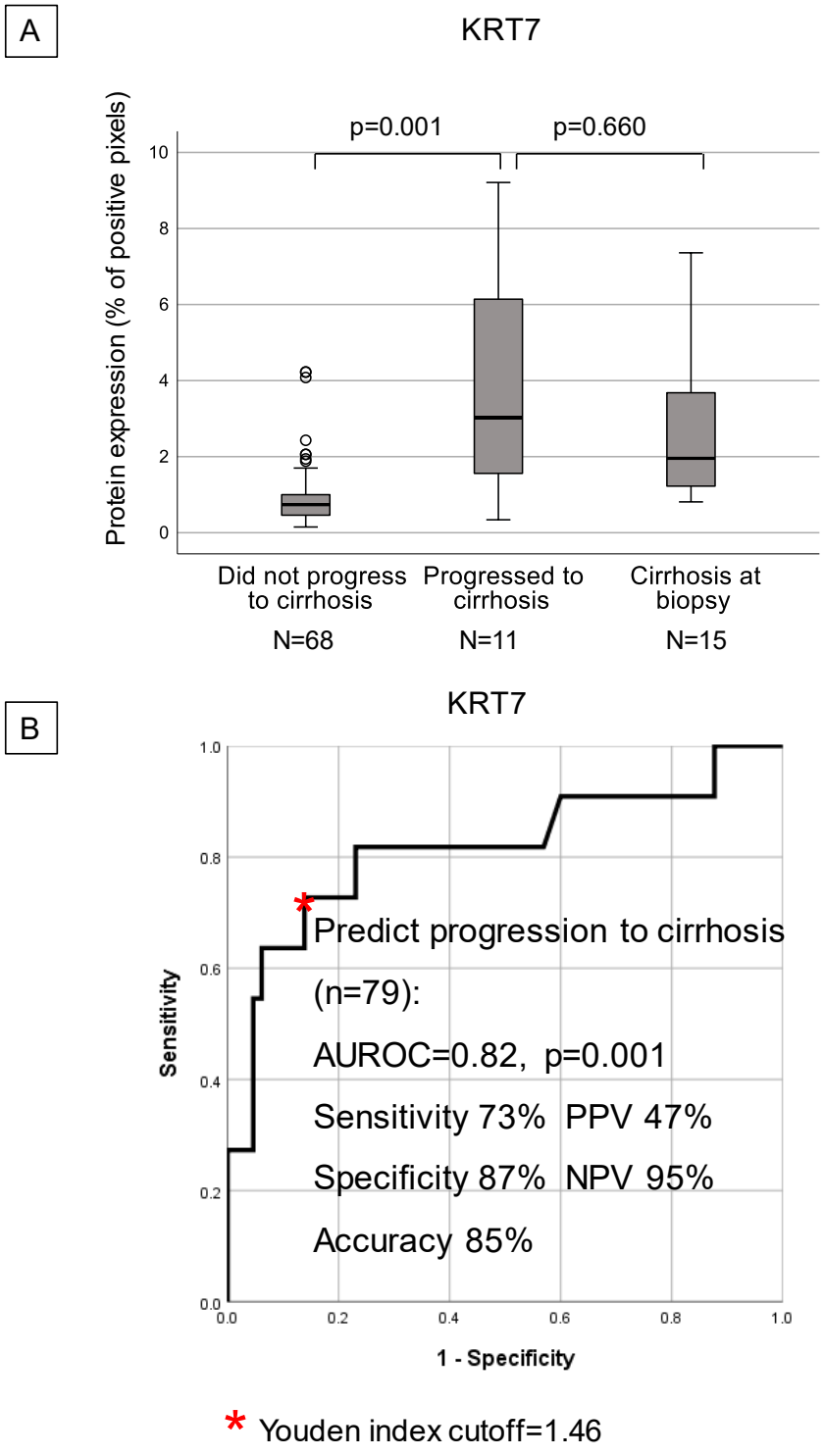

Figure 7.6. KRT7 protein expression predicts progression to cirrhosis.
(A) Patients progressed to cirrhosis had significantly higher KRT7 expression compared to patients who did not progress (p=0.001). (B) KRT7 had an area under the receiver operating characteristic curve (AUROC) of 0.82 to predict progression to cirrhosis.

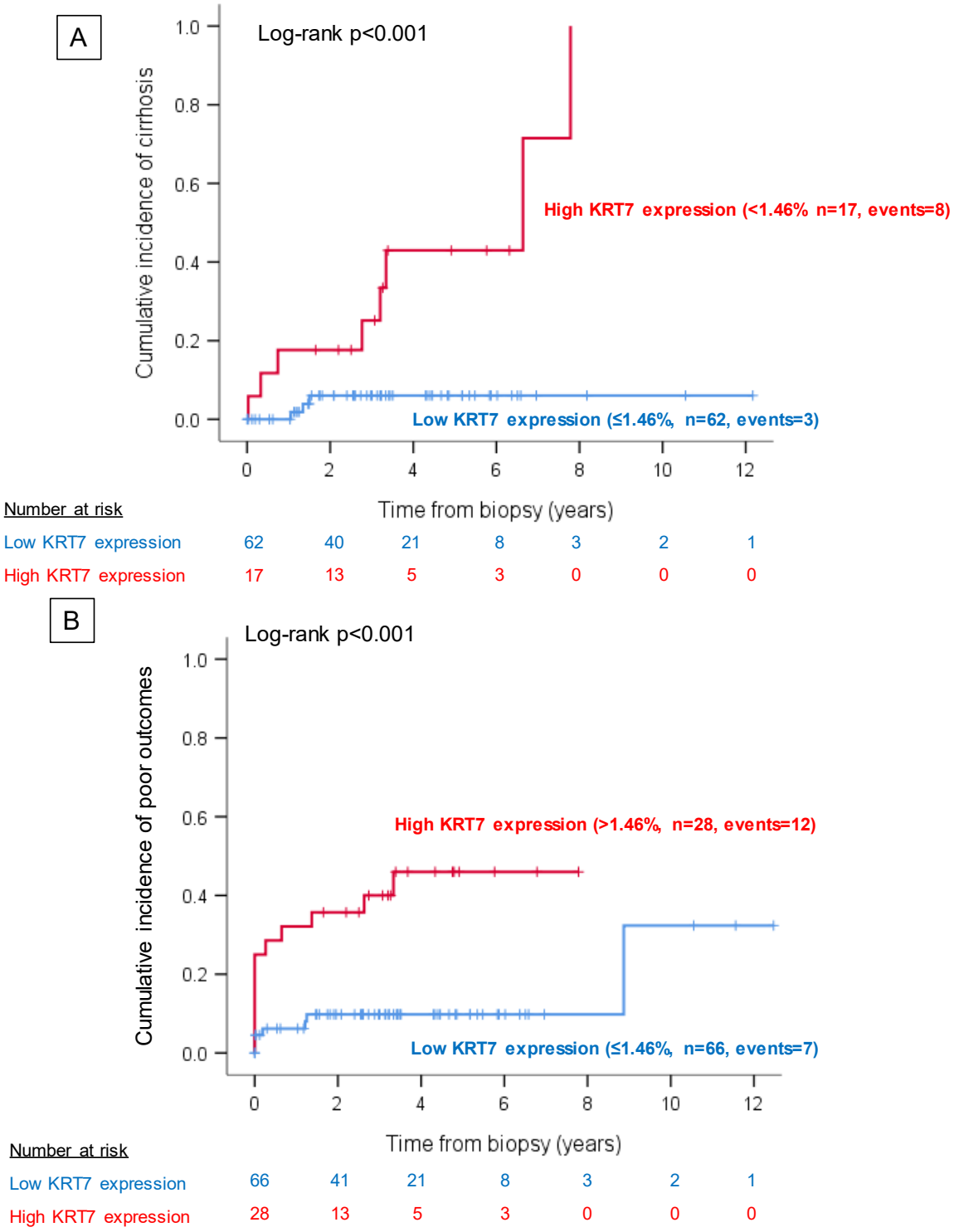

Figure 7.7. Cumulative incidence of (A) cirrhosis and (B) poor outcomes stratified by KRT7 protein expression.

7.5 – References

1. Hernandez-Gea V, Friedman SL. Pathogenesis of liver fibrosis. Annu Rev Pathol 2011;6:425-456.

2. Kaur S, Siddiqui H, Bhat MH. Hepatic Progenitor Cells in Action: Liver Regeneration or Fibrosis? Am J Pathol 2015 Sep;185(9):2342-2350.

3. Richardson MM, Jonsson JR, Powell EE, Brunt EM, Neuschwander-Tetri BA, Bhathal PS, et al. Progressive fibrosis in nonalcoholic steatohepatitis: association with altered regeneration and a ductular reaction. Gastroenterology 2007 Jul;133(1):80-90.

4. Clouston AD, Powell EE, Walsh MJ, Richardson MM, Demetris AJ, Jonsson JR. Fibrosis correlates with a ductular reaction in hepatitis C: roles of impaired replication, progenitor cells and steatosis. Hepatology 2005 Apr;41(4):809-818.

5. Roskams T, Yang SQ, Koteish A, Durnez A, DeVos R, Huang X, et al. Oxidative stress and oval cell accumulation in mice and humans with alcoholic and nonalcoholic fatty liver disease. Am J Pathol 2003 Oct;163(4):1301-1311.

6. Yoon SM, Gerasimidou D, Kuwahara R, Hytiroglou P, Yoo JE, Park YN, et al. Epithelial cell adhesion molecule (EpCAM) marks hepatocytes newly derived from stem/progenitor cells in humans. Hepatology 2011 Mar;53(3):964-973.

7. Roskams T, Katoonizadeh A, Komuta M. Hepatic progenitor cells: an update. Clin Liver Dis 2010 Nov;14(4):705-718.

8. Sancho-Bru P, Altamirano J, Rodrigo-Torres D, Coll M, Millan C, Jose LJ, et al. Liver progenitor cell markers correlate with liver damage and predict short-term mortality in patients with alcoholic hepatitis. Hepatology 2012 Jun;55(6):1931-1941.

9. Bedossa P, Poynard T. An algorithm for the grading of activity in chronic hepatitis C. The METAVIR Cooperative Study Group. Hepatology 1996 Aug;24(2):289-293.

10. Brunt EM, Janney CG, Di Bisceglie AM, Neuschwander-Tetri BA, Bacon BR. Nonalcoholic steatohepatitis: a proposal for grading and staging the histological lesions. Am J Gastroenterol 1999 Sep;94(9):2467-2474.

11. Singh S, Muir AJ, Dieterich DT, Falck-Ytter YT. American Gastroenterological Association Institute Technical Review on the Role of Elastography in Chronic Liver Diseases. Gastroenterology 2017 May;152(6):1544-1577.

12. Ebadi M, Bhanji RA, Mazurak VC, Lytvyak E, Mason A, Czaja AJ, et al. Severe vitamin D deficiency is a prognostic biomarker in autoimmune hepatitis. Aliment Pharmacol Ther 2019 Jan;49(2):173-182.

13. Wong VW, Vergniol J, Wong GL, Foucher J, Chan HL, Le BB, et al. Diagnosis of fibrosis and cirrhosis using liver stiffness measurement in nonalcoholic fatty liver disease. Hepatology 2010 Feb;51(2):454-462.

14. Lens S, Torres F, Puigvehi M, Marino Z, Londono MC, Martinez SM, et al. Predicting the development of liver cirrhosis by simple modelling in patients with chronic hepatitis C. Aliment Pharmacol Ther 2016 Feb;43(3):364-374.

15. Manousou P, Burroughs AK, Tsochatzis E, Isgro G, Hall A, Green A, et al. Digital image analysis of collagen assessment of progression of fibrosis in recurrent HCV after liver transplantation. J Hepatol 2013 May;58(5):962-968.

16. Friedman LS. Surgery in the patient with liver disease. Trans Am Clin Climatol Assoc 2010;121:192-204.

17. Williams MJ, Clouston AD, Forbes SJ. Links between hepatic fibrosis, ductular reaction, and progenitor cell expansion. Gastroenterology 2014 Feb;146(2):349-356.

Chapter 8: Discussion and Future Directions

8.1 – General discussion

Cirrhosis is a late stage of liver fibrosis caused by many forms of chronic liver diseases (1). As disease progresses, increased scar tissue forms which in turn impedes liver functions. The liver damage caused by cirrhosis is difficult to reverse and cirrhosis is life-threatening with a high mortality rate (2). However, if cirrhosis/advanced fibrosis is predicted early and the cause is treated, early fibrosis can be reversed and further liver damage can be prevented. This means prevention of poor outcomes (liver decompensation, need for liver transplantation, or liver-related death).

The gold standard in assessing liver fibrosis is liver needle biopsy examined by histopathology (3). However, histopathology of liver biopsy suffers from sampling error, inter-observer variability, and cannot predict fibrosis progression (4-6). Up to 33% of error rates for diagnosis of advanced fibrosis had been reported (7). The invasive nature of biopsy and inherent limitations of histopathology have led to the development of noninvasive diagnostic tests (imaging methods and serum biomarkers), but none of them were proven to be adequate to identify progressive fibrosis (8). Imaging methods can detect fibrosis only when it is manifested at the histological level by measuring liver stiffness, but can give significant false positive results when there is fatty liver, acute inflammation, or biliary obstruction (9, 10). Serum biomarkers also cannot reliably identify progressive fibrosis and have limitations such as not being liver specific, inability to differentiate intermediate fibrosis stages, and confounder effect of liver inflammation and steatosis (8). Given these constraints and limitations, there is an unmet and urgent clinical need for a surrogate biomarker to predict progressive fibrosis and poor clinical outcomes in patients with chronic

liver disease.

Advanced fibrosis is a shared histological phenotype for late-stage liver disease by different etiologies. However, it is yet unknown if there is a common molecular signature of progressive liver fibrosis that is shared by a variety of chronic liver diseases. If we can understand molecular events that drive progressive fibrosis, then we may predict which patients will progress to advanced fibrosis before the development of well-established pathology.

In Chapter 2, 304 Affymetrix microarrays of fresh livers from 312 patients with different chronic liver diseases were analyzed. I identified a common 48-gene signature associated with advanced fibrosis that is shared by different liver diseases in humans. This was the first comprehensive collection of gene expression signatures that drives advanced liver fibrosis in the context of various common causes of liver disease in humans. This new understanding defines a quantitative surrogate biomarker for advanced liver fibrosis.

Despite the impressive findings in Chapter 2, it is yet unknown if the 48-gene signature can be reliably measured in clinical liver biopsies because formalin-fixed paraffin-embedded (FFPE) tissues are known to suffer from RNA degradation and cross-linkage and there is limited amount of tissue after sectioning for routine histological analysis. Therefore, in Chapter 3, I analyzed 348 clinical liver biopsies and studied the feasibility and reliability of measuring the 48-gene signature using NanoString platform. An additional 30 samples (15 paired fresh and FFPE liver biopsies) were studied using NanoString and the transcript counts between paired fresh versus FFPE samples were compared. I had 99% success rate to isolate enough RNA from paraffin sections of clinical liver biopsies, which were up to 18 years old and had a minimum of 1 mm tissue in length. NanoString gene expression levels

in fresh biopsies were strongly correlated with paired FFPE biopsies ($r=0.944$, $p<0.001$). Moreover, NanoString gene expression measurements were highly reproducible across different RNA input quantities ($r=0.946$-0.995, $p<0.001$), in repeat runs by one operator ($r=0.950$-0.990, $p<0.001$) or by different operators ($r=0.949$-0.992, $p<0.001$), and across different lots of reagents ($r=0.998$-0.999, $p<0.001$). This chapter established a feasible and robust protocol for multiplexed gene expression profiling in clinical liver biopsies.

With supporting results that NanoString is a robust platform for measuring multiplex gene expression signature in clinical liver biopsies, I analyzed if the 48-gene signature can predict fibrosis progression and poor outcomes in a total of 299 patients with post-transplant recurrent viral hepatitis C (HCV) (Chapter 4), autoimmune hepatitis (AIH) (Chapter 5), and non-alcoholic fatty liver disease (NAFLD) (Chapter 6).

Before direct-acting antiviral treatment was available for patients with HCV, virologic recurrence after transplantation was universal and triggered an accelerated progression of fibrosis (11). In Chapter 4, I used post-transplant patients with recurrent HCV, before the direct-acting antiviral treatment was available, as a human disease model for progressive liver fibrosis. I analyzed if the 48-gene signature can predict adverse outcomes, which was defined as progression to one or more of the followings: advanced fibrosis, liver decompensation, requirement for liver transplantation, or liver-related death. This cohort was composed of 62 Edmonton and 60 Toronto patients. Each patient had an early (median: 6-months) and late biopsy (median: 2 to 3 years) post-transplantation. During the entire follow-up period (median 8.4 years for Edmonton patients and 3.1 years for Toronto patients), 42% Edmonton and 13% Toronto patients progressed to adverse outcomes (progressors). The median of the 48-gene signature in early biopsies with F0-F1 fibrosis was significantly higher

in both Edmonton and Toronto progressors compared with non-progressors (p=0.013, 0.008, respectively), but Metavir-fibrosis stage was not (p=0.779, 0.513, respectively). I used the median of 48-gene signature in the 62 Edmonton early biopsies to assign patients to two groups: high and low 48-gene signature and validated the cutoff in Edmonton late biopsies and Toronto early biopsies. In Edmonton patients with F0 or F1 fibrosis in early biopsy, there were significantly more patients with a high 48-gene signature progressed to adverse outcomes compared to patients with a low 48-gene signature (50% vs. 21%, p=0.040), but the percentage of patients progressed to adverse outcomes was similar between F0 and F1 fibrosis (32% vs. 35%, p=1.000). In Toronto early biopsies with F0 or F1 fibrosis, there were also significantly more patients with a high 48-gene signature progressed to adverse outcomes compared to patients with a low 48-gene signature (25% vs. 3%, p=0.035), but the percentage of patients progressed to adverse outcomes was similar between F0 and F1 fibrosis (9% vs. 15%, p=0.689). This chapter showed the 48-gene signature in clinical liver biopsies can predict progression to adverse outcomes earlier than histopathology.

Early prediction of progression to cirrhosis in patients with AIH at disease onset is an unmet clinical need. In Chapter 5, I analyzed if the 48-gene signature can predict progression to cirrhosis in 76 patients with AIH. Eleven (14.5%) patients had cirrhosis at disease onset. Of the 65 patients without cirrhosis at disease onset, 13 (17.1%) progressed to cirrhosis (progressors) during a median of 8.5 years of follow-up. Median 48-gene signature in biopsies was significantly higher progressors compared with non-progressors (p=0.001), but Metavir activity score and fibrosis stages were not (p=0.298, 0.345, respectively). I then derived a 48-gene signature cut-off at 113.56 (Youden index) for progression to cirrhosis from receiver operating characteristic curve analysis in 65 patients without cirrhosis at

disease onset. Of the 65 patients without cirrhosis at disease onset, patients with a high 48-gene signature had significantly higher probability of progression to cirrhosis compared to patients with a low 48-gene signature (53% vs. 7%, log-rank $p<0.001$), but similar between F2-F3 vs. F0-F1 fibrosis (24% vs. 15%, log-rank $p=0.420$) and A2-A3 vs. A1 activity (24% vs. 7%, log-rank $p=0.133$). This chapter showed the 48-gene signature in clinical liver biopsies can predict progression to cirrhosis earlier than histopathology in patients with AIH at disease onset. This prognostic information can provide risk stratification and help guide personalized treatment regimens.

NAFLD is the most common chronic liver disease and is predicted as the most common indication for liver transplantation in 2025 (12). Therefore, drug development for treating non-alcoholic steatohepatitis (NASH) is currently a hot topic. Several ongoing phase III pivotal trials will likely report initial results around 2021 (13). This raises an unmet clinical need for a surrogate biomarker to accurately predict fibrosis progression and to identify patients who may benefit from drug treatments to prevent further liver damage and poor outcomes (14). In Chapter 6, I analyzed if the 48-gene signature can predict progression to cirrhosis and poor outcomes in 101 patients with different severity of NAFLD. The 48-gene signature had an area under the receiver operator characteristic curve of 0.89 (95% confidence interval, 0.82-0.95, $p<0.001$) and the Youden index cutoff at 69.34 had 86% sensitivity, 80% specificity, and 83% of accuracy for NASH. Based on this cutoff, the 48-gene signature was stratified into two groups, low and high 48-gene signature. Seventeen (16.8%) patients had cirrhosis at biopsy. Of 84 patients without cirrhosis at biopsy, patients with a high 48-gene signature had a marginally significantly higher probability of progression to cirrhosis compared to patients with a low 48-gene signature (21% vs. 4%, log-

rank p=0.05). However, the probability of progression to cirrhosis was similar between F0-F1 vs. F2-F3 (9% vs. 19%, log-rank p=0.172). This chapter showed the 48-gene signature in clinical liver biopsies predicts progression to cirrhosis earlier than histopathology in patients with NAFLD. This prognostic information can provide risk stratification and help to identify patients who may benefit from upcoming drug treatments to prevent further liver damage.

It is well-known that mRNA levels may or may not correspond to the protein content in the tissues, and while protein is the key molecule that mediates catalytic and enzymatic functions. Protein level validation will facilitate therapeutics development. Therefore, Chapter 7 analyzed the protein expression of EPCAM and KRT7 that were in the 48-gene signature and found quantification of immunohistochemistry slides of protein immunostained in the liver tissue using an objective quantitative computer imaging analysis can predict progression to cirrhosis in patients with different liver diseases. This suggested EPCAM and KRT7 could serve as a surrogate marker, which can be applied in routine diagnostic liver biopsies, for predicting progression to cirrhosis.

8.2 – Clinical significance

This thesis identified a 48-gene signature associated with advanced liver fibrosis that is shared by different liver diseases in humans. Based on this knowledge, I developed a 48-gene signature genomic test enables early diagnosis of progressive fibrosis in patients with different chronic liver diseases. This molecular test is compatible with standard procurement and work-up of diagnostic liver biopsies from patients with problems in clinic.

As for clinical relevance, the 48-gene signature test could provide risk stratification of progression to advanced fibrosis or cirrhosis for patients with chronic liver disease, earlier

than histology or current available imaging methods. The test could identify patients that are at high-risk of fibrosis progression for timely clinical management. This test could be also applied into anti-fibrotic drug trials for liver fibrosis. Enrolling patients with similar histological fibrosis stages, which most clinical trials did, could not represent these patients had similar phenotype for fibrosis progression (i.e. similar fibrosis progression rate). Implications of the 48-gene signature in clinical trials when selecting patients could provide unambiguous findings because fibrosis progression rates are similar in both placebo and treatment group. If enrolling only the high-risk patients for fibrosis progression (patients with a high 48-gene signature), results could be achieved in a relatively shorter study interval, as differences between a placebo and treatment group would emerge more rapidly if the drug is effective. Moreover, the 48-gene signature could also possibly be used as an earlier indicator of meaningful therapeutic response (if the 48-gene signature has decreased after the treatment).

8.3 – Project strengths and limitations

The major strength of this thesis was that I included a large number of patients (n=312) with a variety chronic liver diseases when identifying a common 48-gene signature for advanced fibrosis (Chapter 2) and the 48-gene signature was validated in multiple independent cohorts of total 299 patients with different chronic liver diseases (Chapters 4, 5, and 6). I also had data to support that the 48-gene signature could be reliably measured in clinical liver biopsies by NanoString (Chapter 3). This made translating the 48-gene signature test into a clinical assay possible using standard liver biopsies performed for clinical indications.

There were limitations to this work. First, in Chapter 6, there was a limited number of NAFLD patients that progressed to cirrhosis (n=10). This was because of the relatively short follow-up period (median 2.6 years). According to previous studies, approximately 25% of patients with NASH and 4% of patients with simple steatosis patients progress to cirrhosis in 10 years of follow-up (15, 16). Therefore, there is a need to validate the 48-gene signature an independent cohort with longer follow-up period. Second, Chapters 4, 5, and 6 were retrospective studies and therefore patient selection bias might occur, as patients who were biopsied usually had a relatively more severe disease. For the AIH cohort, selection bias was minimal as all patients were biopsied at disease onset. For the recurrent HCV and NAFLD cohorts, most biopsies were indication biopsy due to elevated transaminases, which may cause a trend to include patients with more advanced liver damage. However, the fibrosis progression rate was similar between this recurrent HCV cohort and a previously published review study (approximately 40-50% progressed to advanced fibrosis five years after transplantation) (11). Therefore, there was no significant selection bias for the recurrent HCV cohort. For the NAFLD cohort, the follow-up time period was too short (median 2.6 years) to compare the fibrosis progression rate with previous published studies. Therefore, validation in an independent cohort with a longer follow-period should be performed to assure confidence in these initial results.

8.4 – Future directions

Despite liver biopsy has been the gold standard for advanced fibrosis, there are well-known limitations including invasiveness, rare but potentially life-threatening complications, and poor acceptability. Due to the epidemic proportion of patients with chronic liver disease

worldwide, liver biopsy evaluation for all patients is impractical. Therefore, as a further step, comparing mRNA and protein expression levels of the fibrosis genes between paired blood and liver biopsy samples and correlating blood results with tissue mRNA expression levels may enable the development of a non-invasive blood test that may predict fibrosis progression in patients with chronic liver disease.

8.5 – References

1. Tsochatzis EA, Bosch J, Burroughs AK. Liver cirrhosis. Lancet 2014 May 17;383(9930):1749-1761.
2. Bataller R, Brenner DA. Liver fibrosis. J Clin Invest 2005 Feb;115(2):209-218.
3. Afdhal NH, Nunes D. Evaluation of liver fibrosis: a concise review. Am J Gastroenterol 2004 Jun;99(6):1160-1174.
4. Bejarano PA, Koehler A, Sherman KE. Second opinion pathology in liver biopsy interpretation. Am J Gastroenterol 2001 Nov;96(11):3158-3164.
5. Bedossa P, Dargere D, Paradis V. Sampling variability of liver fibrosis in chronic hepatitis C. Hepatology 2003 Dec;38(6):1449-1457.
6. Netto GJ, Watkins DL, Williams JW, Colby TV, dePetris G, Sharkey FE, et al. Interobserver agreement in hepatitis C grading and staging and in the Banff grading schema for acute cellular rejection: the "hepatitis C 3" multi-institutional trial experience. Arch Pathol Lab Med 2006 Aug;130(8):1157-1162.
7. Regev A, Berho M, Jeffers LJ, Milikowski C, Molina EG, Pyrsopoulos NT, et al. Sampling error and intraobserver variation in liver biopsy in patients with chronic HCV infection. Am J Gastroenterol 2002 Oct;97(10):2614-2618.
8. EASL-ALEH Clinical Practice Guidelines: Non-invasive tests for evaluation of liver disease severity and prognosis. J Hepatol 2015 Jul;63(1):237-264.
9. Myers RP, Pomier-Layrargues G, Kirsch R, Pollett A, Duarte-Rojo A, Wong D, et al. Feasibility and diagnostic performance of the FibroScan XL probe for liver stiffness

measurement in overweight and obese patients. Hepatology 2012 Jan;55(1):199-208.

10. Wilder J, Patel K. The clinical utility of FibroScan((R)) as a noninvasive diagnostic test for liver disease. Med Devices (Auckl) 2014;7:107-114.

11. Berenguer M, Schuppan D. Progression of liver fibrosis in post-transplant hepatitis C: mechanisms, assessment and treatment. J Hepatol 2013 May;58(5):1028-1041.

12. Charlton MR, Burns JM, Pedersen RA, Watt KD, Heimbach JK, Dierkhising RA. Frequency and outcomes of liver transplantation for nonalcoholic steatohepatitis in the United States. Gastroenterology 2011 Oct;141(4):1249-1253.

13. Sanyal AJ. Past, present and future perspectives in nonalcoholic fatty liver disease. Nat Rev Gastroenterol Hepatol 2019 Jun;16(6):377-386.

14. Sanyal AJ, Friedman SL, McCullough AJ, Dimick-Santos L. Challenges and opportunities in drug and biomarker development for nonalcoholic steatohepatitis: findings and recommendations from an American Association for the Study of Liver Diseases-U.S. Food and Drug Administration Joint Workshop. Hepatology 2015 Apr;61(4):1392-1405.

15. Ekstedt M, Franzen LE, Mathiesen UL, Thorelius L, Holmqvist M, Bodemar G, et al. Long-term follow-up of patients with NAFLD and elevated liver enzymes. Hepatology 2006 Oct;44(4):865-873.

16. Calzadilla BL, Adams LA. The Natural Course of Non-Alcoholic Fatty Liver Disease. Int J Mol Sci 2016 May 20;17(5).

Bibliography

Abdel-Misih SR, Bloomston M. Liver anatomy. Surg Clin North Am 2010 Aug;90(4):643-653.

Abdueva D, Wing M, Schaub B, Triche T, Davicioni E. Quantitative expression profiling in formalin-fixed paraffin-embedded samples by affymetrix microarrays. J Mol Diagn 2010 Jul;12(4):409-417.

Adams LA, Bulsara M, Rossi E, DeBoer B, Speers D, George J, et al. Hepascore: an accurate validated predictor of liver fibrosis in chronic hepatitis C infection. Clin Chem 2005 Oct;51(10):1867-1873.

Afdhal NH, Nunes D. Evaluation of liver fibrosis: a concise review. Am J Gastroenterol 2004 Jun;99(6):1160-1174.

Affo S, Dominguez M, Lozano JJ, Sancho-Bru P, Rodrigo-Torres D, Morales-Ibanez O, et al. Transcriptome analysis identifies TNF superfamily receptors as potential therapeutic targets in alcoholic hepatitis. Gut 2013 Mar;62(3):452-460.

Agarwal K, Czaja AJ, Donaldson PT. A functional Fas promoter polymorphism is associated with a severe phenotype in type 1 autoimmune hepatitis characterized by early development of cirrhosis. Tissue Antigens 2007 Mar;69(3):227-235.

Agarwal K, Czaja AJ, Jones DE, Donaldson PT. Cytotoxic T lymphocyte antigen-4 (CTLA-4) gene polymorphisms and susceptibility to type 1 autoimmune hepatitis. Hepatology 2000 Jan;31(1):49-53.

Ahmad W, Ijaz B, Hassan S. Gene expression profiling of HCV genotype 3a initial liver fibrosis and cirrhosis patients using microarray. J Transl Med 2012;10:41.

Ahrens M, Ammerpohl O, von SW, Kolarova J, Bens S, Itzel T, et al. DNA methylation analysis in nonalcoholic fatty liver disease suggests distinct disease-specific and remodeling signatures after bariatric surgery. Cell Metab 2013 Aug 6;18(2):296-302.

Aizarani N, Saviano A, Sagar, Mailly L, Durand S, Herman JS, et al. A human liver cell atlas reveals heterogeneity and epithelial progenitors. Nature 2019 Aug;572(7768):199-204.

Ajuebor MN, Carey JA, Swain MG. CCR5 in T cell-mediated liver diseases: what's going on? J Immunol 2006 Aug 15;177(4):2039-2045.

Alberti A, Chemello L, Benvegnu L. Natural history of hepatitis C. J Hepatol 1999;31 Suppl 1:17-24.

Albino D, Longoni N, Curti L, Mello-Grand M, Pinton S, Civenni G, et al. ESE3/EHF controls epithelial cell differentiation and its loss leads to prostate tumors with mesenchymal and stem-like features. Cancer Res 2012 Jun 1;72(11):2889-2900.

Alexander JF, Lischner MW, Galambos JT. Natural history of alcoholic hepatitis. II. The long-term prognosis. Am J Gastroenterol 1971 Dec;56(6):515-525.

Andersen JB, Spee B, Blechacz BR, Avital I, Komuta M, Barbour A, et al. Genomic and genetic characterization of cholangiocarcinoma identifies therapeutic targets for tyrosine kinase inhibitors. Gastroenterology 2012 Apr;142(4):1021-1031.

Anderson LR, Owens TW, Naylor MJ. Structural and mechanical functions of integrins. Biophys Rev 2014 Jun;6(2):203-213.

Angulo P, Hui JM, Marchesini G, Bugianesi E, George J, Farrell GC, et al. The NAFLD fibrosis score: a noninvasive system that identifies liver fibrosis in patients with NAFLD. Hepatology 2007 Apr;45(4):846-854.

Angulo P, Kleiner DE, Dam-Larsen S, Adams LA, Bjornsson ES, Charatcharoenwitthaya P, et al. Liver Fibrosis, but No Other Histologic Features, Is Associated With Long-term Outcomes of Patients With Nonalcoholic Fatty Liver Disease. Gastroenterology 2015 Aug;149(2):389-397.

Angus PW. Role of endothelin in systemic and portal resistance in cirrhosis. Gut 2006 Sep;55(9):1230-1232.

Anthony PP, Ishak KG, Nayak NC, Poulsen HE, Scheuer PJ, Sobin LH. The morphology of cirrhosis: definition, nomenclature, and classification. Bull World Health Organ 1977;55(4):521-540.

Asselah T, Bieche I, Laurendeau I, Paradis V, Vidaud D, Degott C, et al. Liver gene expression signature of mild fibrosis in patients with chronic hepatitis C. Gastroenterology 2005 Dec;129(6):2064-2075.

Baiocchini A, Montaldo C, Conigliaro A, Grimaldi A, Correani V, Mura F, et al. Extracellular Matrix Molecular Remodeling in Human Liver Fibrosis Evolution. PLoS One 2016;11(3):e0151736.

Barr RG, Ferraioli G, Palmeri ML, Goodman ZD, Garcia-Tsao G, Rubin J, et al. Elastography Assessment of Liver Fibrosis: Society of Radiologists in Ultrasound Consensus Conference Statement. Radiology 2015 Sep;276(3):845-861.

Barry-Hamilton V, Spangler R, Marshall D, McCauley S, Rodriguez HM, Oyasu M, et al. Allosteric inhibition of lysyl oxidase-like-2 impedes the development of a pathologic microenvironment. Nat Med 2010 Sep;16(9):1009-1017.

Basra S, Anand BS. Definition, epidemiology and magnitude of alcoholic hepatitis. World J Hepatol 2011 May 27;3(5):108-113.

Bataller R, Brenner DA. Liver fibrosis. J Clin Invest 2005 Feb;115(2):209-218.

Bataller R, Gabele E, Schoonhoven R, Morris T, Lehnert M, Yang L, et al. Prolonged infusion of angiotensin II into normal rats induces stellate cell activation and proinflammatory events in liver. Am J Physiol Gastrointest Liver Physiol 2003 Sep;285(3):G642-G651.

Bataller R, Rombouts K, Altamirano J, Marra F. Fibrosis in alcoholic and nonalcoholic steatohepatitis. Best Pract Res Clin Gastroenterol 2011 Apr;25(2):231-244.

Bataller R, Schwabe RF, Choi YH, Yang L, Paik YH, Lindquist J, et al. NADPH oxidase signal transduces angiotensin II in hepatic stellate cells and is critical in hepatic fibrosis. J Clin Invest 2003 Nov;112(9):1383-1394.

Bateman AC, Hubscher SG. Cytokeratin expression as an aid to diagnosis in medical liver biopsies. Histopathology 2010 Mar;56(4):415-425.

Beckebaum S, Iacob S, Klein CG, Dechene A, Varghese J, Baba HA, et al. Assessment of allograft fibrosis by transient elastography and noninvasive biomarker scoring systems in liver transplant patients. Transplantation 2010 Apr 27;89(8):983-993.

Bedossa P, Dargere D, Paradis V. Sampling variability of liver fibrosis in chronic hepatitis C. Hepatology 2003 Dec;38(6):1449-1457.

Bedossa P, Poynard T. An algorithm for the grading of activity in chronic hepatitis C. The METAVIR Cooperative Study Group. Hepatology 1996 Aug;24(2):289-293.

Bejarano PA, Koehler A, Sherman KE. Second opinion pathology in liver biopsy interpretation. Am J Gastroenterol 2001 Nov;96(11):3158-3164.

Bellentani S, Marino M. Epidemiology and natural history of non-alcoholic fatty liver disease (NAFLD). Ann Hepatol 2009;8 Suppl 1:S4-S8.

Benhamou Y, Bochet M, Di M, V, Charlotte F, Azria F, Coutellier A, et al. Liver fibrosis progression in human immunodeficiency virus and hepatitis C virus coinfected patients. The Multivirc Group. Hepatology 1999 Oct;30(4):1054-1058.

Berenguer J, Zamora FX, Aldamiz-Echevarria T, Von Wichmann MA, Crespo M, Lopez-Aldeguer J, et al. Comparison of the prognostic value of liver biopsy and FIB-4 index in patients coinfected with HIV and hepatitis C virus. Clin Infect Dis 2015 Mar 15;60(6):950-958.

Berenguer M, Schuppan D. Progression of liver fibrosis in post-transplant hepatitis C: mechanisms, assessment and treatment. J Hepatol 2013 May;58(5):1028-1041.

Blake DJ, Weir A, Newey SE, Davies KE. Function and genetics of dystrophin and dystrophin-related proteins in muscle. Physiol Rev 2002 Apr;82(2):291-329.

Blach S, Zeuzem S, Manns M, Altraif I, Duberg AS, Muljono D, et al. Global prevalence and genotype distribution of hepatitis C virus infection in 2015: a modelling study. Lancet Gastroenterol Hepatol 2017 Mar;2(3):161-176.

Borkham-Kamphorst E, Weiskirchen R. The PDGF system and its antagonists in liver fibrosis. Cytokine Growth Factor Rev 2016 Apr;28:53-61.

Bota S, Herkner H, Sporea I, Salzl P, Sirli R, Neghina AM, et al. Meta-analysis: ARFI elastography versus transient elastography for the evaluation of liver fibrosis. Liver Int 2013 Sep;33(8):1138-1147.

Boulter L, Govaere O, Bird TG, Radulescu S, Ramachandran P, Pellicoro A, et al. Macrophage-derived Wnt opposes Notch signaling to specify hepatic progenitor cell fate in chronic liver disease. Nat Med 2012 Mar 4;18(4):572-579.

Bourd-Boittin K, Bonnier D, Leyme A, Mari B, Tuffery P, Samson M, et al. Protease profiling of liver fibrosis reveals the ADAM metallopeptidase with thrombospondin type 1 motif, 1 as a central activator of transforming growth factor beta. Hepatology 2011 Dec;54(6):2173-2184.

Brenner DA, Kisseleva T, Scholten D, Paik YH, Iwaisako K, Inokuchi S, et al. Origin of myofibroblasts in liver fibrosis. Fibrogenesis Tissue Repair 2012;5(Suppl 1):S17.

Brunt EM, Janney CG, Di Bisceglie AM, Neuschwander-Tetri BA, Bacon BR. Nonalcoholic steatohepatitis: a proposal for grading and staging the histological lesions. Am J Gastroenterol 1999 Sep;94(9):2467-2474.

Buch S, Stickel F, Trepo E, Way M, Herrmann A, Nischalke HD, et al. A genome-wide association study confirms PNPLA3 and identifies TM6SF2 and MBOAT7 as risk loci for alcohol-related cirrhosis. Nat Genet 2015 Dec;47(12):1443-1448.

Caillot F, Derambure C, Bioulac-Sage P, Francois A, Scotte M, Goria O, et al. Transient and etiology-related transcription regulation in cirrhosis prior to hepatocellular carcinoma occurrence. World J Gastroenterol 2009 Jan 21;15(3):300-309.

Caillot F, Hiron M, Goria O, Gueudin M, Francois A, Scotte M, et al. Novel serum markers of fibrosis progression for the follow-up of hepatitis C virus-infected patients. Am J Pathol 2009 Jul;175(1):46-53.

Calabro NE, Kristofik NJ, Kyriakides TR. Thrombospondin-2 and extracellular matrix assembly. Biochim Biophys Acta 2014 Aug;1840(8):2396-2402.

Cales P, Oberti F, Michalak S, Hubert-Fouchard I, Rousselet MC, Konate A, et al. A novel panel of blood markers to assess the degree of liver fibrosis. Hepatology 2005 Dec;42(6):1373-1381.

Cales P, Veillon P, Konate A, Mathieu E, Ternisien C, Chevailler A, et al. Reproducibility of blood tests of liver fibrosis in clinical practice. Clin Biochem 2008 Jan;41(1-2):10-18.

Calzadilla BL, Adams LA. The Natural Course of Non-Alcoholic Fatty Liver Disease. Int J Mol Sci 2016 May 20;17(5).

Cassiman D, van PJ, De VR, Van LF, Desmet V, Yap SH, et al. Synaptophysin: A novel marker for human and rat hepatic stellate cells. Am J Pathol 1999 Dec;155(6):1831-1839.

Castera L, Forns X, Alberti A. Non-invasive evaluation of liver fibrosis using transient elastography. J Hepatol 2008 May;48(5):835-847.

Castera L. Noninvasive methods to assess liver disease in patients with hepatitis B or C. Gastroenterology 2012 May;142(6):1293-1302.

Chalasani N, Younossi Z, Lavine JE, Charlton M, Cusi K, Rinella M, et al. The diagnosis and management of nonalcoholic fatty liver disease: Practice guidance from the American Association for the Study of Liver Diseases. Hepatology 2018 Jan;67(1):328-357.

Chang SK, Noss EH, Chen M, Gu Z, Townsend K, Grenha R, et al. Cadherin-11 regulates fibroblast inflammation. Proc Natl Acad Sci U S A 2011 May 17;108(20):8402-8407.

Chang TT, Liaw YF, Wu SS, Schiff E, Han KH, Lai CL, et al. Long-term entecavir therapy results in the reversal of fibrosis/cirrhosis and continued histological improvement in patients with chronic hepatitis B. Hepatology 2010 Sep;52(3):886-893.

Chaqour B, Goppelt-Struebe M. Mechanical regulation of the Cyr61/CCN1 and CTGF/CCN2 proteins. FEBS J 2006 Aug;273(16):3639-3649.

Charlton MR, Burns JM, Pedersen RA, Watt KD, Heimbach JK, Dierkhising RA. Frequency and outcomes of liver transplantation for nonalcoholic steatohepatitis in the United States. Gastroenterology 2011 Oct;141(4):1249-1253.

Chen M, Tabaczewski P, Truscott SM, Van KL, Stroynowski I. Hepatocytes express abundant surface class I MHC and efficiently use transporter associated with antigen processing, tapasin, and low molecular weight polypeptide proteasome subunit components of antigen processing and presentation pathway. J Immunol 2005 Jul 15;175(2):1047-1055.

Choi SS, Diehl AM. Epithelial-to-mesenchymal transitions in the liver. Hepatology 2009 Dec;50(6):2007-2013.

Clouston AD, Powell EE, Walsh MJ, Richardson MM, Demetris AJ, Jonsson JR. Fibrosis correlates with a ductular reaction in hepatitis C: roles of impaired replication, progenitor cells and steatosis. Hepatology 2005 Apr;41(4):809-818.

Cochet-Bissuel M, Lory P, Monteil A. The sodium leak channel, NALCN, in health and disease. Front Cell Neurosci 2014;8:132.

Cohen-Dvashi H, Ben-Chetrit N, Russell R, Carvalho S, Lauriola M, Nisani S, et al. Navigator-3, a modulator of cell migration, may act as a suppressor of breast cancer progression. EMBO Mol Med 2015 Mar;7(3):299-314.

Colmenero J, Bataller R, Sancho-Bru P, Dominguez M, Moreno M, Forns X, et al. Effects of losartan on hepatic expression of nonphagocytic NADPH oxidase and fibrogenic genes in patients with chronic hepatitis C. Am J Physiol Gastrointest Liver Physiol 2009 Oct;297(4):G726-G734.

Cong M, Iwaisako K, Jiang C, Kisseleva T. Cell signals influencing hepatic fibrosis. Int J Hepatol 2012;2012:158547.

Couinaud C. [Dorsal sector of the liver]. Chirurgie 1998 Feb;123(1):8-15.

Czaja AJ, Carpenter HA. Decreased fibrosis during corticosteroid therapy of autoimmune hepatitis. J Hepatol 2004 Apr;40(4):646-652.

Czaja AJ, Carpenter HA. Progressive fibrosis during corticosteroid therapy of autoimmune hepatitis. Hepatology 2004 Jun;39(6):1631-1638.

Czaja AJ, Cookson S, Constantini PK, Clare M, Underhill JA, Donaldson PT. Cytokine polymorphisms associated with clinical features and treatment outcome in type 1 autoimmune hepatitis. Gastroenterology 1999 Sep;117(3):645-652.

Czaja AJ. Drug choices in autoimmune hepatitis: part A--Steroids. Expert Rev Gastroenterol Hepatol 2012 Sep;6(5):603-615.

Czaja AJ. Features and consequences of untreated type 1 autoimmune hepatitis. Liver Int 2009 Jul;29(6):816-823.

Danford CJ, Connelly MA, Shalaurova I, Kim M, Herman MA, Nasser I, et al. A Pathophysiologic Approach Combining Genetics and Insulin Resistance to Predict the Severity of Nonalcoholic Fatty Liver Disease. Hepatol Commun 2018 Dec;2(12):1467-1478.

Davis GL, Czaja AJ, Ludwig J. Development and prognosis of histologic cirrhosis in corticosteroid-treated hepatitis B surface antigen-negative chronic active hepatitis. Gastroenterology 1984 Dec;87(6):1222-1227.

Dolle L, Theise ND, Schmelzer E, Boulter L, Gires O, van Grunsven LA. EpCAM and the biology of hepatic stem/progenitor cells. Am J Physiol Gastrointest Liver Physiol 2015 Feb 15;308(4):G233-G250.

D'Onofrio M, Crosara S, De RR, Canestrini S, Demozzi E, Gallotti A, et al. Acoustic radiation force impulse of the liver. World J Gastroenterol 2013 Aug 14;19(30):4841-4849.

Dooley S, ten DP. TGF-beta in progression of liver disease. Cell Tissue Res 2012 Jan;347(1):245-256.

Dranoff JA, Wells RG. Portal fibroblasts: Underappreciated mediators of biliary fibrosis. Hepatology 2010 Apr;51(4):1438-1444.

Duarte S, Baber J, Fujii T, Coito AJ. Matrix metalloproteinases in liver injury, repair and fibrosis. Matrix Biol 2015 May;44-46:147-156.

EASL 2017 Clinical Practice Guidelines on the management of hepatitis B virus infection. J Hepatol 2017 Aug;67(2):370-398.

EASL Clinical Practice Guidelines: Autoimmune hepatitis. J Hepatol 2015 Oct;63(4):971-1004.

EASL Clinical Practice Guidelines: Management of alcohol-related liver disease. J Hepatol 2018 Jul;69(1):154-181.

EASL-ALEH Clinical Practice Guidelines: Non-invasive tests for evaluation of liver disease severity and prognosis. J Hepatol 2015 Jul;63(1):237-264.

EASL-EASD-EASO Clinical Practice Guidelines for the management of non-alcoholic fatty liver disease. J Hepatol 2016 Jun;64(6):1388-1402.

EASL-EORTC clinical practice guidelines: management of hepatocellular carcinoma. J Hepatol 2012 Apr;56(4):908-943.

Ebadi M, Bhanji RA, Mazurak VC, Lytvyak E, Mason A, Czaja AJ, et al. Severe vitamin D deficiency is a prognostic biomarker in autoimmune hepatitis. Aliment Pharmacol Ther 2019 Jan;49(2):173-182.

Ekstedt M, Franzen LE, Mathiesen UL, Thorelius L, Holmqvist M, Bodemar G, et al. Long-term follow-up of patients with NAFLD and elevated liver enzymes. Hepatology 2006 Oct;44(4):865-873.

Ekstedt M, Hagstrom H, Nasr P, Fredrikson M, Stal P, Kechagias S, et al. Fibrosis stage is the strongest predictor for disease-specific mortality in NAFLD after up to 33 years of follow-up. Hepatology 2015 May;61(5):1547-1554.

Ellis EL, Mann DA. Clinical evidence for the regression of liver fibrosis. J Hepatol 2012 May;56(5):1171-1180.

Elpek GO. Cellular and molecular mechanisms in the pathogenesis of liver fibrosis: An update. World J Gastroenterol 2014 Jun 21;20(23):7260-7276.

El-Serag HB. Epidemiology of viral hepatitis and hepatocellular carcinoma. Gastroenterology 2012 May;142(6):1264-1273.

Eslam M, Hashem AM, Leung R, Romero-Gomez M, Berg T, Dore GJ, et al. Interferon-lambda rs12979860 genotype and liver fibrosis in viral and non-viral chronic liver disease. Nat Commun 2015 Mar 5;6:6422.

Fattovich G. Natural history and prognosis of hepatitis B. Semin Liver Dis 2003 Feb;23(1):47-58.

Fausto N, Campbell JS. The role of hepatocytes and oval cells in liver regeneration and repopulation. Mech Dev 2003 Jan;120(1):117-130.

Fontana RJ, Goodman ZD, Dienstag JL, Bonkovsky HL, Naishadham D, Sterling RK, et al. Relationship of serum fibrosis markers with liver fibrosis stage and collagen content in patients with advanced chronic hepatitis C. Hepatology 2008 Mar;47(3):789-798.

Forns X, Ampurdanes S, Llovet JM, Aponte J, Quinto L, Martinez-Bauer E, et al. Identification of chronic hepatitis C patients without hepatic fibrosis by a simple predictive model. Hepatology 2002 Oct;36(4 Pt 1):986-992.

Fredriksson L, Li H, Eriksson U. The PDGF family: four gene products form five dimeric isoforms. Cytokine Growth Factor Rev 2004 Aug;15(4):197-204.

Frevert U, Engelmann S, Zougbede S, Stange J, Ng B, Matuschewski K, et al. Intravital observation of Plasmodium berghei sporozoite infection of the liver. PLoS Biol 2005 Jun;3(6):e192.

Friedman LS. Surgery in the patient with liver disease. Trans Am Clin Climatol Assoc 2010;121:192-204.

Friedman SL, Neuschwander-Tetri BA, Rinella M, Sanyal AJ. Mechanisms of NAFLD development and therapeutic strategies. Nat Med 2018 Jul;24(7):908-922.

Friedman SL, Ratziu V, Harrison SA, Abdelmalek MF, Aithal GP, Caballeria J, et al. A randomized, placebo-controlled trial of cenicriviroc for treatment of nonalcoholic steatohepatitis with fibrosis. Hepatology 2018 May;67(5):1754-1767.

Friedman SL. Evolving challenges in hepatic fibrosis. Nat Rev Gastroenterol Hepatol 2010 Aug;7(8):425-436.

Friedman SL. Hepatic stellate cells: protean, multifunctional, and enigmatic cells of the liver. Physiol Rev 2008 Jan;88(1):125-172.

Friedman SL. Liver fibrosis -- from bench to bedside. J Hepatol 2003;38 Suppl 1:S38-S53.

Friedman SL. Mechanisms of hepatic fibrogenesis. Gastroenterology 2008 May;134(6):1655-1669.

Gabbiani G. The myofibroblast in wound healing and fibrocontractive diseases. J Pathol 2003 Jul;200(4):500-503.

Galambos JT. Natural history of alcoholic hepatitis. 3. Histological changes. Gastroenterology 1972 Dec;63(6):1026-1035.

Gandhi CR, Behal RH, Harvey SA, Nouchi TA, Olson MS. Hepatic effects of endothelin. Receptor characterization and endothelin-induced signal transduction in hepatocytes. Biochem J 1992 Nov 1;287 (Pt 3):897-904.

Geiss GK, Bumgarner RE, Birditt B, Dahl T, Dowidar N, Dunaway DL, et al. Direct multiplexed measurement of gene expression with color-coded probe pairs. Nat Biotechnol 2008 Mar;26(3):317-325.

Gillet JP, Calcagno AM, Varma S, Marino M, Green LJ, Vora MI, et al. Redefining the relevance of established cancer cell lines to the study of mechanisms of clinical anti-cancer drug resistance. Proc Natl Acad Sci U S A 2011 Nov 15;108(46):18708-18713.

Gleeson D, Heneghan MA. British Society of Gastroenterology (BSG) guidelines for management of autoimmune hepatitis. Gut 2011 Dec;60(12):1611-1629.

Goodman ZD. Grading and staging systems for inflammation and fibrosis in chronic liver diseases. J Hepatol 2007 Oct;47(4):598-607.

Gressner AM, Weiskirchen R, Breitkopf K, Dooley S. Roles of TGF-beta in hepatic fibrosis. Front Biosci 2002 Apr 1;7:d793-d807.

Gressner OA, Gressner AM. Connective tissue growth factor: a fibrogenic master switch in fibrotic liver diseases. Liver Int 2008 Sep;28(8):1065-1079.

Grotendorst GR, Rahmanie H, Duncan MR. Combinatorial signaling pathways determine fibroblast proliferation and myofibroblast differentiation. FASEB J 2004 Mar;18(3):469-479.

Hanley KP, Oakley F, Sugden S, Wilson DI, Mann DA, Hanley NA. Ectopic SOX9 mediates extracellular matrix deposition characteristic of organ fibrosis. J Biol Chem 2008 May 16;283(20):14063-14071.

Hara H, Uchida S, Yoshimura H, Aoki M, Toyoda Y, Sakai Y, et al. Isolation and characterization of a novel liver-specific gene, hepassocin, upregulated during liver regeneration. Biochim Biophys Acta 2000 Jun 21;1492(1):31-44.

Harrison SA, Abdelmalek MF, Caldwell S, Shiffman ML, Diehl AM, Ghalib R, et al. Simtuzumab Is Ineffective for Patients With Bridging Fibrosis or Compensated Cirrhosis Caused by Nonalcoholic Steatohepatitis. Gastroenterology 2018 Oct;155(4):1140-1153.

Harrison SA, Oliver D, Arnold HL, Gogia S, Neuschwander-Tetri BA. Development and validation of a simple NAFLD clinical scoring system for identifying patients without advanced disease. Gut 2008 Oct;57(10):1441-1447.

Hellemans K, Michalik L, Dittie A, Knorr A, Rombouts K, De JJ, et al. Peroxisome proliferator-activated receptor-beta signaling contributes to enhanced proliferation of hepatic stellate cells. Gastroenterology 2003 Jan;124(1):184-201.

Henderson NC, Arnold TD, Katamura Y, Giacomini MM, Rodriguez JD, McCarty JH, et al. Targeting of alphav integrin identifies a core molecular pathway that regulates fibrosis in several organs. Nat Med 2013 Dec;19(12):1617-1624.

Henderson NC, Mackinnon AC, Farnworth SL, Poirier F, Russo FP, Iredale JP, et al. Galectin-3 regulates myofibroblast activation and hepatic fibrosis. Proc Natl Acad Sci U S A 2006 Mar 28;103(13):5060-5065.

Hennes EM, Zeniya M, Czaja AJ, Pares A, Dalekos GN, Krawitt EL, et al. Simplified criteria for the diagnosis of autoimmune hepatitis. Hepatology 2008 Jul;48(1):169-176.

Hernandez-Gea V, Friedman SL. Pathogenesis of liver fibrosis. Annu Rev Pathol 2011;6:425-456.

Heyes S, Pratt WS, Rees E, Dahimene S, Ferron L, Owen MJ, et al. Genetic disruption of voltage-gated calcium channels in psychiatric and neurological disorders. Prog Neurobiol 2015 Nov;134:36-54.

Hoeroldt B, McFarlane E, Dube A, Basumani P, Karajeh M, Campbell MJ, et al. Long-term outcomes of patients with autoimmune hepatitis managed at a nontransplant center. Gastroenterology 2011 Jun;140(7):1980-1989.

Hold GL, Untiveros P, Saunders KA, El-Omar EM. Role of host genetics in fibrosis. Fibrogenesis Tissue Repair 2009 Dec 4;2(1):6.

Hoshida Y, Villanueva A, Sangiovanni A, Sole M, Hur C, Andersson KL, et al. Prognostic gene expression signature for patients with hepatitis C-related early-stage cirrhosis. Gastroenterology 2013 May;144(5):1024-1030.

Housset C, Rockey DC, Bissell DM. Endothelin receptors in rat liver: lipocytes as a contractile target for endothelin 1. Proc Natl Acad Sci U S A 1993 Oct 15;90(20):9266-9270.

Hu K, Olsen BR, Besschetnova TY. Cell autonomous ANTXR1-mediated regulation of extracellular matrix components in primary fibroblasts. Matrix Biol 2017 Oct;62:105-114.

Huang H, Shiffman ML, Cheung RC, Layden TJ, Friedman S, Abar OT, et al. Identification of two gene variants associated with risk of advanced fibrosis in patients with chronic hepatitis C. Gastroenterology 2006 May;130(6):1679-1687.

Huang H, Shiffman ML, Friedman S, Venkatesh R, Bzowej N, Abar OT, et al. A 7 gene signature identifies the risk of developing cirrhosis in patients with chronic hepatitis C. Hepatology 2007 Aug;46(2):297-306.

Hui AY, Chan HL, Wong VW, Liew CT, Chim AM, Chan FK, et al. Identification of chronic hepatitis B patients without significant liver fibrosis by a simple noninvasive predictive model. Am J Gastroenterol 2005 Mar;100(3):616-623.

Ihn H. Pathogenesis of fibrosis: role of TGF-beta and CTGF. Curr Opin Rheumatol 2002 Nov;14(6):681-685.

Imbert-Bismut F, Ratziu V, Pieroni L, Charlotte F, Benhamou Y, Poynard T. Biochemical markers of liver fibrosis in patients with hepatitis C virus infection: a prospective study. Lancet 2001 Apr 7;357(9262):1069-1075.

Inoue T, Ohbayashi T, Fujikawa Y, Yoshida H, Akama TO, Noda K, et al. Latent TGF-beta binding protein-2 is essential for the development of ciliary zonule microfibrils. Hum Mol Genet 2014 Nov 1;23(21):5672-5682.

Ishak K, Baptista A, Bianchi L, Callea F, De GJ, Gudat F, et al. Histological grading and staging of chronic hepatitis. J Hepatol 1995 Jun;22(6):696-699.

Islam S, Antonsson L, Westin J, Lagging M. Cirrhosis in hepatitis C virus-infected patients can be excluded using an index of standard biochemical serum markers. Scand J Gastroenterol 2005 Jul;40(7):867-872.

Itoh T. Stem/progenitor cells in liver regeneration. Hepatology 2016 Aug;64(2):663-668.

Ivanov AI, Romanovsky AA. Putative dual role of ephrin-Eph receptor interactions in inflammation. IUBMB Life 2006 Jul;58(7):389-394.

Ji J, Eggert T, Budhu A, Forgues M, Takai A, Dang H, et al. Hepatic stellate cell and monocyte interaction contributes to poor prognosis in hepatocellular carcinoma. Hepatology 2015 Aug;62(2):481-495.

Kagan HM, Li W. Lysyl oxidase: properties, specificity, and biological roles inside and outside of the cell. J Cell Biochem 2003 Mar 1;88(4):660-672.

Kalluri R, Weinberg RA. The basics of epithelial-mesenchymal transition. J Clin Invest 2009 Jun;119(6):1420-1428.

Kang KW, Kim YG, Cho MK, Bae SK, Kim CW, Lee MG, et al. Oltipraz regenerates cirrhotic liver through CCAAT/enhancer binding protein-mediated stellate cell inactivation. FASEB J 2002 Dec;16(14):1988-1990.

Karsten SL, Van Deerlin VM, Sabatti C, Gill LH, Geschwind DH. An evaluation of tyramide signal amplification and archived fixed and frozen tissue in microarray gene expression analysis. Nucleic Acids Res 2002 Jan 15;30(2):E4.

Kaur S, Siddiqui H, Bhat MH. Hepatic Progenitor Cells in Action: Liver Regeneration or Fibrosis? Am J Pathol 2015 Sep;185(9):2342-2350.

Kawasaki K, Ushioda R, Ito S, Ikeda K, Masago Y, Nagata K. Deletion of the collagen-specific molecular chaperone Hsp47 causes endoplasmic reticulum stress-mediated apoptosis of hepatic stellate cells. J Biol Chem 2015 Feb 6;290(6):3639-3646.

Kazankov K, Barrera F, Moller HJ, Bibby BM, Vilstrup H, George J, et al. Soluble CD163, a macrophage activation marker, is independently associated with fibrosis in patients with chronic viral hepatitis B and C. Hepatology 2014 Aug;60(2):521-530.

Kelleher TB, Mehta SH, Bhaskar R, Sulkowski M, Astemborski J, Thomas DL, et al. Prediction of hepatic fibrosis in HIV/HCV co-infected patients using serum fibrosis markers: the SHASTA index. J Hepatol 2005 Jul;43(1):78-84.

Khalid SS, Hamid S, Siddiqui AA, Qureshi A, Qureshi N. Gene profiling of early and advanced liver disease in chronic hepatitis C patients. Hepatol Int 2011 Sep;5(3):782-788.

Kiernan F, Green J. XXIX. The anatomy and physiology of the liver. Philosophical Transactions of the Royal Society of London 1833 Jan 1.

Kim JH, Sohn BH, Lee HS, Kim SB, Yoo JE, Park YY, et al. Genomic predictors for recurrence patterns of hepatocellular carcinoma: model derivation and validation. PLoS Med 2014 Dec;11(12):e1001770.

Kim MY, Cho MY, Baik SK, Jeong PH, Suk KT, Jang YO, et al. Beneficial effects of candesartan, an angiotensin-blocking agent, on compensated alcoholic liver fibrosis - a randomized open-label controlled study. Liver Int 2012 Jul;32(6):977-987.

Kim SG, Kim YM, Choi JY, Han JY, Jang JW, Cho SH, et al. Oltipraz therapy in patients with liver fibrosis or cirrhosis: a randomized, double-blind, placebo-controlled phase II trial. J Pharm Pharmacol 2011 May;63(5):627-635.

Kim YJ, Sano T, Nabetani T, Asano Y, Hirabayashi Y. GPRC5B activates obesity-associated inflammatory signaling in adipocytes. Sci Signal 2012 Nov 20;5(251):ra85.

King LY, Canasto-Chibuque C, Johnson KB, Yip S, Chen X, Kojima K, et al. A genomic and clinical prognostic index for hepatitis C-related early-stage cirrhosis that predicts clinical deterioration. Gut 2015 Aug;64(8):1296-1302.

Kinnman N, Housset C. Peribiliary myofibroblasts in biliary type liver fibrosis. Front Biosci 2002 Feb 1;7:d496-d503.

Kleiner DE, Brunt EM, Van NM, Behling C, Contos MJ, Cummings OW, et al. Design and validation of a histological scoring system for nonalcoholic fatty liver disease. Hepatology 2005 Jun;41(6):1313-1321.

Kmiec Z. Cooperation of liver cells in health and disease. Adv Anat Embryol Cell Biol 2001;161:III-151.

Knop V, Hoppe D, Welzel T, Vermehren J, Herrmann E, Vermehren A, et al. Regression of fibrosis and portal hypertension in HCV-associated cirrhosis and sustained virologic response after interferon-free antiviral therapy. J Viral Hepat 2016 Dec;23(12):994-1002.

Kobayashi M, Harada K, Negishi M, Katoh H. Dock4 forms a complex with SH3YL1 and regulates cancer cell migration. Cell Signal 2014 May;26(5):1082-1088.

Koda M, Matunaga Y, Kawakami M, Kishimoto Y, Suou T, Murawaki Y. FibroIndex, a practical index for predicting significant fibrosis in patients with chronic hepatitis C. Hepatology 2007 Feb;45(2):297-306.

Kolios G, Valatas V, Kouroumalis E. Role of Kupffer cells in the pathogenesis of liver disease. World J Gastroenterol 2006 Dec 14;12(46):7413-7420.

Kondoh N, Imazeki N, Arai M, Hada A, Hatsuse K, Matsuo H, et al. Activation of a system A amino acid transporter, ATA1/SLC38A1, in human hepatocellular carcinoma and preneoplastic liver tissues. Int J Oncol 2007 Jul;31(1):81-87.

Kotronen A, Johansson LE, Johansson LM, Roos C, Westerbacka J, Hamsten A, et al. A common variant in PNPLA3, which encodes adiponutrin, is associated with liver fat content in humans. Diabetologia 2009 Jun;52(6):1056-1060.

Kozlitina J, Smagris E, Stender S, Nordestgaard BG, Zhou HH, Tybjaerg-Hansen A, et al. Exome-wide association study identifies a TM6SF2 variant that confers susceptibility to nonalcoholic fatty liver disease. Nat Genet 2014 Apr;46(4):352-356.

Kraft P, Wacholder S, Cornelis MC, Hu FB, Hayes RB, Thomas G, et al. Beyond odds ratios--communicating disease risk based on genetic profiles. Nat Rev Genet 2009 Apr;10(4):264-269.

Kraus MR, Clauin S, Pfister Y, Di MM, Ulinski T, Constam D, et al. Two mutations in human BICC1 resulting in Wnt pathway hyperactivity associated with cystic renal dysplasia. Hum Mutat 2012 Jan;33(1):86-90.

Krawitt EL. Autoimmune hepatitis. N Engl J Med 2006 Jan 5;354(1):54-66.

Krishnan A, Li X, Kao WY, Viker K, Butters K, Masuoka H, et al. Lumican, an extracellular matrix proteoglycan, is a novel requisite for hepatic fibrosis. Lab Invest 2012 Dec;92(12):1712-1725.

Lai CL, Ratziu V, Yuen MF, Poynard T. Viral hepatitis B. Lancet 2003 Dec 20;362(9401):2089-2094.

Lampi MC, Reinhart-King CA. Targeting extracellular matrix stiffness to attenuate disease: From molecular mechanisms to clinical trials. Sci Transl Med 2018 Jan 3;10(422).

Lavanchy D. The global burden of hepatitis C. Liver Int 2009 Jan;29 Suppl 1:74-81.

Lee CH, Shah B, Moioli EK, Mao JJ. CTGF directs fibroblast differentiation from human mesenchymal stem/stromal cells and defines connective tissue healing in a rodent injury model. J Clin Invest 2010 Sep;120(9):3340-3349.

Lee YA, Friedman SL. Reversal, maintenance or progression: what happens to the liver after a virologic cure of hepatitis C? Antiviral Res 2014 Jul;107:23-30.

Leivas A, Jimenez W, Bruix J, Boix L, Bosch J, Arroyo V, et al. Gene expression of endothelin-1 and ET(A) and ET(B) receptors in human cirrhosis: relationship with hepatic hemodynamics. J Vasc Res 1998 May;35(3):186-193.

Lens S, Torres F, Puigvehi M, Marino Z, Londono MC, Martinez SM, et al. Predicting the development of liver cirrhosis by simple modelling in patients with chronic hepatitis C. Aliment Pharmacol Ther 2016 Feb;43(3):364-374.

Leroy V, Monier F, Bottari S, Trocme C, Sturm N, Hilleret MN, et al. Circulating matrix metalloproteinases 1, 2, 9 and their inhibitors TIMP-1 and TIMP-2 as serum markers of liver fibrosis in patients with chronic hepatitis C: comparison with PIIINP and hyaluronic acid. Am J Gastroenterol 2004 Feb;99(2):271-279.

Levy MT, Trojanowska M, Reuben A. Oncostatin M: a cytokine upregulated in human cirrhosis, increases collagen production by human hepatic stellate cells. J Hepatol 2000 Feb;32(2):218-226.

Li J, Xin J, Zhang L, Wu J, Jiang L, Zhou Q, et al. Human hepatic progenitor cells express hematopoietic cell markers CD45 and CD109. Int J Med Sci 2014;11(1):65-79.

Liaskou E, Wilson DV, Oo YH. Innate immune cells in liver inflammation. Mediators Inflamm 2012;2012:949157.

Liberal R, Grant CR. Cirrhosis and autoimmune liver disease: Current understanding. World J Hepatol 2016 Oct 8;8(28):1157-1168.

Lipson KE, Wong C, Teng Y, Spong S. CTGF is a central mediator of tissue remodeling and fibrosis and its inhibition can reverse the process of fibrosis. Fibrogenesis Tissue Repair 2012;5(Suppl 1):S24.

Liu C, Schreiter T, Dirsch O, Gerken G, Oldhafer KJ, Broelsch CE, et al. Presence of markers for liver progenitor cells in human-derived intrahepatic biliary epithelial cells. Liver Int 2004 Dec;24(6):669-678.

Liu LX, Huang S, Zhang QQ, Liu Y, Zhang DM, Guo XH, et al. Insulin-like growth factor binding protein-7 induces activation and transdifferentiation of hepatic stellate cells in vitro. World J Gastroenterol 2009 Jul 14;15(26):3246-3253.

Liu SB, Ikenaga N, Peng ZW, Sverdlov DY, Greenstein A, Smith V, et al. Lysyl oxidase activity contributes to collagen stabilization during liver fibrosis progression and limits spontaneous fibrosis reversal in mice. FASEB J 2016 Apr;30(4):1599-1609.

Liu YL, Reeves HL, Burt AD, Tiniakos D, McPherson S, Leathart JB, et al. TM6SF2 rs58542926 influences hepatic fibrosis progression in patients with non-alcoholic fatty liver disease. Nat Commun 2014 Jun 30;5:4309.

Lo RC, Kim H. Histopathological evaluation of liver fibrosis and cirrhosis regression. Clin Mol Hepatol 2017 Dec;23(4):302-307.

Lok AS, Ghany MG, Goodman ZD, Wright EC, Everson GT, Sterling RK, et al. Predicting cirrhosis in patients with hepatitis C based on standard laboratory tests: results of the HALT-C cohort. Hepatology 2005 Aug;42(2):282-292.

Loomba R, Lawitz E, Mantry PS, Jayakumar S, Caldwell SH, Arnold H, et al. The ASK1 inhibitor selonsertib in patients with nonalcoholic steatohepatitis: A randomized, phase 2 trial. Hepatology 2017 Sep 11.

Lorena D, Darby IA, Reinhardt DP, Sapin V, Rosenbaum J, Desmouliere A. Fibrillin-1 expression in normal and fibrotic rat liver and in cultured hepatic fibroblastic cells: modulation by mechanical stress and role in cell adhesion. Lab Invest 2004 Feb;84(2):203-212.

Lozano R, Naghavi M, Foreman K, Lim S, Shibuya K, Aboyans V, et al. Global and regional mortality from 235 causes of death for 20 age groups in 1990 and 2010: a systematic analysis for the Global Burden of Disease Study 2010. Lancet 2012 Dec 15;380(9859):2095-2128.

Luo BH, Springer TA. Integrin structures and conformational signaling. Curr Opin Cell Biol 2006 Oct;18(5):579-586.

MacSween RN, Burt AD. Histologic spectrum of alcoholic liver disease. Semin Liver Dis 1986 Aug;6(3):221-232.

Manousou P, Burroughs AK, Tsochatzis E, Isgro G, Hall A, Green A, et al. Digital image analysis of collagen assessment of progression of fibrosis in recurrent HCV after liver transplantation. J Hepatol 2013 May;58(5):962-968.

Marcellin P, Gane E, Buti M, Afdhal N, Sievert W, Jacobson IM, et al. Regression of cirrhosis during treatment with tenofovir disoproxil fumarate for chronic hepatitis B: a 5-year open-label follow-up study. Lancet 2013 Feb 9;381(9865):468-475.

Marcolongo M, Young B, Dal PF, Fattovich G, Peraro L, Guido M, et al. A seven-gene signature (cirrhosis risk score) predicts liver fibrosis progression in patients with initially mild chronic hepatitis C. Hepatology 2009 Oct;50(4):1038-1044.

Marra F, Tacke F. Roles for chemokines in liver disease. Gastroenterology 2014 Sep;147(3):577-594.

Marrone G, Shah VH, Gracia-Sancho J. Sinusoidal communication in liver fibrosis and regeneration. J Hepatol 2016 Sep;65(3):608-617.

Maslak E, Gregorius A, Chlopicki S. Liver sinusoidal endothelial cells (LSECs) function and NAFLD; NO-based therapy targeted to the liver. Pharmacol Rep 2015 Aug;67(4):689-694.

Massague J. TGFbeta in Cancer. Cell 2008 Jul 25;134(2):215-230.

Matsue Y, Tsutsumi M, Hayashi N, Saito T, Tsuchishima M, Toshikuni N, et al. Serum osteopontin predicts degree of hepatic fibrosis and serves as a biomarker in patients with hepatitis C virus infection. PLoS One 2015;10(3):e0118744.

Matsui T, Kunishima S, Hamako J, Katayama M, Kamiya T, Naoe T, et al. Interaction of von Willebrand factor with the extracellular matrix and glycocalicin under static conditions. J Biochem 1997 Feb;121(2):376-381.

Mauro E, Crespo G, Montironi C, Londono MC, Hernandez-Gea V, Ruiz P, et al. Portal pressure and liver stiffness measurements in the prediction of fibrosis regression after sustained virological response in recurrent hepatitis C. Hepatology 2018 May;67(5):1683-1694.

McHutchison J, Goodman Z, Patel K, Makhlouf H, Rodriguez-Torres M, Shiffman M, et al. Farglitazar lacks antifibrotic activity in patients with chronic hepatitis C infection. Gastroenterology 2010 Apr;138(4):1365-73, 1373.

McPherson S, Hardy T, Henderson E, Burt AD, Day CP, Anstee QM. Evidence of NAFLD progression from steatosis to fibrosing-steatohepatitis using paired biopsies: implications for prognosis and clinical management. J Hepatol 2015 May;62(5):1148-1155.

McPherson S, Wilkinson N, Tiniakos D, Wilkinson J, Burt AD, McColl E, et al. A randomised controlled trial of losartan as an anti-fibrotic agent in non-alcoholic steatohepatitis. PLoS One 2017;12(4):e0175717.

Meissner EG, McLaughlin M, Matthews L, Gharib AM, Wood BJ, Levy E, et al. Simtuzumab treatment of advanced liver fibrosis in HIV and HCV-infected adults: results of a 6-month open-label safety trial. Liver Int 2016 Dec;36(12):1783-1792.

Mezzano SA, Ruiz-Ortega M, Egido J. Angiotensin II and renal fibrosis. Hypertension 2001 Sep;38(3 Pt 2):635-638.

Mills SE. Histology for pathologists. 4th ed.

Miyazaki T, Kanou Y, Murata Y, Ohmori S, Niwa T, Maeda K, et al. Molecular cloning of a novel thyroid hormone-responsive gene, ZAKI-4, in human skin fibroblasts. J Biol Chem 1996 Jun 14;271(24):14567-14571.

Mizejewski GJ. Role of integrins in cancer: survey of expression patterns. Proc Soc Exp Biol Med 1999 Nov;222(2):124-138.

Montano-Loza AJ, Thandassery RB, Czaja AJ. Targeting Hepatic Fibrosis in Autoimmune Hepatitis. Dig Dis Sci 2016 Nov;61(11):3118-3139.

Moon HJ, Finney J, Ronnebaum T, Mure M. Human lysyl oxidase-like 2. Bioorg Chem 2014 Dec;57:231-241.

Moore K, Wendon J, Frazer M, Karani J, Williams R, Badr K. Plasma endothelin immunoreactivity in liver disease and the hepatorenal syndrome. N Engl J Med 1992 Dec 17;327(25):1774-1778.

Moran CJ, Ramesh A, Brama PA, O'Byrne JM, O'Brien FJ, Levingstone TJ. The benefits and limitations of animal models for translational research in cartilage repair. J Exp Orthop 2016 Dec;3(1):1.

Morgan TR, Ghany MG, Kim HY, Snow KK, Shiffman ML, De Santo JL, et al. Outcome of sustained virological responders with histologically advanced chronic hepatitis C. Hepatology 2010 Sep;52(3):833-844.

Moylan CA, Pang H, Dellinger A, Suzuki A, Garrett ME, Guy CD, et al. Hepatic gene expression profiles differentiate presymptomatic patients with mild versus severe nonalcoholic fatty liver disease. Hepatology 2014 Feb;59(2):471-482.

Muir AJ, Levy C, Janssen HLA, Montano-Loza AJ, Shiffman ML, Caldwell S, et al. Simtuzumab for Primary Sclerosing Cholangitis: Phase 2 Study Results With Insights on the Natural History of the Disease. Hepatology 2018 Aug 28.

Muller T, Buch S, Berg T, Hampe J, Stickel F. Distinct, alcohol-modulated effects of PNPLA3 genotype on progression of chronic hepatitis C. J Hepatol 2011 Sep;55(3):732-733.

Munshaw S, Hwang HS, Torbenson M, Quinn J, Hansen KD, Astemborski J, et al. Laser captured hepatocytes show association of butyrylcholinesterase gene loss and fibrosis progression in hepatitis C-infected drug users. Hepatology 2012 Aug;56(2):544-554.

Myers RP, Pomier-Layrargues G, Kirsch R, Pollett A, Duarte-Rojo A, Wong D, et al. Feasibility and diagnostic performance of the FibroScan XL probe for liver stiffness measurement in overweight and obese patients. Hepatology 2012 Jan;55(1):199-208.

Nasr P, Ignatova S, Kechagias S, Ekstedt M. Natural history of nonalcoholic fatty liver disease: A prospective follow-up study with serial biopsies. Hepatol Commun 2018 Feb;2(2):199-210.

Nejjari M, Couvelard A, Mosnier JF, Moreau A, Feldmann G, Degott C, et al. Integrin up-regulation in chronic liver disease: relationship with inflammation and fibrosis in chronic hepatitis C. J Pathol 2001 Nov;195(4):473-481.

Netto GJ, Watkins DL, Williams JW, Colby TV, dePetris G, Sharkey FE, et al. Interobserver agreement in hepatitis C grading and staging and in the Banff grading schema for acute cellular rejection: the "hepatitis C 3" multi-institutional trial experience. Arch Pathol Lab Med 2006 Aug;130(8):1157-1162.

Neubauer K, Baruch Y, Lindhorst A, Saile B, Ramadori G. Gelsolin gene expression is upregulated in damaged rat and human livers within non-parenchymal cells and not in hepatocytes. Histochem Cell Biol 2003 Oct;120(4):265-275.

Neuschwander-Tetri BA, Loomba R, Sanyal AJ, Lavine JE, Van Natta ML, Abdelmalek MF, et al. Farnesoid X nuclear receptor ligand obeticholic acid for non-cirrhotic, non-alcoholic steatohepatitis (FLINT): a multicentre, randomised, placebo-controlled trial. Lancet 2015 Mar 14;385(9972):956-965.

Ngu JH, Gearry RB, Frampton CM, Stedman CA. Predictors of poor outcome in patients w ith autoimmune hepatitis: a population-based study. Hepatology 2013 Jun;57(6):2399-2406.

Nielsen T, Wallden B, Schaper C, Ferree S, Liu S, Gao D, et al. Analytical validation of the PAM50-based Prosigna Breast Cancer Prognostic Gene Signature Assay and nCounter Analysis System using formalin-fixed paraffin-embedded breast tumor specimens. BMC Cancer 2014 Mar 13;14:177.

Obesity linked to dramatic rise in liver disease: Alarming new statistics show that 1 in 4 Canadians may be affected by liver disease. 2016. Available at: https://www.liver.ca/press-releases/ (Accessed: Jul-13-2017).

Orman ES, Odena G, Bataller R. Alcoholic liver disease: pathogenesis, management, and novel targets for therapy. J Gastroenterol Hepatol 2013 Aug;28 Suppl 1:77-84.

O'Shea RS, Dasarathy S, McCullough AJ. Alcoholic liver disease. Hepatology 2010 Jan;51(1):307-328.

Paradis V, Dargere D, Bonvoust F, Vidaud M, Segarini P, Bedossa P. Effects and regulation of connective tissue growth factor on hepatic stellate cells. Lab Invest 2002 Jun;82(6):767-774.

Parikh CR, Thiessen-Philbrook H. Key concepts and limitations of statistical methods for evaluating biomarkers of kidney disease. J Am Soc Nephrol 2014 Aug;25(8):1621-1629.

Parola M, Pinzani M. Hepatic wound repair. Fibrogenesis Tissue Repair 2009 Sep 25;2(1):4.

Patel K, Bedossa P, Castera L. Diagnosis of liver fibrosis: present and future. Semin Liver Dis 2015 May;35(2):166-183.

Patel K, Gordon SC, Jacobson I, Hezode C, Oh E, Smith KM, et al. Evaluation of a panel of non-invasive serum markers to differentiate mild from moderate-to-advanced liver fibrosis in chronic hepatitis C patients. J Hepatol 2004 Dec;41(6):935-942.

Patsenker E, Stickel F. Role of integrins in fibrosing liver diseases. Am J Physiol Gastrointest Liver Physiol 2011 Sep;301(3):G425-G434.

Pellicoro A, Ramachandran P, Iredale JP, Fallowfield JA. Liver fibrosis and repair: immune regulation of wound healing in a solid organ. Nat Rev Immunol 2014 Mar;14(3):181-194.

Penland SK, Keku TO, Torrice C, He X, Krishnamurthy J, Hoadley KA, et al. RNA expression analysis of formalin-fixed paraffin-embedded tumors. Lab Invest 2007 Apr;87(4):383-391.

Perez TR. Is cirrhosis of the liver experimentally produced by CCl4 and adequate model of human cirrhosis? Hepatology 1983 Jan;3(1):112-120.

Pfisterer U, Kirkeby A, Torper O, Wood J, Nelander J, Dufour A, et al. Direct conversion of human fibroblasts to dopaminergic neurons. Proc Natl Acad Sci U S A 2011 Jun 21;108(25):10343-10348.

Philadelphia : Wolters Kluwer Health/Lippincott Williams & Wilkins., 2012.

Pineau P, Volinia S, McJunkin K, Marchio A, Battiston C, Terris B, et al. miR-221 overexpression contributes to liver tumorigenesis. Proc Natl Acad Sci U S A 2010 Jan 5;107(1):264-269.

Poisson J, Lemoinne S, Boulanger C, Durand F, Moreau R, Valla D, et al. Liver sinusoidal endothelial cells: Physiology and role in liver diseases. J Hepatol 2017 Jan;66(1):212-227.

Popper H, Elias H, Petty DE. Vascular pattern of the cirrhotic liver. Am J Clin Pathol 1952 Aug;22(8):717-729.

Poynard T, Mathurin P, Lai CL, Guyader D, Poupon R, Tainturier MH, et al. A comparison of fibrosis progression in chronic liver diseases. J Hepatol 2003 Mar;38(3):257-265.

Poynard T, Munteanu M, Deckmyn O, Ngo Y, Drane F, Messous D, et al. Applicability and precautions of use of liver injury biomarker FibroTest. A reappraisal at 7 years of age. BMC Gastroenterol 2011 Apr 14;11:39.

Pradere JP, Kluwe J, De MS, Jiao JJ, Gwak GY, Dapito DH, et al. Hepatic macrophages but not dendritic cells contribute to liver fibrosis by promoting the survival of activated hepatic stellate cells in mice. Hepatology 2013 Oct;58(4):1461-1473.

Qiu Q, Hernandez JC, Dean AM, Rao PH, Darlington GJ. CD24-positive cells from normal adult mouse liver are hepatocyte progenitor cells. Stem Cells Dev 2011 Dec;20(12):2177-2188.

Quan TE, Bucala R. Culture and analysis of circulating fibrocytes. Methods Mol Med 2007;135:423-434.

Ramachandran P, Dobie R, Wilson-Kanamori JR, Dora EF, Henderson BEP, Luu NT, et al. Resolving the fibrotic niche of human liver cirrhosis at single-cell level. Nature 2019 Oct 9.

Ramnath D, Irvine KM, Lukowski SW, Horsfall LU, Loh Z, Clouston AD, et al. Hepatic expression profiling identifies steatosis-independent and steatosis-driven advanced fibrosis genes. JCI Insight 2018 Jul 26;3(14).

Rappaort AM, BOROWY ZJ, LOUGHEED WM, LOTTO WN. Subdivision of hexagonal liver lobules into a structural and functional unit; role in hepatic physiology and pathology. Anat Rec 1954 May;119(1):11-33.

Ratziu V, Charlotte F, Heurtier A, Gombert S, Giral P, Bruckert E, et al. Sampling variability of liver biopsy in nonalcoholic fatty liver disease. Gastroenterology 2005 Jun;128(7):1898-1906.

Ratziu V. A critical review of endpoints for non-cirrhotic NASH therapeutic trials. J Hepatol 2018 Feb;68(2):353-361.

Regev A, Berho M, Jeffers LJ, Milikowski C, Molina EG, Pyrsopoulos NT, et al. Sampling error and intraobserver variation in liver biopsy in patients with chronic HCV infection. Am J Gastroenterol 2002 Oct;97(10):2614-2618.

Reilkoff RA, Bucala R, Herzog EL. Fibrocytes: emerging effector cells in chronic inflammation. Nat Rev Immunol 2011 Jun;11(6):427-435.

Reis PP, Waldron L, Goswami RS, Xu W, Xuan Y, Perez-Ordonez B, et al. mRNA transcript quantification in archival samples using multiplexed, color-coded probes. BMC Biotechnol 2011;11:46.

Richard AC, Lyons PA, Peters JE, Biasci D, Flint SM, Lee JC, et al. Comparison of gene expression microarray data with count-based RNA measurements informs microarray interpretation. BMC Genomics 2014;15:649.

Richardson MM, Jonsson JR, Powell EE, Brunt EM, Neuschwander-Tetri BA, Bhathal PS, et al. Progressive fibrosis in nonalcoholic steatohepatitis: association with altered regeneration and a ductular reaction. Gastroenterology 2007 Jul;133(1):80-90.

Rinella ME. Nonalcoholic fatty liver disease: a systematic review. JAMA 2015 Jun 9;313(22):2263-2273.

Roberts SK, Therneau TM, Czaja AJ. Prognosis of histological cirrhosis in type 1 autoimmune hepatitis. Gastroenterology 1996 Mar;110(3):848-857.

Rockey DC, Bell PD, Hill JA. Fibrosis--a common pathway to organ injury and failure. N Engl J Med 2015 Mar 19;372(12):1138-1149.

Rockey DC, Caldwell SH, Goodman ZD, Nelson RC, Smith AD. Liver biopsy. Hepatology 2009 Mar;49(3):1017-1044.

Roderburg C, Urban GW, Bettermann K, Vucur M, Zimmermann H, Schmidt S, et al. Micro-RNA profiling reveals a role for miR-29 in human and murine liver fibrosis. Hepatology 2011 Jan;53(1):209-218.

Roderfeld M, Weiskirchen R, Atanasova S, Gressner AM, Preissner KT, Roeb E, et al. Altered factor VII activating protease expression in murine hepatic fibrosis and its influence on hepatic stellate cells. Liver Int 2009 May;29(5):686-691.

Rodriguez-Pascual F, Busnadiego O, Gonzalez-Santamaria J. The profibrotic role of endothelin-1: is the door still open for the treatment of fibrotic diseases? Life Sci 2014 Nov 24;118(2):156-164.

Romeo S, Kozlitina J, Xing C, Pertsemlidis A, Cox D, Pennacchio LA, et al. Genetic variation in PNPLA3 confers susceptibility to nonalcoholic fatty liver disease. Nat Genet 2008 Dec;40(12):1461-1465.

Rosenberg WM, Voelker M, Thiel R, Becka M, Burt A, Schuppan D, et al. Serum markers detect the presence of liver fibrosis: a cohort study. Gastroenterology 2004 Dec;127(6):1704-1713.

Roskams T, Katoonizadeh A, Komuta M. Hepatic progenitor cells: an update. Clin Liver Dis 2010 Nov;14(4):705-718.

Roskams T, Yang SQ, Koteish A, Durnez A, DeVos R, Huang X, et al. Oxidative stress and oval cell accumulation in mice and humans with alcoholic and nonalcoholic fatty liver disease. Am J Pathol 2003 Oct;163(4):1301-1311.

Rotman Y, Koh C, Zmuda JM, Kleiner DE, Liang TJ. The association of genetic variability in patatin-like phospholipase domain-containing protein 3 (PNPLA3) with histological severity of nonalcoholic fatty liver disease. Hepatology 2010 Sep;52(3):894-903.

Ruehl M, Erben U, Schuppan D, Wagner C, Zeller A, Freise C, et al. The elongated first fibronectin type III domain of collagen XIV is an inducer of quiescence and differentiation in fibroblasts and preadipocytes. J Biol Chem 2005 Nov 18;280(46):38537-38543.

Rutkauskas S, Gedrimas V, Pundzius J, Barauskas G, Basevicius A. Clinical and anatomical basis for the classification of the structural parts of liver. Medicina (Kaunas) 2006;42(2):98-106.

Sakai N, Chun J, Duffield JS, Wada T, Luster AD, Tager AM. LPA1-induced cytoskeleton reorganization drives fibrosis through CTGF-dependent fibroblast proliferation. FASEB J 2013 May;27(5):1830-1846.

Sancho-Bru P, Altamirano J, Rodrigo-Torres D, Coll M, Millan C, Jose LJ, et al. Liver progenitor cell markers correlate with liver damage and predict short-term mortality in patients with alcoholic hepatitis. Hepatology 2012 Jun;55(6):1931-1941.

Sandrin L, Fourquet B, Hasquenoph JM, Yon S, Fournier C, Mal F, et al. Transient elastography: a new noninvasive method for assessment of hepatic fibrosis. Ultrasound Med Biol 2003 Dec;29(12):1705-1713.

Sanyal AJ, Friedman SL, McCullough AJ, Dimick-Santos L. Challenges and opportunities in drug and biomarker development for nonalcoholic steatohepatitis: findings and recommendations from an American Association for the Study of Liver Diseases-U.S. Food and Drug Administration Joint Workshop. Hepatology 2015 Apr;61(4):1392-1405.

Sanyal AJ. Past, present and future perspectives in nonalcoholic fatty liver disease. Nat Rev Gastroenterol Hepatol 2019 Jun;16(6):377-386.

Sarin SK, Kumar M, Lau GK, Abbas Z, Chan HL, Chen CJ, et al. Asian-Pacific clinical practice guidelines on the management of hepatitis B: a 2015 update. Hepatol Int 2016 Jan;10(1):1-98.

Schilsky RL, Doroshow JH, Leblanc M, Conley BA. Development and use of integral assays in clinical trials. Clin Cancer Res 2012 Mar 15;18(6):1540-1546.

Schueler M, Braun DA, Chandrasekar G, Gee HY, Klasson TD, Halbritter J, et al. DCDC2 mutations cause a renal-hepatic ciliopathy by disrupting Wnt signaling. Am J Hum Genet 2015 Jan 8;96(1):81-92.

Schuppan D, Kim YO. Evolving therapies for liver fibrosis. J Clin Invest 2013 May;123(5):1887-1901.

Schweitzer A, Horn J, Mikolajczyk RT, Krause G, Ott JJ. Estimations of worldwide prevalence of chronic hepatitis B virus infection: a systematic review of data published between 1965 and 2013. Lancet 2015 Oct 17;386(10003):1546-1555.

Seth D, Leo MA, McGuinness PH, Lieber CS, Brennan Y, Williams R, et al. Gene expression profiling of alcoholic liver disease in the baboon (Papio hamadryas) and human liver. Am J Pathol 2003 Dec;163(6):2303-2317.

Shah H, Bilodeau M, Burak KW, Cooper C, Klein M, Ramji A, et al. The management of chronic hepatitis C: 2018 guideline update from the Canadian Association for the Study of the Liver. CMAJ 2018 Jun 4;190(22):E677-E687.

Shang L, Hosseini M, Liu X, Kisseleva T, Brenner DA. Human hepatic stellate cell isolation and characterization. J Gastroenterol 2018 Jan;53(1):6-17.

Sharma B, John S. Hepatic Cirrhosis. StatPearls Publishing, 2019.

Siegmund SV, Schlosser M, Schildberg FA, Seki E, De MS, Uchinami H, et al. Serum Amyloid A Induces Inflammation, Proliferation and Cell Death in Activated Hepatic Stellate Cells. PLoS One 2016;11(3):e0150893.

Singh S, Allen AM, Wang Z, Prokop LJ, Murad MH, Loomba R. Fibrosis progression in nonalcoholic fatty liver vs nonalcoholic steatohepatitis: a systematic review and meta-analysis of paired-biopsy studies. Clin Gastroenterol Hepatol 2015 Apr;13(4):643-654.

Singh S, Muir AJ, Dieterich DT, Falck-Ytter YT. American Gastroenterological Association Institute Technical Review on the Role of Elastography in Chronic Liver Diseases. Gastroenterology 2017 May;152(6):1544-1577.

Smedsrod B, Le CD, Ikejima K, Jaeschke H, Kawada N, Naito M, et al. Hepatic sinusoidal cells in health and disease: update from the 14th International Symposium. Liver Int 2009 Apr;29(4):490-501.

Smith MW, Walters KA, Korth MJ, Fitzgibbon M, Proll S, Thompson JC, et al. Gene expression patterns that correlate with hepatitis C and early progression to fibrosis in liver transplant recipients. Gastroenterology 2006 Jan;130(1):179-187.

Smith MW, Yue ZN, Korth MJ, Do HA, Boix L, Fausto N, et al. Hepatitis C virus and liver disease: global transcriptional profiling and identification of potential markers. Hepatology 2003 Dec;38(6):1458-1467.

Sookoian S, Castano GO, Burgueno AL, Gianotti TF, Rosselli MS, Pirola CJ. A nonsynonymous gene variant in the adiponutrin gene is associated with nonalcoholic fatty liver disease severity. J Lipid Res 2009 Oct;50(10):2111-2116.

Soule B, Tirucherai G, Kavita U, Kundu S, Christian R. Safety, tolerability, and pharmacokinetics of BMS-986263/ND-L02-s0201, a novel targeted lipid nanoparticle delivering HSP47 siRNA, in healthy participants: A randomised, placebo-controlled, double-blind, phase 1 study. Journal of Hepatology 2018 Apr 1;68:S112.

Speliotes EK, Butler JL, Palmer CD, Voight BF, Hirschhorn JN. PNPLA3 variants specifically confer increased risk for histologic nonalcoholic fatty liver disease but not metabolic disease. Hepatology 2010 Sep;52(3):904-912.

Staels B, Rubenstrunk A, Noel B, Rigou G, Delataille P, Millatt LJ, et al. Hepatoprotective effects of the dual peroxisome proliferator-activated receptor alpha/delta agonist, GFT505, in rodent models of nonalcoholic fatty liver disease/nonalcoholic steatohepatitis. Hepatology 2013 Dec;58(6):1941-1952.

Standish RA, Cholongitas E, Dhillon A, Burroughs AK, Dhillon AP. An appraisal of the histopathological assessment of liver fibrosis. Gut 2006 Apr;55(4):569-578.

Sterling RK, Lissen E, Clumeck N, Sola R, Correa MC, Montaner J, et al. Development of a simple noninvasive index to predict significant fibrosis in patients with HIV/HCV coinfection. Hepatology 2006 Jun;43(6):1317-1325.

Stickel F, Buch S, Lau K, Meyer zu SH, Berg T, Ridinger M, et al. Genetic variation in the PNPLA3 gene is associated with alcoholic liver injury in caucasians. Hepatology 2011 Jan;53(1):86-95.

Sud A, Hui JM, Farrell GC, Bandara P, Kench JG, Fung C, et al. Improved prediction of fibrosis in chronic hepatitis C using measures of insulin resistance in a probability index. Hepatology 2004 May;39(5):1239-1247.

Suriawinata A, Thung S. Liver Pathology: An Atlas and Concise Guide. 2011.

Tacke F, Zimmermann HW. Macrophage heterogeneity in liver injury and fibrosis. J Hepatol 2014 May;60(5):1090-1096.

Talwalkar JA, Yin M, Fidler JL, Sanderson SO, Kamath PS, Ehman RL. Magnetic resonance imaging of hepatic fibrosis: emerging clinical applications. Hepatology 2008 Jan;47(1):332-342.

Tapper EB, Castera L, Afdhal NH. FibroScan (vibration-controlled transient elastography): where does it stand in the United States practice. Clin Gastroenterol Hepatol 2015 Jan;13(1):27-36.

Taura K, Miura K, Iwaisako K, Osterreicher CH, Kodama Y, Penz-Osterreicher M, et al. Hepatocytes do not undergo epithelial-mesenchymal transition in liver fibrosis in mice. Hepatology 2010 Mar;51(3):1027-1036.

Terrault NA, Lok ASF, McMahon BJ, Chang KM, Hwang JP, Jonas MM, et al. Update on prevention, diagnosis, and treatment of chronic hepatitis B: AASLD 2018 hepatitis B guidance. Hepatology 2018 Apr;67(4):1560-1599.

Theise ND, Saxena R, Portmann BC, Thung SN, Yee H, Chiriboga L, et al. The canals of Hering and hepatic stem cells in humans. Hepatology 1999 Dec;30(6):1425-1433.

Tian C, Stokowski RP, Kershenobich D, Ballinger DG, Hinds DA. Variant in PNPLA3 is associated with alcoholic liver disease. Nat Genet 2010 Jan;42(1):21-23.

Torok J, Dranoff JA, Schuppan D, Friedman SL. Strategies and endpoints of antifibrotic drug trials: Summary and recommendations from the AASLD Emerging Trends Conference, Chicago, June 2014. Hepatology 2015 Jan 27.

Trepo E, Goossens N, Fujiwara N, Song WM, Colaprico A, Marot A, et al. Combination of Gene Expression Signature and Model for End-Stage Liver Disease Score Predicts Survival of Patients With Severe Alcoholic Hepatitis. Gastroenterology 2018 Mar;154(4):965-975.

Trepo E, Gustot T, Degre D, Lemmers A, Verset L, Demetter P, et al. Common polymorphism in the PNPLA3/adiponutrin gene confers higher risk of cirrhosis and liver damage in alcoholic liver disease. J Hepatol 2011 Oct;55(4):906-912.

Trepo E, Pradat P, Potthoff A, Momozawa Y, Quertinmont E, Gustot T, et al. Impact of patatin-like phospholipase-3 (rs738409 C>G) polymorphism on fibrosis progression and steatosis in chronic hepatitis C. Hepatology 2011 Jul;54(1):60-69.

Trepo E, Romeo S, Zucman-Rossi J, Nahon P. PNPLA3 gene in liver diseases. J Hepatol 2016 Aug;65(2):399-412.

Trivedi PJ, Hubscher SG, Heneghan M, Gleeson D, Hirschfield GM. Grand round: Autoimmune hepatitis. J Hepatol 2019 Apr;70(4):773-784.

Tsochatzis EA, Bosch J, Burroughs AK. Liver cirrhosis. Lancet 2014 May 17;383(9930):1749-1761.

Tsuchida T, Friedman SL. Mechanisms of hepatic stellate cell activation. Nat Rev Gastroenterol Hepatol 2017 Jul;14(7):397-411.

Tyekucheva S, Martin NE, Stack EC, Wei W, Vathipadiekal V, Waldron L, et al. Comparing Platforms for Messenger RNA Expression Profiling of Archival Formalin-Fixed, Paraffin-Embedded Tissues. J Mol Diagn 2015 Jul;17(4):374-381.

Valenti L, Al-Serri A, Daly AK, Galmozzi E, Rametta R, Dongiovanni P, et al. Homozygosity for the patatin-like phospholipase-3/adiponutrin I148M polymorphism influences liver fibrosis in patients with nonalcoholic fatty liver disease. Hepatology 2010 Apr;51(4):1209-1217.

Valenti L, Rumi M, Galmozzi E, Aghemo A, Del MB, De NS, et al. Patatin-like phospholipase domain-containing 3 I148M polymorphism, steatosis, and liver damage in chronic hepatitis C. Hepatology 2011 Mar;53(3):791-799.

van DF, Olinga P, Poelstra K, Beljaars L. Targeted Therapies in Liver Fibrosis: Combining the Best Parts of Platelet-Derived Growth Factor BB and Interferon Gamma. Front Med (Lausanne) 2015;2:72.

Vashchenko G, Macgillivray RT. Functional role of the putative iron ligands in the ferroxidase activity of recombinant human hephaestin. J Biol Inorg Chem 2012 Dec;17(8):1187-1195.

Vehvilainen P, Hyytiainen M, Keski-Oja J. Matrix association of latent TGF-beta binding protein-2 (LTBP-2) is dependent on fibrillin-1. J Cell Physiol 2009 Dec;221(3):586-593.

Veldman-Jones MH, Brant R, Rooney C, Geh C, Emery H, Harbron CG, et al. Evaluating Robustness and Sensitivity of the NanoString Technologies nCounter Platform to Enable Multiplexed Gene Expression Analysis of Clinical Samples. Cancer Res 2015 Jul 1;75(13):2587-2593.

Veldman-Jones MH, Lai Z, Wappett M, Harbron CG, Barrett JC, Harrington EA, et al. Reproducible, Quantitative, and Flexible Molecular Subtyping of Clinical DLBCL Samples Using the NanoString nCounter System. Clin Cancer Res 2015 May 15;21(10):2367-2378.

Venkatesh SK, Yin M, Ehman RL. Magnetic resonance elastography of liver: technique, analysis, and clinical applications. J Magn Reson Imaging 2013 Mar;37(3):544-555.

Vogel A, Strassburg CP, Manns MP. Genetic association of vitamin D receptor polymorphisms with primary biliary cirrhosis and autoimmune hepatitis. Hepatology 2002 Jan;35(1):126-131.

Vrba J, Modriansky M. Oxidative burst of Kupffer cells: target for liver injury treatment. Biomed Pap Med Fac Univ Palacky Olomouc Czech Repub 2002 Dec;146(2):15-20.

Wai CT, Greenson JK, Fontana RJ, Kalbfleisch JD, Marrero JA, Conjeevaram HS, et al. A simple noninvasive index can predict both significant fibrosis and cirrhosis in patients with chronic hepatitis C. Hepatology 2003 Aug;38(2):518-526.

Wake K. "Sternzellen" in the liver: perisinusoidal cells with special reference to storage of vitamin A. Am J Anat 1971 Dec;132(4):429-462.

Wakim KG. Physiology of the liver. Am J Med 1954 Feb;16(2):256-271.

Wang M, Gong Q, Zhang J, Chen L, Zhang Z, Lu L, et al. Characterization of gene expression profiles in HBV-related liver fibrosis patients and identification of ITGBL1 as a key regulator of fibrogenesis. Sci Rep 2017 Mar 6;7:43446.

Wardle EN. Kupffer cells and their function. Liver 1987 Apr;7(2):63-75.

Wells RG. The portal fibroblast: not just a poor man's stellate cell. Gastroenterology 2014 Jul;147(1):41-47.

Welter D, MacArthur J, Morales J, Burdett T, Hall P, Junkins H, et al. The NHGRI GWAS Catalog, a curated resource of SNP-trait associations. Nucleic Acids Res 2014 Jan;42(Database issue):D1001-D1006.

Westbrook RH, Dusheiko G. Natural history of hepatitis C. J Hepatol 2014 Nov;61(1 Suppl):S58-S68.

Wilder J, Patel K. The clinical utility of FibroScan((R)) as a noninvasive diagnostic test for liver disease. Med Devices (Auckl) 2014;7:107-114.

Williams MJ, Clouston AD, Forbes SJ. Links between hepatic fibrosis, ductular reaction, and progenitor cell expansion. Gastroenterology 2014 Feb;146(2):349-356.

Williams R, Aspinall R, Bellis M, Camps-Walsh G, Cramp M, Dhawan A, et al. Addressing liver disease in the UK: a blueprint for attaining excellence in health care and reducing premature mortality from lifestyle issues of excess consumption of alcohol, obesity, and viral hepatitis. Lancet 2014 Nov 29;384(9958):1953-1997.

Wong VW, Vergniol J, Wong GL, Foucher J, Chan HL, Le BB, et al. Diagnosis of fibrosis and cirrhosis using liver stiffness measurement in nonalcoholic fatty liver disease. Hepatology 2010 Feb;51(2):454-462.

Wurmbach E, Chen YB, Khitrov G, Zhang W, Roayaie S, Schwartz M, et al. Genome-wide molecular profiles of HCV-induced dysplasia and hepatocellular carcinoma. Hepatology 2007 Apr;45(4):938-947.

Wynn TA, Ramalingam TR. Mechanisms of fibrosis: therapeutic translation for fibrotic disease. Nat Med 2012 Jul 6;18(7):1028-1040.

Xian ZH, Cong WM, Wang YH, Wang B, Wu MC. Expression and localization of aquaporin-1 in human cirrhotic liver. Pathol Res Pract 2009;205(11):774-780.

Xie G, Diehl AM. Evidence for and against epithelial-to-mesenchymal transition in the liver. Am J Physiol Gastrointest Liver Physiol 2013 Dec;305(12):G881-G890.

Xin X, Mains RE, Eipper BA. Monooxygenase X, a member of the copper-dependent monooxygenase family localized to the endoplasmic reticulum. J Biol Chem 2004 Nov 12;279(46):48159-48167.

Xu B, Broome U, Uzunel M, Nava S, Ge X, Kumagai-Braesch M, et al. Capillarization of hepatic sinusoid by liver endothelial cell-reactive autoantibodies in patients with cirrhosis and chronic hepatitis. Am J Pathol 2003 Oct;163(4):1275-1289.

Xu J, Liu X, Koyama Y, Wang P, Lan T, Kim IG, et al. The types of hepatic myofibroblasts contributing to liver fibrosis of different etiologies. Front Pharmacol 2014;5:167.

Xu X, Li YM, Ji H, Hou CZ, Cheng YB, Ma FP. Changes of ECM and CAM gene expression profile in the cirrhotic liver after HCV infection: analysis by cDNA expression array. World J Gastroenterol 2005 Apr 14;11(14):2184-2187.

Yeh MM, Brunt EM. Pathological features of fatty liver disease. Gastroenterology 2014 Oct;147(4):754-764.

Yildiz G, Arslan-Ergul A, Bagislar S, Konu O, Yuzugullu H, Gursoy-Yuzugullu O, et al. Genome-wide transcriptional reorganization associated with senescence-to-immortality switch during human hepatocellular carcinogenesis. PLoS One 2013;8(5):e64016.

Yin C, Evason KJ, Asahina K, Stainier DY. Hepatic stellate cells in liver development, regeneration, and cancer. J Clin Invest 2013 May;123(5):1902-1910.

Yokomori H, Oda M, Yasogawa Y, Nishi Y, Ogi M, Takahashi M, et al. Enhanced expression of endothelin B receptor at protein and gene levels in human cirrhotic liver. Am J Pathol 2001 Oct;159(4):1353-1362.

Yoon SM, Gerasimidou D, Kuwahara R, Hytiroglou P, Yoo JE, Park YN, et al. Epithelial cell adhesion molecule (EpCAM) marks hepatocytes newly derived from stem/progenitor cells in humans. Hepatology 2011 Mar;53(3):964-973.

Yoon YJ, Friedman SL, Lee YA. Antifibrotic Therapies: Where Are We Now? Semin Liver Dis 2016 Feb;36(1):87-98.

Yoshida EM, Sulkowski MS, Gane EJ, Herring RW, Jr., Ratziu V, Ding X, et al. Concordance of sustained virological response 4, 12, and 24 weeks post-treatment with sofosbuvir-containing regimens for hepatitis C virus. Hepatology 2015 Jan;61(1):41-45.

Younossi ZM, Koenig AB, Abdelatif D, Fazel Y, Henry L, Wymer M. Global epidemiology of nonalcoholic fatty liver disease-Meta-analytic assessment of prevalence, incidence, and outcomes. Hepatology 2016 Jul;64(1):73-84.

Younossi ZM, Ratziu V, Loomba R, Rinella M, Anstee QM, Goodman Z, et al. Obeticholic acid for the treatment of non-alcoholic steatohepatitis: interim analysis from a multicentre, randomised, placebo-controlled phase 3 trial. Lancet 2019 Dec 14;394(10215):2184-2196.

Younossi ZM, Stepanova M, Afendy M, Fang Y, Younossi Y, Mir H, et al. Changes in the prevalence of the most common causes of chronic liver diseases in the United States from 1988 to 2008. Clin Gastroenterol Hepatol 2011 Jun;9(6):524-530.

Yovchev MI, Grozdanov PN, Joseph B, Gupta S, Dabeva MD. Novel hepatic progenitor cell surface markers in the adult rat liver. Hepatology 2007 Jan;45(1):139-149.

Zatloukal K, Stumptner C, Fuchsbichler A, Fickert P, Lackner C, Trauner M, et al. The keratin cytoskeleton in liver diseases. J Pathol 2004 Nov;204(4):367-376.

Zeng MD, Lu LG, Mao YM, Qiu DK, Li JQ, Wan MB, et al. Prediction of significant fibrosis in HBeAg-positive patients with chronic hepatitis B by a noninvasive model. Hepatology 2005 Dec;42(6):1437-1445.

Zeremski M, Dimova RB, Pillardy J, de Jong YP, Jacobson IM, Talal AH. Fibrosis Progression in Patients With Chronic Hepatitis C Virus Infection. J Infect Dis 2016 Oct 15;214(8):1164-1170.

Zhang DY, Goossens N, Guo J, Tsai MC, Chou HI, Altunkaynak C, et al. A hepatic stellate cell gene expression signature associated with outcomes in hepatitis C cirrhosis and hepatocellular carcinoma after curative resection. Gut 2016 Oct;65(10):1754-1764.

Zhou S, Zhu Y, Mashrah M, Zhang X, He Z, Yao Z, et al. Expression pattern of DKK3, dickkopf WNT signaling pathway inhibitor 3, in the malignant progression of oral submucous fibrosis. Oncol Rep 2017 Feb;37(2):979-985.

Appendix A

Detailed protocol for preparation of formalin-fixed paraffin-embedded tissues cutting for RNA extraction.

Equipment and supplies

- Microtome
- RNase AWAY™ Decontamination Reagent
- Xylene
- Blades
- Gloves
- RNase and DNAse free microcentrifuge tubes (1.5 mL)

Procedure

1. Wipe equipment clean with xylene and dry with kimwipes (repeat between samples to minimize carry-over of wax and cross-contamination of tissue).

2. Decontaminate all equipment (including microtome, forceps, scalpel blade holder, and macrodissecting cutting surface) before preparation of each sample using RNase AWAY™ Decontamination Reagent. Use a new blade for cutting each block.

3. Commence sectioning at 5-µm thickness and discard top few whole sections (to avoid using the oxidized/contaminated surface of tissue block).

4. Set to microtome to cut 20-µm sections and cut 3-8 curls.

5. Place sections immediately into a labeled RNase-free microcentrifuge tube, close cap.

6. Repeat steps 1–5 until all samples are prepared. Change new gloves before cutting a new sample.

Appendix B

Detailed protocol for RNA isolation using RecoverAll™ Total Nucleic Acid Isolation Kit (Ambion).

Equipment and supplies

- RNase and DNAse free pipettes and filtered tips
- RNase AWAY™ Decontamination Reagent
- RNAse and DNAse free microcentrifuge (1.5 mL) tubes
- Nuclease-free water
- Modular tube rack
- Waste bucket
- Sharpie
- Dry block heaters
- Microfuge
- Centrifuge
- Vortex mixer
- Biosafety hood
- Ice and ice bucket
- RecoverAll™ Total Nucleic Acid Isolation Kit
- Xylene
- 100% ethanol
- Gloves

Before You Begin

1. RNase precautions:

Clean the lab, bench, tube rack and pipettes, with an RNase decontamination solution.

2. Prepare wash solutions:

a. Add 42 mL of ACS grade 100% ethanol to the bottle labeled Wash 1 Concentrate. Mix well.

b. Add 48 mL of ACS grade 100% ethanol to the bottle labeled Wash 2/3 Concentrate. Mix well.

c. Cap the wash solution bottles tightly to prevent evaporation.

d. Mark the labels to indicate that the ethanol has been added.

The final solutions will be referred to as ***Wash 1*** and ***Wash 2/3*** in the procedure.

Procedure

A. Deparaffinization

1. Add 1 mL 100% xylene, mix, and incubate for 3 min at 50°C:

a. Under Fumehood: Add 1 mL 100% xylene to the sample.

b. Vortex briefly to mix.

c. Centrifuge briefly to bring any tissue that is stuck to the sides of the tube down into the xylene.

d. Heat the sample for 3 min at 50°C to melt the paraffin.

2. Centrifuge for 4 min at maximum speed, and discard the xylene:

a. Centrifuge the sample for 4 min at room temperature and maximum speed to pellet the tissue.

b. Under fume hood: Use 1000 µL pipette to remove the xylene without disturbing the pellet. Discard the xylene.

c. Repeat 1a to 1c and 2a to 2b again. Don't heat the sample this time.

- At this step, the tissue is usually clear and can be difficult to see. If the pellet is loose, you may need to leave some xylene in the tube to avoid removing any tissue pieces.

3. Wash the pellet 3 times with 1 mL 100% ethanol:

a. Under fume hood: Add 1 mL of 100% ethanol (room temperature) to the sample and vortex to mix.

b. Centrifuge the sample for 2 min at room temperature and maximum speed to pellet tissue.

c. Use 1000 µL pipette to remove and discard the ethanol without disturbing the pellet.

d. Repeat steps 3a–3c twice to wash with 1 mL of 100% ethanol.

e. Briefly centrifuge again (1 min) to collect any remaining drops of ethanol in the bottom of the tube. Use 200 µL pipette to remove as much residual ethanol as possible without disturbing the pellet.

4. Air dry for 60-90 min at room temperature under the fume hood to remove residual ethanol.

B. Protease Digestion

1. Add Digestion Buffer and Protease:

a. Add 100 µL of Digestion Buffer needed for your tissue sample.

- Keep all enzymes on ice.

- Clean ice-bucket with RNase AWAY™ Decontamination Reagent beforehand.

b. Add 4 µL Protease to each sample.

c. [Do no vortex]: Mix and immerse the tissue (dislodge the pellet by pippetting up and down gently). If tissue sticks to the sides of the tube, use a pipette tip to push it into the solution, or briefly centrifuge to bring the tissue down into the solution.

2. Incubate for 15 min at 50°C, then 15 min at 80°C:

Incubate the sample in heat blocks for 15 min at 50°C, then 15 min at 80°C.

C. Nucleic Acid Isolation

1. Prepare Isolation Additive/ethanol mixture:

Combine the indicated amounts of Isolation Additive and ethanol, according to the volume of Digestion Buffer used in your sample.

For multiple samples, prepare a master mix for all samples plus ~5% overage.

Component	Amount (per sample)
Isolation Additive	120 µL
100% ethanol	275 µL
Total	395 µL

2. Add Isolation Additive/ethanol and mix:

a. Add 395 µL of Isolation Additive/ethanol mixture to each sample.

b. Mix by pipetting up and down five times. Some samples may appear white and cloudy after mixing.

3. Pass the mixture through a Filter Cartridge:

a. For each sample, place a Filter Cartridge in one of the Collection Tubes supplied.

b. Pipette up to 700 µL of the sample/ethanol mixture (from step 2) onto the Filter Cartridge and close the lid.

- To prevent clogging of the filter, avoid pipetting large pieces of undigested tissue onto the Filter Cartridge.

- Do not centrifuge Filter Cartridges at relative centrifugal forces greater than 10,000 g; higher forces may damage the filters.

c. Centrifuge at 10,000g for 1 min to pass the mixture through the filter.

d. Discard the flow-through, and re-insert the Filter Cartridge in the same Collection Tube.

4. Wash with 700 µL of Wash 1:

a. Add 700 µL of Wash 1 to the Filter Cartridge.

b. Centrifuge for 1 min at 10,000 g to pass the mixture through the filter.

c. Discard the flow-through, and re-insert the Filter Cartridge in the same Collection Tube.

5. Wash with 500 µL of Wash 2/3, and then centrifuge to remove residual fluid:

a. Add 500 µL of Wash 2/3 to the Filter Cartridge.

b. Centrifuge for 1 min at 10,000 g to pass the mixture through the filter.

c. Discard the flow-through, and re-insert the Filter Cartridge in the same Collection Tube.

d. Centrifuge for another 1 min at 10,000 g to remove residual fluid from the filter.

D. Nuclease Digestion and Final Nucleic Acid Purification

1. Prepare DNase mixture

Combine the indicated amounts of Nuclease-free Water, 10X DNase Buffer, and DNAse.

For multiple samples, prepare a master mix for all samples plus ~5% overage.

Component	Amount (per sample)
Nuclease-free Water	50 µL
10X DNase Buffer	6 µL
DNase	4 µL
Total	60 µL

2. RNA isolation: add 60 µL of DNA mixture and incubate for 30 min at room temp:

a. Add 60 µL of the DNase mixture to the center of each Filter Cartridge.

b. Cap the tube and incubate for 30 min at room temperature.

3. Wash with 700 µL of Wash 1:

a. Add 700 µL of Wash 1 to the Filter Cartridge.

b. Incubate for 1 min at room temperature.

c. Centrifuge for 1 min at 10,000 g.

d. Discard the flow-through, and re-insert the Filter Cartridge in the same Collection Tube.

4. Wash twice with 500 µL of Wash 2/3, then centrifuge to remove residual fluid:

a. Add 500 µL of Wash 2/3 to the Filter Cartridge.

b. Centrifuge for 1 min at 10,000 g.

c. Discard the flow-through, and re-insert the Filter Cartridge in the same Collection Tube.

d. Repeat steps a–c to wash a second time with 500 µL of Wash 2/3.

e. Centrifuge the assembly for 1 min at 10,000 g to remove residual fluid from the filter.

f. Transfer the filter cartridge to a new collection tube and proceed with the following.

5. Elute with 60 µL nuclease-free water at room temp:

a. Apply 60 µL of nuclease-free water to the center of the filter, and close the cap.

b. Allow the sample to sit at room temperature for 1 min.

c. Centrifuge for 1 min at maximum speed to pass the mixture through the filter (the eluate contains the RNA), put the samples on ice immediately after centrifuging.

d. Continue on to ethanol precipitation.

E. Ethanol precipitation of RNA:

1. Initial Precipitation

a. Add 0.1 volumes (6 µL) 3M sodium acetate (pH 5.2). Pipetting up and down to mix.

b. Add 2.2 volumes (132 µL) ice cold 100% ethanol. Mix thoroughly.

c. Place the tubes in the -80°C freezer overnight.

2. Withdrawing RNA

a. Keep the sample on ice whenever possible.

b. Mix the ethanol precipitate.

c. Spin the tube 10 minutes in a 4 degree microcentrifuge at 14,000 g. Be sure the hinge of the tube is facing out so that you know where the pellet will be later (it is often invisible).

d. Decant the supernatant.

e. Add 500 µL ice cold 70% ethanol to the tube.

f. Spin the tube 10 minutes in the microcentrifuge at 14,000 g.

g. Remove the ethanol by decanting with a pipettor (recommend 200 µL pipette).

h. Invert the tubes on a towel under the fume hood and allow the pellet to dry 60-90 min.

i. Dissolve the sample in 20 µL of nuclease-free water.